



Daniel Gossen

A Semi-Automated Design Method for Anthropomorphic Robot Hands

A Semi-Automated Design Method for Anthropomorphic Robot Hands

Eine Teilautomatisierte Designmethode für Anthropomorphe Roboterhände

Von der Fakultät für Maschinenwesen der
Rheinisch-Westfälischen Technischen Hochschule Aachen
zur Erlangung des akademischen Grades eines
DOKTORS DER INGENIEURWISSENSCHAFTEN
genehmigte Dissertation

vorgelegt von

Daniel Gossen

Berichter: apl. Prof. Dr.-Ing. Mathias Hüsing
Univ.-Prof. Dr.-Ing. Dr. h. c. (UPT) Burkhard Corves
Prof. Clément Gosselin

Tag der mündlichen Prüfung: 16.12.2025

Diese Dissertation ist auf den Internetseiten der Universitätsbibliothek online verfügbar.



DOI: 10.18154/RWTH-2026-02184

Acknowledgements

This thesis was written during my tenure as a research assistant at the Institute of Mechanism Theory, Machine Dynamics, and Robotics at RWTH Aachen University from 2021 to 2025.

First of all, I want to thank my supervisors, Professor Mathias Hüsing and Professor Burkhard Corves, for the opportunity to pursue my doctoral thesis during my time at the IGMR, for the trust placed in me in many projects and in my position as group leader, and for how much I learned during that time under their leadership.

I also thank Stefan Ruland and Axel Sommer for their constant IT support and I thank all my colleagues for making this time so memorable.

I further want to express my special thanks to my third examiner, Prof. Clément Gosselin. I still remember my excitement when I was granted the opportunity to show my work to Prof. Gosselin. Since then, I have been very grateful for all the feedback, guidance, and many inspiring technical discussions we had. I have very fond memories of the visit to his laboratory in the beautiful city of Québec (generously funded by the German Academic Exchange Service), and I appreciate how my collaboration with Prof. Gosselin contributed greatly to the success of my dissertation.

I further thank all the students who supported me. Special thanks go to Tianyi “Reinhold” Jin, Mark Witte, and Sebastian Polzin, who accompanied me as student assistants on this journey over a long period of time. I would especially like to thank Sebastian, whose thesis was the first I supervised and who later became the first student assistant I supervised, for the invaluable work over the years and the time we spent together.

I want to thank my families and friends for their continuous encouragement. To all my friends who endured / enjoyed these many long days during our studies: Thank you for sharing these memorable times that made me the academic I am today. To my parents: Thank you for encouraging me to study in the first place and motivating me throughout the entire time.

And lastly, to my fiancée, Jasmin: Thank you for the greatest support, for always understanding, and for always listening so attentively and enthusiastically to the same old stories.

Cologne, December 16, 2025

Daniel Gossen

Funding

Funded by the Deutsche Forschungsgemeinschaft (DFG, German Research Foundation) under Germany's Excellence Strategy – EXC-2023 Internet of Production – 390621612.

Abstract

With demographic change driving the demand for robotic assistance in complex grasping tasks, robot hands are emerging as a promising solution. However, the growing interest in anthropomorphic robot hands is difficult to address: The complex and multifaceted mechanical design creates high entry hurdles for new designers. This slows the growth in the number of experts and complicates finding relevant information, even for experienced designers. This is particularly evident in the conceptual design phase, when determining joint configuration, their coordination, and relative allocation. Guidance in the form of a knowledge-based design assistance system could address these problems by automating the decision-making parts of the design process, presenting solutions with reference to literature and offering recommendations for the conceptual design. This dissertation addresses the question of how such a guidance can be developed. A hypothesis is formulated and three objectives are pursued to test it: (1) develop a literature-linked knowledge base on joint configuration and coordination of tendon-driven rigid-sequential anthropomorphic robot hands to systematically generate conceptual designs, (2) develop a method to identify optimal designs based on user requirements, and (3) develop an automated evaluation method to select the most suitable design from the generated options. For the first objective, a knowledge base is developed, organizing relevant information into a non-redundant list of 23 fields of interest and 30 principal solutions, each linked to its original references. Arranged in morphological boxes, the knowledge base is applied to a methodically derived joint configuration of the human hand to generate approximately 8.5 billion conceptual designs. For the second, a heuristic is developed to identify Pareto-optimal designs based on desired grasp types (performance) and a choice between dexterity and design simplicity (preference). Suitable joint configurations and coordination strategies, drawn from literature, are ranked according to the user's preference. For the third, the developed control system evaluates designs using a utility analysis of the principal solutions, with scores adjusted by preference and relevance weights to align with the heuristic. The resulting guidance is implemented as a graphical user interface and verified to replicate the intended recommendations. An example application of the guidance presents, to the best of the author's knowledge, the first task-based design of an anthropomorphic robot hand with references to original sources.

By lowering entry barriers in early-stage anthropomorphic robot hand design, this dissertation lays a foundation for accelerating mechanical and control development, with potential to meet growing demand and reduce costs. It also presents the first framework for task-based robot hand design with meaningful results, despite gaps in the state of the art limiting a full analysis.

Zusammenfassung

Mit dem demografischen Wandel steigt die Nachfrage nach robotischer Assistenz bei komplexen Greifaufgaben, und Roboterhände gewinnen zunehmend an Bedeutung. Das wachsende Interesse an anthropomorphen Roboterhänden ist jedoch schwer zu adressieren: Das komplexe mechanische Design schafft hohe Einstiegshürden für neue Entwickler und verlangsamt damit den Zuwachs erfahrener Fachkräfte und die Identifikation relevanter Informationen. Dies ist besonders im Konzeptentwurf deutlich, wenn die Gelenkkonfiguration, -koordination und -anordnung definiert werden. Eine wissensbasierte Designunterstützung hat das Potenzial, diese Probleme zu adressieren, indem sie Entscheidungsprozesse automatisiert, Literaturreferenzen bereitstellt und Empfehlungen gibt. Diese Dissertation behandelte die Frage, wie eine solche Unterstützung entwickelt werden kann. Dazu wurde eine Hypothese formuliert und drei Ziele verfolgt: (1) Aufbau einer literaturverknüpften Wissensbasis zur Gelenkkonfiguration und -koordination seilgetriebener, rigide-sequenzieller anthropomorpher Roboterhände zur systematischen Generierung von Konzeptentwürfen, (2) Entwicklung einer Methode zur Identifikation optimaler Entwürfe auf Basis von Nutzeranforderungen und (3) Entwicklung einer automatisierten Bewertungsmethode für die im ersten Ziel generierten Optionen. Für das erste Ziel wurde eine Wissensbasis erstellt, welche relevante Informationen aus der Literatur in 23 Interessensfeldern und 30 Prinziplösungen organisiert und verlinkt. Die Wissensbasis wurde in Form von morphologischen Kästen auf eine methodisch abgeleitete Gelenkkonfiguration der menschlichen Hand angewendet und ermöglichte die Generierung von rund 8,5 Milliarden Konzeptentwürfen. Für das zweite Ziel wurde eine Heuristik entwickelt, die Pareto-optimale Entwürfe basierend auf der vom Nutzer gewünschten Leistung (Griffe) und Präferenz (Dexterität oder Einfachheit) identifiziert. Für das dritte Ziel wurde eine Inferenzmaschine entwickelt, die mithilfe einer Nutzwertanalyse und identifizierter Präferenz- und Relevanzgewichte die Entwürfe gemäß der Heuristik bewertet. Die entwickelte Designunterstützung wurde als grafische Benutzeroberfläche implementiert und reproduzierte erfolgreich bekannte Empfehlungen. Eine umgesetzte Beispielanwendung stellt nach Kenntnis des Autors erstmals ein aufgabenspezifisches Design einer anthropomorphen Roboterhand mit direkten Literaturverweisen dar.

Die Arbeit trägt damit zum einen dazu bei, Einstiegshürden zu senken, zum anderen legt sie ein methodisches Fundament für die zukünftige Entwicklung aufgabenbasierter Entwürfe mit ersten belastbaren Ergebnissen, auch wenn bestehende Lücken im Stand der Technik derzeit eine vollständige Analyse einschränken. Diese Dissertation verspricht daher Expertise zugänglicher zu machen, Entwicklungen zu beschleunigen und Kosten zu reduzieren.

Contents

| | |
|---|-------------|
| List of Figures | iii |
| List of Tables | viii |
| Nomenclature | xi |
| 1 Introduction | 1 |
| 1.1 Objectives | 2 |
| 1.2 Methodology and Structure | 4 |
| 2 Fundamentals and Research Positioning | 7 |
| 2.1 Knowledge-Based Systems | 7 |
| 2.2 Robot Hand Fundamentals | 8 |
| 2.2.1 Anthropomorphic Nomenclature | 8 |
| 2.2.2 Actuation Architectures | 10 |
| 2.2.3 Classification and Evaluation of Robot Hand Designs | 12 |
| 2.3 Current Conceptual Design Process | 15 |
| 2.3.1 Anthropomorphic Dimensions | 16 |
| 2.3.2 Approaches | 18 |
| 2.4 Related Work | 20 |
| 2.4.1 Knowledge Bases | 20 |
| 2.4.2 Design Methods | 21 |
| 2.5 Conclusion | 24 |
| 3 Guidance Knowledge Base | 25 |
| 3.1 Problem Statement and Approach | 25 |
| 3.2 Anthropomorphic Reference Model | 26 |
| 3.2.1 Human Hand Analysis | 26 |
| 3.2.2 Successful Robot Hands | 27 |
| 3.2.3 Initial Maximum DOF Configuration | 29 |
| 3.3 FoIs and PSs | 31 |
| 3.3.1 Data Structure | 32 |
| 3.3.2 Notation | 34 |

| | | |
|----------|--|------------|
| 3.3.3 | Review Systematic | 35 |
| 3.3.4 | Results | 37 |
| 3.3.4.1 | Joint Configuration | 38 |
| 3.3.4.2 | Joint Coordination | 42 |
| 3.4 | Hand Concepts | 47 |
| 3.5 | Conclusion | 49 |
| 4 | Design Recommendation | 51 |
| 4.1 | Problem Statement and Approach | 51 |
| 4.2 | Relevant Studies | 53 |
| 4.3 | Foundation for Task-Based Recommendation | 58 |
| 4.3.1 | Criteria | 59 |
| 4.3.2 | Requirement Combinations | 61 |
| 4.3.3 | Recommendations for Joint Configuration | 62 |
| 4.3.4 | Recommendations for Joint Coordination | 64 |
| 4.4 | Conclusion | 66 |
| 5 | Guidance Control System Design | 67 |
| 5.1 | Problem Statement and Approach | 67 |
| 5.2 | Inference Component | 69 |
| 5.2.1 | Weights | 69 |
| 5.2.2 | Criteria | 70 |
| 5.2.2.1 | Notation | 71 |
| 5.2.2.2 | Superior Qualities | 73 |
| 5.2.2.3 | Input Dependency | 74 |
| 5.2.3 | Metric | 75 |
| 5.2.4 | Influence Identification | 77 |
| 5.3 | Interfaces | 89 |
| 5.4 | Conclusion | 93 |
| 6 | Application and Evaluation | 97 |
| 6.1 | Methodology Validation | 97 |
| 6.2 | Guidance Verification | 99 |
| 6.3 | Example Application | 101 |
| 7 | Discussion | 105 |
| 8 | Conclusion and Outlook | 115 |

| | |
|---|----------------|
| Supervised Student Theses | I |
| Bibliography | III |
| Appendix | XXI |
| A Joint Allocation Information | XXIII |
| B Entity-Relation Models | XXIX |
| C Collected Robot Hands | XXXIII |
| D Library of Approaches Examples | XXXVII |
| E Lists of Entities and Instances | XLIII |
| F Fields of Interest Compatibility Matrix | LI |
| G Illustration of Derivation of Hand Concepts | LIII |
| H Programming Implementation Details | LVII |
| H.1 Hand Concept Creation | LVII |
| H.2 Recommendation Generation | LVIII |
| H.3 Hand Concept Illustration | LIX |
| H.4 Data Files Programming Excerpts | LX |
| H.5 Flow Charts | LXI |
| I Guidance GUI Design Illustrations | LXIX |
| J Influence Value Derivation | LXXI |
| K Quality Criteria and Quality Profile Illustrations | LXXV |
| L Influence Values | LXXXIII |

List of Figures

| | | |
|------|--|----|
| 1.1 | Proposed conceptual design process preceding the preliminary and detailed design. | 2 |
| 1.2 | Structure of this dissertation. | 6 |
| 2.1 | Architecture of knowledge-based systems with three individuals as users illustrate the system's universal usability. | 8 |
| 2.2 | Anatomical planes and directions in the human hand. Skeleton taken from International (2024) | 10 |
| 2.3 | Anthropomorphic joint terminology. Skeleton taken from International (2024) | 10 |
| 2.4 | Illustration of anthropomorphic hand movements. | 11 |
| 2.5 | Illustration of workspaces for fully actuated, coupled, and underactuated fingers. | 12 |
| 2.6 | Reduced grasp taxonomy by Feix et al. (2015) with illustrations created by the author. | 14 |
| 2.7 | Thumb opposition test procedure by Kapandji (1986) | 15 |
| 3.1 | Illustration of the proposed morphological box structure. | 26 |
| 3.2 | Human hand analysis resulting range of joint configurations †, ©2011 IEEE. . | 28 |
| 3.3 | Joint configurations and DOFs of qualitatively evaluated robot hands †, ©2011 IEEE. | 29 |
| 3.4 | Initial Maximum DOF Configuration with 24 DOFs †, ©2011 IEEE. | 30 |
| 3.5 | SRH joint configurations trade-off. | 30 |
| 3.6 | Kinematic structure comparison of all unsuccessful (right hand side) and a single successful robot hand with minimal DOF (left hand side) †, ©2011 IEEE. | 31 |
| 3.7 | QR code for the publicly launched LoA. | 31 |
| 3.8 | Illustration of the applied systematic mapping process †. | 33 |
| 3.9 | Illustration of identified thumb joint configurations †. | 39 |
| 3.10 | Cumulative illustration of thumb configuration frequencies †. | 39 |
| 3.11 | Illustration of identified finger joint configurations †. | 40 |
| 3.12 | Illustration of identified robot hand HMC joint configurations †. | 42 |
| 3.13 | Conceptual illustration of different thumb joint coordinations (brown: linkages, blue: tendons, striped: underactuated) †. | 43 |

| | | |
|------|---|----|
| 3.14 | Illustration of identified finger joint coordinations (brown: linkages, blue: tendons, striped: underactuated) †. | 45 |
| 3.15 | Percentile distribution of the number of underactuated fingers among the 29 evaluated tendon-driven robot hands †. | 47 |
| 3.16 | Example Hand Concept with given GFPSs (blue: tendons, striped: underactuated). | 48 |
| 4.1 | Illustration of optimization problem in multiple trade-offs. | 52 |
| 4.2 | SRHs' joint configurations with assigned GFPSs and illustrated trade-off. | 54 |
| 4.3 | SRHs' joint coordinations with assigned GFPSs and illustrated trade-off. | 55 |
| 4.4 | Rehabilitation tests: (a) Box and Block Test, (b) Nine Hole Peg Test, and (c) Groved Pegboard Test (Frommelt and Lösslein 2011). | 56 |
| 4.5 | Joint coordination strategies from the work by Tavakoli et al. (2015) (see Table 4.2) assigned to grasps from Feix's taxonomy. | 57 |
| 4.6 | Derived requirements of Anthropomorphic Movements criteria for grasps from the reduced Feix taxonomy. Colored criteria are required for the respective grasp. | 62 |
| 4.7 | Derived requirements of Movement Independence criteria for grasps from the reduced Feix taxonomy. Colored criteria are required for the respective grasp. | 65 |
| 5.1 | Example pairwise evaluation approach in methodical product development. | 67 |
| 5.2 | Presentation of the parameters to be identified according to the classic approach. | 68 |
| 5.3 | Standardization of Quality Profile aggregate values. | 80 |
| 5.4 | Standardization of a Hand Concept's Quality Profile-magnitude without weighting. | 80 |
| 5.5 | A Hand Concept's Quality Profile-magnitude with relevance weight. | 80 |
| 5.6 | A Hand Concept score without relevance weight and with preference weight towards Simplicity. | 80 |
| 5.7 | Method illustration for influence value identification. | 81 |
| 5.8 | Influenced Superior Qualities per FoI category (brown: positive influence, blue: negative influence). | 82 |
| 5.9 | Discretized Trade-Off Illustration of Hand Concepts (FoI category "Joint Configuration"). | 83 |
| 5.10 | Summary of the identified Major Quality and Superior Quality aggregate values. | 88 |
| 5.11 | Design of the guidance's Dialog Component. | 90 |
| 5.12 | Design of the guidance's Explanation Component. | 90 |
| 5.13 | Design of the guidance's Knowledge Acquisition Component. | 93 |
| 5.14 | Illustration of the Quality Criteria (enlarged version in Figure K.1). | 94 |
| 5.15 | Example visualization of the Quality Profile for the PS p_{16} (enlarged version in Figure K.2). | 94 |

| | | |
|------|--|-------|
| 6.1 | Quality Profile illustration of $gfps_8$ (enlarged version in Figure K.3). | 98 |
| 6.2 | Quality Profile illustration of $gfps_{78}$ (enlarged version in Figure K.4). | 98 |
| 6.3 | Aggregate Quality Profile values for $gfps_8$ and $gfps_{78}$ | 98 |
| 6.4 | Relevance-weighted aggregate Quality Profile values for $gfps_8$ and $gfps_{78}$ in two scenarios. | 98 |
| 6.5 | Guidance's recommendations for FoI-C Joint Configuration considering different user preferences. | 100 |
| 6.6 | Consistent alignment of gripper images using fixed height and vertical centering. | 102 |
| 6.7 | Required guidance input for the example application 'Care'. | 102 |
| 6.8 | Guidance's recommendation for the example application 'Care' with example positioning of the commercially available Shadow Dexterous Hand. | 103 |
| 6.9 | QP-illustration of the example recommendation (enlarged version in Figure K.6). | 104 |
| 6.10 | Quality Profile illustration of the Shadow Dexterous Robot Hand (enlarged version in Figure K.7). | 104 |
| | | |
| A.1 | Developed robot hand dimensions. Measures without unit are given in mm. | XXIII |
| A.2 | Developed robot hand prototype according to the IMDC joint structure. | XXIV |
| A.3 | Developed robot hand Kapandji Test results. | XXIV |
| A.4 | Exploded view of the developed robot hand prototype. | XXV |
| A.5 | Exploded view of the developed robot hand's middle finger. | XXVI |
| A.6 | Illustration of MCP joint design. | XXVI |
| | | |
| B.1 | Entity-Relation model of the Quality Criteria data structure. | XXIX |
| B.2 | Entity-Relation Model of the LoA data structure. | XXX |
| B.3 | Entity-Relation Model of three data bases: LoA, Configuration, and Exploration. | XXXI |
| B.4 | Entity-Relationship model for the relationship between the data files Qualities, GFPS, and Grasps. | XXXII |
| | | |
| C.1 | Time line of the collected Significant Robot Hands †. | XXXIV |
| C.2 | Time line of the collected robot hands analyzed for thumb contributions †. | XXXV |
| C.3 | Time line of the collected robot hands analyzed for interfinger underactuation contributions †. | XXXVI |
| | | |
| G.1 | Illustration of FoI combinations for five FoIs with up to two combined FoIs. | LIV |
| G.2 | Illustration of IMDC combination with FoI_2 and FoI_8 | LIV |
| G.3 | Illustration of IMDC combination with PSs from FoI_2 and FoI_8 | LV |
| G.4 | Illustration of G-expansion from a given FoI combinations to a GFoI combination with FoI_2 and FoI_6 | LV |

| | | |
|------|---|---------|
| G.5 | Illustration of concatenated expansion from a given FoI combinations to a GFPS combination with FoI ₂ and FoI ₆ | LVI |
| H.1 | Design of the guidance' tab for advanced settings. | LVIII |
| H.2 | Flowchart for Hand Concept creation. | LXII |
| H.3 | Flowchart for FoI combinations creation. | LXIII |
| H.4 | Flowchart for GFoI combinations creation. | LXIII |
| H.5 | Flowchart for GFPS combinations creation. | LXIV |
| H.6 | Flowchart for Effect combinations creation. | LXIV |
| H.7 | Flowchart for main process. | LXV |
| H.8 | Flowchart for input processing. | LXVI |
| H.9 | Flowchart for identification of recommended Hand Concepts. | LXVII |
| H.10 | Flowchart for creation of recommendation. | LXVIII |
| I.1 | Implementation of the guidance's Dialog Component. | LXIX |
| I.2 | Implementation of the guidance's Knowledge Acquisition Component. | LXIX |
| I.3 | Implementation of the guidance's Explanation Component. | LXX |
| I.4 | Implementation of the guidance's advanced settings tab. | LXX |
| J.1 | Discretized Trade-Off Illustration of Hand Concepts (FoI-C Intrafinger Joint Coordination) | LXXII |
| K.1 | Illustration of the Quality Criteria (enlarged version of Figure 5.14). | LXXVI |
| K.2 | Example visualization of influence values for PS p_{16} as the Quality Profile illustration (enlarged version of Figure 5.15). | LXXVII |
| K.3 | Quality Profile illustration of $gfps_8$ (enlarged version of Figure 6.1). | LXXVIII |
| K.4 | Quality Profile illustration of $gfps_{78}$ (enlarged version of Figure 6.2). | LXXIX |
| K.5 | Quality Profile illustration of the IMDC. | LXXX |
| K.6 | Quality Profile illustration of the example recommendation (enlarged version of Figure 6.9). | LXXXI |
| K.7 | Quality Profile illustration of the Shadow Dexterous Robot Hand (enlarged version of Figure 6.10). | LXXXII |

List of Tables

| | | |
|-----|---|----|
| 2.1 | Collected holistic review papers, evaluated for alignment with this dissertation's objective and the development of a database (✓: fulfilled, ✗: not fulfilled) †. . | 21 |
| 2.2 | Design Methods for anthropomorphic robot hands, evaluated on four criteria (✓: fulfilled, ✗: not fulfilled, (✓): partly fulfilled). | 22 |
| 3.1 | Human hand joint type and DOF analysis ("*": DOF only in little and ring finger; "***": unclear or missing information) ‡, ©2011 IEEE. | 27 |
| 3.2 | Kapandji, Feix, and Cutkosky evaluations of robotic hands (*no distinction made). Names in beige meet the scoring criteria ‡, ©2011 IEEE. | 28 |
| 3.3 | Thumb MB excerpt: Thumb-specific FoIs and PSs for joint configurations †. . | 38 |
| 3.4 | Index finger MB excerpt: FoIs and PSs for joint configuration †. | 40 |
| 3.5 | KBC MB excerpt: KBC-specific FoIs and PSs for joint configurations †. . . . | 41 |
| 3.6 | Thumb MB excerpt: Thumb-specific FoIs and PSs for joint coordination †. . . | 42 |
| 3.7 | Index finger morphological box excerpt: index finger-specific FoIs and PSs for joint coordination †. | 44 |
| 3.8 | KBC MB excerpt: KBC-specific FoIs and PSs for joint coordination †. | 45 |
| 3.9 | Transmission MB excerpt: Transmission-specific FoIs and PSs for joint coordination †. | 46 |
| 4.1 | Dexterity Scores under different immobilization conditions from the work by Saliba, Chetcuti and Farrugia Saliba et al. 2013. | 56 |
| 4.2 | Actuation strategy names with corresponding recommended joint coordination from the work by Tavakoli et al. (2015). | 58 |
| 4.3 | Criteria for Anthropomorphic Movements and Movement Independence for all fingers. | 60 |
| 4.4 | Criteria combination of Anthropomorphic Movements and Movement Independence for three defined grasp scenarios: 1) LF A-A movement not needed; 2) LF A-A movement needed with independent actuation; 3) LF A-A movement needed and may be coordinated. | 61 |
| 8.1 | Student theses supervised in the doctoral period that contribute to this dissertation. | I |
| 8.2 | Student theses supervised in the doctoral period that have not contributed to this dissertation. | II |

| | | |
|------|--|----------|
| A.1 | ROM value from literature for different finger | XXVII |
| A.2 | Robot hand finger phalanx dimensions in mm for a hand length of 195 mm. | XXVIII |
| D.1 | LoA examples: Thumb - elim. 1 TMC P-S DOF | XXXVII |
| D.2 | LoA examples: Thumb - Elim. 2 DOA - tendon underactuation | XXXVIII |
| D.3 | LoA examples: Thumb - elim. 1 MCP A-A DOF | XXXVIII |
| D.4 | LoA examples: Thumb - elim. 1 TMC P-S and 1 MCP A-A DOF | XXXIX |
| D.5 | LoA examples: Thumb - elim. 1 TMC P-S and 2 MCP DOF | XL |
| D.6 | LoA examples: Thumb - elim. TMC P-S and F-E and MCP A-A DOF | XL |
| D.7 | LoA examples: Elim. 1 DOA - Tendon Coupling | XLI |
| D.8 | LoA examples: Thumb: Elim. 1 DOA - Linkage Coupling | XLI |
| E.1 | List of instances of the entity "Group" (see Entity-Relation model in Figure B.2). | XLIII |
| E.2 | List of instances of the entity "FoI" (see Entity-Relation model in Figure B.2). | XLIV |
| E.3 | List of instances of the entity "Principal Solutions" (see Entity-Relation model in Figure B.2). | XLV |
| E.4 | List of instances of the entity "GFPS" (see Entity-Relation model in Figure B.2). | XLVIII |
| E.5 | List of instances of the entity "Major Quality" (see Entity-Relation model in Figure B.1). | XLVIII |
| E.6 | List of instances of the entity "Superior Quality" (see Figure B.1). | XLIX |
| E.7 | List of instances of the entity "Quality" (see Entity-Relation model in Figure B.1). | L |
| F.1 | Compatibility Matrix for FoIs with beige illustrating compatibility. | LII |
| G.1 | 53 valid FoI combinations for FoI-C ₁ grouped by size (1-4 FoIs) | LIII |
| L.1 | Influence values for FoI: Eliminating 1 TMC Joint DOF | LXXXIII |
| L.2 | Influence values for FoI <i>Eliminating 1 MCP Joint DOF</i> | LXXXIV |
| L.3 | Influence values for FoI <i>Eliminating 1 IP Joint DOF</i> | LXXXV |
| L.4 | Influence values for G-FoI <i>LF-Eliminating 1 IP Joint DOF</i> | LXXXV |
| L.5 | Influence values for FoI <i>Eliminating 2 TMC Joint DOF</i> | LXXXVI |
| L.6 | Influence values for FoI <i>Eliminating 2 MCP Joint DOF</i> | LXXXVI |
| L.7 | Influence values for FoI <i>Eliminating 1 HMC Joint DOF</i> | LXXXVII |
| L.8 | Influence values for FoI <i>Eliminating 2 HMC Joint DOF</i> | LXXXVII |
| L.9 | Influence values for FoI <i>Elim. 1 DOA HMC Joint</i> | LXXXVIII |
| L.10 | Influence values for FoI <i>Elim. 1 DOA MCP-PIP Joints</i> | LXXXIX |
| L.11 | Influence values for FoI <i>Elim. 2 DOA TMC-MCP-IP Joints</i> | XC |

| | | |
|------|--|--------|
| L.12 | Influence values for FoI <i>Elim. 3 DOA TMC-MCP-IP Joints</i> | XCI |
| L.13 | Influence values for FoI <i>Elim. 1 DOA PIP-DIP Joints</i> | XCII |
| L.14 | Influence values for FoI <i>Elim. 2 DOA MCP-PIP-DIP Joints</i> | XCIII |
| L.15 | Influence values for FoI <i>Elim. 3 DOA MCP-DIP-PIP Joints</i> | XCIV |
| L.16 | Influence values for FoI <i>Eliminating 1 DOA F-E LF-RF</i> | XCIV |
| L.17 | Influence values for FoI <i>Eliminating 1 DOA F-E MF-IF</i> | XCIV |
| L.18 | Influence values for FoI <i>Eliminating 2 DOA F-E RF-MF-IF</i> | XCIV |
| L.19 | Influence values for FoI <i>Eliminating 2 DOA F-E LF-RF-MF</i> | XCVI |
| L.20 | Influence values for FoI <i>Eliminating 2 DOA A-A LF-RF-IF</i> | XCVI |
| L.21 | Influence values for FoI <i>Eliminating 3 DOA F-E LF-RF-MF-IF</i> | XCVII |
| L.22 | Influence values for FoI <i>Eliminating 4 DOA F-E LF-RF-MF-IF-Tb</i> | XCVIII |
| L.23 | Influence values for FoI <i>Eliminating 4 DOA A-A LF-RF-MF-IF-Tb</i> | XCIX |

Nomenclature

General Convention

| | |
|----------------------|--|
| Scalar | Lowercase (italic) <i>a</i> |
| Vector | Lowercase (bold and italic) <i>a</i> |
| Array | Capital (bold and italic) <i>A</i> |
| Set | Throughout this dissertation, mathematical sets are denoted, where subscripts are used solely for ease of reference and do not imply any ordering of the set. The elements of the set are textual labels and not numerical values. |
| Evaluation Criterion | Throughout this dissertation, robot hand evaluation criteria are defined. Their abbreviations include periods to distinguish them from other abbreviations. |

Abbreviations

| | |
|--------|--|
| A-A | Adduction-Abduction, page 9 |
| A.M. | Anthropomorphic Movements — introduced evaluation criterion category (Superior Quality), page 61 |
| BBT | Box and Block Test, page 57 |
| BMBF | Federal Ministry of Education and Research (B undes m inisterium für B ildung und F orschung), page 1 |
| C.C. | Contact Condition — introduced evaluation criterion category (Superior Quality), page 77 |
| CMC | Carpometacarpal, page 9 |
| D.o.A. | Degree of Actuation — introduced evaluation criterion category (Superior Quality), page 77 |
| DIP | Distal Interphalangeal, page 10 |
| DOA | Degree of Actuation, page 5 |
| DOF | Degree of Freedom, page 2 |
| F-E | Flexion-Extension, page 9 |
| FoI | Field of Interest — introduced term for robot hand focus areas identified in this dissertation, page 5 |
| FoI-C | Field of Interest (FoI) Category — introduced term for categorization of defined FoIs, page 34 |
| GFoI | Group-specific Field of Interest (FoI) — introduced term for FoIs |

| | |
|------|--|
| | depending on the assigned morphological box (MB), page 37 |
| GFPS | Group- and Field of Interest (FoI)-specific principal solution (PS) — introduced term for PSs depending on the assigned morphological box (MB) and FoI, page 37 |
| GPT | Groved Pegboard Test , page 57 |
| GUI | Graphical User Interface , page 33 |
| HC | Hand Concept — introduced term for a robot hand conceptual design, page 5 |
| HMC | Hamatometacarpal , page 9 |
| IF | Index Finger , page 9 |
| IMDC | Initial Maximum Degree of Freedom Configuration — introduced term for a defined human hand reference model, page 5 |
| IP | Interphalangeal , page 10 |
| KBC | Kinematic Base Chain — introduced term for a Morphological Box (MB) name in the Library of Approaches (LoA), page 34 |
| LF | Little Finger , page 9 |
| LoA | Library of Approaches — introduced term for collected morphological boxes (MBs) in this dissertation, page 33 |
| M. | Manipulability — introduced evaluation criterion category (Superior Quality), page 78 |
| M.A. | Motion Ability — introduced evaluation criterion category (Superior Quality) for the subset of dexterity relevant to this dissertation, page 13 |
| M.D. | Mechanical Design — introduced evaluation criterion category (Superior Quality), page 78 |
| M.I. | Movement Independence — introduced evaluation criterion category (Superior Quality), page 61 |
| MB | Morphological Box , page 5 |
| MCP | Metacarpophalangeal , page 9 |
| MF | Middle Finger , page 9 |
| MQ | Major Qualities , page 75 |
| NHPT | Nine-Hole-Peg-Test , page 57 |
| P-S | Pronation-Supination , page 9 |
| PIP | Proximal Interphalangeal , page 9 |
| PS | Principal Solution , page 5 |
| RF | Ring Finger , page 9 |
| ROM | Range of Motion , page 14 |
| SQ | Superior Qualities , page 75 |

| | |
|-----|---|
| SRH | S uccessful R obot H ands — introduced term for the set of successfully evaluated robot hands found in literature, page 29 |
| Th | T humb, page 9 |
| TMC | T rapezi m etacarpal, page 9 |
| UM | U nderactuated M echanism, page 11 |

Formula Symbols

| | |
|------------------------------------|--|
| $\mathbf{p}_Q^{\text{gfps}_u}$ | Quality Profile of a given gfps_u — vector of $p_{q_i}^{\text{gfps}_u}$ for all i , page 79 |
| $\mathbf{p}_Q^{\text{HC}_l}$ | Quality Profile of a given HC_l — vector of $p_{q_i}^{\text{HC}_l}$ for all i , page 80 |
| \mathbf{p}_S | Start Vector assigning an HC initial values for the MQ, page 81 |
| $\mathbf{p}_{R-Q}^{\text{gfps}_u}$ | Relevance-weighted Quality Profile of a given gfps_u , page 80 |
| $\mathbf{p}_{R-Q}^{\text{HC}_l}$ | Relevance-weighted Quality Profile of a given HC_l , page 80 |
| \mathbf{v} | Vector of all (input-dependent) relevance weight values, page 79 |
| \mathbf{w} | Preference weight, page 81 |
| \mathbf{w} | Weighting factor for evaluation of criteria associated to the Major Qualities (MQs), page 73 |
| ϕ_{MQ} | Mapping that specifies assignment of Q to Q_{MQ} , page 77 |
| ϕ_Q | Mapping that specifies assignment of Q to Q_{SQ} , page 76 |
| ϕ_{SQ} | Mapping that specifies assignment of Q_{SQ} to Q_{MQ} , page 76 |
| a | Number of unsuitable FoIs applied to an HC in FoI-C ₁ , page 89 |
| b | Number of reduced DOF through suitable FoIs applied to an HC in FoI-C ₁ , page 88 |
| c | Number of suitable FoIs applied to an HC in FoI-C ₂ , page LXXI |
| F | Set of identified Fields of Interest (FoIs), page 36 |
| f^{gfps_u} | Mapping that assigns defined numerical values to each q_i for a given gfps_u , page 79 |
| f_a | Element of the set of Fields of Interest (F), with reference label a , page 36 |
| G | Set of identified groups, page 36 |
| g_r | Element of the set of groups (G), with reference label r , page 36 |
| GF | Set of identified Group-specific Fields of Interest (GFoIs), page 37 |
| g_f_s | Element of the set of Group-specific Fields of Interest (GF), with reference label s , page 37 |
| $GFPS$ | Set of identified Group-, and Fields of Interest (FoI)-specific principal solutions (GFPSs), page 37 |
| $gfps_u$ | Element of the set of Group-, and Fields of Interest (FoI)-specific principal solutions ($GFPS$), with reference label u , page 37 |
| HC | Set of identified robot hand conceptual designs (HCs), page 49 |
| HC_l | Element of the set of robot hand conceptual designs (HC), with reference label l , page 49 |
| m_C | Number of identified robot hand conceptual designs (HCs), page 49 |
| m_F | Number of identified Fields of Interest (FoIs), page 36 |
| m_G | Number of identified groups, page 36 |

| | |
|------------------------------|---|
| m_P | Number of identified principal solutions (PSs), page 36 |
| m_Q | Number of defined Qualities, page 75 |
| m_S | Number of identified Group-specific Fields of Interest (GFoIs), page 37 |
| m_U | Number of identified Group-, and Fields of Interest (FoI)-specific principal solutions (GFPSs), page 37 |
| m_{MQ} | Number of defined Major Qualities (MQ), page 76 |
| m_{SQ} | Number of defined Superior Qualities (SQ), page 76 |
| n | Number of unsuitable FoIs applied to an HC in FoI-C ₂ , page LXXIII |
| P | Set of identified principal solutions (PSs), page 36 |
| p_v | Element of the set of principal solutions (P), with reference label v , page 36 |
| p_{f_1} | Amount by which $p_{MQ_1}^{\text{FoI-C}_1}$ is reduced after inversion through the relevance weight in case of an unsuitable FoI, page 89 |
| p_{f_2} | Amount by which $p_{MQ_2}^{\text{FoI-C}_2}$ is reduced after inversion through the relevance weight in case of an unsuitable FoI, page 89 |
| $p_{MQ_k}^{\text{gfps}_u}$ | Aggregate (sum) value of $p_{SQ_j}^{\text{gfps}_u}$ for all q_{SQ_j} in $Q_{q_{MQ_k}}$, page 79 |
| $p_{MQ_k}^{\text{HC}_l}$ | Aggregate (sum) value of $p_{SQ_j}^{\text{HC}_l}$ for all q_{SQ_j} in $Q_{q_{MQ_k}}$, page 80 |
| $p_{q_i}^{\text{gfps}_u}$ | Numerical value (influence) assigned to q_i by the gfps_u , page 79 |
| $p_{q_i}^{\text{HC}_l}$ | Total influence on a given q_i by all gfps_u applied to a given HC_l , page 80 |
| $p_{R-MQ_k}^{\text{gfps}_u}$ | Relevance-weighted aggregate (sum) value of $p_{R-SQ_j}^{\text{gfps}_u}$ for all q_{SQ_j} in $Q_{q_{MQ_k}}$, page 80 |
| $p_{R-MQ_k}^{\text{HC}_l}$ | Aggregate (sum) value of $p_{R-SQ_j}^{\text{HC}_l}$ for all q_{SQ_j} in $Q_{q_{MQ_k}}$, page 80 |
| $p_{R-q_i}^{\text{gfps}_u}$ | Relevance-weighted influence value $p_{q_i}^{\text{gfps}_u}$ on a Quality q_i of a given gfps_u , page 80 |
| $p_{R-q_i}^{\text{HC}_l}$ | Relevance-weighted influence value $p_{q_i}^{\text{HC}_l}$ on a Quality q_i of a given HC_l , page 80 |
| $p_{R-SQ_j}^{\text{gfps}_u}$ | Relevance-weighted aggregate (sum) value of $p_{R-q_i}^{\text{gfps}_u}$ for all q_i in $Q_{q_{SQ_j}}$, page 80 |
| $p_{R-SQ_j}^{\text{HC}_l}$ | Aggregate (sum) value of $p_{R-q_i}^{\text{HC}_l}$ for all q_i in $Q_{q_{SQ_j}}$, page 80 |
| $p_{SQ_j}^{\text{gfps}_u}$ | Aggregate (sum) value of $p_{q_i}^{\text{gfps}_u}$ for all q_i in $Q_{q_{SQ_j}}$, page 79 |
| $p_{SQ_j}^{\text{HC}_l}$ | Aggregate (sum) value of $p_{q_i}^{\text{HC}_l}$ for all q_i in $Q_{q_{SQ_j}}$, page 80 |
| Q | Set of Qualities, page 75 |
| Q_I | Set of Qualities q_i that are required by the input, page 80 |
| q_i | Element of the set of Qualities (Q), with reference label i , page 75 |
| Q_R | Set of Qualities q_i that are not required by the input (residual), page 80 |
| q_{MQ_k} | Element of the set of Major Qualities (Q_{MQ}), with reference label k , |

| | |
|----------------|---|
| | page 76 |
| Q_{MQ} | Set of Major Qualities, page 76 |
| $Q_{q_{MQ_k}}$ | Subset that assigns a set of q_{SQ_j} to a specific q_{MQ_k} , page 76 |
| $Q_{q_{SQ_j}}$ | Subset that assigns a set of q_i to a specific q_{SQ_j} , page 76 |
| q_{SQ_j} | Element of the set of Superior Qualities (Q_{SQ}), with reference label j , page 76 |
| Q_{SQ} | Set of Superior Qualities (SQ), page 76 |
| x^{HC_i} | Robot hand conceptual design (HC) dependent evaluation score, page 81 |

Symbols

- † Denotes material reused with permission from Gossen et al. (2025b), page 20
- ‡ Denotes material reused with permission from Gossen et al. (2025a), ©2011 IEEE, page 29

Ambiguous Operators

- Dot product, page 81
- function composition operator, page 77
- ⊙ Hadamard (elementwise) product, page 80

Glossar

| | |
|--------------------|---|
| Hand Concept | Introduced term for a robot hand conceptual design, comprising the implemented joints, their degrees of freedom and which degrees of freedom are coupled or underactuated, page 5 |
| Knowledge Engineer | Terminology from the research field of knowledge-based systems, describing a person with expert knowledge that sets up a knowledge-based system, page 7 |
| Major Qualities | Introduced term for robot hand evaluation criteria categories, under which Superior Qualities are categorized., page 75 |
| Motion Ability | Introduced term as a quality measure comprising the fingers' addressable workspace of a robot hand and how well the individual workspaces are harmonized. It is introduced to establish a more concise reference compared to alternative terminologies, such as the frequently used and ambiguously defined term <i>dexterity</i> , page 13 |
| Qualities | Introduced term for robot hand evaluation criteria on the lowest level of introduced categorization., page 75 |
| Quality Criteria | Introduced term for robot hand evaluation criteria., page 75 |
| Quality Profile | Introduced term for a vector of influence values of all evaluation criteria for a given conceptual robot hand design. This dissertation established a dedicated illustration of the Quality Profile, page 79 |
| Superior Qualities | Introduced terminology for robot hand evaluation criteria categories, under which Qualities are categorized., page 75 |

1 Introduction

Demographic change increasingly requires robotic assistance in different domains. Due to demographic change, a shortage of skilled workers in sectors, such as industry and healthcare, is anticipated (BMWK 2020). To address the anticipated shortage, among others, robotic assistance in form of mobile manipulators and humanoid robots is being explored to perform complex manipulation tasks as a solution (BMBF 2024; BMBF 2023)¹.

The increasing interest in application of humanoids can be seen currently. Current analyses predict that global humanoid robot shipments may reach 160 thousand units by 2032 (Interact Analysis 2024). This number is supported by current commercial statements and governmental directives, including Tesla's CEO Elon Musk's announcement to build "several thousand" humanoid robots in 2025 (Fortune Editors 2025), and the Chinese government's directive to promote the use of humanoid robots in elderly care by 2030 (Xinhua 2025), which aims to address an increasingly aging society.

These recent developments provide great opportunity for robot hands. To fulfill the designated goal of addressing the shortage of skilled workers, dexterous grippers are required to perform complex grasping and manipulation tasks. This presents one of the main bottlenecks in current application of humanoids (The Robot Report 2025). The application of anthropomorphic robot hands becomes, thus, increasingly interesting for addressing the above challenges in industrial and social domain. Already in the study by Saliba et al. (2013), the development of anthropomorphic hands was motivated by an impending age of humanoid robots.

However, the growing interest in anthropomorphic robot hands is difficult to address. Besides current challenges in control complexity, the mechanical design is very complex, extensive and multifaceted. Firstly, this presents great entry hurdles for new researchers and secondly, even for experts, identifying relevant information is laborous. It can be assumed that these reasons lead to the current high costs of up to £95,000 for commercially available robot hands (Shadow Robot Company 2020)², due to few available experts, lengthy development times and overly complex designs.

Especially in early design, the conceptual design phase plays a crucial role. In that phase,

¹The sources are announcements by the Federal Ministry of Education and Research (BMBF) on the implementation of the Federal Government's Future Strategy for Research and Innovation.

²The cost is given for the Shadow Robot Hand. The referenced price list was received by the author via email from the Shadow Company in 2021 and is not publicly available. The price varies depending on equipment and robot hand complexity.

designers define the kinematic structure and kinematic parameters. Considering the prevalent approach of modeling the human hand, this refers in particular to the definition of the joint *configuration* (i.e., relevant joints and their degrees of freedom (DOFs)) and *coordination* (i.e., application of coupling or underactuation), and joint *allocation* (i.e. their relative alignment), respectively. As the literature is ambiguous in these aspects, expertise in the field is required. The conceptual design determines the future complexity, establishing the basis for the addressable workspace and consequently future dexterity.

The conceptual design phase can be organized into knowledge- and application-based parts. A proposed design process is given in Figure 1.1. Knowledge-parts (blue in Figure 1.1) require the designer to have and/or find relevant information and to make decisions regarding the joint related questions. Application-parts (beige in Figure 1.1) require the designer to evaluate the decisions, which is often performed experimentally and requires a prototype. If a poor decision is made in the knowledge part, the prototype needs to be adjusted and re-evaluated. This process explains the laborious and iterative nature of robot hand designs.

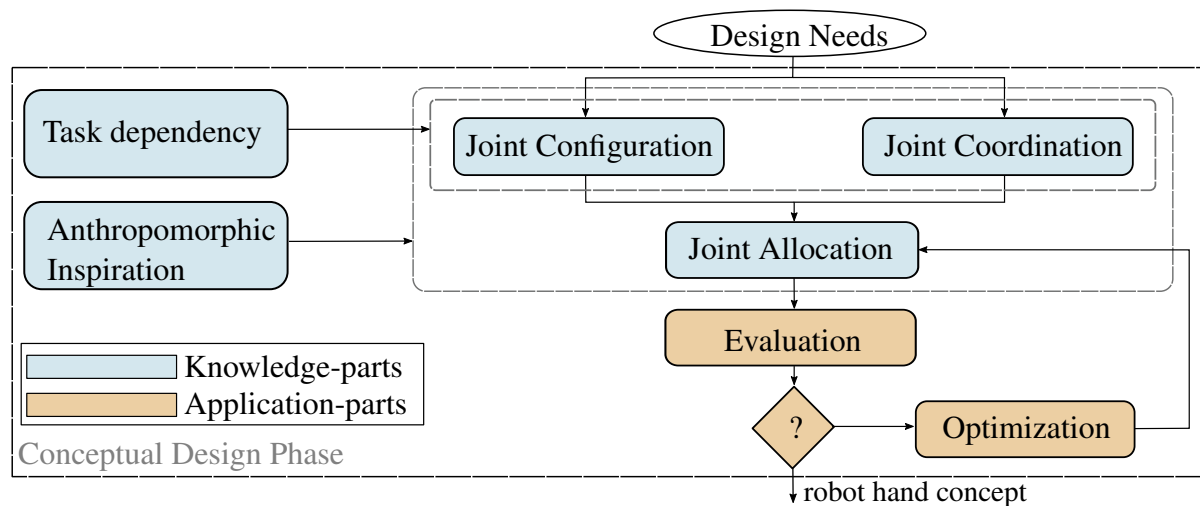


Figure 1.1: Proposed conceptual design process preceding the preliminary and detailed design.

1.1 Objectives

Guidance in the form of a knowledge-based design assistance could address the above challenges. If a system could be developed to guide designers by presenting relevant information, possible solutions and suggestions for the knowledge parts, only the application part would remain. This would significantly reduce the entry barriers for novice designers and help both novice and experienced designers to find relevant information. A semi-automation of the conceptual design process is thus proposed, implemented through a knowledge-based design

assistance system that automatically provides possible solutions, suggestions and relevant information for the knowledge parts of the process. To the best of the authors' knowledge, no such guidance exists for the (conceptual) design of anthropomorphic robot hands.

Thereby, the simultaneous recommendation of relevant literature serves an important function. First, it ensures that the rapidly evolving nature of the field of anthropomorphic robot hands is taken into account, rather than treating the subject as a closed and self-contained body of knowledge. Second, literature sources provide transparency for the system's suggestions. Third, they enable the designer to deepen their understanding of the recommendations provided, and last, they allow for proper scientific citation. In conclusion, the proposed system is intended as a guidance tool and should be understood as a form of support, helping designers to identify, comprehend, and further explore relevant knowledge in this field.

Based on the above proposal, the following research question is defined for this dissertation:



How can a guidance in form of a design assistance system be developed that guides designers through the conceptual design by presenting possible solutions with relevant literature for the knowledge parts and summarized suggestions for the overall conceptual design?

To address the derived research question, the following assumptions are made. The architecture of knowledge-based systems is considered, consisting of a knowledge base and a control system. The knowledge base incorporates embedded knowledge and the control system processes this knowledge (see Section 2.1). First, regarding the knowledge base, the intended guidance should present possible solutions for the individual knowledge-parts, rather than only offering summarized suggestions in the form of complete conceptual designs. A direct classification of existing conceptual designs is considered impractical and, therefore, inappropriate. Second, for the control system, it is assumed that no single ideal robot hand design, and therefore no universal conceptual design, exists. Instead, an optimal design must be identified, which is based on user requirements. These considerations lead to the following hypothesis:



The proposed guidance can be developed as a knowledge-based system in which the knowledge base allows to generate conceptual design solutions from embedded, literature-linked knowledge on joint configuration and coordination, and the control system allows the evaluation of the design solutions based on user requirements and the recommendation of the most appropriate solution along with the underlying embedded knowledge and its associated literature sources.

For a structured treatment of the hypothesis, it is dissected into three specific objectives:

- (O1) Develop a knowledge base with literature-linked knowledge on joint configuration and coordination of tendon-driven rigid-sequential anthropomorphic robot hands that allows the systematic generation of conceptual design solutions.
- (O2) Develop a method for identification of optimal conceptual designs based on user requirements.
- (O3) Develop a method for automated evaluation of conceptual designs based on user requirements, for identifying the most suitable solution (according to (O2)) among the available options (from (O1)).

First, focus is made on tendon-driven rigid-sequential robot hand designs, to limit the scope of this dissertation. Second, it is distinguished between objectives (O2) and (O3): (O3) refers to the development of the guidance's control system, defining how designs are automatically evaluated, where (O2) defines the goal towards which designs are evaluated.

1.2 Methodology and Structure

This work is structured in eight chapters, each fulfilling a distinct role in answering the research question. Chapter 2 lays the theoretical foundation of this work. The presented fundamentals and state of the art justify claimed limitations and challenges. Chapters 3, 4 and 5 address the objectives (O1) to (O3), respectively. The work concludes with an evaluation and discussion of the results in Chapter 7 and summary and outlook in Chapter 8. The individual connections of the chapters are illustrated in Figure 1.2.

The overarching methodology is separated in individual methodologies for each objective. To motivate the methodologies, Chapters 3, 4 and 5 contain a problem statement in which associated challenges are defined. The problem statements refer to the results of the preceding chapters and the state of the art for a better understanding. Therefore, they are not given here and reference is made to them for the underlying motivation instead. In the following, for each chapter, the applied methodologies are presented.

Chapter 2 lays the informational foundation of this dissertation. In Section 2.1 and 2.2, the architecture of knowledge-based systems and robot hand fundamentals are given, respectively. In Section 2.3, the current conceptual design process provides background information and justifies claimed limitations. In Section 2.4, related work is evaluated.

Chapter 3 addresses Objective (O1), establishing the knowledge base. As no suitable database for robot hand designs was identified (see Section 3.1), a dedicated methodology was developed. Due to the impracticality of capturing all existing conceptual designs, the approach defines

a conceptual design through the combination of, first, a robot hand joint configuration and, second, design approaches that modify joint configuration and coordination. Thus, in a first step, a unique robot hand joint configuration is defined. Second, a structured set of design approaches towards the modification of joint configuration and coordination found in literature is defined. This structure enables each design approach to be directly linked to its original literature source(s), providing literature references for any generated conceptual design through the concatenation.

The initial robot hand joint configuration is derived in Section 3.2 with a proper methodology. Inspired by the design process (see Figure 1.1), in which anthropomorphic inspiration is typically used to create a technical replica, the defined joint configuration shall represent an initial maximum DOF configuration (IMDC), which is then reduced by applying the defined design approaches. Therefore, studies of human anatomy are collected and the suggested joints are compared to those implemented in current, successful robot hands.

The design approaches are defined in Section 3.3 through a systematic mapping. To adequately represent the state of the art in mechanical design, four distinct search strategies are employed, each identifying a different set of studies with a specific focus. Further, the PRISMA guideline (Page et al. 2021) is followed to guarantee thoroughness and reproducibility. Design knowledge is captured in morphological boxes (MBs), synthesizing initially unknown *Fields of Interest* (FoIs) and principal solutions (PSs). FoIs reflect design objectives, while PSs represent the design approaches and describe how these objectives are realized and are linked to literature. To enable the intended application to the IMDC, the terminology of FoIs and PSs is aligned accordingly, with names referencing specific joints and implying the reduction of DOF or degrees of actuation (DOA). Finally, derived PSs are combined with the IMDC to generate a set of robot hand conceptual designs, referred to as *Hand Concepts* (HCs), from which the recommendation can choose.

Chapter 4 addresses the objective (O2), identifying optimal conceptual designs based on user requirements. User requirements most frequently relate to the performance of a specified task. However, task-based recommendation yields multiple equally suitable conceptual designs, with the optimum depending on the user's preference for other design qualities (see Section 4.1). Thus, a dedicated methodology is developed for selecting a Hand Concept as a task- and user-preference dependent optimization problem. A task requirement is used to preselect eligible conceptual designs, and a quality preference is used to identify the optimal design within that set in a trade-off. As an example implementation, task requirements for grasping and the trade-off between simplicity and dexterity are considered, allowing the user to specify those. The preference-dependent optimum is simply identified by sorting the preselected set towards their number of DOF or DOA. For identification of the preselected set, relevant studies are analyzed in Section 4.2. Finally, Section 4.3 consolidates these findings into a single foundation

for task-based preselection.

Chapter 5 addresses the objective (O3), developing a method to automatically evaluate all Hand Concepts. The chapter begins in Section 5.1 with a description of the associated challenges for the development of the method. From here on, the chapter is organized according to the architecture of a knowledge based system's control system. Section 5.2 addresses the method for the automated evaluation, while Section 5.3 addresses the different communication interfaces for user input and output and system maintenance.

As the set of Hand Concepts and the approach of task- and preference-dependent trade-off selection is introduced in this dissertation for the first time, a dedicated methodology is developed for the according automated Hand Concept evaluation. A scoring method is applied in which each PS influences defined criteria. Consequently, each Hand Concept is assigned a constant score depending on the applied PSs. However, these scores change, first, according to the specified task requirement, and second, according to the specified preference. For the former, an implemented weighting allows to flip the score of those Hand Concepts that are not part of the preselected set according to the results from Chapter 4, depending on the specified task-requirement. Regarding the latter, another weighting modifies the scores so that the Hand Concepts are ordered in terms of simplicity. The sorting direction depends on the user preference. The Hand Concept(s) with the highest score(s), together with their associated PSs and the associated literature references of these PSs, are recommended.

The main body of this dissertation focuses on the derived methodologies and methods. Readers interested in details of the programming implementation are referred to the appendix. The actual implementation of data files and algorithms represents an essential component of this dissertation and required considerable time and effort. Nevertheless, it is regarded as the realization of the established methods and derived methodologies. Therefore, references to the appendix are provided at appropriate points for details, in order to maintain the primary focus of the thesis on the conceptual and methodological foundations. All algorithms and data files are implemented in Python and JSON, respectively.

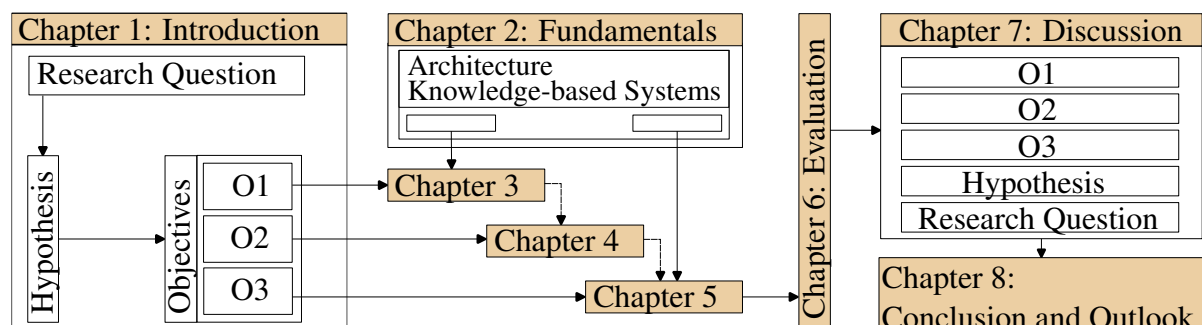


Figure 1.2: Structure of this dissertation.

2 Fundamentals and Research Positioning

This chapter presents fundamentals, basic information and background relevant for understanding the remainder of the work. In Section 2.1, knowledge-based systems are introduced and their architecture described. In Section 2.2, robot hand fundamentals are presented. Subsequently, the current process of conceptual design is presented, including information on joint allocation relevant for the recommendation. Finally, the goals of this dissertation are compared to those of related work from literature.

2.1 Knowledge-Based Systems

A knowledge-based system is defined by two main characteristics. First, it uses embedded knowledge to solve a certain problem. Second, it clearly distinguishes the knowledge base and the knowledge processing. (Altenkrüger and Büttner 2013) Since many programs use knowledge, a distinction is often difficult to make.

The architecture of a knowledge-based system has been defined to enable clear identification. The two main components *Knowledge Base* and *Control System* are shown in the center of Figure 2.1, with knowledge processing taking place in the depicted Control System. Typically, the people involved are distinguished as the Knowledge Engineer (right), who sets up the system, and the user (left). Thus, a knowledge-based system typically enables non-experts to interact with it (Altenkrüger and Büttner 2013) ¹.

The control system is therefore divided into four sub-components. The *Inference Component* processes information from the knowledge base. The *Dialogue Component* represents the interface through which the user communicates and provides input. The *Explanation Component* provides another interface through which the user can receive outputs. This is particularly important for a knowledge-based system as it enables the user to comprehend the results. Lastly, the Control System often incorporates a *Knowledge Acquisition Component*. This allows the Knowledge Engineer to manually expand or modify the knowledge base. (Altenkrüger and Büttner 2013)

¹Three individuals from diverse backgrounds illustrate the system's universal usability.

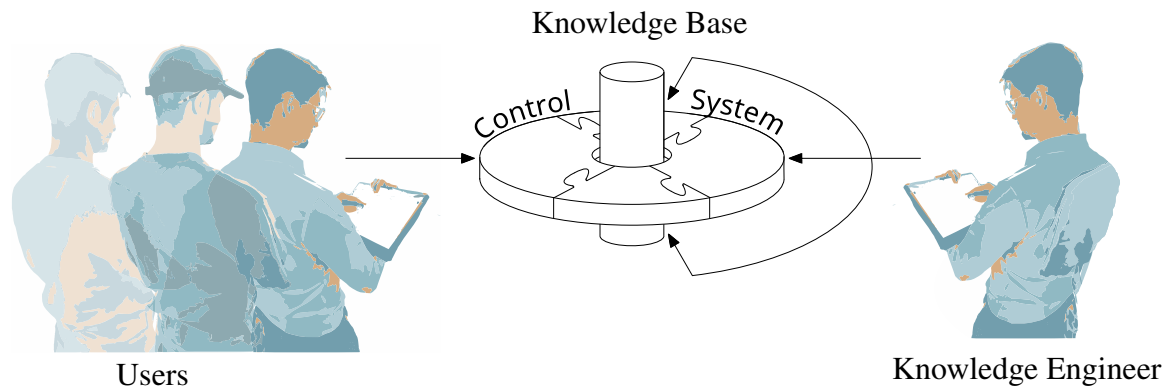


Figure 2.1: Architecture of knowledge-based systems with three individuals as users illustrate the system's universal usability.

2.2 Robot Hand Fundamentals

This section presents the fundamentals of robot hands, which are critical for understanding the content of this dissertation. It starts with the anthropomorphic nomenclature to establish the scope of the intended design and a common vocabulary. Actuation architectures are then presented to introduce fundamental concepts such as underactuation in robot hand designs. Lastly, the section presents current methods of classifying anthropomorphic robot hands. This section illustrates the qualities by which robot hands are currently distinguished, how they are defined, and how they are evaluated.

2.2.1 Anthropomorphic Nomenclature

This subsection aims at reaching two objectives. First, anthropomorphism is defined in the context of robotic hand design to clarify design requirements. Second, basic terminologies for fingers, joints, and movements are introduced to establish a consistent vocabulary.

Identifying an exact definition of when a gripper is anthropomorphic is difficult. Many studies limit the definition to the presence of several fingers and an opposable thumb (Martell and Giuseppina 2007; Puig et al. 2008b). Other definitions define anthropomorphism in robotic hands as the partial or complete imitation of the human hand (Puig et al. 2008b; Biagiotti et al. 2004), in factors such as shape, size, consistency, color, temperature and aesthetic factors (Gama Melo et al. 2014). Biagiotti et al. (2004) introduced an anthropomorphism index that weights kinematics, contact surfaces and size.

Since no clear design requirements can be derived from the above definition, the following requirements for an anthropomorphic robotic hand are derived for this dissertation: First, four

fingers and thumb are present at all times, to correspond to above requirements of multiple fingers and a thumb. Secondly, all achievable movements correspond to anthropomorphic movements as they are known in the human hand. This requires the fingers to be located in relation to one another in the same way as in the human hand. Thus, the definition regarding kinematics, form and aesthetics is complied with. Third, all applied joints correspond to anthropomorphic joints, as they are known from a human hand.

For the underlying terminologies, first, a distinction is made between the terms finger and digit. The term finger refers specifically to the index finger (IF), middle finger (MF), ring finger (RF), and little finger (LF). The thumb (Th) is excluded from that definition. Referring to all four fingers and the thumb collectively, the term *digit* is used. (Biesecker et al. 2009)

Further, anatomical planes are introduced. According to Güçlü and Cora (2023) and Zimmer and Appell (2021b), the coronal, sagittal and transverse planes are defined as illustrated in Figure 2.2. Further, six different directions are given. Proximal and distal describe relative proximity to the carpus. Palmar and dorsal refer to directions on the palm and backhand side, respectively. Ulnar indicates a position towards the ulna, while radial denotes a position towards the radius.

Third, the terms for the anthropomorphic movements are defined. The terms include *Flexion*, *Extension* (F-E), and *Abduction*, *Adduction* (A-A). Flexion refers to the movement of a finger towards the palm, while extension describes its return to the extended starting position, given in Figure 2.4a. Abduction generally describes a movement away from the Sagittal Plane. Thereby, it is distinguished between different A-A for fingers and thumb. The index finger A-A and thumb palmar A-A is illustrated in Figure 2.4b. Thumb radial A-A is illustrated in Figure 2.4c. Another movement that is not illustrated is the axial rotation of the thumb, which is essential for full opposition. This movement enables the pad of the thumb to face the pads of the fingers, typically involving a rotation of up to 180 degrees around the thumb's own axis. It is often referred to as the *Pronation-Supination* (P-S) DOF of the thumb. (Zimmer and Appell 2021b; Güçlü and Cora 2023)

Finally, the joint terminology is described, as illustrated in Figure 2.3. The finger structure consists of multiple articulated bones. The carpal bones form the structure of the palm. For each finger, the carpal bones connect to the metacarpal bones. The articulation between the carpal and metacarpal bones is known as the Carpometacarpal (CMC) joint. For better distinction, the commonly used alternatives of Hamatometacarpal (HMC) for the fingers and Trapeziometacarpal (TMC) for the thumb are used. At the distal end of the metacarpal bones, they connect to the proximal phalanges through the Metacarpophalangeal (MCP) joint. The fingers then continue with the medial phalanges, which articulate with the Proximal Interphalangeal (PIP) joint. Finally, the distal phalanges are connected to the medial phalanges

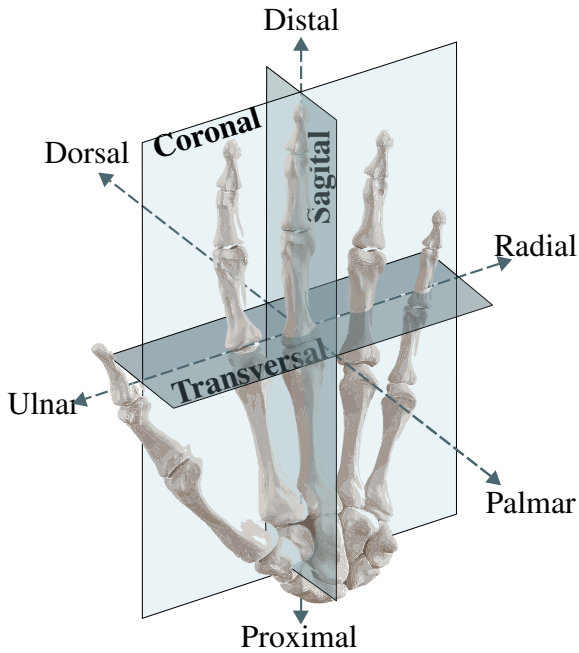


Figure 2.2: Anatomical planes and directions in the human hand. Skeleton taken from International (2024)

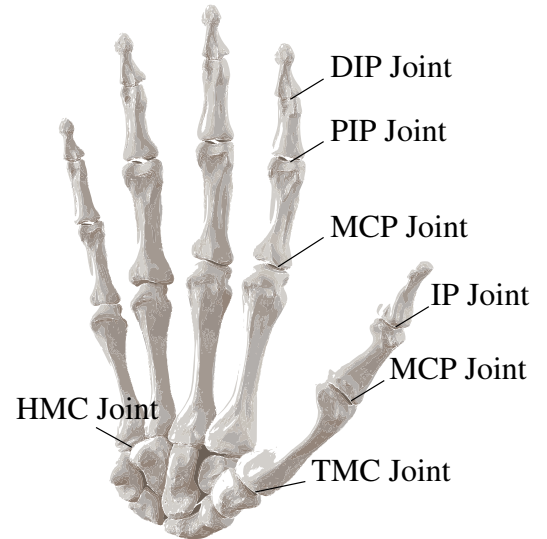


Figure 2.3: Anthropomorphic joint terminology. Skeleton taken from International (2024)

via the Distal Interphalangeal (DIP) joint. The thumb's structure slightly differs from the finger's, lacking a medial phalanx. Instead, its proximal phalanx is directly connected to the distal phalanx via the Interphalangeal (IP) joint. (Marieb and Hoehn 2007) Muscles, tendons, and ligaments, as well as the remaining bones are not given in detail. For further information, the reader is referred to the work of Hirt et al. (2015) and Kapandji (1987).

2.2.2 Actuation Architectures

For the design of anthropomorphic robotic hands, three actuation architectures can be distinguished: fully-actuated, coupled, and underactuated. In consideration of the conceptual design, the key information is whether a particular joint is independently actuated or coordinated with another joint. This coordination can be either a coupling or an underactuation. The three types are explained in more detail in the following.

Fully-actuated robotic hands offer remarkable dexterity but face challenges due to the high number of motors. Fully-actuated refers to a system in which each designated joint experiences an independent torque applied by a dedicated actuator. As a result, fully-actuated mechanisms have the same number of DOFs as the DOAs, which correspond to the number of actuators

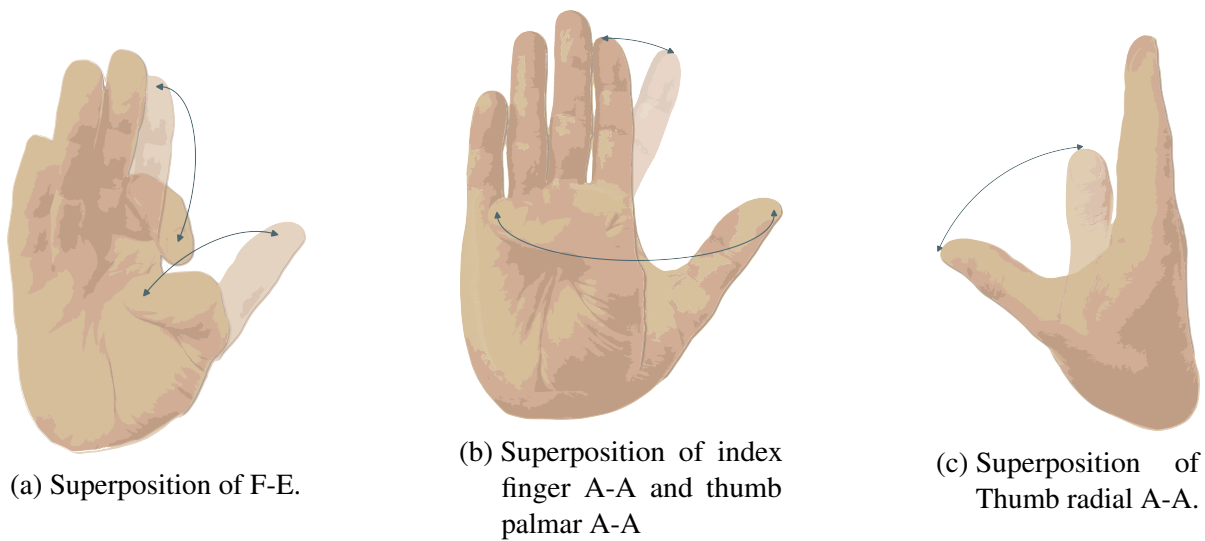


Figure 2.4: Illustration of anthropomorphic hand movements.

(Birglen et al. 2008). The number of independent actuators enables complex movements and thus great dexterity, as illustrated as a brown area in Figure 2.5 (a). However, firstly, a large number of motors occupy substantial space and add weight (Birglen et al. 2008). Furthermore, with each additional motor, the control complexity increases, turning even a simple grasping task into a highly coordinated operation involving many motors.

Joint coupling offers a solution to reduce the number of actuators but simultaneously sacrifices dexterity. A coupling mechanism within a finger interconnects two or more phalanges, enforcing synchronous movement. By reducing the DOA, this approach minimizes occupied space, weight, and control complexity. However, the same reduction in DOA occurs for the DOF, thereby limiting the finger's workspace. Without description of specific mechanisms, the resulting limitation in workspace is illustrated in Figure 2.5 (b): The two-dimensional workspace of a fully-actuated finger is reduced to a one-dimensional path. Additionally, a coupled mechanism restricts adaptability to objects: once one of the interconnected phalanges is blocked, none of the phalanges can continue to move. (Birglen et al. 2008)

Underactuated mechanisms offer an alternative solution to reduce the number of actuators while imposing comparatively fewer restrictions on dexterity (Piazza et al. 2019). An underactuated mechanism (UM) within a finger, similar to a coupled mechanism, interconnects two or more phalanges, creating synchronous movement. However, unlike coupled mechanisms, UMs allow the interconnected phalanges to deviate from synchronous movement. This additional DOF is kinematically constrained by passive elements, such as springs, which must be overcome. Thus, when one phalanx makes contact with an object, the remaining phalanges can continue

to deflect, allowing for passive adaptation to the object (Gosselin 2006). This behavior is illustrated in Figure 2.5 (c), visualizing in three cases how the underactuated finger can make use of the entire workspace, provided the object geometry allows it. Compared to coupled mechanisms, underactuated mechanisms are characterized by a number of DOAs smaller than the number of DOFs, reducing thus only the DOA, compared to a fully actuated design. Summarizing, the application of underactuated and coupled mechanisms introduce a popular trade-off in the design of anthropomorphic robotic hands, balancing simplification and dexterity. On the one hand, the use of those mechanisms allows to reduce DOA, thereby decreasing occupied space, weight, and control complexity. In the particular case of UMs, the passive adaptation to objects is highly valuable for grasping objects of complex or unknown geometry. On the other hand, compared to fully actuated designs, the addressable workspace is limited in the absence of external forces. If high dexterity with independent movements for complex manipulations is required, a reduction of DOA must be carefully evaluated.

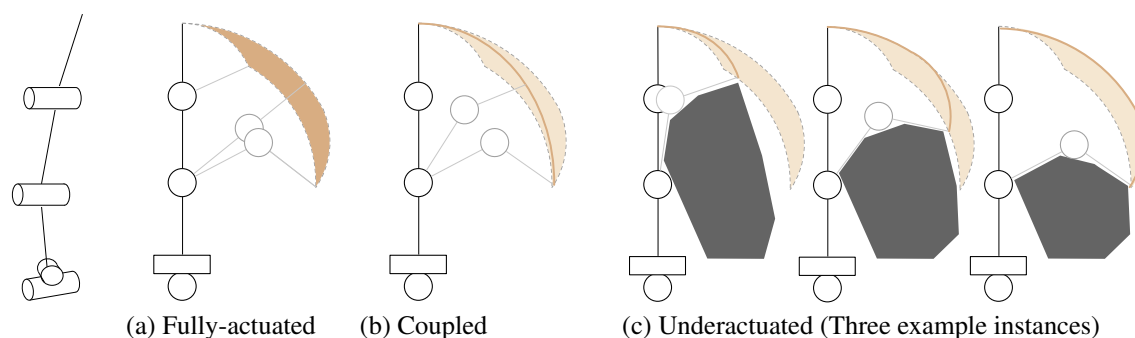


Figure 2.5: Illustration of workspaces for fully actuated, coupled, and underactuated fingers.

2.2.3 Classification and Evaluation of Robot Hand Designs

A classification of robot hands is usually closely linked to its evaluation. Within a given classification, captured robot hands are compared to one another in a specific aspect. For identification of that specific aspect, the robot hand is evaluated against that aspect. The type of evaluation depends on the aspect of interest.

Over the years, robot hand designs have been evaluated against many aspects. Popular evaluation involve the form, feature and performance. An evaluation of the form captures the characteristics of a hand, such as its size, or weight. An evaluation of the features records the equipment of a hand, such as the sensors installed or the actuators used. (Sureshbabu et al. 2019) Other popular choices comprise classification regarding the simplicity, level of anthropomorphism or field of application, where the former evaluates the number of DOF or DOA. These categories are particularly common for comparing robot hands and can be found

in, e.g., the work by Piazza et al. (2019).

In the context of the conceptual design, the evaluation of performance and simplicity is most meaningful. A conceptual design does not feature any applied peripherals (Feature) or provide finite information on the form. However, it lays the foundation for future performance and its associated complexity/simplicity. While the level of simplicity is easy to identify, performance can be measured in different ways. The following presents different performance measures and evaluation methods, limiting the scope to those relevant for the conceptual design.

Performance involves the two actions *grasping* and *manipulation*. Grasping is commonly defined as the secure fixation of an object (e.g. Birglen et al. 2008), whereby slight variations of definition can be found. For example, Bicchi (2000) defines the secure fixation as lack of relative motion between the object and hand, even under external disturbances. Manipulation describes the control of the position and the orientation of an object (e.g. Birglen et al. 2008), and can be further classified into *in-hand manipulation*, *non-grasping manipulation*, and *gesturing*. Sureshbabu et al. (2019) define in-hand manipulation as manipulation within the hand without placing the object down. Non-grasping manipulation involves tasks such as pushing and shoving. A detailed discussion on the concept of manipulation can be found in the work of Mason (2018).

As summarized by Roa and Suárez (2015), the following properties are taken into account for a successful grasp: disturbance resistance, equilibrium, stability and dexterity. The main problems of these properties involve, first, the determination of appropriate contact points on the object, second, the determination and control of proper contact forces, third, the control of restitution forces when the grasp is moved away from equilibrium, and lastly, the determination of the proper hand configuration, respectively (Roa and Suárez 2015).

Therefore, it is reasoned in this dissertation that, for performance evaluation of the conceptual design, solely the geometric ability to reach a given hand configuration is meaningful. The aspects of disturbance resistance, equilibrium and stability can be neglected, as no piece of software is written at the time of the conceptual design and no information on motors or inertia are known for calculation of forces. The same is true for kinematic and dynamic properties of the required hand configuration. The geometric ability to reach a set of required fingertip poses is the result of the fingers' workspaces and how well they are harmonized. To address both aspects, the term of a robot hand's *Motion Ability* (M.A.) is introduced in this work, to establish a more concise reference compared to alternative terminologies, such as the frequently used and ambiguously defined term *dexterity*.

The use of grasp taxonomies has become established for evaluating the Motion Ability Grasp taxonomies define a set of human grasps and are used in physiotherapy and rehabilitation (Feix et al. 2015). Depending on the chosen taxonomy, a certain number of grasps is defined and a robot hand can be evaluated regarding the number of successfully implemented grasps.

The most comprehensive taxonomy to date was established by Feix et al. (2015). In their study, 211 different examples of grasps were identified and used to synthesize 33 grasp types. The 33 grasps are further classified according to other aspects, such as the grip nature (power, precision, intermediate), or the number of fingers involved. A representative set, including one grasp per category, includes 17 grasps and is illustrated in Figure 2.6. It is referred to as the reduced Feix taxonomy in the following. Alternative methods for evaluating the Motion Ability exist

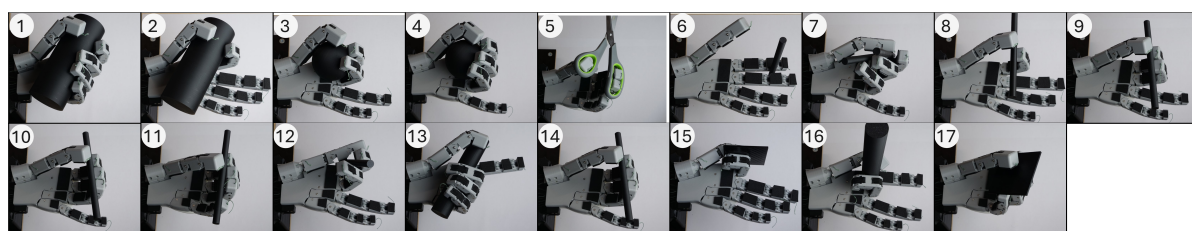


Figure 2.6: Reduced grasp taxonomy by Feix et al. (2015) with illustrations created by the author.

but are less commonly used. The first alternative by Cutkosky (1989) defines 16 grasp types. While Cutkosky's taxonomy is comprehensive, Feix's taxonomy offers a more extensive grasp database. Therefore, a detailed presentation of the Cutkosky taxonomy is omitted here, and reference is instead made to the work of Cutkosky (1989). A second alternative is not a grasp taxonomy but a definition of objects from the work of Calli et al. (2015).

Besides the whole hand's performance, the thumb's Motion Ability is commonly evaluated separately. The Opposition Test from the work of Kapandji (1986) has become an established method for robot hand evaluation, adapted from originally clinical applications. The test procedure is illustrated in Figure 2.7. The thumb tip must touch a total of eleven defined points on the hand. The procedure illustrates that successful execution requires not just adequate thumb range of motion (ROM), but the reconciliation of all fingers' ROM. In summary, roboticists evaluate the performance that results from the conceptual design by assessing the Motion Ability. To evaluate the complete hand, grasps from taxonomies are implemented and assessed using a binary success criterion. The taxonomy proposed by Feix et al. (2015) has become widely adopted for this purpose, with less comprehensive alternatives, such as the taxonomy by Cutkosky (1989). Given the importance of the thumb for overall performance, its Motion Ability is evaluated separately with the test from Kapandji (1986). For a comprehensive list of evaluation methods for other aspects than the Motion Ability, the reader is referred to the thesis from Polzin (2024).

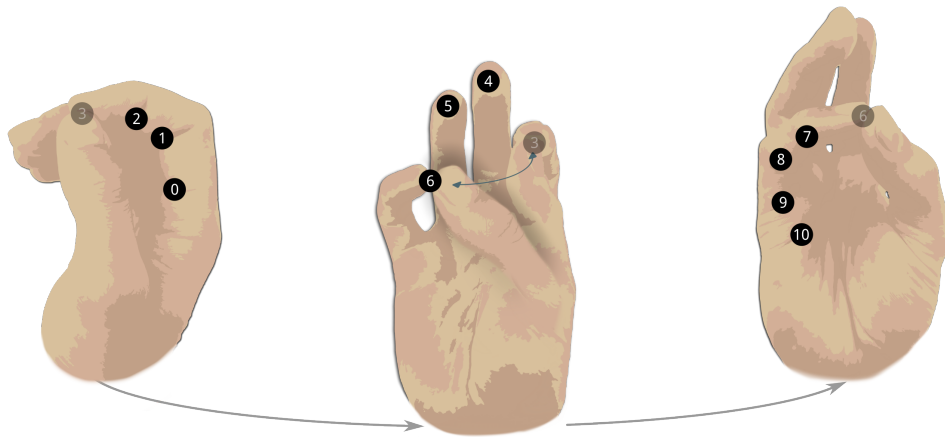


Figure 2.7: Thumb opposition test procedure by Kapandji (1986)

2.3 Current Conceptual Design Process

This chapter serves as a foundation to (1) illustrate the entry barrier claimed in the introduction and (2) clearly position the contribution of this dissertation within the design procedure, providing the basis for distinguishing it from comparable studies in Section 2.4. The presented design procedure aims to demonstrate why novice designers initially need to acquire expertise in a time-consuming manner, why the design process is highly iterative, and consequently, why high entry barriers exist. Additionally, by outlining the conceptual design procedure, this chapter establishes which part of the procedure should be automated, referring to the defined goal of semi-automation in the process.

For this purpose, the state of the art of the conceptual design procedure is presented in the following, referring to the design process in Figure 1.1. The process is introduced in this dissertation due to the lack of alternatives, as it is shown in Section 2.4. The process is derived through analysis of the approaches described in the literature for various robotic hands. As discussed above, the conceptual design phase encompasses four aspects: Joint configuration, joint coordination, joint allocation and evaluation of the derived conceptual design. Generally for this phase, relevant joints and their number of DOFs are identified, the application of coupling and underactuation is defined, the joints are arranged in relation to one another and the derived conceptual design is evaluated and, if necessary, iteratively adjusted and re-evaluated. In the following, further insights are given from the perspective of an expert.

Experienced designers base their choice of relevant joints and the number of degrees of freedom on their own past iterations and results in the literature. Historically, robot hand design has been inspired by the human hand. Depending on the chosen interpretation of the human hand and multiple iterative adaptations of this derived joint configuration, experienced designers

have proposed many different successful robot hand designs. Thus, no single correct robotic hand design can be identified. Therefore, new designers must either go through the extensive process of multiple iterations or study extensive literature on robot hand designs. In both cases, the process is laborious and requires them to acquire knowledge and find relevant information. The same applies to joint coordination. Roboticians work on mechanisms and coordination strategies, often with different goals. While some focus on the development of ingenious mechanisms that allow to implement as few DOA as possible while maintaining as much of the dexterity as possible (e.g. Birglen et al. 2008), others focus on keeping the dexterity of a fully actuated hand as much as possible while reducing the number of DOA (e.g. Grebenstein 2016). Consequently, a substantial body of knowledge exists, presenting various robot hand designs that have all been successfully evaluated. However, the evaluation depends on the designer's goal. Novice designers first need to familiarize themselves with the mechanisms involved, then evaluate or read about different coordination strategies to find many equally viable alternatives. Besides joint configuration and coordination, further information are presented on joint allocation and overall design approaches. The former involves important dimensional parameters. The latter describes how roboticians establish the conceptual design.

2.3.1 Anthropomorphic Dimensions

The information presented in this section are obtained in the systematic study presented in Chapter 3. As such, it should be presented in Chapter 3, as part of the results for the knowledge-parts of the design process. However, it is given here for the sake of describing the claimed entry hurdles for novice designers. The content is previously published in similar form in Gossen et al. (2025b), which was produced in the course of this dissertation.

First, the relevance of anthropomorphic proportions in robot hand designs is briefly reflected. Besides aesthetic goals in prosthetics, robot hand designs could demonstrate the functional importance of anthropomorphic proportions. For example, an earlier iteration of the iCub robot hand by Sureshbabu et al. (2015) with an extended thumb resulted in reduced dexterity and awkward grip postures. Adjusting the thumb to human-like length in a subsequent design iteration improved the performance (Sureshbabu et al. 2015). Other studies, e.g. by Kawasaki et al. (2011), similarly evaluated the importance of anthropomorphic relations for enhanced manipulation. Examples include studies from robot hand design by Kawasaki et al. (2011) or from the medical field. Chalon et al. (2010) describe the surgical procedure *pollicisation*, where a missing thumb is reconstructed using anthropomorphic proportions.

Anthropomorphic dimensions can be obtained by own measurements or from literature. For example, the standard DIN 33402-2 (Deutsches Institut für Normung e.V. 2020) categorized 21 dimensions of the human hand, including finger widths and lengths as well as palm dimensions. Alternatively, the work of Vergara et al. (2018), 99 dimensions were identified in 134 test

subjects. While further works exist, such as the work of Jee et al. (2016), the work of Vergara et al. (2018) presents the most comprehensive collection.

Specifically for the ROM values of the individual joints, a number of studies can be identified². For reasons of clarity, a table with the ROM values proposed in these studies is created and presented in the Appendix A.

For phalanx lengths, further studies discuss the required ratios. The general existence and relevance of phalanx length ratios is discussed in the work of Chalon et al. (2010), identifying consistent ratios across different individuals. For the ratios, the work by van der Hulst et al. (2012) and Peña-Pitarch et al. (2014) define the dependency of phalanx lengths to the total hand length. The lengths of the proximal, medial and distal phalanges are described to be 21.8%, 14.1%, 8.6% of hand length for the index finger, 24.5%, 15.8%, 9.8% for the middle finger, 22.2%, 15.3%, 9.7% for the ring finger, 17.7%, 10.8%, 8.6% for the little finger, and 17.1%, 12.1% for the thumb (van der Hulst et al. 2012). Peña-Pitarch et al. (2014) further describes the metacarpal length of each finger, including 25.1% of hand length for the thumb, 37.4% for the index finger, 37.3% for the middle finger, and 33.6% and 29.5% for the ring and little finger. Besides phalanx lengths and joint ROMs, inclination and twist angles between adjacent joints have been proposed. Grebenstein (2016) discusses the use of inclination and twist angles to optimize grasping performance with compensation of an eliminated thumb's Pronation-Supination DOF. Inclination is the angle between the joint's axis of motion and the vertical position. It allows the fingers to be parallel to each other at rest and to tilt towards the sagittal plane during flexion (Grebenstein et al. 2010). The twist is the deviation of the joint axis around the longitudinal axis. It enables the fingers common vanishing point on the palm during flexion (Kapandji 1987) through an inward rotation of the finger towards the palm (Grebenstein 2016). Grebenstein (2016) experimentally evaluated the impact of inclination and twist angles in the thumb. For four different thumb configurations (no inclination/twist, only twist, only inclination, with both inclination and twist) are used to perform the Kapandji Test and various grasps. The results indicate the dependence of an optimum. For example, without implemented inclination and twist for the Kapandji test, a better reachability of the MCP joints for the Kapandji Test and better fingertip contact for the key grip could be shown. However, with inclination and twist implemented, grasps of large cylindrical objects could be optimized.

On this basis, recommendations for the thumb were made in the work of Grebenstein (2016) that depend on user preference. Generally, the use of inclination and twist angles is recommended for the thumb. If key grasps are dominantly present, an outwards twist is recommended; if grasps of large cylinders are preferred, an inwards twist is recommended. In addition, the

²The interested reader is referred to the works by Becker and Thakor (1988), Hume et al. (1990), El-Shennawy et al. (2001), Cobos et al. (2008), Barakat et al. (2013), Ngeo et al. (2014), Peña-Pitarch et al. (2014), Bain et al. (2015), and K.-S. Lee and Jung (2015)

inclination and twist should be fine-tuned for power grasps of small objects. Recommended value ranges describe 0° - 5° for inclination and 0° - 9° for twist. For the little finger, ring finger and index finger, similar experiments are conducted and recommendations are made. They are identified to be beneficial for power grasps and spherical objects. However, the specific angles need to be fine-tuned, to account for robot hand specific factors, such as thumb positioning, finger lengths and palm dimensions. For fine-tuning the inclination angles, Grebenstein (2016) suggests starting with large inclination angles, to balance finger overlapping and opposition improvement, proceeding from index finger to little finger. Final adjustments should be made on a physical prototype to account for opposition compensation through finger pads. Approximate ranges are recommended to involve $5^{\circ} - 9^{\circ}$ for the little finger, and $10^{\circ} - 14^{\circ}$ for the ring finger. The inclination angle in the middle finger is negligibly small.

For positioning of the TMC, HMC and MCP joints, it can be concluded that no unique values can be identified. In contrast to phalanx lengths, the positioning of base joints could not yet be uniquely defined through ratios. (van der Hulst et al. 2012; Peña-Pitarch et al. 2014) Among other factors, it demonstrates the variance found in humans: As stated by Grebenstein (2016), eight billion working kinematic structures can be found on earth.

For identification of appropriate TMC, HMC and MCP joint positions, different sources have been used. First, measurements of the own hand can be taken to identify the base joint's positions. However, a difficulty lies in the soft tissue displacement that lead to inaccurate results. Second, MRI-based models by van der Smagt and Stillfried (2007)³, or defined standards allow precise localization of joint positions, offering the advantage of avoiding soft tissue displacement during measurements. However, the descriptions are often not intended for direct technical application. Additionally, they are based on 50–100 scans of a single hand, limiting their generalizability. Third, existing dimensions from previous iterations or other robot hands in literature can be used, in rare cases where they are mentioned in publication.

For example, the second has been applied to various robot hand designs, including the Kinematic Humanoid Hand (Kawasaki et al. 2004), the EthoHand (Konnaris et al. 2016), the ACT Hand (Deshpande et al. 2013), or the HBA Hand (Xu and Todorov 2016). Further information in form of examples for the others and more detailed descriptions can be found in the associated publication (Gossen et al. 2025b).

2.3.2 Approaches

In this section, the approaches to go through the steps of the conceptual design process are presented. In the preceding section, it is detailed how designers find relevant information for the individual knowledge-parts of the conceptual design process. However, in this section, it is

³The reader is also referred to the subsequent works from the years 2009; 2010; 2014.

presented how the information are applied and the evaluation is performed.

Generally, the robot hand's performance is evaluated. As described in Section 2.2.3, the Motion Ability is evaluated. Commonly, a grasp taxonomy, such as the one by Feix et al. (2015), is implemented for binary evaluation of success.

The most common approach to perform a grasp taxonomy is a prototypical implementation. The gathered information regarding joint configuration, coordination and allocation is implemented in form of a prototype and experimentally evaluated. The use of simulation is an obvious choice but presents significant challenges for novice designers. It involves considerable effort in modeling contact conditions to extract meaningful insights from the simulation. Furthermore, assessing whether an object has been successfully grasped based solely on simulation is difficult. Without a background in grasp kinematics, it is not intuitive to decide when a kinematic successfully performed a grasp and therefore unsuitable for beginners.

An alternative to a fully implemented prototype is presented in the work of Grebenstein (2016), utilizing cardboard models. The method is based on the idea that even an untrained observer can determine whether a kinematic structure appears human-like. A cardboard model of a hand is cut out, where joints are simulated by folds at the corresponding positions. With the cardboard replica, the grasps from the Feix taxonomy are performed, allowing to assess the "naturalness" of the appearance. According to the proposed philosophy, if the appearance seems natural, the kinematic is considered human-like and therefore successful. The advantage of this approach is that it allows for quick iteration of joint positions and arrangements with minimal effort, without requiring specialized expertise.

In case of unsuccessful evaluation, the conceptual design needs to be adjusted. Commonly, the chosen joint configuration and coordination remains untouched, unless major flaws are apparent. The same is true for the joint allocation within fingers: the defined ratios provide a robust basis and do not need to be adjusted. However, the applied inclination and twist angles, as well as base joint positions are subject to optimization during evaluation.

Alternative approaches for identification of base joint positions can be found in literature. The approaches vary from guidance to practical instruction. For TMC joint positioning, approaches can be found in works from Kawasaki et al. (2002a), Kawasaki et al. (2002a), Kawasaki et al. (2011), H. Wang et al. (2017a), H. Wang et al. (2012), Peerdeman et al. (2014), and Savić et al. (2016). Detailed presentations are given in the associated publication (Gossen et al. 2025b). It is omitted here for the sake of conciseness: the goal of this section is to demonstrate that, first, no unique solution can be found; second, the optimization is often performed experimentally and iteratively; and third, many different practical approaches exist. The pure reference to the aforementioned works serves to illustrate the difficulty a novice designer has when navigating the vast body of existing literature.

2.4 Related Work

This dissertation identifies related works in relation to its objectives. The aim is to develop guidance for designers through a semi-automated design method in the form of a knowledge-based assistance system. Therefore, two directions are used to identify such works. Firstly, works that contribute to the creation of a knowledge base are identified in order to evaluate whether such a base exists. Secondly, the literature is searched for design methods. The identified options are then compared with regard to the objectives of this dissertation.

2.4.1 Knowledge Bases

Review papers are analyzed to identify existing knowledge bases. This procedure is based on the assumption that the creation of a knowledge base involves extensive research. Most likely, those results are presented in the form of a review.

Therefore, the focus of the analyses is on holistic review papers. These are review papers that evaluate the hand as a whole, rather than focusing on individual parts such as the fingers or thumb. The aim is to eliminate from the beginning a large number of works that only deal with individual parts and do not fit the objectives of this dissertation. The collection of holistic review paper has been previously published in Gossen et al. (2025b). The text and figures have been reused with permission from the publisher. All figures originating from that publication are marked with a dagger symbol (†) in their captions.

To comply with the PRISMA guideline, the following documents the search strategy used for the identification of holistic review papers. By May 2023, the first ten pages of Google Scholar using the keywords "robotic hands" OR "anthropomorphic gripper" AND "review" OR "overview" are assessed, yielding 213 studies. To limit the scope, reviews were excluded if they are published before 2000 (16 studies), are not freely accessible through RWTH Aachen University or do not investigate holistically robot hands. For the latter, this comprises studies on single aspects (e.g., sensors), single fields of application (e.g., agriculture) or non-anthropomorphic designs. Finally, 15 studies are identified and listed in Table 2.1.

The captured holistic review papers are examined in terms of two aspects: the objective and the outcome. Firstly, it is evaluated whether the objective of the study is the structured organization of mechanical design approaches as PSs in MBs. This would enable the information to be used for the purposes of this dissertation. Secondly, it is evaluated whether the studies create a database. If so, the suitability of the database for the objectives of this dissertation is evaluated. Regarding the first aspect, while the collected reviews offer comprehensive and valuable overviews, none share the same objective as this dissertation, as summarized in Table 2.1. The reviews predominantly focus on robot-hand-specific discussions, such as identifying trends, performing comparisons, or evaluating grasping performance. None identify overall valid,

| Reference | Objective | Database |
|------------------------------|-----------|----------|
| Biagiotti et al. (2004) | × | × |
| Martell and Gini (2007) | × | × |
| Nazma and Mohd (2012) | × | × |
| Belter et al. (2013) | × | × |
| Gama Melo et al. (2014) | × | × |
| Melchiorri and Kaneko (2016) | × | × |
| Ten Kate et al. (2017) | × | × |
| Piazza et al. (2019) | × | ✓ |
| Difonzo et al. (2020) | × | × |
| Vertongen et al. (2020) | × | × |
| Mendez et al. (2021) | × | × |
| Mansoor et al. (2023) | × | × |
| Parveen et al. (2023) | × | × |

Table 2.1: Collected holistic review papers, evaluated for alignment with this dissertation’s objective and the development of a database (✓: fulfilled, ×: not fulfilled) †.

robot-hand-unspecific principal design solutions, with references to specific robot hands.

It should be noted that some studies, such as the work by Piazza et al. (2019), present summaries on joint design that could be considered principal solutions. However, firstly, the results are not structured as such, secondly, this is not the overall goal of the study, and lastly, PSs are not derived for other aspects.

Regarding the second aspect, only a single study presents a database as the outcome of the review. In the review by Piazza et al. (2019), a databases can be downloaded in a pdf format. It contains a large collection of robot hands with information on their DOFs and DOAs or number of fingers, among others. According to the derivation in Section 2.2.3, this refers to classifications regarding form, feature and simplicity. However, no database is presented for the objectives of this dissertation using design PSs (which would allow a classification of robot hands regarding their design).

2.4.2 Design Methods

Existing design methods are identified and analyzed regarding the objectives of this dissertation. The analysis evaluates whether methods (1) consider robotic hands holistically, (2) address the conceptual design, (3) allow the user to modify the output according to the needs and (4) provide solutions from literature. The first aims to classify all those methods that focus on individual parts of a robot hands instead of the holistic structure. The second aims to identify if the method addresses the aspects of joint configuration, coordination and allocation in a holistic robot hand design. The third aims to identify if the method generates a user-specific design, taking task-requirements into account. The last aims to identify if the method is providing

solutions from literature and can thus be considered guidance, rather than creating a unique solution based on a defined metric, without supporting literature references.

The following search strategy is applied for the identification of design methods. A Google Scholar search is conducted, using keywords "design" AND "method" OR "methodology" AND "anthropomorphic robotic hand" OR "robotic hand", limiting the results to the first ten pages. The results are illustrated in Table 2.2. Studies that are focused on non-anthropomorphic grippers are excluded from the results.

The first group of identified studies comprise design methods that do not address robot hands

| Reference | Holistic | Concept. Design | User- Centric | References |
|-------------------------------|----------|--------------------|------------------|------------|
| Chalon et al. (2010) | × | × | × | × |
| Ciocarlie and Allen (2010) | × | × | × | × |
| Sardo et al. (2006) | × | × | × | × |
| Le et al. (2016) | × | × | × | × |
| Chew et al. (1991) | ✓ | × | × | × |
| Hassanzadeh et al. (2016) | ✓ | × | × | × |
| You, Y. Lee, et al. (2019) | ✓ | × | × | × |
| Hazard et al. (2020) | ✓ | × | ✓ | × |
| Martell and Giuseppina (2007) | ✓ | × | ✓ | × |
| Tian et al. (2020) | ✓ | (✓) | × | × |
| Puig et al. (2008a) | ✓ | × | × | × |

Table 2.2: Design Methods for anthropomorphic robot hands, evaluated on four criteria (✓: fulfilled, ×: not fulfilled, (✓): partly fulfilled).

holistically. In Table 2.2, a non-exhaustive list of representative examples are given in the first four rows. The examples include the work by Chalon et al. (2010) and Ciocarlie and Allen (2010) for thumb design, the work by Sardo et al. (2006) for fingertip design and the work by Le et al. (2016) for robot hand skin design. In general, none of these works align with the objectives of this study, as they only address sub-parts of the robot hand and not the whole hand. Besides, no work could be identified that recommends a (sub-)design based on user specification and uses literature references for the output, to comply with the guidance objective.

The second group of identified studies comprise design methods that address the kinematic structure of robot hands. Significant examples are given in the subsequent four rows in Table 2.2, comprising the works by Chew et al. (1991), Hassanzadeh et al. (2016), You, Y. Lee, et al. (2019), and Hazard et al. (2020). The found studies consider the robot hand holistically by investigating its overall kinematic structure. However, none of the works addresses completely the conceptual design, focussing solely on the joint configuration and allocation. Besides, only the work by Hazard et al. (2020) offers an automated user-centric design. In their study, the

generated kinematic structure is based on specified manipulation tasks. However, the method leverages a derived metric and does thus not refer to (alternative) solutions found in literature. The last group of identified studies comprises design methods for automated robot hand design. This group comprises three works which are given in more detail in the following.

The work by Martell and Giuseppina (2007) presents a method for identifying suitable actuators and sensors for a given robot hand design. In their study, the authors derive a unique robot hand joint configuration and allocation for a set of frequent grasps using the dimensions of the designer's hand. This virtual model is then used to generate requirements for sensors and actuators based on the user-specified task requirements. This study thus partly complies with the objectives of this dissertation: While considering robot hands holistically and user input for output generation, the task-based design focuses on actuator and sensor requirements rather than the conceptual design. Furthermore, it does not refer to solutions in the literature, but rather generates suitable solutions itself.

The work by Tian et al. (2020) presents a method for automated generation of a robot hand design. The developed framework uses a 3D scan of a human hand to generate a fully 3D-printable robot hand design, including joint configuration, coordination and allocation. While considering the robot hand holistically and allowing the user to adjust the solution to some extent, the method does not comply with the overall objectives of this dissertation. First, the conceptual design can not be modified but is automatically created once. Therefore, in Table 2.2, this aspect is evaluated to be only partly fulfilled. Further, besides the dimensions given through the 3D scan, the user can not adapt the design based on task requirements. Lastly, the method does not refer to solutions in the literature, but rather generates suitable solutions itself. The work by Puig et al. (2008a) presents a design process plan for multi-fingered robot hands. To the best of the author's knowledge, it is the only existing process diagram. As stated in the study, the process plan is derived from the authors' experience over many years of robot hand design. It addresses the complete robot hand design, covering steps for the preliminary and for the detailed design. This study thus partly complies with the objectives of this dissertation, as it considers the robot hand holistically and offers some form of guidance for designers. However, the study does not comply with the objectives of this dissertation. The conceptual design is addressed by a single step, called "Analyze Human Hand", which, firstly, does not provide sufficient guidance for a designer in form of recommendation or instructions, and hence, can not process user-requirements. Lastly, no literature references are given for the individual steps of the process plan.

In conclusion, after analyzing the state of the art, no related work was found that complies with the objectives of this study. Firstly, no database presenting principle solutions for the conceptual design of robot hands was found. Secondly, no design method could be identified that (semi-)automates the conceptual design process according to the objectives of this dissertation.

Comparable design methods either do not consider the design of robot hands holistically, do not focus on conceptual design, or do not allow user-centered modification. None of the design methods found refer to existing solutions in the literature, but rather generate new solutions.

2.5 Conclusion

Based on the preceding three sections, conclusions can be drawn for this dissertation. These conclusions are presented below, following the chapter structure of fundamentals, state of the art, and related work.

Based on Section 2.1, the remainder of this dissertation is organized around the two core components of a knowledge-based system: a knowledge base (Chapter 3) and a control system (Chapter 5). Chapter 4 defines the decision logic by which the control system exploits that knowledge.

From the robot hand fundamentals in Section 2.2, this dissertation defines user requirements (see Objective (O2)) for the conceptual design as grasping tasks, using the taxonomy by Feix et al. (2015) for specification. The required Motion Ability is thus dependent on the specified tasks. Consequently, there is no overall valid configuration of joints, their DOF and their coordination, but a most optimal solution based on the user requirements.

From elaborations in Section 2.3, three relevant aspects can be identified. First, the elaborations demonstrate the high entry hurdles claimed in the Introduction. Second, the scope of the joint allocation merits merit its own dissertation. And third, the elaborations highlight how experienced designers could equally benefit from the proposed guidance.

Regarding the second point, the ambiguity of the joint allocation is presented. It is shown that, to date, no unique set of dimensional parameters could be derived for an anthropomorphic robot hand. Consequently, an evaluation is frequently used for iterative fine-tuning before the design is validated. Based on this finding, it is concluded that no task-dependent joint allocation is derived in this dissertation, as this would exceed the scope. Instead, for the guidance, the user is referred to a single set of working dimensional parameters.

Regarding the third point, experienced designers could use the guidance to be referred to better solutions. Although they know the design process, fine-tuning dimensional parameters can still yield only a local optimum: The applied performance evaluation is binary, leaving the question open as to whether alternative kinematics with fewer DOFs or DOAs exist. By considering existing expert knowledge, designers might learn about other successfully evaluated designs with less DOF or DOA.

The discussion in Section 2.4 reveals that no prior study shares the objectives of this dissertation. To the best of the author's knowledge, neither a database suited to these objectives nor a design method with equivalent aims exist.

3 Guidance Knowledge Base

To answer the research question, this chapter deals with the first objective (O1). The chapter begins with a problem description in section 3.1, followed by the development of the knowledge base with literature-linked knowledge on joint configuration and coordination of tendon-driven rigid-sequential anthropomorphic robot hands in Section 3.3. For the systematic generation of conceptual designs, the anthropomorphic reference model is defined in Section 3.2, which is combined to the derived knowledge base in Section 3.4.

3.1 Problem Statement and Approach

The problem for defining the knowledge base can be summarized in two questions:

- (Q1) How to capture knowledge about the mechanical design for the comprehensive and diverse field of study, allowing systematic generation of conceptual design solutions and association of relevant literature sources?
- (Q2) How to design the knowledge base development to be user-friendly and scalable?

Regarding (Q1), the design of anthropomorphic robot hands is characterized by a wide range of currently incomparable different designs. Although numerous individual solutions and design approaches have been proposed in the literature, this knowledge is tailored to specific applications. Furthermore, the knowledge is not centrally structured. This lack of norms makes it difficult to systematically compare, combine and reuse existing design knowledge. As described in Section 2.2.3, current approaches to comparing robotic hands use form, features, performance or simplicity. To date, no existing approaches allow the classification of robot hands according to their design.

Question (Q2) refers to the scope in setting up the knowledge base. It must be ensured that the setup is feasible for the Knowledge Engineer and scales, to enable easy inclusion of future information or modifications. For instance, capturing knowledge about the mechanical design in form of complete robot hand designs would not be appropriate: Considering a single finger alone, the number of possible joint configurations and joint coordinations and their combinations are large. Considering further multiple fingers and allowing differences among them¹ results in a unfeasible number of options for such classification.

¹Differences among fingers regarding their joint configuration and/or coordination is common and an important tool for reducing mechanical complexity.

Above questions motivate the derivation of a novel methodology, as it is introduced in Section 1.2. Capturing design knowledge in MBs allows to address (Q1). Knowledge is abstractly captured in FoIs and PSs, as illustrated in Figure 3.1. With a uniquely defined joint configuration, any robot hand design from the literature can be represented by a unique combination of that joint configuration and certain PSs. It allows thus to, first, capture knowledge abstractly, second, refer to the original sources where the approaches have been found, and last, generate any conceptual design. As a single PS relates to multiple robot hand designs, ambiguity is avoided, and thus, (Q2) is addressed.

The chapter is thus structured as follows. First, the IMDC is derived in Section 3.2. Second, the PSs are captured through a systematic mapping of existing knowledge of mechanical design in Section 3.3. To ensure thoroughness, the PRISMA guideline (Page et al. 2021) is followed in the systematic mapping. Third, the automated combination of PSs for definition of robot hand conceptual designs is presented in Section 3.4.

| Morphological Box | | | |
|-------------------|------|------|------|
| FoI | PS 1 | PS 2 | PS 3 |
| | | | |
| | | | |
| | | | |

Figure 3.1: Illustration of the proposed morphological box structure.

3.2 Anthropomorphic Reference Model

For the anthropomorphic reference model, the IMDC is identified. The IMDC needs to be a standard that allows to identify any robot hand (conceptual) design from literature through reducing that standard's DOF or DOA. For identification, a two-step analysis is performed. First, an upper bound joint configuration is determined by analyzing human hand joint configuration studies. Second, the literature is reviewed to determine which of the upper bound joint configuration's DOFs have been implemented in current successful robot hands. All joints that have been used at least once are considered for the IMDC. This section is based on the author's previously published work (Gossen et al. 2025a). Text and figures are reused with permission from the publisher and marked here with a double dagger (‡) (©2011 IEEE).

3.2.1 Human Hand Analysis

For analysis, the anthropomorphic joint types and their DOFs are recorded from studies that analyzed the human hand and are presented in Table 3.1. Various specialist books (Duruoz

2014; Kapandji 2007; Marieb and Hoehn 2007; Zimmer and Appell 2021a; Woo 2019) and other scientific works serve as sources of information. In Table 3.1, the IP, DIP and PIP joints are not given, as they are uniformly understood as hinge joints with a single DOF. Only the TMC, HMC and MCP joints are listed, as there is a particular discrepancy in the literature. These joints are discordantly identified to be either saddle, condyloid, ellipsoid, ball-joints, or amphiarthroses. The latter describes a joint that is severely restricted in its movement by ligaments and tendons. Regarding the associated DOFs, a clear discrepancy is evident in the literature. Two joints of the same type may have different numbers of DOFs. Often, if fewer DOFs are assumed, the joint is argued to be strongly constrained by ligaments and tendons (Zilles and Tillmann 2010). If more DOFs are assumed, the joint is considered to have elasticity and clearance. For example, the saddle joint is defined as having two rotational DOFs about the transverse axes. However, a third passive rotational DOF about the longitudinal axis is occasionally attributed to this joint type (Woo 2019). Notably, two studies suggest that the HMC joint is only relevant for the little and ring fingers, due to the greater restriction in the other fingers (Van Der Hulst et al. 2012; Peña-Pitarch et al. 2012).

In summary, the analysis of the human hand results in a range of configurations. The range is illustrated in Fig. 3.2 with a lower bound joint configuration on the left and the upper bound joint configuration on the right. The upper bound joint configuration includes 33 DOFs, while the lower bound joint configuration includes only 20. The main difference between the two configurations lies in the thumb kinematic structure, the number of DOFs in the fingers' MCP joints, and the general consideration of HMC joints. The large interval clearly demonstrates the disagreement and lack of unambiguous definition.

| | TMC | | Thumb MCP | | HMC | | Finger MCP | |
|-----------------------------|-------|-----|-----------|-----|---------|-----|------------|-----|
| | Type | DOF | Type | DOF | Type | DOF | Type | DOF |
| Duruoz (2014) | Sadle | 2 | Ellip. | 2 | Sadle | 1 | Ellip. | 2 |
| Kapandji (2007) | Sadle | 2 | | 3 | ** | ** | Cond. | 2 |
| Zimmer and Appell (2021a) | Sadle | 2 | Ball | 3 | A.-Thr. | 0 | Ball | 3 |
| Woo (2019) | Sadle | 3 | Cond. | 3 | ** | ** | ** | ** |
| Van Der Hulst et al. (2012) | Sadle | 2 | Cond. | 3 | ** | 1* | Cond. | 3 |
| Peña-Pitarch et al. (2012) | ** | 2 | ** | 2 | ** | 2* | ** | 2 |
| Zilles and Tillmann (2010) | Sadle | 3 | Cond. | 1 | A.-Thr. | 0 | Ball | 2 |

Table 3.1: Human hand joint type and DOF analysis ("*": DOF only in little and ring finger; "***": unclear or missing information) ‡, ©2011 IEEE.

3.2.2 Successful Robot Hands

Current successful robot hands (SRHs) are identified in this dissertation to verify the upper bound joint configuration's DOFs. Robot hands are considered successful if they pass the

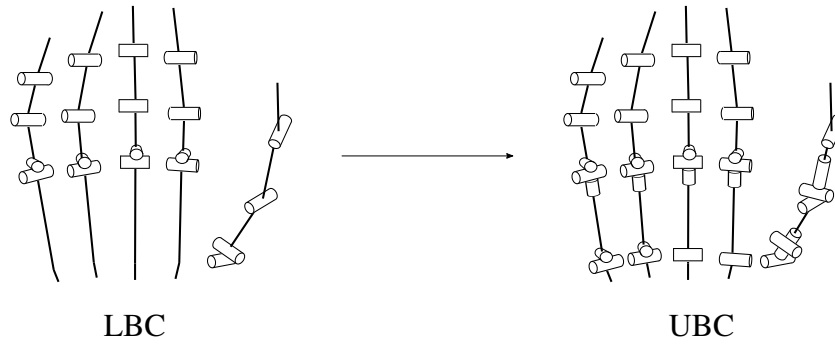


Figure 3.2: Human hand analysis resulting range of joint configurations ‡, ©2011 IEEE.

Kapandji test and either the Feix or Cutkosky taxonomy.

For identification, a search is conducted. On *Google Scholar*, the keywords "robotic hand" AND "Kapandji" AND "Feix" OR "Cutkosky" yielded 16 hands on the first ten pages that used these tests. Four of these hands have no rigid-sequential design and are thus neglected. The remaining twelve evaluated robot hands are presented in Table 3.2 with their names and test performances.

The SRH are identified among the evaluated robot hands. Six of the evaluated robot hands

| | Kapandji (11) | Feix (33) | Cutkosky (16) |
|--|--------------------------|----------------------|--------------------------|
| 3D-Printed Soft Robotic Hand (Shorthose et al. 2022) | 11 | 32 | - |
| Soft-Rigid H.S. (C. Zhang et al. 2023) | 7 | 32 | - |
| BCL-26 Hand (J. Zhou et al. 2019) | 11 | 33 | - |
| MCR-Hand II (H. Yang et al. 2021b) | 11 | - | 16 |
| ISR Alpha Hand (Farinha and Lima 2016) | 9 | 41/49 (33+16)* | - |
| TSA Gripper (Konda et al. 2022) | 6 | 31 | - |
| Gesture Based Robotic Hand (Tian et al. 2021) | 11 | 33 | - |
| ACB Hand (Tasi et al. 2019) | 11 | 33 | - |
| X-Hand (Xiong et al. 2016) | 8 | 30 | - |
| X-Hand III (Chu et al. 2024) | 9 | 30 | - |
| MSRH Hand (P. Lee et al. 2023) | 11 | 33 | - |
| Awiji Hand (Grebenstein 2016) | 11 | 33 | 16 |

Table 3.2: Kapandji, Feix, and Cutkosky evaluations of robotic hands (*no distinction made). Names in beige meet the scoring criteria ‡, ©2011 IEEE.

passed successfully all eleven Kapandji poses and all 33 grasps of Feix's taxonomy or all 16 grasps from Cutkosky's taxonomy. They are highlighted in beige in Table 3.2.

The joint configurations of evaluated robot hands are illustrated in Fig. 3.3 for easier comparison. Each robot hand is a distinct color assigned and the kinematic structure is illustrated by a series of connected dots. Each dot represent a certain joint, with the name given on the vertical axis

and its DOF on the horizontal axis. Further, the total DOFs of each evaluated robot hand are displayed on the right side, noting that the actual applied DOFs may be lower, as only implemented joints are considered, excluding underactuation.

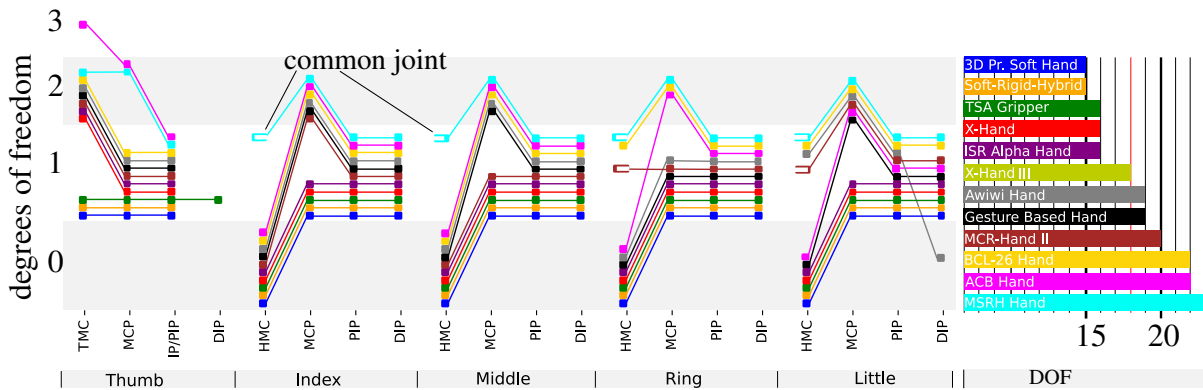


Figure 3.3: Joint configurations and DOFs of qualitatively evaluated robot hands ‡, ©2011 IEEE.

3.2.3 Initial Maximum DOF Configuration

The illustration of the evaluated robot hands in Figure 3.2 facilitates the identification of the IMDC. The identification of the IMDC results from the comparison of the upper bound joint configuration with the SRH. Using Figure 3.2, the maximum applied DOF per joint can easily be identified by evaluating the figure row by row. E.g. the only joint that has been identified to feature three DOF in SRHs is the TMC joint. Thus, all other joints of the upper bound joint configuration with three DOF can be reduced by one DOF (e.g. MCP joints).

The resulting IMDC is illustrated in Figure 3.4. It features a total of 24 DOFs, with one DOF attributed to each IP joint (P-IP, D-IP), two DOFs to each MCP joint, three DOFs to the TMC joint, and one DOF to the little and ring finger HMC joints, respectively. With regard to the programming implementation, the interested reader is referred to Appendix H.1 for the detailed implementation. The data file is structured as a dictionary, where each entry represents a joint identified by a set of parameters. The parameters are used later in this thesis for illustration purposes only.

On a minor note, the identified SRH configurations illustrate well the lack of a clear definition for necessary DOFs for successful grasping. Analyzing the kinematic chains of the six hands shows that no definitive conclusions can be made about the required DOFs. Two minimal configurations with 19 DOFs are identified in the Gesture-Based Hand (Tian et al. 2021) and the Awiwi Hand (Greibenstein 2016), which differ as well. Thus, there is no unique "minimum configuration". The remaining four designs have more DOFs, often due to HMC joints or different thumb configurations. However, this information alone does not imply that these four

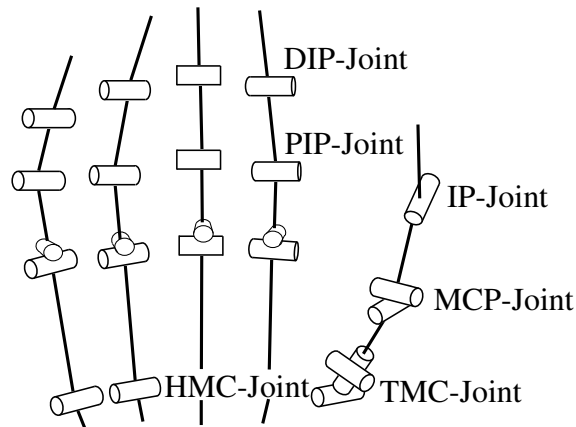


Figure 3.4: Initial Maximum DOF Configuration with 24 DOFs ‡, ©2011 IEEE.

hands have unnecessary DOFs: As the applied tests are of qualitative nature, it is not possible to simply conclude on their lack of relevance. Instead, it must be assumed that a quantitative trade-off is present between simplicity and Motion Ability, as illustrated in Figure 3.5. In

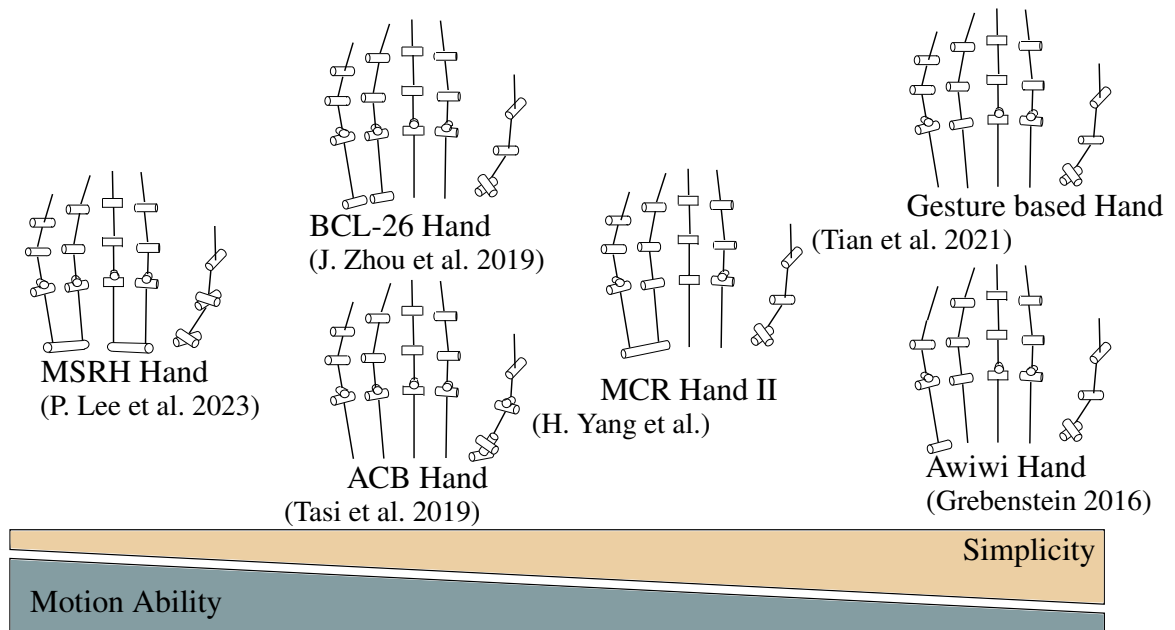


Figure 3.5: SRH joint configurations trade-off.

addition to identifying the IMDC, notable observations about the kinematic structure of SRHs are made. Fig. 3.6 illustrates all unsuccessful evaluated robot hands configurations on the three right, and a successful hand with minimum DOF on the left. A key difference for the grasping performance appears to be the presence of A-A DOFs in the finger's MCP joints, which is applied in all SRHs. Thereby, additionally, three of the six SRHs do not use the A-A DOF for the ring finger. Besides differences, a 2-1-1 thumb configuration is not only found in

unsuccessful hands, but also in four of the six SRHs.

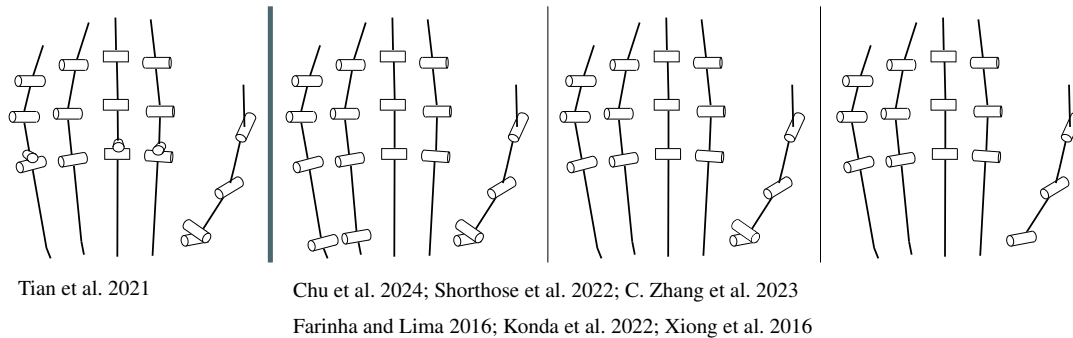


Figure 3.6: Kinematic structure comparison of all unsuccessful (right hand side) and a single successful robot hand with minimal DOF (left hand side) ‡, ©2011 IEEE.

3.3 Fols and PSs

In this section, the FoIs and PSs for the joint configuration and coordination found in robot hand designs in literature are derived. The gathered information are the result of a systematic mapping, following the PRISMA guideline (Page et al. 2021). The methodology and results in this section are based on the author's previously published work (Gossen et al. 2025b). Text, figures and tables are reused with permission from the publisher and marked here with a dagger (†). Interested readers are referred to the publication, where all results are presented as the *Library of Approaches* (LoA) with more references and examples. The LoA can further be found online in a publicly launched graphical user interface (GUI) under the link "<https://loa.igmr.rwth-aachen.de>" or by scanning the QR-code in Figure 3.7.

The methodology is applied as follows. Literature is systematically collected, to adequately



Figure 3.7: QR code for the publicly launched LoA.

represent the existing knowledge in a manageable set. In a second step, the gathered knowledge is used to synthesize FoIs and PSs as the summary of the found content as the smallest demoninator. These FoIs and PSs are then assigned to MBs. All MBs together form the LoA. Further, the captured information are organized using Entity–Relation modeling to assign

literature references to the PSs, to enable automated processing of the PSs, and to reduce ambiguity and enable retrospective information integration.

The section is structured as follows. First, the methodology is described, including the applied data structure (Section 3.3.1), naming convention (Section 3.3.2), and review systematic (Section 3.3.3). Subsequently, the synthesized FoIs and PSs are presented in Section 3.3.4. For improved readability, the identified FoIs and PSs are categorized and separately presented in FoI categories (FoI-C) *Joint Configuration* and *Joint Coordination*, analogously to the design flowchart in Figure 1.1.

3.3.1 Data Structure

The goal of the structure is to enable a concise presentation of existing approaches for the mechanical design of anthropomorphic robot hands and to allow differentiation between them. Therefore, a structuring into MBs was chosen. The FoIs abstractly capture the research or application objectives. For a given FoI, PSs are identified that describe how these objectives can be realized. The PSs are also high-level and generic, not tied to specific design solutions. Specific design solutions can be found in the relevant literature linked to a particular PS.

The structuring process is illustrated in Figure 3.8. At the top of the figure are the collected papers that provide the information that is structured. The systematic way in which this information has been collected is presented in section 3.3.3. Relevant information from a paper is then either used to create a FoI and PS, or assigned to an already established FoI and PS, as shown in the center of the figure as highlighted cards. Thereby, multiple works can contribute to the creation of a certain FoI, while being attributed to distinct PSs (illustrated in brown and blue in the figure). Finally, the established FoIs and PSs are assigned to the relevant MBs, as shown at the bottom of the figure. The variables in Figure 3.8 are introduced in Section 3.3.2 and given prior for the sake of conciseness. Further, it is noted that the studies related to the covering have been collected for the original study of the LoA but are not presented in this dissertation, as they do not contribute to the conceptual design.

Eight MBs have been created to promote concise links to relevant literature. One morphological box represents one Group, containing multiple FoIs and PSs. A Group is created for every major component of an anthropomorphic robot hand: "Thumb", "Index Finger", "Middle Finger", "Ring Finger", "Little Finger", "Covering", "Transmission" and "Kinematic Base Chain" (KBC). The KBC contains important aspects of global connection of the individual components. The fingers receive individual groups to enable the automated processing of the LoA. The Covering Group is neglected in this dissertation.

FoIs are subject to defined rules. Generally, the naming of FoIs and PSs is kept generic and does not directly refer to a specific design. Instead, references to the literature are used for this purpose. A FoI refers to any design field of interest that roboticists address with specific

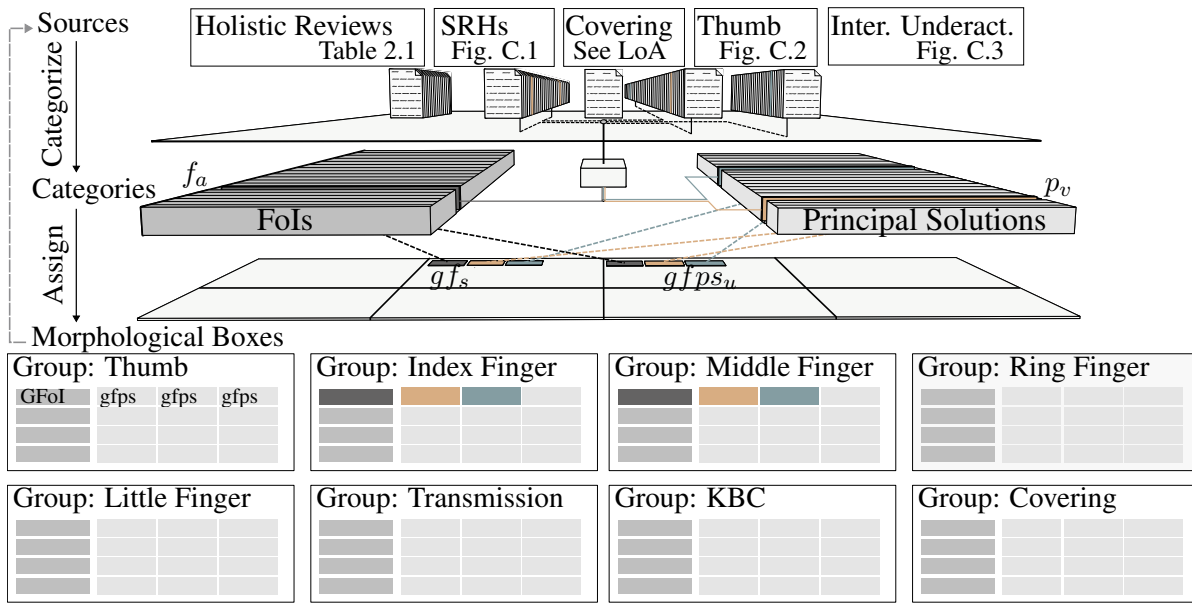


Figure 3.8: Illustration of the applied systematic mapping process †.

approaches. However, to ensure applicability, several constraints must be met. First, the name must be formulated as an action title and contain a gerund-form verb to express the core activity or outcome (e.g. eliminating). Second, the action must be clearly associated with a specific joint or group of joints in the IMDC. Finally, the compatibility of FoIs must be explicitly definable, meaning that for any two FoIs, it must be possible to determine whether they are compatible (i.e. can be applied simultaneously) or mutually exclusive.

PSs are defined by similar rules. Similar to FoIs, each PS must be formulated as an action title with a gerund-form verb and must reference a specific joint or group of joints. However, in contrast to FoIs, the terminology of PSs conveys how the corresponding FoI action is to be implemented. Furthermore, the PSs associated with a given FoI represent alternative solutions, i.e. form an OR-relation, and only one PS per FoI may be applied at a time.

The compatibility requirement for FoIs necessitated multiple iterations during their definition in this dissertation. In several cases, design approaches from the literature were successfully captured as FoIs, along with their corresponding PSs representing OR alternatives within each FoI. However, it was observed that while two FoIs themselves were incompatible by definition, some of their respective PSs were, in fact, compatible. Those observations led to an iterative refinement of the FoI definitions: instead of broad or overlapping formulations, FoIs were incrementally decomposed to ensure well-defined OR-solution spaces both within individual FoIs and between compatible FoIs. This rule is thus of utmost importance to enable the automated use of identified FoIs and PSs for the intended framework.

3.3.2 Notation

Entity–Relation modeling was used for organizing the FoIs and PSs, avoiding redundancy and linking additional information. An Entity–Relation model illustrates how individual data elements are related. It does not describe any process and therefore has no reading direction. An illustration of the modeled data structure is given in Figure B.2 in the appendix. Eight entities are established, including literature sources, robot hand names and author names, besides the Groups, FoIs and PSs. From a programming perspective, an entity is a stand-alone data file. Within an entity, information is captured as an instance with a unique identifier. For example this allows to assign a certain PS (instance) of that entity to multiple MBs (~Groups) (illustrated in Figure 3.8) and thus avoid redundancy in the classification of mechanical design approaches. Those assignments, once again, receive a unique identifier in a proper entity *GFPS*. Furthermore, the modeling allows any amount of information to be added to an instance of an entity. Generally, Entity–Relation modeling simplifies any subsequent modification of terminology or the retrospective inclusion of further instances, such as PSs.

Further, for the introduced entities FoI, PS and their assignments, the respective mathematical representations are introduced for clear future reference. These and further entities are defined throughout this dissertation as mathematical sets, where subscripts are used solely for ease of reference and do not imply any ordering of the set. The elements of the set are textual labels and not numerical values.

The set of identified FoIs is described by

$$F = \{f_1, f_2, \dots, f_a, \dots, f_{m_F}\}, \quad (3.1)$$

whereby m_F is the total number of identified FoIs and $a \in \{1, \dots, m_F\}$.

The set of identified PSs is described by

$$P = \{p_1, p_2, \dots, p_v, \dots, p_{m_P}\}, \quad (3.2)$$

whereby m_P is the total number of identified PSs and $v \in \{1, \dots, m_P\}$.

The set of defined Groups is described by

$$G = \{g_1, g_2, \dots, g_r, \dots, g_{m_G}\}, \quad (3.3)$$

whereby $m_G = 8$ is the total number of defined groups and $r \in \{1, \dots, m_G\}$.

From these minimal sets, the entries can be assigned to one another, to enable referring to the application of PSs in different Groups. For instance, a given PS p_v can be assigned to a given FoI f_a , which can be assigned to multiple Groups. Even though the particular PS p_v is the same in all those assignments, it is important to distinguish between the different assignments for

future use. Therefore, it is necessary to define the set of Group-specific FoI (GFoI) as

$$GF = \{gf_1, gf_2, \dots, gf_s, \dots, gf_{m_S}\}, \quad (3.4)$$

whereby m_S is the total number of defined GFoI entries, and each gf_s serves as a label referring to a specific $f_a \in F$ in a unique assignment to a specific $g_r \in G$. Further, the same approach is applied for PSs. The set of Group-, and FoI-specific PSs (GFPSs) are defined as

$$GFPS = \{gfps_1, gfps_2, \dots, gfps_u, \dots, gfps_{m_U}\}, \quad (3.5)$$

whereby m_U is the total number of defined GFPS entries, and each $gfps_u$ serves as a label referring to a specific $p_v \in P$ in a unique assignment to a specific $f_a \in F$, within a specific $g_r \in G$, for $u \in \{1, \dots, m_U\}$.

Similar to Groups, FoIs and PSs, other entities of the Entity–Relation model are equally treated: A set of robot hand names, literature sources, and author names is defined. For all those entities, from a programming point of view, an instance is linked to a unique ID that can be referred to. For the sake of conciseness, the sets of author names, robot hand names and literature sources are not described in detail here and can be found in the LoA.

3.3.3 Review Systematic

For the intended data structuring, a systematic for capturing literature is defined to adequately cover the state of the art in the mechanical design of tendon-driven, rigid-sequential anthropomorphic robotic hands. Since no PSs or FoIs had been defined at the time of literature collection, it was not possible to explicitly screen the literature based on these criteria. Therefore, the primary objective was to gather an adequate set of literature with various focal points within the domain of mechanical design.

Five independent systematic approaches were applied to collect relevant literature with different focal points. In a first step, the holistic review papers, collected in Section 2.4, were used. These studies holistically examine the research, developments, and trends in robotic hands. They are thus chosen under the assumption that, after approximately 150 years of research on robotic hands (Piazza et al. 2019), much of the relevant information has already been published and reviewed and can be found there. In the second step, an analysis of existing robotic hands was conducted to identify additional FoIs and PSs. The scope of this analysis is defined by a set of *Significant Robot Hands*, which were extracted from the holistic review papers. To further address the particularly relevant fields of thumb design and underactuation design, additional robotic hands were identified with corresponding focus. Lastly, a separate review was conducted to identify PS for the development of coverings. This information is solely given

for the sake of completeness, referring to the published study for more information and results. It is not further mentioned in this dissertation, as the results are irrelevant for the conceptual design. The execution of all five systematic approaches was completed by end of May 2023. The set of significant robot hands is defined through an analysis of the holistic review papers as those robot hands mentioned at least twice. A single mention results in a total of 135 robotic hands. The threshold was chosen to create a more manageable set of frequently discussed designs. The set of significant robot hands comprises 24 robotic hands, analyzed across 31 studies covering different iterations of their designs. It is emphasized that the chosen terminology does not imply the insignificance of other robotic hands but serves solely as a defined systematic approach due to the lack of alternatives. A complete collection of significant robot hands is presented in a timeline in Figure C.1 in the appendix.

For the identification of robotic hands with thumb design contribution, two search strategies are applied. In a first step, a backwards-snowballing approach is applied. The review by Nanayakkara et al. (2017) is chosen as the starting point for its matching focus, as it provides an extensive literature overview of anthropomorphic robotic hands with a focus on the mechanical realizations of their thumbs. For the backwards-snowballing approach, all references cited in that work are reviewed and presented robot hand designs are captured. For thoroughness, former and past iterations of that robot hand are further identified in literature. The approach resulted in 183 studies. Based on an analysis of the title and abstract, 82 of the 183 studies are chosen for detailed analysis. After a detailed analysis of the studies, 61 out of the 82 studies are identified with an actual matching focus, including any predecessor or successor versions of a robot hand. In a second step, a keyword-based search is performed to identify those relevant robot hand designs published after the work by Nanayakkara et al. (2017). A search on ResearchGate using the keywords "anthropomorphic robotic thumb" OR "robotic thumb" was conducted. The search revealed 40 studies, considering the first two pages, respectively. Based on an analysis of the title and abstract if a contribution to mechanical thumb design is addressed, nine potentially interesting studies are chosen for further analysis. Out of these, six further studies are identified. Thus, in total, 67 studies are chosen for the identification of PSs, addressing the development of robot hand designs in multiple iterations. A complete collection of the resulting 34 robot hands is presented in a timeline in Figure C.2 in the appendix.

For the identification of robot hands focusing on interfinger underactuation, a keyword-based search strategy is performed. The keywords "between fingers" AND "robotic hands" AND "underactuated" OR "underactuation", AND "wire-driven" OR "tendon-driven" are used on Google Scholar. The keyword "between fingers" was added to filter out studies predominantly focused on underactuated mechanisms within fingers. As these are considered to be part of finger design, those PSs are aimed to be captured through the thumb design studies. The search was limited to the first three pages, yielding 58 studies. These studies were evaluated based

on their titles and abstracts to determine whether they investigated tendon-driven mechanisms for interfinger underactuation. As a result, 16 studies were selected for detailed analysis². To identify relevant robotic hands, the sources of the 16 studies were further examined. Ultimately, a total of 29 robot hands were identified for the analysis of approaches toward interfinger underactuation. A complete collection of the collected robot hands is presented in a timeline in Figure C.3 in the appendix.

3.3.4 Results

A total of 23 FoIs and 30 PSs are defined in this dissertation. Summarized presentations are given in Tables E.1, E.2, and E.3 for the Groups, FoIs and PSs, respectively. The assignment of the PSs to different FoIs and Groups led to a definition of 86 GFPSs. The complete list is given in Table E.4. The thereby established 42 GFoIs are not given in an individual table, as they can be seen in Table E.4, whereby some GFoIs appear multiple times in a row. Further, the results yield 87 robot hands from 110 authors. A summarized illustration in tables is omitted. Instead, it is referred to Table 3.2 and Figures C.1, C.2, C.3 for the robot hands and to the bibliography for authors and references.

The illustration of entity programming is omitted here, as the tables summarize the results sufficiently. However, the example excerpt in Listing 3.1 from the FoI entity demonstrates how the data is implemented. The attributes (such as "id" and "name") can be taken from the Entity–Relation model in Figure B.2 for each entity. Finally, the implementation allows to assigns PSs, FoIs, and references in the GFPS entity, as given in listing 3.2.

Listing 3.1: Example extract from the FoI entity data file

```

1      {
2          "id": "F001",
3          "name": "Eliminating 1 IP Joint DOF" },
4      ...

```

Listing 3.2: Example extract from the GFPS entity data file

```

1      {
2          "GFPS001": {"G001": {"F001": {"PS001": "REF014"}}},
3          ... }

```

²Notably, the book *Underactuated Robotic Hands* by Birglen et al. (2008) emerged as a frequently cited and influential source in the field, considered the pioneering work exclusively focused on underactuated hands.

In the following, FoIs and PSs are presented in form of excerpts of the MBs. To be able to give reference to literature, GFPS are presented. Thereby, instead of presenting 86 GFPSs, only 28 GFPS are presented, covering all PSs and FoIs. Further, for better readability, the GFPSs are presented for each FoI category separately.

3.3.4.1 Joint Configuration

| |
|-----------------------|
| Elim. 1 MCP Joint DOF |
| Elim. MCP A-A DOF |
| Elim. 2 MCP Joint DOF |
| Elim. MCP Joint |
| Elim. 1 TMC Joint DOF |
| Elim. TMC P-S DOF |
| Elim. 2 TMC Joint DOF |
| Elim. TMC P-S and F-E |

Table 3.3: Thumb MB excerpt: Thumb-specific FoIs and PSs for joint configurations †.

For Thumb Group, the assigned FoI and their PS are given in Table 3.3. For the MCP joint, two FoIs are identified, eliminating either one or two DOFs. For the former, the PS describes eliminating the A-A DOF of that joint, thereby limiting the MCP joint to a single F-E DOF (e.g. H. Wang et al. 2017a). For the latter, the PS describes the complete removal of the MCP joint, where a fixed angle is implemented in its place (e.g. Pulleyking et al. 2016). For the TMC joint, two FoIs are identified, eliminating either one or two DOFs. For the former, the PS describes eliminating the Pronation-Supination DOF, allowing the TMC joint to retain two remaining DOFs (e.g. Lotti et al. 2005a)³. For the latter, the PS describes eliminating the Pronation-Supination and the F-E DOF, resulting in a TMC joint with only a single A-A DOF (e.g. Peerdeman et al. 2014).

The possible combination of the identified GFPSs found in literature are presented as joint configurations in Figure 3.9. Five different joint configurations for the thumb are identified in the literature, each representing a combination of the identified GFoI and their GFPS. They allow a maximum of five DOFs for the thumb, achieved by 3-1-1 and 2-2-1 configurations. The minimum of three DOFs is achieved by 2-0-1 and 1-1-1 configurations. Finally, intermediate four DOF 2-1-1 configurations are also identified. Each configuration has been successfully

³Thereby, the eliminated Pronation-Supination DOF is often passively compensated for through skillful choice of inclination and twist angles between the remaining joints (Greibenstein 2016).

applied in robotic hand designs. Examples for each configuration with reference to literature and additional information are given in the Appendix in D. A comparison of the frequencies

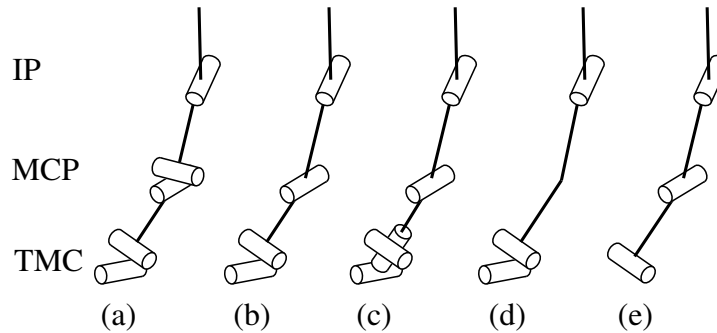


Figure 3.9: Illustration of identified thumb joint configurations †.

of the individual configurations of the thumb is shown in the cumulative representation in Fig. 3.10. As shown in the examples, a relative frequency of the 2-1-1 configuration is evident and continues to increase. However, in recent years, there has also been an increase in more complex configurations, such as the 3-1-1 or 2-2-1 configurations. This may be due to advances in control techniques or a recent desire for more dexterous robot hands. On the other hand, there is also an increase in comparatively simpler configurations, such as the 1-1-1 or 2-0-1 configurations. On the one hand, this can be attributed to the desire for simpler control. On the other hand, configurations such as the 2-0-1 configuration can be understood as a correlation with improvements in the medical domain. In Table 3.4, the FoIs and PSs for index finger joint

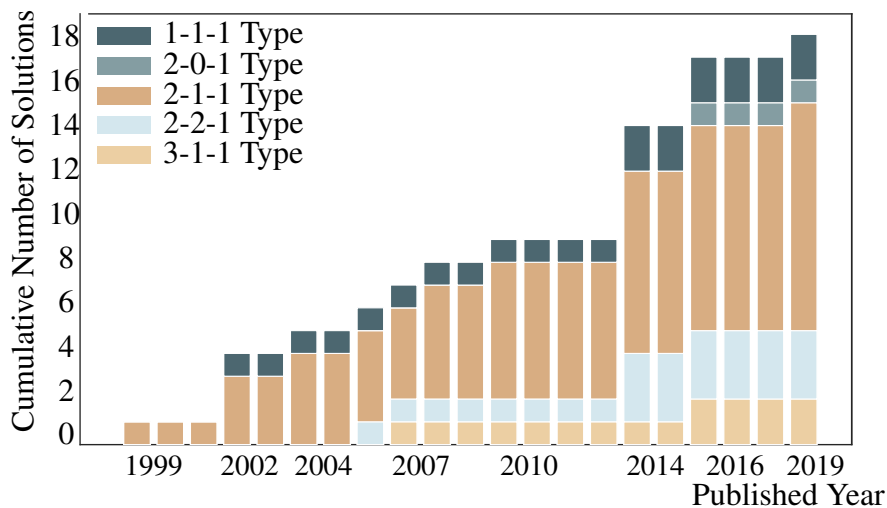


Figure 3.10: Cumulative illustration of thumb configuration frequencies †.

configuration are presented. First, the elimination of MCP joint A-A DOF could be identified in the literature. Notably, this elimination is controversially discussed in the literature. For

| |
|-------------------------|
| Elim. 1 MCP Joint DoF |
| Elim. MCP Add./Abd. DOF |
| Elim. 1 IP Joint DOF |
| Elim. PIP/DIP Joint |

Table 3.4: Index finger MB excerpt: FoIs and PSs for joint configuration †.

successful grasping, many robot hand designs implement A-A in all fingers but middle finger (e.g. J. Zhou et al. 2019)⁴. However, the complete elimination of all A-A DOF is comparably frequent in robot hand designs to reduce complexity. Second, the elimination of DIP or PIP joint can be identified. In such instances, the joint is replaced with a constant angle between the two adjacent phalanges. An Example can be found, for instance, in the Mia Hand from Prensilia[®] (2024).

The combinations of the above identified PSs for finger joint configuration found in literature are given in Figure 3.11. As illustrated, six different combinations are depicted. The setup ranges from configurations with four DOF to configurations with only two DOF. Examples from the literature can be found in the corresponding PSs of the LoA, such as the work by Leonardis and Frisoli (2020) for configuration (f), or Konnaris et al. (2016) for configuration (b). For configurations (c) and (d), no sources are captured in the LoA. However, they are illustrated for the sake of completeness, as the lack of sources are interpreted as a limitation of this dissertation rather than an indication of the absence of such finger joint configurations.

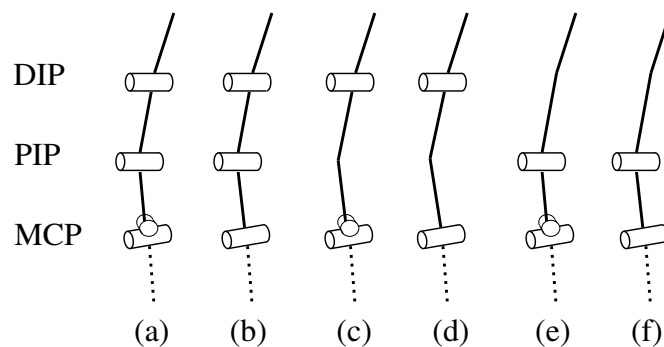


Figure 3.11: Illustration of identified finger joint configurations †.

⁴See also works by Grebenstein (2016) and Tian et al. (2021).

| Eliminating 1 HMC Joint DOF | | |
|-----------------------------|-------------------------------------|------------------------------------|
| Eliminating RF HMC joint | Implementing joined LF-RF HMC joint | Eliminating joined IF-MF HMC joint |

Table 3.5: KBC MB excerpt: KBC-specific FoIs and PSs for joint configurations †.

In Table 3.5, the Fields and PSs for the elimination of HMC joints are presented for the KBC Group. HMC joints can be argued to belong to the respective finger and should thus be considered in the respective Group of the LoA. However, in this dissertation, they are considered in the KBC Group as they are located in the palm, can be assigned to more than one finger and are frequently considered for the cupping movement of the palm.

The general relevance of HMC joints is discussed in multiple works. Konnaris et al. (2016) proposes two additional HMC joints for ring- and little finger to achieve palm-arch capabilities. Similarly, Grebenstein (2016) proposes a little finger HMC joint for the Awiwi Hand to improve the grasp of small spherical objects. Including an HMC joint, the workspace is turned inward and, thus, the opposition with the thumb is improved.

The identified PS for the elimination of 1 HMC joint DOF include three options. The first PS describes the elimination of the joined index finger and middle finger HMC joint. This is the most common choice, considering the low number of robot hands that apply HMC joints for the index finger and middle finger. In the course of this study, no robot hand with individual HMC joints for the index finger and middle finger could be identified. However, examples such as the MSRH Hand by P. Lee et al. (2023) performed successfully all Feix grasps and the Kapandji test with a joined index finger and middle finger HMC joint. The second PS describes application of a joined little finger and ring finger HMC joint, found in MSRH Hand or in the MCR Hand II by H. Yang et al. (2021a). The third PS describes an elimination of ring finger HMC joint, as found in examples such as the Awiwi Hand by Grebenstein (2016). Similarly, H. Yang et al. (2021a) and Z. Zhang et al. (2018) propose a palm design split into two parts using a single joint at HMC base between ring- and middle finger. No consideration of HMC joints (elimination of three HMC joint DOFs) is the most common choice in robot hand designs. Examples include the iCub Hand Serie (Davis et al. 2008; Sureshbabu et al. 2015), the ACB Hand (Chu et al. 2024) or the ISR Alpha Hand by Farinha and Lima (2016).

The combinations of the above identified PSs for HMC joint configuration found in literature are given in Figure 3.12. Illustrated are configurations with no HMC joints, a single HMC joint little finger, a single common HMC joint for little and ring finger, and two individual HMC joints for little and ring finger. They are given from (a) to (d), respectively.

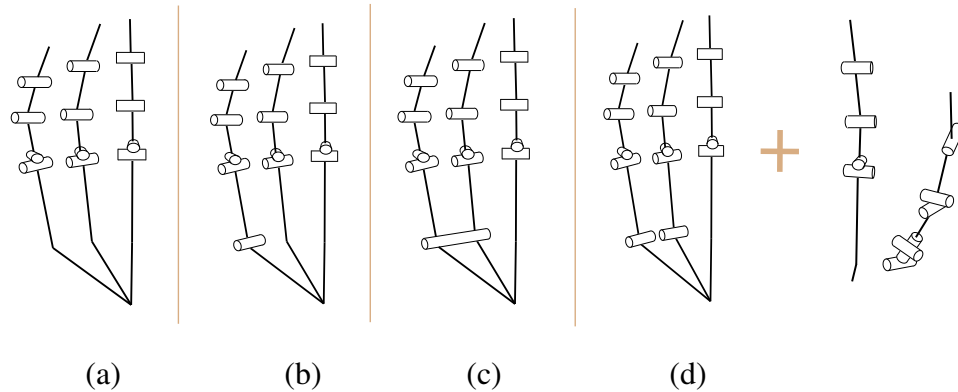


Figure 3.12: Illustration of identified robot hand HMC joint configurations †.

3.3.4.2 Joint Coordination

The PS collected in this FoI category include approaches for connecting joints rather than eliminating them. For this reason, the elimination of DOA is chosen as the naming for the FoIs. For the elimination of DOA, UMs or couplings are applied. Even though the latter also eliminates a DOF, the PSs are not considered within the FoI "Elim. DOF", as no joint is eliminated.

For Thumb Group-specific examples, identified FoI and their PS are given in Table 3.6. A distinction is made between the elimination of a single DOA, two DOAs and three DOAs. Within these FoIs, the PSs differ with respect to the application of an underactuation or coupling and with respect to the application of tendons or linkages. The FoIs and their corresponding PSs are described in more detail below.

The identified PS for the coordination of joints are conceptually illustrated in Figure 3.13. For

| | | |
|----------------------------------|--------------------------------|----------------------------------|
| Elim. 1 DOA MCP-PIP Joints | | |
| Tendon coupling of two joints | Linkage coupling of two joints | Linkage UA of two joints |
| Elim. 2 DOA TMC-MCP-PIP Joints | | |
| Linkage UA of three joints | Tendon UA of three joints | Linkage coupling of three joints |
| Elim. 3 DOA TMC-MCP-PIP Joints | | |
| Linkage coupling of three joints | | |

Table 3.6: Thumb MB excerpt: Thumb-specific FoIs and PSs for joint coordination †.

the joint coordination, a new notation is introduced. If two adjacent joints in a consecutive kinematic (i.e. in a finger) are colored, they are coordinated. Thereby, a blue color refers to a

coordination by tendon and a brown color to a coordination by linkages. If the joints are striped, an underactuation is implemented. Otherwise, a coupling is implemented. Important to note, the illustrated joints are not necessarily applied in the robot hands that are mentioned. Here, it is solely referred to the applied coordination of joints. Further PSs for the elimination of DOF can be applied.

The identified PSs for the reduction of one DOA in the thumb all refer to the coordinaton of the

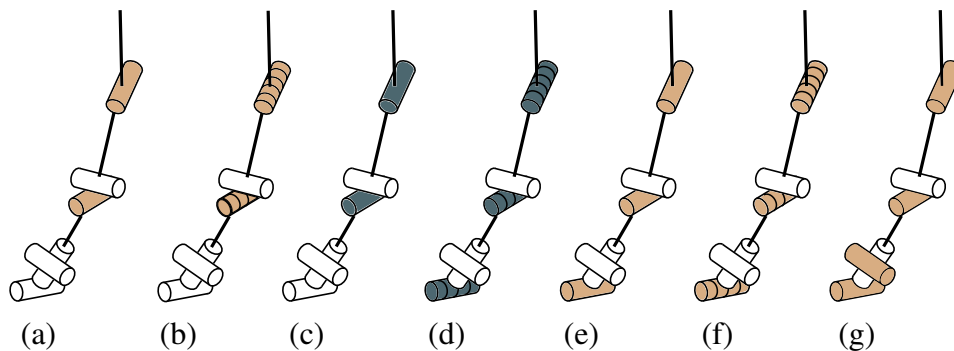


Figure 3.13: Conceptual illustration of different thumb joint coordinations (brown: linkages, blue: tendons, striped: underactuated) †.

MCP and IP joints, as given in Table 3.6. First, the tendon coupling of MCP and IP joints (see Figure 3.13 (c)) could be identified in literature (e.g. Butterfass et al. n.d.). Second the linkage coupling (see Figure 3.13 (a), (e.g. Liu et al. 2008)), and third a linkage underactuation could be identified (see Figure 3.13 (b), (e.g. D.-p. Yang et al. 2009)). For a tendon actuated robot hand, the tendon coupling is comparably easy to implement. As a result, this is a common choice and often argued to be analogously to the coordination of MCP and IP joints in human thumbs (Berselli et al. 2009). For tendon coupling of MCP and IP joints, examples from literature are given in Table D.7. Examples for the linkage coupling are given in Table D.8.

The identified PSs for the reduction of two DOA in the thumb refer to the coordination of the TMC, MCP and IP joints, as given in Table 3.6. Three different PSs to eliminate two DOA in a thumb design are identified: First, a linkage coupling of three joints (see Figure 3.13 (e), (e.g. Rodriguez et al. 2006)); second, a linkage underactuation of the three joints (see Figure 3.13 (f), (e.g. Laliberté and Gosselin 2001)); and last, a tendon underactuation of the three joints (see Figure 3.13 (d), (e.g. Gosselin et al. 2008)). For the last, an detailed example from literature is given in Table D.2.

For the elimination of three DOA in thumb design, only a single PS could be identified in literature. In the work by Tae-uk and Yonghwan (2014) a spherical five-bar mechanism and two underactuated four-bar linkages are applied. The applied mechanism allows the connection of IP F-E, MCP F-E and TMC F-E and A-A DOFs, as illustrated in figure (see Figure 3.13 (g)). For Finger Group-specific examples, the FoIs and PSs for the reduction of DOA are presented

| | | | |
|--------------------------------|--------------------------------|----------------------------------|---------------------------------|
| Elim. 1 DOA DIP-PIP Joints | | | |
| Tendon coupling of two joints | Linkage coupling of two joints | Linkage UA of two joints | |
| Elim. 1 DOA MCP-PIP Joints | | | |
| Tendon coupling of two joints | Linkage coupling of two joints | Linkage UA of two joints | |
| Elim. 2 DOA MCP-PIP-DIP Joints | | | |
| Linkage UA of three joints | Tendon UA of three joints | Linkage coupling of three joints | Tendon Coupling of three joints |
| Elim. 3 DOA MCP-PIP-DIP Joints | | | |
| Linkage UA of three joints | | | |

Table 3.7: Index finger morphological box excerpt: index finger-specific FoIs and PSs for joint coordination †.

tn Table 3.7. Even though the PSs are identical to those from the "Thumb" Group for reduction of DOA, the location of application is different and thus worth to mention. For the reduction of one DOA, two main principles can be found. Either the DIP and PIP joint, or the MCP and PIP joint are connected. The former is a comparably common choice, imitating human physiology. The latter is usually combined with the elimination of the DIP joint, as presented above as a PS. For the elimination of two DOA, a tendon or linkage UA or coupling can be found in the literature, similar to those for the thumb. Further, an elimination of three DOA in finger design could be found in the literature. In the work by Tae-uk and Yonghwan (2014), a spherical five-bar mechanism is proposed for a finger operation in space rather than in a plane. Thus, the A-A movement is included in the UA.

An illustration of applied DOA reduction strategies from literature are given in Figure 3.14. A prominent design choice is to neither couple nor underactuate the A-A DOF in the MCP joint. Only one out of eight cases in Figure 3.14 includes this DOF for a coordination. For this one case, examples in literature are rare. Besides, four out of the eight cases involve coupling or underactuation of the F-E DOF of the MCP joint, achieved through either tendons or linkages. The remaining options focus on connecting only the DIP and PIP joints, mimicking human physiology while creating additional workspace by independently actuating the MCP joint⁵.

In Table 3.8, FoIs and PSs are presented for joint coordination involving HMC joints. Two

⁵Examples for the given DOA reduction strategies are (from left to right) the work by Kawasaki et al. (2002b), D.-p. Yang et al. (2009), Davis et al. (2008), Kyberd et al. (2001), Laliberté and Gosselin (2001), and Pons et al. (2004), again Gosselin et al. (2008), and, lastly, Tae-uk and Yonghwan (2014).

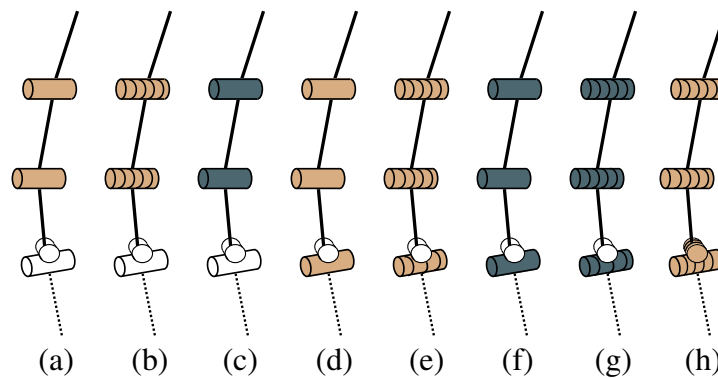


Figure 3.14: Illustration of identified finger joint coordinations (brown: linkages, blue: tendons, striped: underactuated) †.

| | |
|---------------------------------------|---------------------------------|
| Eliminating 1 DOA HMC Joint | |
| Linkage Underactuation HMC-MCP Joints | Linkage Coupling HMC-MCP Joints |

Table 3.8: KBC MB excerpt: KBC-specific FoIs and PSs for joint coordination †.

PSs are collected for eliminating one DOA at HMC joints: First, a linkage underactuation of the HMC with the corresponding MCP joints is identified in literature. For example, in the work by Ambrose et al. (2000), the underactuated palm is able to cup in a human-like way without the fingers colliding. Similarly, Z. Zhang et al. (2018) apply an underactuated DOF at the palm that relies on ring and little fingers' flexion. Second, a linkage coupling of the HMC joint with the corresponding MCP joint could be identified. Konnaris et al. (2016) propose two HMC joints of ring- and little finger in the dorsal region of the palm. Both of them are directly coupled with the F-E of the MCP joint. In Table 3.9, FoIs and PSs are presented for joint coordination between fingers. In the established terminology, those PSs relate to interfinger joint coordination. The identified FoIs differ in number of fingers and chosen fingers. The eliminated DOA are considered to be equal to the number of coordinated fingers. Thereby, it is irrelevant if the respective finger is otherwise coordinated within the finger design. All FoIs are given in more detail in the following.

Elimination of one DOA involves the coordination of two fingers. The decision to underactuate two fingers in certain robotic hands is driven by specific goals. For example, Dalley et al. (2009) aimed to achieve maximum continuous grasp force, while Wiste and Goldfarb (2017) sought to simplify control and mechanical structure. The RTR II hand was designed by Massa et al. (2002) with a total of three fingers, including the thumb. Therefore, in this design, the two fingers, apart from the thumb, were underactuated to enhance the hand's adaptability to the

shape of objects.

Elimination of two DOA involves the coordination of three fingers. Two different combinations could be found for underactuation of three fingers. In the work by Cipriani et al. (2010), the coordination of little finger, ring finger and middle finger is argued based on a statistical investigation of the human hand. The study by Ingram et al. (2008) revealed that the thumb is the most independent finger, followed by the index finger, which led to the decision to underactuate the middle, ring, and little fingers. This approach was also supported by Kyberd et al. (2001), who provided a similar rationale for underactuating these particular fingers (the ability to pick up small objects with the index finger and thumb). Besides underactuation, a tendon coupling could also be identified in literature (e.g. Schmitz et al. 2010).

The elimination of three DOA is the most common choice and involves an underactuation of all fingers but the thumb. In this configuration, an additional actuator is dedicated to the thumb (e.g. Kontoudis et al. 2015)⁶. Possibly, further actuators are considered in the robot hand to enable A-A movements, enhancing dexterity (Kontoudis et al. 2019).

The elimination of four DOA incorporates the thumb in the coordination. All captured

| | | |
|---|---|---|
| Eliminating 1 DOA F-E LF-RF | Eliminating 1 DOA F-E MF-IF | |
| Tendon Underactuation F-E LF-RF | Tendon Underactuation F-E MF-IF | |
| Eliminating 2 DOA A-A LF-RF-IF | Eliminating 2 DOA F-E MF-IF-Th | |
| Tendon coupling A-A LF-RF-IF | Tendon Underactuation F-E MF-IF-Th | |
| Eliminating 2 DOA F-E RF-MF-IF | Eliminating 3 DOA F-E LF-RF-MF-IF | |
| Tendon Underactuation F-E RF-MF-IF | Tendon Underactuation F-E LF-RF-MF-IF | |
| Eliminating 4 DOA A-A LF-RF-MF-IF-Th | Eliminating 4 DOA F-E LF-RF-MF-IF-Th | |
| Tendon Underactuation A-A LF-RF-MF-IF-Tb | Tendon Underactuation F-E LF-RF-MF-IF-Tb | Tendon Underactuation/Coupling F-E LF-RF-MF-IF-Tb |

Table 3.9: Transmission MB excerpt: Transmission-specific FoIs and PSs for joint coordination †.

robot hands with four coordinated fingers excluded the thumb from coordination but coupled it, enabling the use of a single actuator to control all digits. This design approach aims to achieve

⁶See also works by Sun et al. (2022) and Tomovic and Boni (1962).

a simpler and lighter robotic hand (e.g. Gosselin et al. 2008)⁷. However, other designs exist that apply an underactuation that incorporates the thumb for F-E (e.g. Catalano et al. 2016) or A-A (e.g. Della Santina et al. 2018). In every case, attention is paid to the thumb's force, which must equal the combined force of the other fingers (Gosselin et al. 2008).

To date, there is no defined standard for a correct number of coordinated fingers for a robotic hand. Therefore, an analysis is performed to understand common choices and trends. In Figure 3.15, a piechart illustration of the distribution of number of underactuated fingers is given. It is apparent that 55% of the 29 evaluated hands feature four underactuated fingers. Additionally, 17% of the hands have five underactuated fingers, while 14% have three, and another 14% have two underactuated fingers.

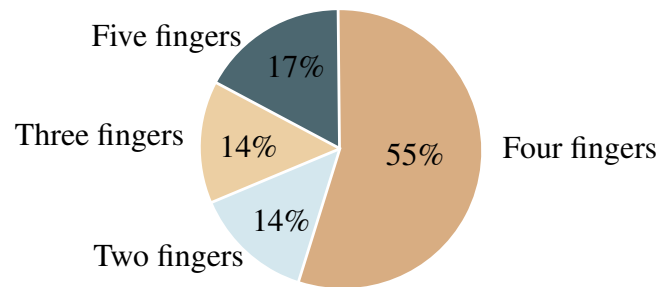


Figure 3.15: Percentile distribution of the number of underactuated fingers among the 29 evaluated tendon-driven robot hands †.

3.4 Hand Concepts

After identifying the FoIs and PSs, their combination to define robot hand conceptual designs is investigated. The general applicability of FoIs and PSs is already shown in the previous section in form of existing thumb, finger or HMC structures. However, in this section, it is demonstrated how the GFPSs are used to define existing robot hand designs.

A Hand Concept (HC) is defined as the conceptual design of a robot hand. Each Hand Concept, with

$$HC = \{HC_1, HC_2, \dots, HC_l, \dots, HC_{m_C}\}, \quad (3.6)$$

being the set of identified Hand Concepts, HC_l being the element of the set of Hand Concepts with reference label l and m_C being the number of identified Hand Concepts, can be described through a combination of the IMDC and GFPSs and illustrates a robot hand's joint configuration and joint coordination. An example is given in Figure 3.16. The illustrated Hand Concept corresponds to the design of the Gesture Based Hand by Tian et al. (2021). Attention is pointed to the notation used, in which the circle refers to the IMDC and the box to a Hand Concept. The

⁷See also works by Baril et al. (2010), Birglen and Gosselin (2006), and Dollar and Howe (2007).

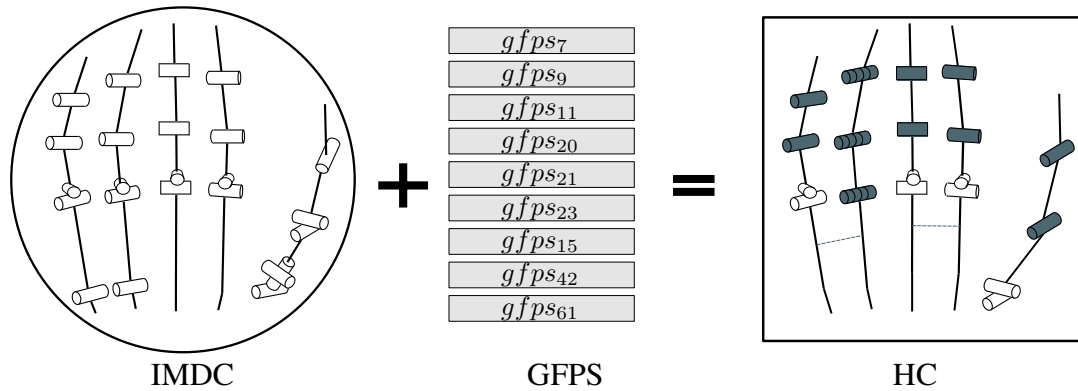


Figure 3.16: Example Hand Concept with given GFPSs (blue: tendons, striped: underactuated).

definition of possible Hand Concepts requires a compatibility analysis. By definition, a Hand Concept is the result of a combination of GFPSs with the IMDC. To identify all possible Hand Concepts, thus, all possible GFPS combinations need to be identified. Thus, a compatibility matrix needs to be defined for all GFPSs.

However, the number of GFPS is comparably big and rules are derived that allow to reduce the manual effort for the Knowledge Engineer, to address the question (Q2). A compatibility analysis for GFPSs requires pairwise comparisons of 86 elements. To reduce the manual effort of the Knowledge Engineer, the previously derived relations of FoI, Group and PS are leveraged to enable the creation of a compatibility matrix for FoIs instead and automatically expand it to a compatibility matrix for GFoIs and subsequently for GFPSs. These derived expansion rules are explained in the following.

To extend the compatibility matrix from the FoI level to the GFoI level, the structural relationship between FoIs and GFoIs is leveraged. A GFoI is defined as a FoI assigned to a specific group, allowing a direct mapping between the two levels. A developed compatibility matrix for 23 FoIs can thus be expanded to a matrix for 42 GFoIs by applying two rules. First, if two FoIs are compatible, all corresponding GFoIs are also compatible, regardless of their group assignment. Second, if two FoIs are incompatible, the corresponding GFoIs remain compatible as long as they are assigned to different groups. Incompatibility at the GFoI level arises only when two incompatible FoIs belong to the same group. For example, the two FoIs f_1 and f_{08} (see Table E.2) are incompatible because a DOF cannot be eliminated and coordinated at the same time. However, at the GFoI level, this conflict only applies within the same group (e.g., little finger). GFoIs in different groups are compatible, since the same DOF can be eliminated in one finger and coordinated in another.

To extent the compatibility matrix from GFoI level to GFPS level, the relation between FoIs and PSs are leveraged. Within a FoI, PSs are defined to be mutually exclusive. As a GFoI is in essence a FoI assigned to a certain group, the same argument applies to the GFPS within a

GFoI: they are mutually exclusive. Thus, two rules are applied. First, for each applied GFoI, either one of its GFPS can be applied. Second, in case of at least two compatible GFoIs, each possible combination of their GFPSs can be applied.

The derived rules enable automated identification of potential Hand Concepts. By applying these rules, the Knowledge Engineer only needs to define a compatibility matrix for 23 FoIs instead of 86 GFPSs, significantly reducing manual effort. The compatibility matrix allows to define viable FoI-combinations. Above expansion rules are then used to automatically identify GFPSs-combinations, which in turn can be applied to the IMDC to define Hand Concepts.

The defined compatibility matrix on FoI level is given in Table F.1. For improved readability, the matrix is given in the Appendix. Thereby, a colored box for two FoIs illustrates the compatibility and results in a possible combination.

Applying the rules, 8, 514, 992, 160 possible Hand Concepts are defined. Only considering the defined FoIs in the first FoI category (FoI-C₁ *Joint Configuration*), a total of 7, 919 Hand Concepts are identified. For the second FoI category (FoI-C₂ *Interfinger Joint Coordination*), 27, 332, 063 Hand Concepts are identified. Lastly, for the third FoI category (FoI-C₃ *Intrafinger Joint Coordination*), 863 Hand Concepts are identified. Considering further the possible combinations of FoIs across the FoI category, the above mentioned approximately 8.5 billion Hand Concepts are identified.

Interested readers can refer to Appendix G for a detailed explanation of how the expansion rules are applied and why this leads to a large number of Hand Concepts. It is explained in detail how, despite the relatively low number of FoIs, the combination of these FoIs, followed by the G-expansion and then the PS-expansion, results in a large number of GFPS-combinations and therefore a large number of Hand Concepts.

Further, interested reader are referred to Appendix H.1 for a detailed explanation of how the creation of Hand Concepts is implemented from a programming perspective.

3.5 Conclusion

This chapter addresses the first objective (O1) of this dissertation. A knowledge base with literature-linked knowledge on joint configuration and coordination must be developed that allows for the systematic generation of conceptual designs.

Due to the lack of alternatives, a methodology is developed to capture design knowledge with specific reference to literature. The knowledge is structured using morphological boxes (~Groups), where each morphological box applies to a major aspect of a robot hand, including each digit, the transmission and the overarching kinematic structure. Each group is assigned Fields of Interest (FoIs) and principal solutions (PSs) that reflect how these FoIs have been addressed in the past. Minimal, non-redundant lists of FoIs and PS are created, with each entry

assigned a unique identifier. Additional indexed lists are defined for literature sources, robot hands and author names, each with unique identifier. Each group- and FoI-specific PS (GFPS) is then linked to relevant literature sources, authors, and robot hand examples.

To identify relevant design knowledge, a second methodology is applied, comprising a systematic mapping process based on the PRISMA guideline. In five distinct search strategies, a total of 147 studies are identified for analyses. The design knowledge regarding joint configuration and joint coordination is gathered in these studies and used to synthesize previously undefined FoIs and PSs. Based on the given information, an identified PS is assigned to the matching morphological box and linked to its source.

For the systematic generation of conceptual designs, a third methodology is developed that defines a conceptual design as the combination of PSs and a defined joint configuration. This defined joint configuration is modeled after the human hand, complying to the usual approach to conceptual design (see Figure 1.1). Therefore, the results of biological studies are compared with the joint configurations used in currently successful robot hands. The outcome is presented as Initial Maximum DOF Configuration (IMDC). To automate the generation of conceptual designs, a compatibility matrix of the GFPSs was created. However, by defining suitable rules, manual effort could be reduced, and the Knowledge Engineer only needs to create a compatibility matrix for the FoIs instead. Finally, the terminology of FoIs and PSs is defined in such a way that they can be applied to the IMDC to either eliminate joints (i.e., reduce DOF) or coordinate them (i.e., reduce DOA).

The applied methodologies led to the following results. A total of 30 PSs and 23 FoIs are defined. With seven defined groups, the PSs are further combined into 86 GFPSs. The IMDC comprises 24 DOF, as illustrated in Figure 3.4. Using the 86 GFPSs and the IMDC, a total of 8,514,992,160 possible robot hand conceptual designs (HCs) are derived. Each HC is specified by the applied GFPSs, which are further linked to relevant literature references where the PS have been applied before, author names, and associated robot hands. Summaries of the identified Groups, FoIs, PSs and GFPSs are given in the Tables E.1, E.2, E.3 and E.4, respectively. Summaries of the identified robot hands are given in Table 3.2 and Figures C.1, C.2, C.3 for the respective search strategy. A summary of literature references is omitted here. Instead, readers are referred to the bibliography. For the specific assignments to the GFPSs, readers are referred to the publicly launched online GUI⁸ or the information in the main body of this dissertation.

As the next step, the derived conceptual designs are used in the guidance as embedded knowledge. The basis on which the hand concepts are chosen from the guidance is determined in Chapter 4. Chapter 5 then implements this methodology in the form of a method.

⁸<https://loa.igmr.rwth-aachen.de/>

4 Design Recommendation

To answer the research question, this chapter deals with the second objective (O2). A method is developed to define optimal conceptual designs based on user requirements. The chapter starts with a problem description in section 4.1. Subsequently, the methodology is derived, which includes the analysis of relevant literature (Section 4.2) and an interpretation of the results for this dissertation in Section 4.3.

4.1 Problem Statement and Approach

The associated challenges for the recommendation can be summarized in two questions:

(Q3) With respect to which requirements is a recommendation made?

(Q4) How to choose among Hand Concepts, given a set of requirements?

Regarding (Q3), possible requirements for a robotic hand design are diverse. Different options for classification and evaluation of robot hand designs are discussed in Section 2.2.3. However, it could be concluded that the evaluation of the performance is most meaningful for the conceptual design. With the performance criterion generally comprising grasping and manipulation, this dissertation focus on grasping to limit the scope. For that, it is established in Section 2.2.3 that *grasping* can be interpreted as the collection of operations (tasks) and grasp taxonomies, such as the one by Feix et al. (2015), are a suitable measure to define individual operations as executable grasps. Lastly, the Motion Ability is introduced in this dissertation as the performance quality that is evaluated during the conceptual design phase, representing the digits' ROMs and how well they are harmonized.

Regarding (Q4), choosing a robot hand design among a set of options is proposed in this dissertation to be an optimization problem. The derivations in Chapter 3 reveal eight billion possible conceptual designs. Choosing among them with given performance requirements most likely lead to multiple viable options. For example, the set of SRHs presents six alternative solutions for successful execution of all Feix grasps. In practice, therefore, performance is often not the only factor considered; the designer also has some preference regarding other qualities, such as the simplicity, considering the eligible number of DOA. Thus, for robot hand designs, a recommendation can not be made based on a metric that considers performance requirements alone.

Against this background, at least two factors are considered in a nested application. Firstly, an initial preselection of a set of eligible Hand Concepts for a necessary performance is made, with, secondly, a subsequent trade-off consideration of that set regarding another factor, such as simplicity. The procedure can be well illustrated using the example of the SRHs. In Figure 3.5, a preselected set of Hand Concepts is shown, ordered by the number of DOA. Depending on the preference for simplicity, either the Hand Concepts on the left side or the right side are preferred. Therefore, in this dissertation, performance requirements in the form of achievable grasps and the preference between Simplicity and Motion Ability is asked of the user.

The concept presented is theoretically also suitable for more factors. If two preselected sets of Hand Concepts are considered that are sorted according to different factors, the Hand Concept that represents the optimum of both preferences is recommended. A qualitative illustration is given in Figure 4.1. Thus, the procedure can be extended for any number of preference factors as long as the preselected sets of Hand Concepts contain a subset of identical Hand Concepts that are not equal to zero. In this dissertation, only the grasp performance and simplicity as a preference factor are implemented as proof of concept.

A remaining challenge is the definition of the preselected set of Hand Concepts for a given

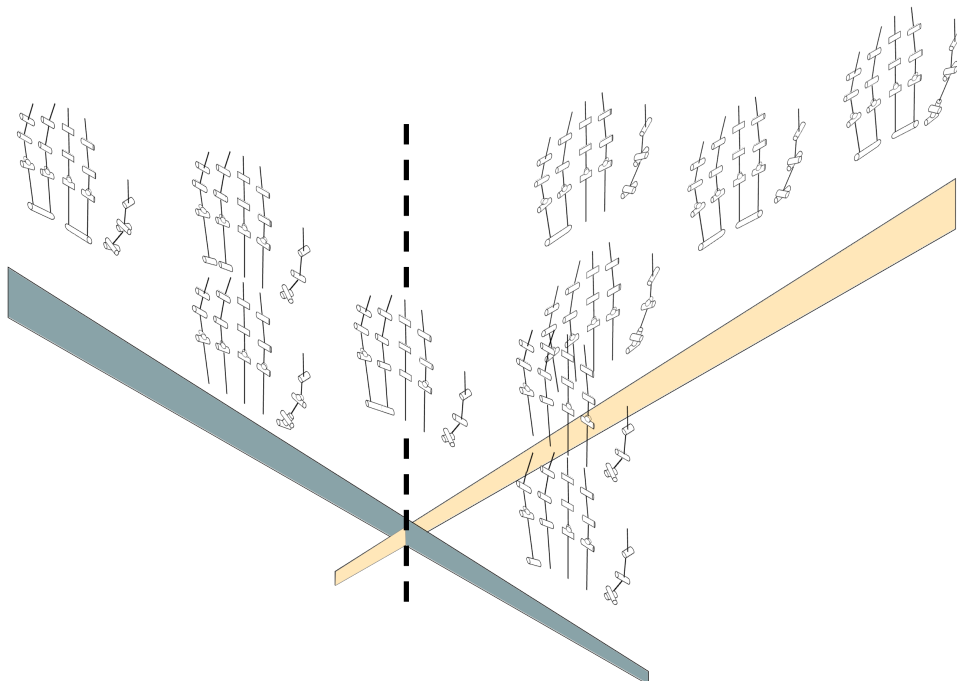


Figure 4.1: Illustration of optimization problem in multiple trade-offs.

input. Given a preselected set of Hand Concept, the simplicity preference can be incorporated by sorting the set by ascending DoA to obtain an ordered list. However, the preselected sets first need to be defined. For each grasp from Feix's taxonomy, the Hand Concepts capable of performing that grasp need to be identified. From a rational point of view, for a defined number of grasps this set will consist of a range of Hand Concepts with the IMDC on one side and a Hand Concept with a minimum number of DOF and DOA on the other side.

The further procedure is derived from these considerations. Literature is reviewed to identify the minimum DOF (relevant FoIs of the first FoI category FoI-C₁) or minimum DOA (FoIs of the second and third FoI category FoI-C₂ and FoI-C₃, respectively) Hand Concept for each Feix grasp.

4.2 Relevant Studies

Before an additional search, the results of the SRHs are a valuable basis. The set of robot hands that can successfully complete all grasps from Feix's taxonomy can be used to investigate successful joint configurations and joint coordinations for maximum performance. However, the remaining question is the necessary minimum configurations and coordinations per grasp. A literature search for robot hands capable of performing isolated Feix grasps does not lead to important results. This may be due to the fact that robot hands are generally designed to perform complex manipulation tasks. The sole completion of individual grasps is reserved for customized industrial grippers.

Therefore, for the joint configuration (~minimal DOF), the literature is analyzed to identify studies on joint relevance. These studies analyze the relevance of individual joints in anthropomorphic robot hands and can be used to identify joints that are irrelevant for isolated grasps. For joint coordination (~minimal DOA), the literature is analyzed for studies on grasp synergies and minimal actuation. This is a popular field in the area of anthropomorphic robot hands, investigating the use of underactuated mechanisms to minimize the number of DOA while maintaining acceptable performance in terms of grasping.

The SRHs are analyzed as the upper boundary in joint configuration and joint coordination for full performance. For a user requirement of full performance, i.e. all grasps from Feix's taxonomy, the SRHs' joint configurations and joint coordinations have been experimentally verified to be successful. To use this information in the context of the terminology derived in Chapter 3, the SRHs are assigned with the respective GFoIs and GFPSs.

An illustration of the SRHs' joint configurations and coordinations with associated GFPSs are given in Figure 4.2 and 4.3, respectively. For both figures, the preselected sets of Hand

Concepts are sorted and shown from left to right with decreasing number of DOA¹. For the joint coordination, in addition to the previously introduced notation, straight lines between fingers indicate the interfinger coordination.

Analysis of the SRH joint configuration indicates that up to five DOFs could be eliminated

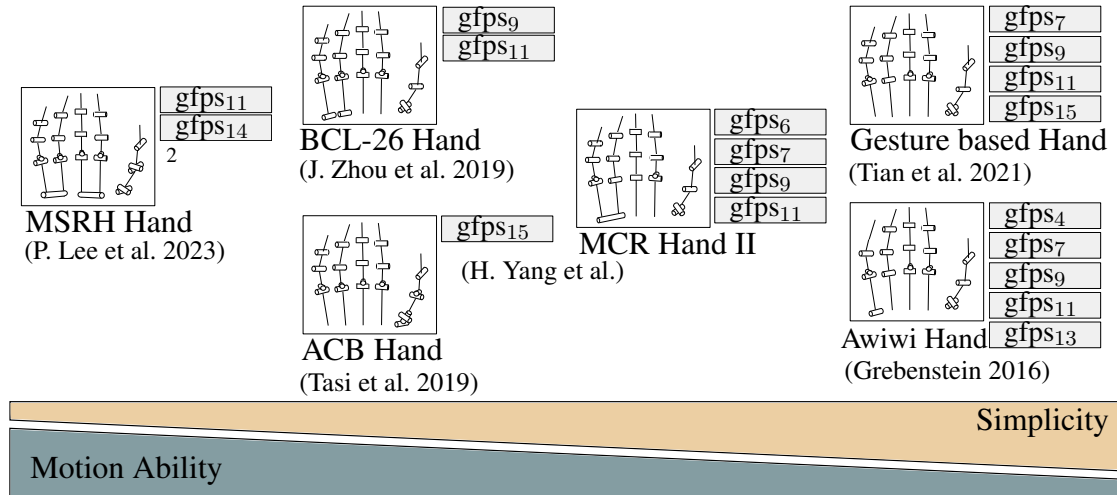


Figure 4.2: SRHs' joint configurations with assigned GFPSs and illustrated trade-off.

compared to the IMDC. Notable are all eliminated DOFs that have been proven to be not required for successful performance: Five of the six SRHs eliminated the Pronation-Supination DOF of the TMC joint; Four SRHs have demonstrated successful performance with a single DOF in the thumb MCP joint; Three SRHs have eliminated the A-A DOF in the ring finger MCP joint; and two SRHs have shown that HMC joints are dispensable. Further, the MCR Hand II does not apply the middle finger's MCP joint A-A DOF.

The analysis of applied joint coordination in the SRHs reveals a possible elimination of up to twelve DOAs. Up to ten DOA are eliminated through intrafinger joint coordination, as given in the Awiwi Hand. Two additional DOA are eliminated through interfinger coordination, combining the little finger with the ring finger and the middle finger with the index finger.

One SRH is not depicted in Figure 4.3. The BCL-26 hand is not listed, as it is pneumatically actuated and has, thus, neither linkage nor tendon coupling/underactuation applied³.

A literature search on joint relevance revealed a single study analyzing the contribution of individual joints to the overall hand dexterity. To the best of the authors' knowledge, the work

¹Where DOA is synonymous with DOF for the joint configuration.

²This SRH features an additional DOF as a joined HMC joint for middle and index finger that is not considered in the IMDC, as biological studies have proven its neglectable ROM, as derived in Section 3.2.

³Nonetheless, the applied sequential design allowed to derive conclusions regarding PSs for joint configuration.

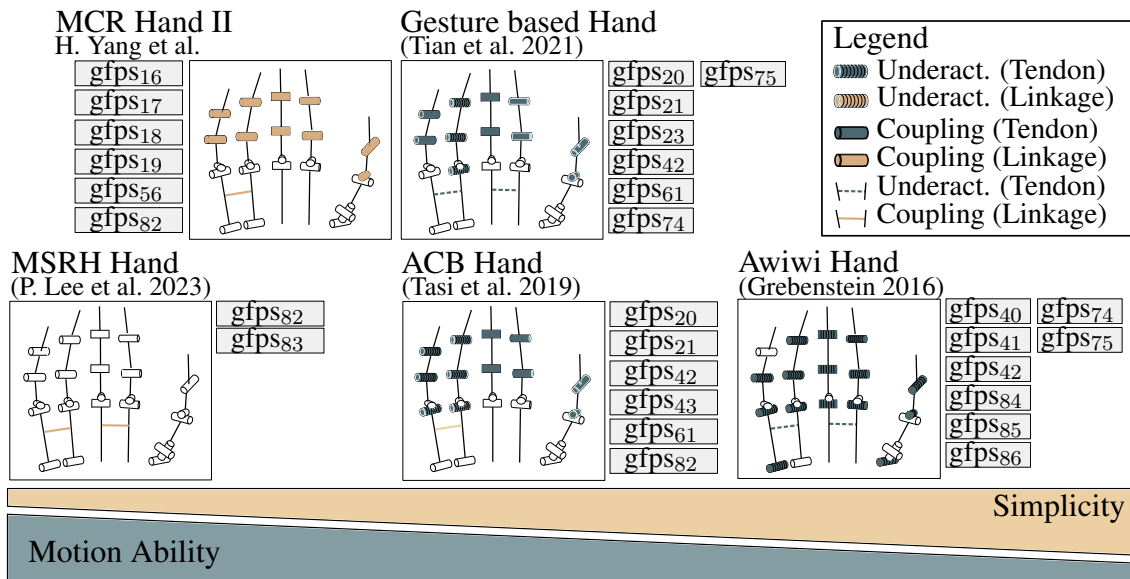


Figure 4.3: SRHs' joint coordinations with assigned GFPSs and illustrated trade-off.

by Saliba et al. (2013) is the only conducted study on joint relevance for anthropomorphic hands. In that comprehensive study, the grasping performance of 40 people was recorded using the *Box and Block Test* (BBT), *Nine-Hole-Peg-Test* (NHPT) and the *Grooved Pegboard Test* (GPT). These tests are popular in rehabilitation and illustrated in Figure 4.4. They require a subject to move an object from a start to an end position. For the Box and Block Test, Nine-Hole-Peg-Test and Grooved Pegboard Test, the objects are different and represent cubes, cylinders and a key-like object, respectively. (Frommelt and Lösslein 2011) For the Nine-Hole-Peg-Test and Grooved Pegboard Test, the objects must be inserted in a designated hole, thus requiring manipulation of the object. In the study, participants repeated the tasks multiple times, each time with different mechanical constraints applied to their hands. A metric was developed to measure how much each constraint affected dexterity, based on the time it took to complete the task.

The study investigated the following hand attributes. First, the elimination of index finger, middle finger, ring finger and little finger are investigated. Second, IP joints are obstructed, for all digits individually and for all together. Third, the A-A DOF of the fingers' MCP joint is obstructed for all fingers together and last, the sense of touch is limited. (Saliba et al. 2013) For this dissertation, only the second and the third is of interest. The elimination of complete fingers is neglected to comply with the definition of anthropomorphism derived in Section 2.2.1. Also, the sense of touch is irrelevant for the conceptual design.

The results of the study relevant to this dissertation are summarized in Table 4.1. Saliba et al. derived that the elimination of individual IP joints has a negligible influence on dexterity. However, the elimination of the IP joints in all digits results in a considerable impairment of

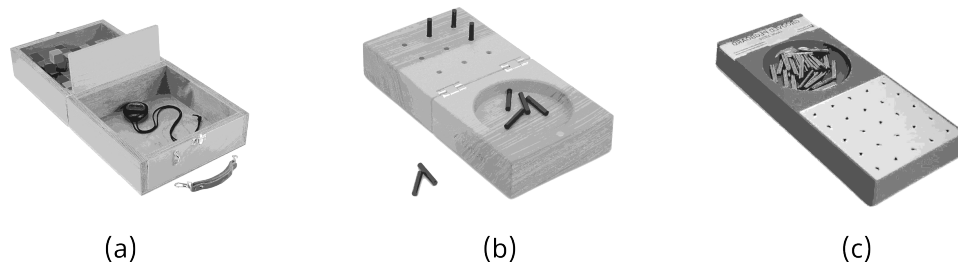


Figure 4.4: Rehabilitation tests: (a) Box and Block Test, (b) Nine Hole Peg Test, and (c) Grooved Pegboard Test (Frommelt and Lösslein 2011).

the dexterity. The elimination of the A-A of all fingers has shown a negligible influence on the Box and Block Test. However, for the Grooved Pegboard Test the influence is significant. For the entirety of the results, the reader is referred to the work by Saliba et al. (2013).

It is further noted that searching for studies on joint relevance turned out to be an effective strategy. Studies could be identified that propose a minimal configuration robot hand (e.g. Dalli and Saliba 2016)⁴, building upon the results of Saliba et al.'s study. This dissertation will therefore do the same and exploit the results to identify minimal configurations. However, for

| | Free | No A-A | Interphalangeal joints immobilized | | | | | |
|---------------------------|-------|--------|------------------------------------|------|------|------|------|------|
| | | | LF | RF | MF | IF | Th | All |
| Dexterity Score (%) (BBT) | 100.0 | 92.0 | 100.8 | 95.7 | 91.8 | 94.4 | 94.4 | 85.6 |
| Dexterity Score (%) (GPT) | 100.0 | 65.3 | 99.0 | 91.7 | 79.7 | 87.6 | 90.1 | 60.1 |

Table 4.1: Dexterity Scores under different immobilization conditions from the work by Saliba, Chetcuti and Farrugia Saliba et al. 2013.

proper interpretation of the results reported by Saliba et al. in the context of this dissertation, their findings must be critically evaluated. First, the experimental tests do not cover a wide range of object geometries and sizes; instead, all tests involve a similarly shaped object of relatively small dimensions. Therefore, the generalizability of the findings is limited and must be questioned. Second, the results obtained from the Box and Block Test and Grooved Pegboard Test should be considered separately. Saliba et al. (2013) note in their work that the Box and Block Test can be divided into four phases: grasping, transferring, releasing the block, and returning the hand. The calculated dexterity metric in this case primarily reflects the grasp phase. In contrast, the Grooved Pegboard Test consists of six phases: grasping, transferring, manipulating, inserting the peg, releasing it, and returning the hand. Accordingly, the derived

⁴Saliba et al. themselves exploited the results as well in a later study for a minimal configuration design.

dexterity metric incorporates time segments related to grasping and manipulation. Since this dissertation focuses primarily on grasping (instead manipulation) and the objects used in both tests are similar in dimension, the results of the Box and Block Test are more relevant to this dissertation than those of the Grooved Pegboard Test.

A literature search on grasp synergies and minimal actuation through underactuation revealed several influential studies. Many of these works investigate how fingers can be coordinated to achieve the best possible synergy among a set of grasps. For the purposes of this study, the most relevant results are presented in the work by Tavakoli et al. (2015). In that study, actuation strategies in the form of finger coordinations are proposed for each grasp from Feix's taxonomy. For the exact process of derivation, it is referred to the work by Tavakoli et al. (2015).

The proposed actuation strategies are summarized in Table 4.2. On the left is the name of the actuation strategy, and on the right is the associated combination of underactuation. A term not separated by a plus sign denotes one DOA for the specified movement. For example, "F-E LF-RF" denotes a single DOA for the F-E of the little finger and ring finger, thus proposing interfinger coordination between the little finger and ring finger, and intrafinger coordination for the F-E within these fingers.⁵

A summarized form of actuation strategy assignments to the Feix's grasps is given in Figure 4.5. In the original work, several possible actuation strategy are given for each grasp. Here, only the minimal actuation strategy is listed. Further, only the grasps from the reduced Feix taxonomy are given, for conciseness.



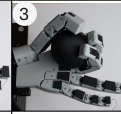
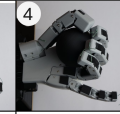
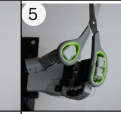
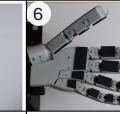
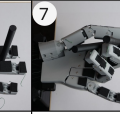
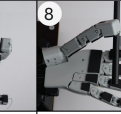
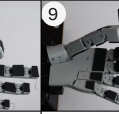
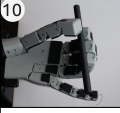


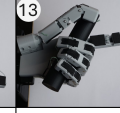
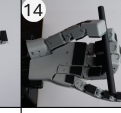
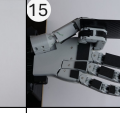
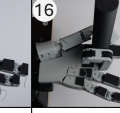
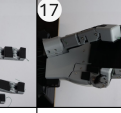
| | | | | | | | | |
|---|---|---|---|---|---|--|---|---|
|  |  |  |  |  |  |  |  |  |
| 1.0 | 3.0 | 2.0M | 1.0 | 3.0 | - | 2.0C | 3.0 | 4.0M |
|  |  |  |  |  |  |  |  | |
| 4.3 | 1.0 | 2.0C | 3.0M | 2.0C | 2.0M | 2.0 | 1.0 | |

Figure 4.5: Joint coordination strategies from the work by Tavakoli et al. (2015) (see Table 4.2) assigned to grasps from Feix's taxonomy.

⁵The terminology used in the work by Tavakoli et al. (2015) is slightly adjusted to comply to the one used in this dissertation.

⁶In the work by Tavakoli et al, "F1" is given. This must be an error, as the notation of the work does not assign any finger to "1". Taking into account the comments assigned to Grasp number 7, the "F1" is replaced by "F5", which is here the little finger.

| Name | Actuation |
|------|---|
| 1.0 | F-E Th, IF, MF, RF, LF |
| 2.0 | F-E Th + F-E IF, MF, RF, LF |
| 2.0C | A-A Th, F-E Th + F-E IF, MF, RF, LF |
| 2.0M | F-E Th + F-E IF, MF, RF, LF + Manual A-A Th |
| 3.0 | F-E Th + F-E IF + F-E MF, RF, LF |
| 3.0C | A-A Th, F-E Th + F-E IF + F-E MF, RF, LF |
| 3.0M | F-E Th + F-E IF + F-E MF, RF, LF + Manual A-A Th |
| 3.1 | A-A Th + F-E Th + F-E IF, MF, RF, LF |
| 3.2 | A-A Th + F-E Th, MF, RF, LF + F-E IF |
| 3.3 | A-A Th + F-E Th, IF + F-E MF, RF, LF |
| 4.0 | A-A Th + F-E Th + F-E IF + F-E MF, RF, LF |
| 4.0M | F-E Th + F-E IF + F3 + F-E RF, LF + Manual A-A Th |
| 4.1 | A-A Th + F-E Th, IF + F-E MF + F-E RF, LF |
| 4.2 | F-E Th + F-E IF + F-E MF + F-E RF, LF |
| 4.3 | F-E Th + F-E IF + F-E MF, RF + F-E LF |
| 5.0 | A-A Th + F-E Th + F-E IF + F-E LF ⁶ + F-E MF, RF |

Table 4.2: Actuation strategy names with corresponding recommended joint coordination from the work by Tavakoli et al. (2015).

4.3 Foundation for Task-Based Recommendation

This section aims at deriving evaluation criteria and, by combining the results from the relevant studies, defining task-based definitions of relevant criteria. The sets of relevant evaluation criteria are associated to individual grasp, respectively, whereby the reduced Feix taxonomy is applied as proof of concept. However, combining the identified works is not possible without further ado. On the one hand, relevant studies that provide the required information on joint configuration and coordination were successfully identified. On the other hand, combining them is difficult, as the studies were performed on different bases and objectives. For instance, the findings from the SRH can only be interpreted for a task description involving all grasps; the findings by Tavakoli et al. (2015) can be interpreted for a task description based on individual grasps; and the findings by Saliba et al. (2013) are not associated to task descriptions involving feix grasps but other test procedures. The interpretation of the results from the last study is particularly challenging. For example, it is stated that 67.8% grasping ability is lost when limiting the middle finger (see Saliba et al. 2013). This allows little practical interpretation, e.g. if the remaining dexterity suffice to securely hold a large cylinder.

Therefore, this dissertation proposes to consolidate the findings in form of evaluation criteria to establish the lowest common denominator. All of the studies analyze the requirements for

grasping or manipulation tasks, regardless of whether the hand is human or robotic. The two types of hand share the same anthropomorphic joint terminology and movements. Therefore, in a first step, existing anthropomorphic movements are defined in form of evaluation criteria. In a second step, for each Feix grasp, it is identified which of the criteria are required (i.e. interpretation of results from Saliba et al. (2013)). The required criteria for a task description involving all grasps must correspond to the findings found in the SRHs.

4.3.1 Criteria

Against above background, this dissertation introduces two task-based evaluation criteria categories *Anthropomorphic Movements* (A.M.) and *Movement Independence* (M.I.). Within the former, existing anthropomorphic movements are captured, where each anthropomorphic movement serves as an evaluation criterion that can be specified if that movement is required for a certain grasp. Within the latter, evaluation criteria are defined that allow specifying which anthropomorphic movements can be coordinated.

The recorded criteria for the Anthropomorphic Movements and Movement Independence are given in Table 4.3. As shown, the movements are assigned to the corresponding finger on the left. On the right, the criteria associated to the Movement Independence allow to specify the necessity of a movement's independence.

The terminology used for the criteria follows defined rules. First, the criteria must enable the identification of the requirements of a given grasp. Second, the criteria must be assignable to the defined GFPSs.

Regarding the first aspect, the criteria are formulated in such a way that the relevance and independence of a movement for a given grasp can be determined through the selection or non-selection of the criteria. For example, selecting "Enable IF F-E" for a given grasp indicates that F-E of the index finger is necessary for that grasp. Further, selecting only "Elim. IF individual DIP F-E" implies that the PIP and DIP joints of the index finger may be coordinated, while the MCP joint must remain independent.

Regarding the second aspect, the criteria are named using the same terminology as the PSs. On the one hand, this ensures that the criteria can be directly addressed by GFPSs, which is applied in Chapter 5 for the automated identification of suitable GFPSs based on selected criteria. On the other hand, it enables checking for completeness: for instance, on the right side of Figure 4.3, coordination of finger F-E is only defined between adjacent fingers, since no GFPSs were found that coordinate non-adjacent fingers.

The presented criteria for Anthropomorphic Movements and Movement Independence are the result of iterative adjustments. Inconsistencies, missing criteria, and unnecessary redundancies were continuously identified and corrected during the identification process. For example, a finger's F-E was initially defined separately for each joint (DIP F-E, PIP F-E, MCP F-E).

| | Anthropomorphic Movements (A.M.) | Movement Independence (M.I.) |
|---------------|--|---|
| Little Finger | Enable LF F-E Enable LF A-A | Elim. LF individual DIP F-E Elim. LF individual PIP F-E Elim. LF individual A-A Elim. LF individual F-E towards RF Elim. LF individual F-E towards A-A |
| Ring Finger | Enable RF F-E Enable RF A-A | Elim. RF individual DIP F-E Elim. RF individual PIP F-E Elim. RF individual A-A Elim. RF individual F-E towards MF Elim. RF individual F-E towards A-A |
| Middle Finger | Enable MF F-E Enable MF A-A | Elim. MF individual DIP F-E Elim. MF individual PIP F-E Elim. MF individual A-A Elim. MF individual F-E towards IF Elim. MF individual F-E towards A-A |
| Index Finger | Enable IF F-E Enable IF A-A | Elim. IF individual DIP F-E Elim. IF individual PIP F-E Elim. IF individual A-A Elim. IF individual F-E towards Th. Elim. IF individual F-E towards A-A |
| Thumb | Enable Th. F-E Enable Th. A-A radial Enable Th. A-A palmar Enable Th. P-S | Elim. Th. individual IP F-E Elim. Th. individual MCP F-E Elim. Th. individual TMC A-A palmar Elim. Th. individual MCP A-A radial towards Th. Elim. Th. individual F-E towards Th. A-A |

Table 4.3: Criteria for Anthropomorphic Movements and Movement Independence for all fingers.

However, this approach posed two main issues. First, it complicated the identification of relevant criteria, as the above relevant studies do not provide sufficient information to determine the importance of individual joints for overall F-E. Second, it became evident that, because of the first, reducing a finger's F-E to a single criterion produced the same overall results.

As another example, it was found that the specification "towards" which finger another finger's F-E is coordinated is relevant. Initially, the criterion "Eliminating LF individual F-E towards R.F." was defined without the specification of the neighboring finger. This turned out to pose a challenge for the definition of appropriate GFPSs. For example, assuming an actuation strategy requires the thumb's A-A and F-E to be combined and all finger's F-E to be coordinated. Regarding the criteria, all "Elim. X individual ..." are chosen. Based on above definition of

requirements, however, many viable solution in terms of appropriate GFPSs existed. Among them, the coordination of all digits F-E and the thumb's A-A would satisfy the requirements. Thus, the requirement rose to define which neighboring fingers may not be coordinated.

Examples of how the criteria are applied can be found in the following section. The examples include the derivation of the identified criteria for the Feix grasps and the presentation of the recommended GFPSs implied by these criteria. To improve clarity, the examples for the Anthropomorphic Movements and Movement Independence are presented separately.

4.3.2 Requirement Combinations

Before recommendations can be derived, an example identification of relevant criteria for different requirements is presented. Three scenarios are defined, involving the criteria from Anthropomorphic Movements and Movement Independence: First, a finger's A-A movement is not needed; Second, a finger's A-A movement is needed and needs to be independently actuated; and lastly, a finger's A-A movement is needed and does not need to be actuated separately. For all three scenarios, the recommendations for the little finger are given in Table 4.4, where relevant criteria are colored blue. As given, for the first scenario, neither criterion is chosen: the movement is not enabled, as it is not required, and its independence can thus also not be eliminated. For the second scenario, only the Anthropomorphic Movements criterion is chosen: The movement is enabled, as it is required, and its independence is not eliminated, as it must be individually actuated. For the third scenario, criteria in both categories are chosen: The movement is enabled, as it is required, and its independence is eliminated, as it is not required.

After discussing how criteria relevance is applied for different scenarios, combination rules

| Scenario 1 | Scenario 2 | Scenario 3 |
|-------------------------|-------------------------|-------------------------|
| Enable LF A-A | Enable LF A-A | Enable LF A-A |
| Elim. LF individual A-A | Elim. LF individual A-A | Elim. LF individual A-A |

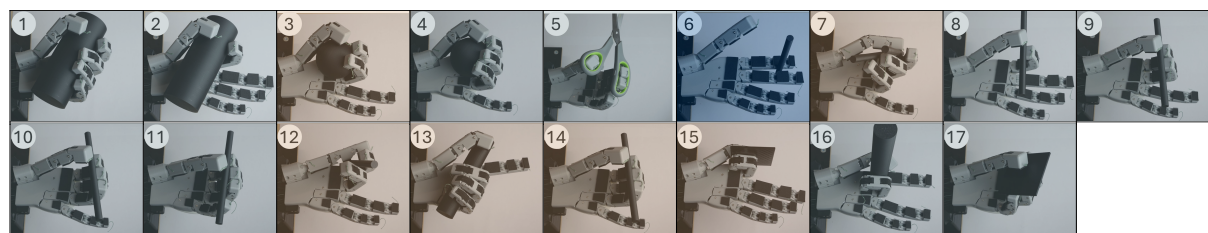
Table 4.4: Criteria combination of Anthropomorphic Movements and Movement Independence for three defined grasp scenarios: 1) LF A-A movement not needed; 2) LF A-A movement needed with independent actuation; 3) LF A-A movement needed and may be coordinated.

in case of multiple requirements are discussed. If criteria are defined for more than one grasp and all grasps have to be considered together for a recommendation, the question arises how to define a combination of all relevant criteria. Because of the different connotations of Anthropomorphic Movements and Movement Independence criteria, the established rules are different. For Anthropomorphic Movements criteria, a criterion is considered relevant if it is

defined as relevant for at least one of the grasps. The rule is based on the logic that a certain movement must be enabled for all grasps if it is relevant for at least one grasp. For Movement Independence criteria, a criterion is only considered relevant if it is defined as relevant for all grasps. The rule follows from the logic that the independence of a movement can only be eliminated if it is legitimate for all the grasps considered.

4.3.3 Recommendations for Joint Configuration

The derived requirements of Anthropomorphic Movements criteria for grasps from the reduced Feix taxonomy are given in Figure 4.6. The figure lists all grasps and assigns the derived required criteria by color to the respective grasps. In the following, the process of derivation is explained in detail. First, it is reasoned about the general requirements of A-A DOFs of middle



| | | |
|----------------------|----------------------|----------------------|
| Enable LF F-E | Enable LF F-E | Enable LF F-E |
| Enable LF A-A | Enable LF A-A | Enable LF A-A |
| Enable RF F-E | Enable RF F-E | Enable RF F-E |
| Enable RF A-A | Enable RF A-A | Enable RF A-A |
| Enable MF F-E | Enable MF F-E | Enable MF F-E |
| Enable MF A-A | Enable MF A-A | Enable MF A-A |
| Enable IF F-E | Enable IF F-E | Enable IF F-E |
| Enable IF A-A | Enable IF A-A | Enable IF A-A |
| Enable T. F-E | Enable T. F-E | Enable T. F-E |
| Enable T. A-A radial | Enable T. A-A radial | Enable T. A-A radial |
| Enable T. A-A palmar | Enable T. A-A palmar | Enable T. A-A palmar |
| Enable T. P-S | Enable T. P-S | Enable T. P-S |

Figure 4.6: Derived requirements of Anthropomorphic Movements criteria for grasps from the reduced Feix taxonomy. Colored criteria are required for the respective grasp.

finger and ring finger. Analyzing the SRH, it is apparent that the MCR Hand II (see Figure 3.5) provides full performance and does not apply the A-A of middle finger and ring finger. It is thus concluded that these DOFs are neglectable for either Feix grasp.

Second, it is reasoned about the requirements of index finger and little finger A-A DOFs. Initially, information can be gained from analysis of SRHs. It can be seen that consideration of A-A DOFs are found to be the sole difference between SRHs and unsuccessful robot hand

designs within the ERHs (see Figure 3.6). It is thus reasoned that the MCP's A-A DOFs of little finger and index finger are required for the complete scope of grasping, whereby it remains unclear how this relates to individual grasps. Subsequently, the suggestions by Tavakoli et al. are taken into account: Besides the thumb's A-A, the fingers' A-A DOFs are not considered in neither of the given actuation strategies. Only for the cigarette grasp, it is stated that the A-A of index finger is required. Comparing that to the unsuccessful robot hands that have the same joint configuration as the SRH besides the A-A DOF, they, indeed, report 32 out of 33 successful grasps. Therefore, it is concluded from this observation that the index finger A-A is only necessary for that single grasp. Otherwise, the index finger and little finger A-A DOF is proven by the unsuccessful ERHs to be neglectable. Especially the latter is supported by the findings of Saliba et al. (2013), where the elimination of the entire little finger resulted in a neglectable degradation of the performance.

To justify the omission of the fingers' A-A DOFs for most grasps, the findings by Saliba et al. (2013) are critically evaluated. Their results initially appear to contradict the elimination of A-A DOFs, reporting an approximately 35% reduction in dexterity when all fingers' A-A DOFs are removed. However, this result is based on the Grooved Pegboard Test, whereas the more relevant Box and Block Test shows a considerably smaller reduction in dexterity. Furthermore, it is acknowledged in the study's limitations that "the abduction/adduction degrees of freedom of the fingers may not have been constrained at their optimal angles." This limitation further weakens the impact of the reported 35% dexterity loss.

There remain concerns that can only be addressed through dedicated analysis in future work. First, it is notable that SRHs typically implement both of these DOFs. Second, the inclusion of an A-A DOF for the little finger seems to be relevant: This DOF is primarily responsible for the inward rotation of the little finger toward the palm, a movement that becomes particularly evident when grasping spherical or large cylindrical objects. It is also worth noting that, from an evolutionary perspective, this DOF appears to have been conserved despite the little finger's limited role in manipulation tasks. The little finger is used almost exclusively for grasping, which might suggest that the presence of this DOF is functionally important and not easily explained by other factors. However, a definitive conclusion would require extensive experimental validation and is therefore left for future work.

As a third step, the relevance of the thumb's Pronation-Supination DOF and its radial A-A DOF is evaluated. The Pronation-Supination DOF is typically associated with the third DOF of the TMC joint, and the radial A-A with the second DOF of the MCP joint, as described in Section 3.2.1. The majority of the SRHs successfully performed all grasps defined by Feix without implementing these DOFs, and reported that compensation was achieved through cleverly applied inclination and twist angles (Greibenstein 2016). It is therefore concluded that neither of these DOFs is strictly required for executing the considered set of grasps.

As a fourth step, the relevance of the thumb's palmar A-A DOF is evaluated. To support a minimal actuation, a basic configuration is defined in which the robot hand has a default posture with the thumb adducted. It is therefore concluded that the palmar A-A DOF is only necessary if a given grasp requires the thumb to be in an abducted or intermediate position. Such a classification is provided, for example, in the work of Tavakoli et al. (2015).

As a fifth step, the relevance of F-E and the contribution of IP joints is discussed. The F-E of each finger is considered relevant for every grasp. Defining otherwise would justify the application of GFPSs that eliminate an entire finger, which is avoided in this dissertation due to the adopted definition of anthropomorphism. Regarding the specific contribution of a finger's IP joints to F-E, a clear conclusion is difficult to draw. The study by Saliba et al. provides limited insight in this respect. On the one hand, the omission of individual IP joints results in only negligible loss of dexterity. On the other hand, the simultaneous elimination of all IP joints leads to a considerable reduction in dexterity. At the same time, all SRHs include implementation of their IP joints. Only the Awiwi Hand by Grebenstein (2016) omits the little finger's DIP joint. This design choice aligns with the findings of Saliba et al., as the little finger is the only finger that maintains nearly 100% dexterity when its DIP joint is removed. It is therefore concluded that the elimination of an IP joint generally has a negative effect on a finger's F-E, with the exception of the little finger.

4.3.4 Recommendations for Joint Coordination

The derived requirements of Movement Independence criteria for grasps from the reduced Feix taxonomy are given in Figure 4.7. The figure lists all grasps and assigns the required criteria by color. The derivation of these requirements is explained in the following.

First, it is reasoned about the requirements of independent movement within a finger. Considering the results from the study by Tavakoli et al., all recommendations are given in form of interfinger coordinations. It is thus concluded that the digits F-E DOFs can be coordinated. Therefore, the corresponding criteria for elimination of their independence are chosen. Identical conclusions are drawn when analyzing the SRHs.

Second, it is reasoned about the requirements of independent A-A movements of the fingers. For the requirements in Anthropomorphic Movements, it is derived that the finger's A-A movement can be neglected for each grasp. Considering the derived scenarios in Table 4.4, the criteria for the independent A-A movements are thus not chosen.

Based on above considerations, only the interfinger coordination for each grasp must be evaluated. If the F-E within a finger is decided to be coordinated for all grasps and each finger's A-A is irrelevant, only the criteria for F-E independence between the fingers is remaining. Therefore, each Feix grasp is evaluated according to the suggestions made by Tavakoli et al. (2015).

Recommendations for grasps with assigned 1.0 actuation strategy are given in Table 4.7 colored

| | | |
|--|-------------------------------|-------------------------------|
| Elim. LF ind. DIP F-E | Elim. LF ind. DIP F-E | Elim. LF ind. DIP F-E |
| Elim. LF ind. PIP F-E | Elim. LF ind. PIP F-E | Elim. LF ind. PIP F-E |
| Elim. LF ind. A-A | Elim. LF ind. A-A | Elim. LF ind. A-A |
| Elim. LF ind. F-E tow. R.F. | Elim. LF ind. F-E tow. R.F. | Elim. LF ind. F-E tow. R.F. |
| Elim. RF ind. DIP F-E | Elim. RF ind. DIP F-E | Elim. RF ind. DIP F-E |
| Elim. RF ind. PIP F-E | Elim. RF ind. PIP F-E | Elim. RF ind. PIP F-E |
| Elim. RF ind. A-A | Elim. RF ind. A-A | Elim. RF ind. A-A |
| Elim. RF ind. F-E tow. M.F. | Elim. RF ind. F-E tow. M.F. | Elim. RF ind. F-E tow. M.F. |
| Elim. MF ind. DIP F-E | Elim. MF ind. DIP F-E | Elim. MF ind. DIP F-E |
| Elim. MF ind. PIP F-E | Elim. MF ind. PIP F-E | Elim. MF ind. PIP F-E |
| Elim. MF ind. A-A | Elim. MF ind. A-A | Elim. MF ind. A-A |
| Elim. MF ind. F-E tow. I.F. | Elim. MF ind. F-E tow. I.F. | Elim. MF ind. F-E tow. I.F. |
| Elim. IF ind. DIP F-E | Elim. IF ind. DIP F-E | Elim. IF ind. DIP F-E |
| Elim. IF ind. PIP F-E | Elim. IF ind. PIP F-E | Elim. IF ind. PIP F-E |
| Elim. IF ind. A-A | Elim. IF ind. A-A | Elim. IF ind. A-A |
| Elim. IF ind. F-E tow. T. | Elim. IF ind. F-E tow. T. | Elim. IF ind. F-E tow. T. |
| Elim. T. ind. IP F-E | Elim. T. ind. IP F-E | Elim. T. ind. IP F-E |
| Elim. T. ind. MCP F-E | Elim. T. ind. MCP F-E | Elim. T. ind. MCP F-E |
| Elim. T. ind. MCP A-A radial | Elim. T. ind. MCP A-A radial | Elim. T. ind. MCP A-A radial |
| Elim. T. ind. F-E tow. T. A-A | Elim. T. ind. F-E tow. T. A-A | Elim. T. ind. F-E tow. T. A-A |
|  | | |
| Elim. LF ind. DIP F-E | Elim. LF ind. DIP F-E | Elim. LF ind. DIP F-E |
| Elim. LF ind. PIP F-E | Elim. LF ind. PIP F-E | Elim. LF ind. PIP F-E |
| Elim. LF ind. A-A | Elim. LF ind. A-A | Elim. LF ind. A-A |
| Elim. LF ind. F-E tow. R.F. | Elim. LF ind. F-E tow. R.F. | Elim. LF ind. F-E tow. R.F. |
| Elim. RF ind. DIP F-E | Elim. RF ind. DIP F-E | Elim. RF ind. DIP F-E |
| Elim. RF ind. PIP F-E | Elim. RF ind. PIP F-E | Elim. RF ind. PIP F-E |
| Elim. RF ind. A-A | Elim. RF ind. A-A | Elim. RF ind. A-A |
| Elim. RF ind. F-E tow. M.F. | Elim. RF ind. F-E tow. M.F. | Elim. RF ind. F-E tow. M.F. |
| Elim. MF ind. DIP F-E | Elim. MF ind. DIP F-E | Elim. MF ind. DIP F-E |
| Elim. MF ind. PIP F-E | Elim. MF ind. PIP F-E | Elim. MF ind. PIP F-E |
| Elim. MF ind. A-A | Elim. MF ind. A-A | Elim. MF ind. A-A |
| Elim. MF ind. F-E tow. I.F. | Elim. MF ind. F-E tow. I.F. | Elim. MF ind. F-E tow. I.F. |
| Elim. IF ind. DIP F-E | Elim. IF ind. DIP F-E | Elim. IF ind. DIP F-E |
| Elim. IF ind. PIP F-E | Elim. IF ind. PIP F-E | Elim. IF ind. PIP F-E |
| Elim. IF ind. A-A | Elim. IF ind. A-A | Elim. IF ind. A-A |
| Elim. IF ind. F-E tow. T. | Elim. IF ind. F-E tow. T. | Elim. IF ind. F-E tow. T. |
| Elim. T. ind. IP F-E | Elim. T. ind. IP F-E | Elim. T. ind. IP F-E |
| Elim. T. ind. MCP F-E | Elim. T. ind. MCP F-E | Elim. T. ind. MCP F-E |
| Elim. T. ind. MCP A-A radial | Elim. T. ind. MCP A-A radial | Elim. T. ind. MCP A-A radial |
| Elim. T. ind. F-E tow. T. A-A | Elim. T. ind. F-E tow. T. A-A | Elim. T. ind. F-E tow. T. A-A |

Figure 4.7: Derived requirements of Movement Independence criteria for grasps from the reduced Feix taxonomy. Colored criteria are required for the respective grasp.

in blue. According to Tavakoli et al., a single actuator need to suffice. Therefore, all finger F-E movements are coordinated towards the neighboring finger, highlighting the respective Movement Independence criteria for independence elimination.

Recommendations for grasps with assigned 3.0 actuation strategy are given in Table 4.7 colored in light blue. From the requirements in Anthropomorphic Movements criteria, it is established that only F-E movements are required. According to the definition of the 3.0 actuation strategy, one actuation is assigned to the thumb, index finger and the remaining fingers, respectively. Thus, the little finger, ring finger and middle finger are coordinated. Therefore, the criteria for elimination of their movement's independence are chosen.

The remaining grasps follow similarly the definition of the assigned actuation strategy. Depending on the given suggestion, the respective fingers are coordinated and the corresponding criteria for elimination of that movement's independence chosen.

4.4 Conclusion

In this chapter, the requirements for optimal robot hand concepts in form of evaluation criteria based on user requirements are derived. In a first step, user requirements relevant for the conceptual design are defined. In a second step, possible evaluation criteria and their overarching categories are established. Thirdly, relevant studies found in the literature are collected. Lastly, the findings of the relevant studies are consolidated in form of specification of relevant evaluation criteria for different user requirements.

Regarding the first point, a recommendation of a robot hand concept is proposed to involve a trade-off between at least two factors. This dissertation proposes the user to (1) select grasps from Feix's taxonomy to define the performance requirements in form of designated grasping tasks and to (2) define preference between design simplicity and Motion Ability. With the performance requirements, a preselected set of viable Hand Concepts can be defined. The preselected set is then sorted with descending number of DOA. Based on the user's preference, either the Hand Concept on the left or the right in the sorted set is recommended.

Regarding the third point, results from literature on joint relevance and minimal actuation are leveraged. The findings from the defined SRH, from the work by Saliba et al. (2013) and from the work by Tavakoli et al. (2015) are used to define requirement criteria for each grasp. These criteria comprise required anthropomorphic movements and their independence and are addressable by GFPSs.

In a subsequent step to the automated task-based identification of relevant evaluation criteria derived in this chapter, an automated task-based generation of a hand concept recommendation is derived in Chapter 5. Based on the derived requirement criteria, viable Hand Concepts for each grasp can be defined by identifying the GFPSs that address these criteria most appropriately.

5 Guidance Control System Design

To answer the research question, this chapter addresses the third objective (O3) by detailing the control system of the guidance framework. Based on the architecture of a knowledge-based system, the control system comprises four sub-components, each covered in this chapter. Section 5.1 introduces the problem. In Section 5.2, the Inference Component is developed and in Section 5.3 the guidance's interfaces are developed, comprising the Dialog, Explanation, and Knowledge Acquisition Components. The Inference Component is responsible for the automated evaluation of a hand concept based on the influence of its respective GFPSs on the evaluation criteria.

5.1 Problem Statement and Approach

The methodology developed in this dissertation is inspired by the classic approach to methodical product development, illustrated in Figure 5.1. As shown, design options are evaluated against defined criteria, weighted, and aggregated into a final score. The option with the highest score is then selected.

The classic approach can be mapped onto the structure and terminology used in this dissertation.

| | Weight | Option 1 | Option 2 | Option 3 |
|------------|--------|----------|----------|----------|
| Criteria 1 | 0.1 | 1 | 3 | 4 |
| Criteria 2 | 0.3 | 4 | 2 | 1 |
| Criteria 3 | 0.2 | 3 | 1 | 1 |
| Criteria 4 | 0.4 | 2 | 4 | 2 |

Figure 5.1: Example pairwise evaluation approach in methodical product development.

The three options shown in Figure 5.1 represent OR alternatives, requiring a choice. In this dissertation's terminology, they correspond to GFPSs within a given GFoI. Following the logic of the classic approach, each GFPS must be evaluated by assigning influence values to each criterion, which are then weighted and summed to yield a score.

This procedure results in an overall score for each Hand Concept from Chapter 3, which enables the guidance to identify the most suitable Hand Concept. Assuming a single GFoI with three GFPSs, the exploration yields four Hand Concepts: three that each apply one GFPS, and

one that applies none. If the GFPSs are evaluated against criteria as described above, each Hand Concept inherits the score of its respective GFPS. The developed guidance would then recommend the Hand Concept with the highest score. Analogous to this example with only one GFoI, the score of an Hand Concept with multiple GFoIs is calculated as the sum of the scores of all applied GFPSs.

Following this procedure, the evaluation would need to be performed for every GFoI and thus in total for 86 GFPSs, as illustrated in Figure 5.2. The given parameter in Figure 5.2 are derived in Section 5.2.2.3 and depicted here for later reference.

The challenge of this approach, apart from the large number of evaluations required, lies in the

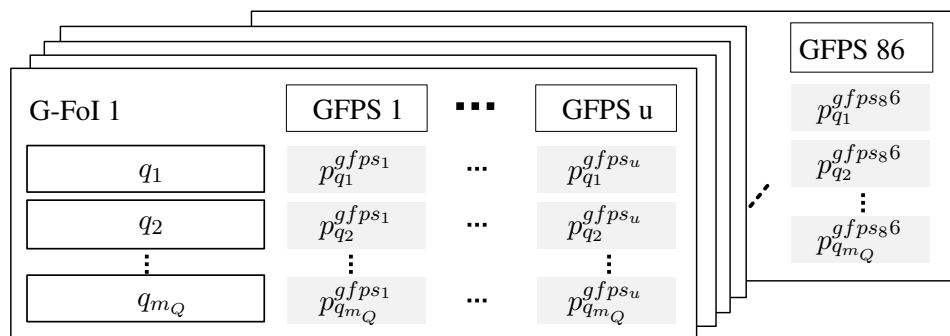


Figure 5.2: Presentation of the parameters to be identified according to the classic approach.

choice of influence values and weighting factors. Assuming that the criteria to be evaluated are defined, the question remains as to how to select influence values and weighting factors in such a way that the correct Hand Concept is selected by the system. In the above considerations, it was derived that each GFPS contributes a score to an Hand Concept and the Hand Concept with the highest score is recommended by the system. With exclusively positive influence values, this will inevitably result in the system always recommending the Hand Concept that applies the most GFPS. However, depending on the user input, it may happen that a Hand Concept that does not apply a certain GFoI (i.e. the GFPSs of this GFoI) is to be recommended. However, such a Hand Concept without this GFoI would only be recommended by the system if all GFPSs in this GFoI only have negative scores and a Hand Concept without the GFoI consequently has a higher overall score. The question therefore arises,

(Q5) how to choose influence values and weight factors to automatically identify the input-dependent (un)suitability of GFoIs .

Further, the knowledge-based assistance system shall reflect the trade-off of simplicity and dexterity and recommend a Hand Concept based on the user preference towards a side. It raises thus the question of

(Q6) how to choose influence values and weight factors to enable the algorithm to account for the trade-off in its recommendation .

A final challenge concerns the user-friendliness of the development. It should be avoided that influence values for 86 GFPSs against m_Q criteria must be manually identified and fine-tuned. Moreover, the method should be scalable and, hence, hard-coded case handling via "if-then" logic should be avoided. It thus raises the question of

(Q7) how to design the system development process to ensure ease of implementation and scalability.

5.2 Inference Component

This Section addresses the development of the Inference Component. To address the derived problems from the previous section, the evaluation criteria, weights and influences are discussed in respective subsections.

5.2.1 Weights

A challenge with weighting lies in its dependency on the user preferences, as the relevance of individual criteria is subjective. In classical product development processes, a pairwise comparison of criteria is often carried out to determine their relative importance. However, due to the anticipated large number of evaluation criteria, such a procedure cannot reasonably be expected from the user, as the use of the guidance must be intuitive and low-threshold.

However, an indispensable input to the system is the user's preference for the trade-off. As discussed in Chapter 4, depending on this preference, the algorithm recommends either the left side of the sorted preselected set of Hand Concepts (preference toward Motion Ability) or the right side (preference toward Simplicity).

To account for the user's preference, a preference weight w is introduced. To enable intuitive and low-threshold usage of the guidance, the user is only required to indicate their preference between Simplicity and Motion Ability. This input is internally processed into two distinct weighting factors w_1 and w_2 . All criteria are grouped according to their affiliation to either Simplicity or Motion Ability, and the respective weighting factor is then applied to each group accordingly. For the sake of simplicity, the preference weight w is restricted to values of either 1 or 3, with 3 being chosen for the preferred performance quality as specified by the user.

To meet the challenges defined in Section 5.1, a second weighting is introduced. The problem of identifying the (un)suitability of GFoIs is essentially linked to the question which evaluation criteria are relevant and if a certain GFoI address them. To identify relevant evaluation criteria,

a relevance weight is introduced here.

Technically, a GFoI is considered unsuitable if all of its associated GFPSs yield only negative scores for all addressed evaluation criteria. As a result, each Hand Concept applying any GFPS from that GFoI obtains a lower overall score than Hand Concepts not applying any of these GFPSs. The guidance would therefore not prioritize these Hand Concepts, since others without these unsuitable GFPSs achieve higher scores, which leads to what is referred to here as the unsuitability of a GFoI.

To implement this system behavior, it must be ensured that unsuitable GFPSs yield negative scores through the use of the relevance weight. Generally, inspired by the classic approach given in Figure 5.1, a GFPS can either positively or negatively address a given evaluation criterion, resulting in two basic cases. Furthermore, as derived in Section 4.3, some criteria are relevant for a given task while others are not, expanding the two cases into four different scenarios. Accordingly, the relevance weight needs to consider relevance of criteria and turn a GFPS' score either solely negative, or turn it positive. For example, positively addressing a criterion that is not desired must be penalized. Conversely, negatively addressing an undesired criterion must be rewarded, as this contributes to a minimal design. The latter is essential, since the PSs (and hence the GFPSs) are negatively connoted. As an illustration, consider the GFPS "Eliminating LF MCP A-A DOF". This GFPS should be applied in a final Hand Concept if that DOF is not required for the task. However, it negatively addresses the criterion "Enable LF A-A", derived in Section 4.3. As the GFPS is desired for the given task, the negative score must be inverted into a positive one.

To implement this type of behavior, the relevance weight v is introduced. Criteria that are not desired by the user are weighted with -1 . This penalizes positive influence on these criteria (representing unnecessary complication of the design) and inverts a negative influence, thereby rewarding desirable design simplification.

The magnitude of influence values remains an important parameter. The question remains as to how the influence values should be selected so that the global score of an undesired GFPS is ultimately negative. The introduction of a relevance weight alone is not effective, as a GFPS can simultaneously address relevant (not penalized) and irrelevant criteria (penalized). If the influence on relevant criteria is comparatively high, the penalized influence irrelevant criteria may only reduce the score rather than render it negative. Therefore, to properly handle the influence values, the criteria themselves are defined in advance in the next step.

5.2.2 Criteria

This section deals with the evaluation criteria. In a first step, the notation is introduced. Subsequently, further criteria necessary for the identification of influence values will be defined. Initially, a uniform terminology is introduced. In this dissertation, the evaluation criteria are

called *Quality Criteria*. The naming primarily serves the purpose of avoiding confusion when using the frequently occurring term "criterion". Further, the name is motivated by the fact that the Motion Ability was derived for the first time in Section 2.2.3 from the grasp qualities defined by Roa and Suárez (2015).

To address the user-friendliness issue described in (Q7), a categorization is applied to the foreseeable large amount of Quality Criteria. The categorization is shown in Fig. B.1 in the form of an Entity-Relation model. At the lowest level, the Quality Criteria consists of here called *Qualities*, which are assigned to *Superior Qualities* (SQs), and in turn grouped under *Major Qualities* (MQs). The Major Qualities represent the already established robot hand qualities Motion Ability and Simplicity. They are composed of their respective Superior Qualities. For the Major Quality Motion Ability, Superior Qualities, such as the Anthropomorphic Movements and Movement Independence are derived in Section 4.3. Correspondingly, the Qualities are the thereby established criteria for addressing the Superior Qualities Anthropomorphic Movements and Movement Independence. As discussed in Section 4.3, Qualities are named using gerund-form verbs so they can be directly addressed by PSs.

The subjective nature of the naming of the individual Qualities is recognized. However, it also is emphasized that the exact naming is irrelevant. As in the classic example given, evaluation criteria are merely used to compare two or more options qualitatively in pairs in order to decide between them. In fact, in the course of the derivation of the inference component in this Section, it is shown that the number of addressed Qualities and the terminology are irrelevant for the proper functioning of the algorithm - only the assignment to the higher-level categories (Superior Quality and Major Quality) is relevant.

5.2.2.1 Notation

The notation is derived in general form before assigning it to any already established Qualities. The Qualities that can be addressed by PSs are defined as

$$Q = \{q_1, q_2, \dots, q_i, \dots, q_{m_Q}\}, \quad (5.1)$$

where m_Q denotes the maximum number of Qualities, and $q_i \forall i \in \{1, \dots, m_Q\}$.

Further, each Superior Quality is given as q_{SQ_j} with

$$Q_{SQ} = \{q_{SQ_1}, q_{SQ_2}, \dots, q_{SQ_j}, \dots, q_{SQ_{m_{SQ}}}\}, \quad (5.2)$$

where m_{SQ} the total number of Superior Qualities and $q_{SQ_j} \forall j \in \{1, \dots, m_{SQ}\}$. Lastly, each Major Quality is given as q_{MQ_k} with

$$Q_{MQ} = \{q_{MQ_1}, q_{MQ_2}, \dots, q_{MQ_k}, \dots, q_{MQ_{m_{MQ}}}\}, \quad (5.3)$$

where m_{MQ} the total number of Major Qualities and $q_{MQ_k} \forall k \in \{1, \dots, m_{MQ}\}$. Next, the mappings of the above categorizations must be defined. While q_i , q_{SQ_j} and q_{MQ_k} are technically stored as strings, they are semantically linked by associations. This allows the definition of a mapping

$$\phi_Q : Q \rightarrow Q_{SQ} \quad (\text{with } \phi_Q(q_i) = q_{SQ_j}), \quad (5.4)$$

which specifies the assignment of a Quality to its corresponding Superior Quality. Formulated as a partition, this allows the definition of a subset

$$Q_{q_{SQ_j}} = \{q_i \in Q \mid \phi_Q(q_i) = q_{SQ_j}\}, \quad (5.5)$$

which assigns a set of q_i to a specific q_{SQ_j} . Furthermore, the surjective mapping from the Superior Qualities to the Major Qualities must be defined. This allows the definition of a mapping

$$\phi_{SQ} : Q_{SQ} \rightarrow Q_{MQ} \quad (\text{with } \phi_{SQ}(q_{SQ_j}) = q_{MQ_k}). \quad (5.6)$$

Thus the subset

$$Q_{q_{MQ_k}} = \{q_{SQ_j} \in Q_{SQ} \mid \phi_{SQ}(q_{SQ_j}) = q_{MQ_k}\} \quad (5.7)$$

can be defined, which assigns a set of q_{SQ_j} to a specific q_{MQ_k} . The following relationship therefore results graphically with both mappings:

$$q_i \xrightarrow{\phi_Q (Q \rightarrow Q_{SQ})} q_{SQ_j} \xrightarrow{\phi_{SQ} (Q_{SQ} \rightarrow Q_{MQ})} q_{MQ_k}.$$

To establish a surjective mapping from the Qualities to the Major Qualities, both mappings must be composed according to

$$\phi_{MQ} = \phi_{SQ} \circ \phi_Q : Q \rightarrow Q_{MQ}, \quad \text{with } \phi_{MQ}(q_i) = q_{MQ_k}, \quad (5.8)$$

where \circ denotes function composition. In conclusion, Equation (5.1) can thus be extended as follows:

$$\begin{aligned}
 Q &= \{q_1, q_2, \dots, q_{m_Q}\} \\
 &= \{Q_{q_{SQ_1}}, Q_{q_{SQ_2}}, \dots, Q_{q_{SQ_{m_{SQ}}}}\} \\
 &= \{Q_{q_{MQ_1}}, Q_{q_{MQ_2}}, \dots, Q_{q_{MQ_{m_{MQ}}}}\} \\
 &= \bigcup_{k=1}^{m_{MQ}} Q_{q_{MQ_k}}.
 \end{aligned} \tag{5.9}$$

5.2.2.2 Superior Qualities

After derived notation, the status quo of defined Quality Criteria from the previous chapters is captured. With the given limitation of this dissertation, only the trade-off between Motion Ability and Simplicity is considered. Therefor, one has $m_{MQ} = 2$ and q_{MQ_1} and q_{MQ_2} corresponding to "Motion Ability" and "Simplicity", respectively (see Table E.5). Furthermore, some Superior Qualities and Qualities are derived in Section 4.3 and presented in Table 4.3. With ascending numbering, the given criteria can be assigned to the introduced notation of Quality Criteria. Thus, q_{SQ_1} = "Anthropomorphic Movements" and q_{SQ_2} = "Movement Independence" (see Table E.6). Further, both are subordinated to q_{MQ_1} by $Q_{q_{MQ_1}} = \{q_{SQ_1}, q_{SQ_2}, \dots\}$. Lastly, twelve Qualities of the Superior Quality Anthropomorphic Movements are defined and can be assigned according to Equation (5.5) as $Q_{q_{SQ_1}} = \{q_1, q_2, \dots, q_{12}\}$. Similarly, the 25 defined Qualities for the Movement Independence can be assigned as $Q_{q_{SQ_2}} = \{q_{13}, \dots, q_{37}\}$. (see Table E.7)

In the given example from classic product development, evaluation criteria are defined by a preceding requirements analysis. Selected design options are then evaluated with regard to these criteria.

The procedure is adapted for the problem at hand in this dissertation. For the defined Major Qualities, it is elaborated which evaluation criteria are generally considered within Motion Ability and Simplicity and which of those are addressed by the captured PSs. This elaboration was performed simultaneously with the systematic mapping described in Chapter 3.

Following this approach, four additional Superior Qualities are defined for this dissertation. The Superior Qualities *Contact Conditions* (C.C.) and *Degree Of Actuation* (D.o.A.) were identified as prominent characteristics of Motion Ability and Simplicity, respectively.¹ In particular, studies addressing design approaches for intrafinger joint coordination highlight the relevance of these Qualities: joint underactuation enables fingers to passively adjust to

¹The specific capital writing "Degree Of Actuation" and notation D.o.A. shall distinguish the Superior Quality from the general term "degree of actuation".

objects of various shapes while simultaneously reducing the number of required motors. This contributes to improvements in both contact conditions and degrees of actuation. However, the finger trajectory becomes predefined due to the coordinated joints, causing the finger to lose part of its addressable workspace. This is not captured by the Superior Quality Anthropomorphic Movements, as the movement itself (F-E) remains possible. Therefore, the Superior Quality *Manipulability* (M.) is introduced to qualitatively capture the reduction in possible movement directions. Additionally, joint coordination increases the effort in mechanical design. To account for this negative impact on Simplicity, the identically named Superior Quality *Mechanical Design* (M.D.) is introduced (see Table E.6).

The assignment of the new Superior Qualities to the Major Qualities follows the derived notation. This results in $m_{SQ} = 6$ and the set of Superior Qualities assigned to

$$\begin{aligned} Q_{SQ} &= \{q_{SQ_1}, q_{SQ_2}, \dots, q_{SQ_6}\} \\ &= \{"A.M.", "M.I.", "C.C.", "M.", "M.D.", "D.o.A." \}. \end{aligned}$$

Identification of the respective Qualities is subject to a later section. For the sake of simplicity, the Qualities are derived when the influence values are defined.

5.2.2.3 Input Dependency

With respect to the introduced relevance weight in Section 5.2.1, input dependencies of the Qualities need to be defined. The relevance weight distinguishes between Qualities that are required by the user and those that are not required. The exact requirements need to be derived, thus, on the lowest level of the Quality Criteria.

As a first step, it is decided which of the Superior Qualities are subject to input dependency. The Qualities of the Superior Qualities Anthropomorphic Movements and Movement Independence have been defined for certain grasps. It is thus established that the corresponding Qualities are input dependent. For the remaining Superior Qualities, it is decided here that they are not in dependency of the input: Disregarding the specific grasp that is required, a simple design, a low DOA, and good contact conditions are always equally relevant. Further, the Superior Quality Manipulability is also decided here to be not input-dependent. A legitimate reduction in manipulability for the defined grasps is already covered by the input-dependent Superior Quality "Anthropomorphic Movements".

The requirements can therefore be summarized as follows. The requirements generally represent the Qualities that are required by an input. Regardless of the input, all Qualities of the Superior Qualities Contact Conditions, Manipulability, Mechanical Design and Degree Of Actuation are required. Only the Qualities of the Superior Qualities Anthropomorphic Movements and Movement Independence are dependent on the grasps selected by the user. A summary of those

requirements are presented in Figures 4.6 and 4.7 for the Superior Qualities Anthropomorphic Movements and Movement Independence, respectively.

5.2.3 Metric

This section derives the metric necessary for the method to calculate a final score of a Hand Concept. In the following, underlying terminologies and notations are introduced.

Each gfps_u addresses the set Q and assigns concrete numerical values to each q_i , which are referred to as the *influence values* in this dissertation. Mathematically, this can be represented by a mapping

$$f^{\text{gfps}_u} : Q \rightarrow \mathbb{R}, \quad f^{\text{gfps}_u}(q_i) = p_{q_i}^{\text{gfps}_u}, \quad (5.10)$$

with $p_{q_i}^{\text{gfps}_u}$ being the influence value, depending on the considered gfps_u and the considered Quality q_i . As a result, for each gfps_u , a vector,

$$\mathbf{p}_Q^{\text{gfps}_u} = \left(p_{q_1}^{\text{gfps}_u}, p_{q_2}^{\text{gfps}_u}, \dots, p_{q_{m_Q}}^{\text{gfps}_u} \right) \in \mathbb{R}^{m_Q}, \quad (5.11)$$

can be defined, which is referred to as the *Quality Profile* of the respective gfps_u . The influence values and thus the Quality Profiles are constant for a given gfps_u .

The Quality Profiles can be used to calculate scalar aggregate values for the Superior Qualities and Major Qualities

$$p_{SQ_j}^{\text{gfps}_u} = \sum_{q_i \in Q_{SQ_j}} p_{q_i}^{\text{gfps}_u} \quad \text{and} \quad p_{MQ_k}^{\text{gfps}_u} = \sum_{q_i \in Q_{MQ_k}} p_{q_i}^{\text{gfps}_u}, \quad (5.12)$$

which are equally constant for a given gfps_u .

Further, the Quality Profile is modified with respect to the relevance of the addressed Qualities by the relevance weight \mathbf{v} , as derived in Section 5.2.1. For this purpose, \mathbf{v} is defined as

$$\mathbf{v} = (v_1, v_2, \dots, v_i, \dots, v_{m_Q}) \in \mathbb{R}^{m_Q}. \quad (5.13)$$

With the Qualities being divided according to

$$Q = Q_I \cup Q_R, \quad (5.14)$$

where Q_I denotes the set of all $q_i \in Q$ that are required by the input, and Q_R represents the set of all remaining q_i , i.e. $Q_R = Q \setminus Q_I$. This now allows the definition of

$$v_i = \begin{cases} 1, & \text{if } q_i \in Q_I \\ -1, & \text{if } q_i \in Q_R \end{cases}$$

and results in \mathbf{v} being not constant but input-dependent.

Using \mathbf{v} , the relevance-weighted Quality Profile $\mathbf{p}_{R-Q}^{\text{gfps}_u}$ of a gfps_u is defined as

$$\mathbf{p}_{R-Q}^{\text{gfps}_u} = \mathbf{v} \odot \mathbf{p}_Q^{\text{gfps}_u} = (v_1 \cdot p_{q_1}^{\text{gfps}_u}, v_2 \cdot p_{q_2}^{\text{gfps}_u}, \dots, v_{m_Q} \cdot p_{q_{m_Q}}^{\text{gfps}_u}) = (p_{R-q_1}^{\text{gfps}_u}, \dots, p_{R-q_{m_Q}}^{\text{gfps}_u}). \quad (5.15)$$

Equally as applied to the Quality Profile, using Equation (5.12), the aggregate values for the Superior Qualities and Major Qualities $p_{R-SQ_j}^{\text{gfps}_u}$ and $p_{R-MQ_k}^{\text{gfps}_u}$ of the relevance-weighted Quality Profile can be defined.

After definition on GFPS level, the same equation shall be derived for a hand concept HC_l . Based on the above derivations, a Quality Profile

$$\mathbf{p}_Q^{\text{HC}_l} = (p_{q_1}^{\text{HC}_l}, p_{q_2}^{\text{HC}_l}, \dots, p_{q_{m_Q}}^{\text{HC}_l}) \in \mathbb{R}^{m_Q} \quad (5.16)$$

can be defined for a hand concept HC_l that applies at least one GFPS. Thereby, each $p_{q_i}^{\text{HC}_l}$ is defined by

$$p_{q_i}^{\text{HC}_l} = \sum_{u \in U_l} p_{q_i}^{\text{gfps}_u}, \quad (5.17)$$

with U_l being the set of all GFPSs applied to a hand concept HC_l . As the individual Quality Profiles are constant, the Hand Concepts' Quality Profiles are constant as well. Based on Equation (5.12), the aggregate values $p_{SQ_j}^{\text{HC}_l}$ and $p_{MQ_k}^{\text{HC}_l}$ can be defined, equally being constant. Further, using the introduced relevance weight \mathbf{v} and (5.15), the relevance-weighted influence values $p_{R-q_i}^{\text{HC}_l}$ and Quality Profile $\mathbf{p}_{R-Q}^{\text{HC}_l}$ of a given hand concept is defined. Finally, based on Equation (5.15), the relevance-weighted aggregate values $p_{R-SQ_j}^{\text{HC}_l}$ and $p_{R-MQ_k}^{\text{HC}_l}$ are defined.

For the next step, a start vector \mathbf{p}_S is required, which assigns an initial value to the Major Qualities. This is necessary by logic for two reasons. First, a Hand Concept needs to have a certain initial Motion Ability assigned to the IMDC, even without an applied GFPS. Second, the trade-off of Motion Ability and Simplicity describes a reduction of Motion Ability with every applied GFPS, which requires an initial Motion Ability to be reduced. The start vector \mathbf{p}_S , with

$$\mathbf{p}_S = (p_{S_1}, p_{S_2}, \dots, p_{S_{m_{MQ}}}), \quad (5.18)$$

is defined once.

Finally, above vectors can be used to define the score

$$x^{\text{HC}_l} = \mathbf{w} \cdot \left(\mathbf{p}_{R-MQ}^{\text{HC}_l} + \mathbf{p}_S \right) = \sum_{k=1}^{m_{MQ}} w_k \cdot \left(p_{R-MQ_k}^{\text{HC}_l} + p_{S_k} \right) \quad (5.19)$$

of a HC_l , where \mathbf{w} is the previously introduced preference weight, with

$$\mathbf{w} = (w_1, w_2, \dots, w_k \dots, w_{m_{MQ}}) \in \mathbb{R}^{m_{MQ}}. \quad (5.20)$$

5.2.4 Influence Identification

In this section, a method is derived that allows identifying the influence values and addressing the issues (Q6)-(Q7). First, it is explained why a reverse engineering approach is pursued in the developed method. Assumptions are then presented which, on the one hand, shall allow such reverse engineering and, on the other hand, shall reduce the number of parameters (~influence values) to be identified.

Some assumptions already made will first be formalized using the newly introduced notation in the form of equations. First, the necessity of the starting value \mathbf{p}_S has already been established. However, from the description, it can be inferred that a starting value is not required for Simplicity. From this, it follows that $\mathbf{p}_S = (p_{S_1}, 0)$. Second, conclusions can be drawn regarding the influence values. The Quality Criteria were introduced to describe the trade-off between Motion Ability and Simplicity in the design of robotic hands. When sorting a preselected set of Hand Concepts, this results in a decrease in Motion Ability and a corresponding increase in Simplicity from one end of the set to the other. Using the derived notation, this implies that the aggregate influence of the Major Quality Motion Ability must be negative ($p_{MQ_1}^{\text{GFPS}_u} < 0$), and the aggregate influence on Simplicity must be positive ($p_{MQ_2}^{\text{GFPS}_u} > 0$) of any given GFPS.

A reverse engineering approach is expedient for determining the influence values. In the classic approach described in Section 5.1, a bottom-up approach is applied: the options are evaluated with regard to the criteria without initial preference and the most suitable option is identified. For the problem of this dissertation, the opposite is the case. Through the derivations in Chapter 3, it is known which GFPSs should be used for which grasp. The identification of the influence values should therefore be rolled backwards to ensure that the correct GFPSs or GFoIs are selected.

The first assumption describes the rationale for not capturing the influence values of individual GFPSs on specific Qualities, but rather capturing the combined influences on Major Qualities

and Superior Qualities at the GFoI level. In a bottom-up approach, the influences $p_{q_i}^{\text{gfps}_u}$ on each q_i would need to be determined for each gfps_u , resulting in a large number of variables that would need to be identified. However, the meaningful grouping into GFoIs can be leveraged. The GFPSs in a given GFoI present alternative solutions and therefore essentially serve the same function. This means that even though the specific addressed Qualities vary among the GFPSs, the addressed Superior Qualities and Major Qualities will be the same. Furthermore, the meaningful grouping into FoI categories has also been introduced. By leveraging this grouping, the addressed Superior Qualities and Major Qualities of all GFoIs within a FoI category must be the same, since they essentially serve the same function (e.g., eliminating joints). This allows the addressed Superior Qualities and Major Qualities to be identified on GFoI level for the three established FoI categories, and these will be valid for all associated GFPSs. As a result, the number of parameters that need to be identified can be drastically reduced, with the influence values for all Qualities associated with an irrelevant Superior Quality set directly to zero.

The second assumption proposes the introduction of a standardized Quality Profile aggregate value $\left| p_{MQ,max}^{\text{gfps}_u} \right|$ per reduced DOA for the best-performing gfps_u in a GFoI. As previously derived, each gfps_u is associated with a constant Quality Profile $p_Q^{\text{gfps}_u}$ which can be aggregated in magnitudes $p_{MQ,k}^{\text{gfps}_u}$ per Major Quality. Within a GFoI, these magnitudes must differ in order to produce distinct scores x^{HC_i} , as one gfps_u within that set of alternatives is more appropriate. The gfps_u with highest magnitude is referred to as the best-performing within the GFoI. However, it becomes evident that such differentiation is only meaningful within a single GFoI, but not necessary across different GFoIs. With multiple GFoIs, the only relevant question is whether a GFoI should be applied for a given input. Accordingly, a binary classification (suitable/unsuitable) is sufficient. The exact contribution of the best-performing GFPS from a suitable GFoI to the overall Hand Concept score is irrelevant. It can thus be concluded that a uniform upper threshold $\left| p_{MQ,max}^{\text{gfps}_u} \right|$ per eliminated DOA can be defined for the best-performing GFPS within a GFoI and applied across all GFoIs, eliminating further variables.

The outcome of the first two assumptions is illustrated as follows: In Figure 5.3, the composition of an Hand Concept's Quality Profile-magnitude (i.e., its unweighted Hand Concept score x^{HC_i}) is shown for the case where a single gfps_u is applied. The initially assigned start value (purely associated to the Motion Ability) is reduced by the influence of the GFPSs on the Qualities associated with the Major Quality Motion Ability (i.e., $-p_{MQ,max}^{\text{gfps}_u}$) and increased by the same amount due to its influence on the Major Quality Simplicity (i.e., $+p_{MQ,max}^{\text{gfps}_u}$). Figure 5.4 shows the Quality Profile-magnitudes for multiple Hand Concepts, each with only best-performing GFPSs applied (first assumption). It illustrates how the introduction of a standardized aggregate value results in uniform Quality Profile-magnitudes across all these Hand Concepts.²

The final determination of the Hand Concept score, based on the two assumptions above, is

²For the representation, each GFPS is assumed to reduce only one DOF.

also illustrated. As argued in the preceding sections, the suitability or non-suitability of a GFPS is derived from the user input and implemented through the relevance weight v . Based on the illustration in Figure 5.4, a qualitative example for a given input is shown in Figure 5.5, depicting how the Quality Profile-magnitudes behave when the relevance weight is applied. Similarly, Figure 5.6 shows the final Hand Concept score x^{HC_i} . For clarity, the relevance weight is not applied in this depiction. Further, an example preference weight reflecting a user preference for Simplicity is applied: the aggregate values $p_{MQ_2}^{HC_i}$ are multiplied by 3, and $p_{MQ_1}^{HC_i}$ by 1. The resulting distribution shows the highest values on the right-hand side, associated with the simplest designs.

Based on the assumptions above, a standardization of the Superior Qualities' influence values can also be performed. If the sum of influences for the Major Qualities is normalized, and the addressed Superior Qualities are identical across all FoIs within a given FoI category, then normalized aggregate sums $p_{SQ_j,max}^{gfps_u}$ can also be defined for the Superior Qualities. In the context of determining the suitability or unsuitability of a FoI, the aggregate values $p_{SQ_1,max}^{gfps_u}$ and $p_{SQ_2,max}^{gfps_u}$ play a key role. These two Superior Qualities are input-dependent and represent the portion of $p_{MQ_1}^{gfps_u}$ that can be inverted, as described in Section 5.2.1. Special attention must therefore be given to determining these values, as they are decisive in whether a FoI is successfully identified as unsuitable (i.e., whether $p_{MQ_1}^{gfps_u}$ becomes sufficiently small).

Finally, the last assumption proposes conducting the analysis at the FoI level, followed by automated mapping back to the GFoI level. In Chapter 3, the compatibility matrix could be developed at FoI level, rather than at the GFPS level, using a targeted set of rules, and then automatically mapped back to the GFPS level. A similar approach is intended here. Since the input-dependent Qualities within the Superior Qualities Anthropomorphic Movements and Movement Independence are aligned with the group-level terminology, it is not strictly necessary to determine the influences at the GFoI level. Instead, the influences can be defined at the FoI level and then automatically assigned to the correct Qualities for the corresponding GFoIs using appropriate loop variables.

A representation of the method derived from the assumptions is shown in Figure 5.7. As suggested in the assumptions, instead of determining the influence values for each GFPS (which would involve $86 \cdot m_Q$ variables, see top left corner of Figure 5.7), the number of parameters to be identified is reduced, and the process is divided into four phases. In Phase 1, the Major Quality aggregate values are defined. In Phase 2, they are used to define the Superior Quality aggregate values. It is noted that the reference to $gfps_u$ in the upper index has been replaced by a reference to the respective FoI category. In Phase 3, the Superior Quality aggregate values are used to define the influence values for the best-performing PS of each FoI on Qualities. In Phase 4, the influences of the remaining PS of that FoI are defined, if the FoI has more than one PS. Lastly, the values are transformed from PS level to GFPS level.

Although this determination is carried out only once for the development of the GUI, the

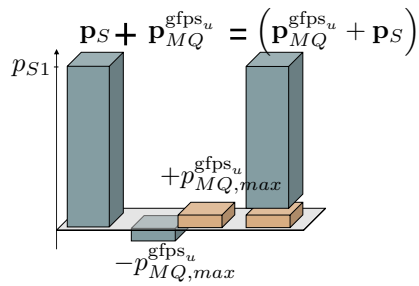


Figure 5.3: Standardization of Quality Profile aggregate values.

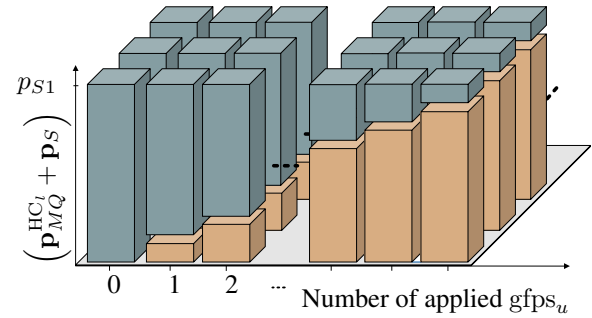


Figure 5.4: Standardization of a Hand Concept's Quality Profile-magnitude without weighting.

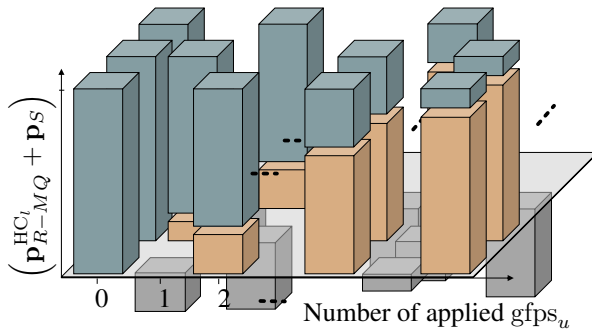


Figure 5.5: A Hand Concept's Quality Profile-magnitude with relevance weight.

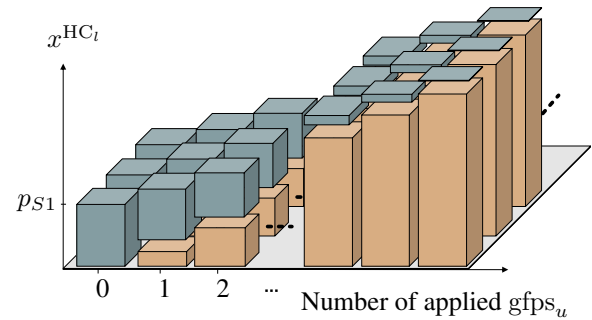


Figure 5.6: A Hand Concept score without relevance weight and with preference weight towards Simplicity.

method was designed to simplify the reconstruction of this dissertation or its adaptation to other applications.

As proposed in the assumptions, depending on the FoI category under consideration, many parameters are automatically set to zero. For example, considering the FoI category "Joint Configuration", the GFPSs in this category do not address the Qualities associated to SQ_2 (Movement Independence). As a result, one parameter in Phase 2 and all parameters in Block II of Phase 3 can be eliminated. Furthermore, it can also be shown that while Block I theoretically provides 12 parameters per FoI, in practice only a few are relevant. This becomes evident in the example implementation presented in Section 5.2.4.

It can also be shown that only Phase 1 and Phase 2 are essential for the successful application of the algorithm. Considering the assumptions above and Equation (5.19) for the overall Hand

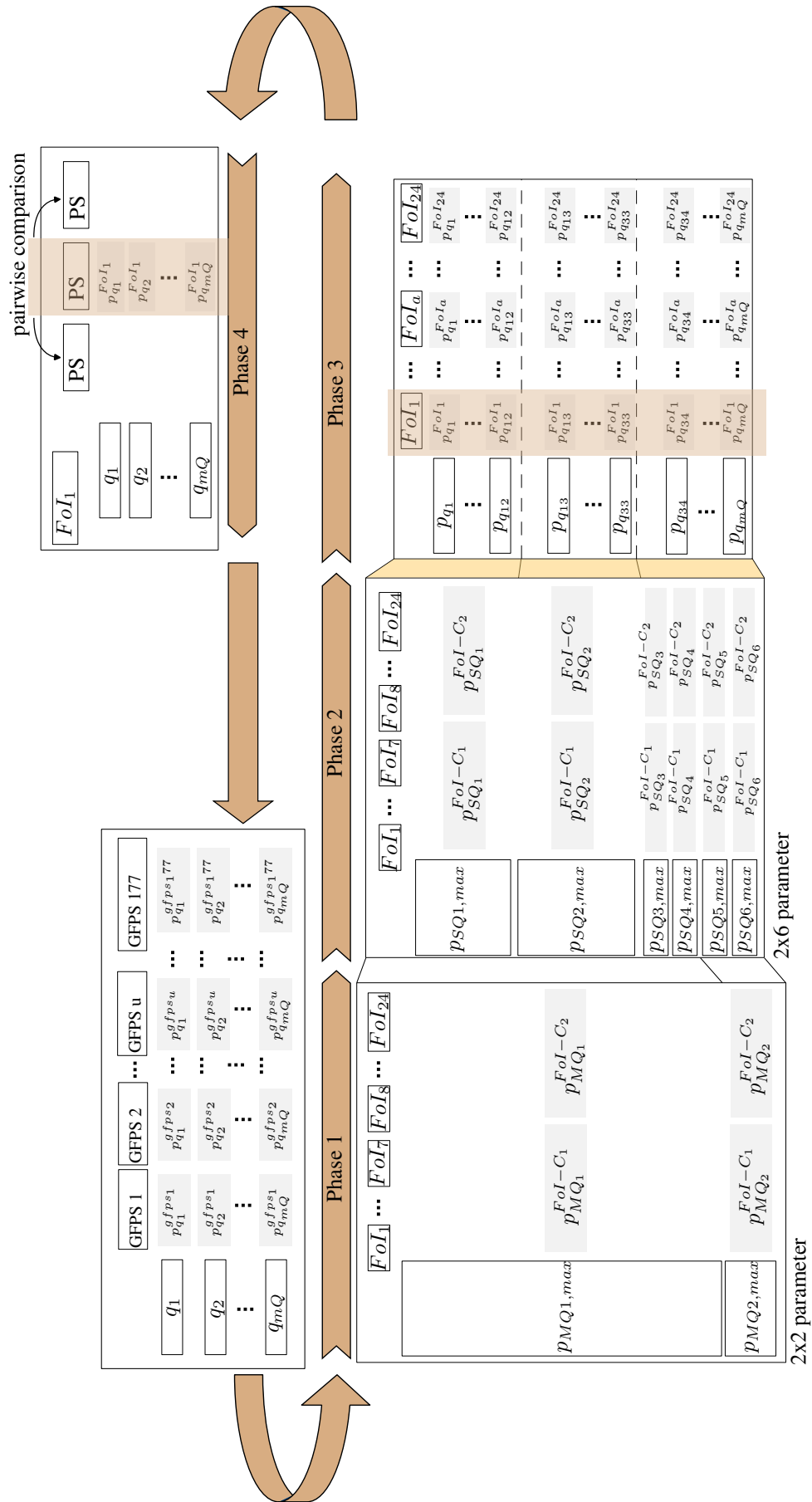


Figure 5.7: Method illustration for influence value identification.

Concept score, it becomes clear that only the aggregate values at the Superior Quality and Major Quality levels are decisive for suitability (or unsuitability) of a FoI. The exact distribution across the individual Qualities within an Superior Quality is not critical. As a result, only $2 + 6$ parameters per FoI category need to be identified for the algorithm to function effectively, instead of the initially stated $86 \cdot m_Q$ parameters. In Figure 5.7, the transition to Phase 3 is therefore highlighted in color. The Qualities and their influence values identified in Phases 3 and 4 are used within the knowledge-based system solely for external communication. They are incorporated in the Explanation Component to justify the selection or exclusion of specific GFPSs.

In a first step implementing the method, the addressed Superior Qualities for each FoI category are defined, as shown in Figure 5.8. The assignment, whether positive or negative, follows the Superior Quality derivation in Section 5.2.2.2. For example, all GFPSs in the FoI category "Joint Configuration" positively influence Qualities in the Superior Qualities Degree Of Actuation and Mechanical Design (colored brown), and negatively influence Qualities in the Superior Qualities Manipulability and Anthropomorphic Movements (colored blue). This default negative influence stems from the negatively connoted terminology of the PSs (e.g., "Eliminate MCP A-A DOF") contrasting the positively connoted Qualities within these Superior Qualities (e.g., "Enable MCP A-A DOF"). Slanted coloring indicated that the influence is inverted when the corresponding Quality is not required by the input. Similarly, GFPSs of the second and third FoI category "Joint Coordination" negatively influence Qualities of the Superior Qualities Manipulability and Mechanical Design while positively influencing Qualities of the Superior Qualities Degree Of Actuation, Contact Conditions, and Movement Independence. This reflects the fact that negatively connoted PSs (e.g., "LF: Elim. 1 DOA PIP-DIP") align with negatively connoted Qualities (e.g., "Eliminate LF individual PIP F-E") and thus support the intended outcome.

The different phases of the method are presented below. A mathematical derivation is provided

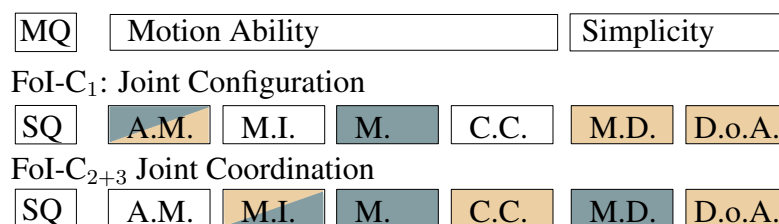


Figure 5.8: Influenced Superior Qualities per FoI category (brown: positive influence, blue: negative influence).

to determine the aggregate values for Major Qualities and Superior Qualities. This takes into account possible input dependencies of the Superior Qualities and supports a deliberate choice

of upper limits to address the challenge of identifying the general suitability of a FoI.

Phase 1

In the following, the derivation is presented for the first FoI category "Joint Configuration". An example preselected set of Hand Concepts with associated scores is shown in Figure 5.9. The SRHs serve as an example of this preselected set. Each Hand Concept is assigned its applied FoI and the corresponding best-performing GFPS (that is applied). Additionally, the qualitative trade-off between Motion Ability and Simplicity is discretized.

The discrete values reflect qualitatively the intended outcome. The centrally positioned

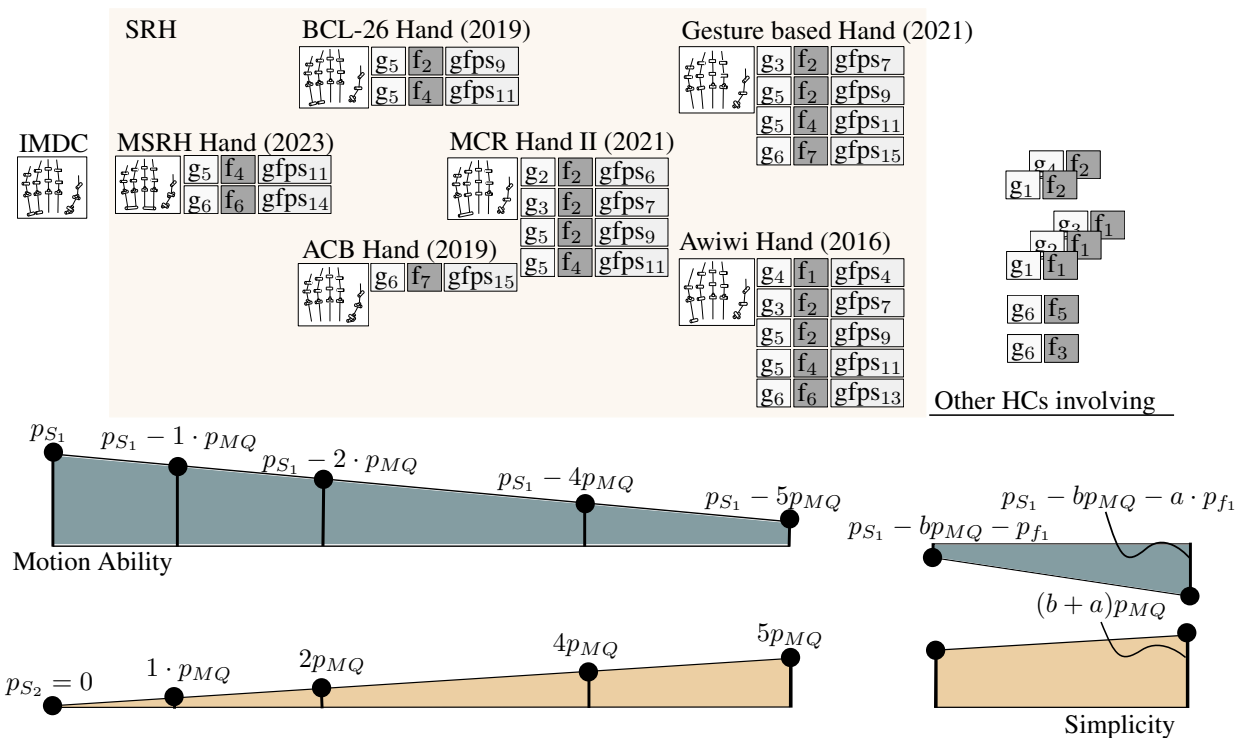


Figure 5.9: Discretized Trade-Off Illustration of Hand Concepts (FoI category "Joint Configuration").

SRHs represent valid solutions and feature thus the step wide reduction of Motion Ability and increase of Simplicity. For undesired GFPSs (see "other Hand Concepts involving" in Figure 5.9), the resulting Hand Concept is inadequate and the Motion Ability score thus negative. Nevertheless, the simplification of the design increases, which is expected to occur with each joint elimination.

The variables can now be determined such that the desired system behavior is achieved for the suitable FoIs. The variables used are already known from the derivation of the metric. For

clarity, the aggregate values are shown without upper indices. Furthermore, to properly test the assumptions, two distinct values are chosen for the Major Quality aggregate values. The system should recommend left-side Hand Concepts when Motion Ability is preferred, and right-side Hand Concepts when Simplicity is preferred. Therefore, mathematically, the condition

$$\begin{aligned} 3(p_{S_1} - b \cdot p_{MQ_1}) + 1 \cdot (b \cdot p_{MQ_2}) &< 3 \cdot p_{S_1} + 1 \cdot 0 \\ 3p_{S_1} - 3bp_{MQ_1} + bp_{MQ_2} &< 3p_{S_1} \end{aligned} \quad (5.21)$$

must hold for preference towards Motion Ability, and the condition

$$\begin{aligned} 1 \cdot p_{S_1} + 3 \cdot 0 &< 1 \cdot (p_{S_1} - b \cdot p_{MQ_1}) + 3 \cdot b \cdot p_{MQ_2} \\ p_{S_1} &< p_{S_1} - bp_{MQ_1} + 3bp_{MQ_2} \end{aligned} \quad (5.22)$$

must hold for preference towards Simplicity. Thereby, the preference weights used are 1 and 3, as previously defined. Further, the variable b represents the number of reduced DOFs through suitable FoIs.

From Equation (5.21) follows that

$$-3bp_{MQ_1} + bp_{MQ_2} < 0 \quad \Rightarrow \quad p_{MQ_2} < 3p_{MQ_1} \quad (5.23)$$

must hold. It can be seen that neither the initial value p_{S_1} nor the number of eliminated DOF b is relevant for the condition to hold.

From Equation (5.22) follows that

$$0 < 3bp_{MQ_2} + bp_{MQ_1} \quad \Rightarrow \quad -\frac{1}{3}p_{MQ_1} < p_{MQ_2}. \quad (5.24)$$

Combining inequalities (5.23) and (5.24) yields the following relationship between the two step sizes

$$-\frac{1}{3}p_{MQ_1} < p_{MQ_2} < 3p_{MQ_1} \quad (5.25)$$

From this, it can be concluded that choosing p_{MQ_2} within the interval defined in Equation (5.25) ensures the desired system recommendation behavior. For simplicity, both aggregate values are considered to be equal ($p_{MQ_2} = p_{MQ_1} = p_{MQ}$), as initially proposed in the assumptions.

The variables can also be set to ensure the desired system behavior on the side of unsuitable FoIs. The remaining question is by how much the inversion (through the relevance weight) must reduce the aggregate value so that a Hand Concept containing even a single unsuitable FoI is not selected by the system. Thus, an equation is derived to reflect this system behavior. For a

hypothetical Hand Concept with b suitable FoIs, the Motion Ability results in $(p_{S_1} - bp_{MQ})$ and the Simplicity score results in bp_{MQ} . For a Hand Concept with a unsuitable FoIs in addition to the b suitable ones, the Motion Ability score results in $(p_{S_1} - bp_{MQ} - ap_{f_1})$ and the Simplicity score in $(b + a)p_{MQ}$, where p_{f_1} is the amount by which p_{MQ_1} is reduced after inversion through the relevance weight in case of an unsuitable FoI. p_{f_1} must be defined.

To ensure the system always selects the Hand Concept with only suitable FoIs, the following condition must hold:

$$3 \cdot (b + a)p_{MQ} + 1 \cdot (p_{S_1} - bp_{MQ} - ap_{f_1}) < 3 \cdot (bp_{MQ}) + 1 \cdot (p_{S_1} - bp_{MQ}). \quad (5.26)$$

Rearranging Equation (5.26) leads to $3p_{MQ} < p_{f_1}$. It can therefore be concluded that the number of desired FoIs (b) as well as the number of undesired FoIs (a) ($a > 0$) do not affect the validity of the condition. As long as $p_{f_1} > 3p_{MQ}$, a Hand Concept with unsuitable FoIs will not be chosen. For simplicity, $p_{f_1} = 4p_{MQ}$ is defined in the following.

In summary, the Major Quality aggregate values are determined as follows: It was shown that a single value p_{MQ} can be used for both Motion Ability and Simplicity, and that this value can be freely chosen. Additionally, it was established that for Hand Concepts containing unsuitable FoIs, the Motion Ability score must result in $-4p_{MQ}$ (instead of $-p_{MQ}$) after inversion by the relevance weight, in order to ensure that such Hand Concepts are not recommended.

Interested readers are referred to Appendix J for the derivation of the other FoI category. It was repeated to demonstrate the general applicability of the approach. It is shown that, first, the method can be applied in the same way to other FoI categories, and second, that selections within different FoI categories do not interfere with one another. The derivation is excluded from the main body for clarity. The exact same conclusions are drawn as they are for the FoI-C₁.

Concluding on both FoI categories, the following summary can be given. For both FoI categories $p_{MQ_1} = p_{MQ_2} = p_{MQ}$ holds true, resulting in two variables $p_{MQ}^{FoI-C_1}$ and $p_{MQ}^{FoI-C_2}$. Further, in order to account for Hand Concepts with unsuitable FoIs, the Motion Ability score need to be switched from $-p_{MQ}$ to $-4p_{MQ}$ by the relevance weight. Therefore, $p_{f_1} = -4p_{MQ}^{FoI-C_1}$ and $p_{f_2} = -4p_{MQ}^{FoI-C_2}$ are introduced. The number of suitable FoIs, unsuitable FoIs or the Motion Ability start value are not relevant for the proper functioning. Since the aggregate values within both FoI categories can be freely chosen and no dependencies between these values across FoI categories have been identified, they are combined for simplicity. It therefore holds that $p_{f_1} = p_{f_2} = p_f$ and $p_{MQ}^{FoI-C_1} = p_{MQ}^{FoI-C_2} = p_{MQ}$ (as used prior in the derivation above).

Phase 2

For the second phase, the determined Major Quality aggregate values are used to derive the corresponding Superior Quality aggregate values. Particular attention must be paid to the input dependencies of the Superior Qualities, as these are responsible for the differing aggregate Motion Ability contributions for suitable FoIs ($-p_{MQ}$) and unsuitable FoIs ($-4p_{MQ}$). The required Superior Quality aggregate values are derived for the FoI category in the following. For the FoI category Joint Configuration, the aggregate values for the Superior Qualities Anthropomorphic Movements and Manipulability (associated with the Major Quality Motion Ability), as well as for Mechanical Design and Degree Of Actuation (associated with the Major Quality Simplicity), must be determined. As in the previous step, the value ranges are derived in a mathematically general form. Thereby, the variables $p_{SQ_x}^{FoI-C_1}$ are modified to directly refer to the specific Superior Quality, to improve readability. For the same reason, the upper index is removed. Taking into account the inversion of influences on non-required Qualities and the two possible total contributions to the Major Quality, the following two conditions can be established:

$$-p_{MQ} = (-1) \cdot (-p_{A.M.}) - p_M. \quad (5.27)$$

$$-4p_{MQ} = -p_{A.M.} - p_M. \quad (5.28)$$

Equation (5.27) represents the case in which a suitable FoI is selected, while Equation (5.28) corresponds to the selection of an unsuitable FoI. In both cases, and in accordance with the derivation of the Superior Qualities in Section 5.2.2.2, the influence of a PS on the Superior Qualities Manipulability and Anthropomorphic Movements must be negative. The only difference between the two equations lies in the inversion of the influence on Qualities in the Superior Quality Anthropomorphic Movements: in the first case, the Qualities addressed within Anthropomorphic Movements are not required, and the influence is therefore inverted³.

From Equation (5.27) follows that:

$$-p_{MQ} = p_{A.M.} - p_M. \quad (5.29)$$

Transferring the result from Equation (5.29) into Equation (5.28) yields:

$$4(p_{A.M.} - p_M.) = -p_{A.M.} - p_M. \Rightarrow p_{A.M.} = \frac{3}{5}p_M. \quad (5.30)$$

³Reminder: A FoI's suitability in the first FoI category is characterized by the elimination of DOFs (i.e., application of PSs) that are not required (i.e., Qualities that are not needed).

This establishes a relationship between the aggregate values of the two Superior Qualities. Substituting this result into Equation (5.29) yields:

$$-p_{MQ} = \frac{3}{5}p_{M.} - p_{M.} \Rightarrow p_{M.} = \frac{5}{2}p_{MQ}, \quad (5.31)$$

which defines the aggregate value for the Superior Quality Manipulability. Inserting this into the earlier equations then gives the aggregate value for the Superior Quality Anthropomorphic Movements:

$$p_{A.M.} = \frac{3}{2}p_{MQ}. \quad (5.32)$$

For the derivation of Superior Quality aggregate values for the second FoI category, interested readers are referred to Appendix J. Similar as for the derivation of the Major Quality aggregate values, the derivation for the Superior Quality aggregate values follows the same pattern for the first and second FoI category. However, the detailed derivation is provided for the sake of completeness, as the second FoI category involves more than two Superior Qualities. As a final result, the following relationships were identified:

$$p_{M.} = 3p_{MQ} \quad p_{C.C.} = 0.5p_{MQ} \quad p_{M.I.} = 1.5p_{MQ}. \quad (5.33)$$

After establishing existing dependencies, numerical values are now assigned for the following considerations. The Major Quality aggregate value p_{MQ} was identified as freely selectable. For simplicity, it is set to $p_{MQ} = 0.1$. The magnitude of the start value p_{S_1} was likewise found to be irrelevant to the functioning of the guidance and can therefore also be freely chosen. It is defined as $p_{S_1} = 2$. All Superior Quality aggregate values are derived as a function of the Major Quality aggregate value. The resulting numerical values are summarized in Figure 5.10. The Superior Quality aggregate values associated with the Major Quality Simplicity were not derived mathematically, as their individual values are irrelevant, as long as their sum corresponds to p_{MQ} . They are thus simply proportionally assigned and may be adjusted for the Explanation Component as needed, depending on the specific GFPS under consideration. In Phases 1 and 2, the total number of parameters to be identified is thus reduced to 14 (see Figure 5.10), instead of the originally assumed $86 \cdot 8$ parameters (i.e., one value per GFPS for each Superior Quality and Major Quality).

Phases 3 and 4

In this section, phases 3 and 4 are performed. As introduced, the addressed Qualities at the lowest level are relevant for the explanation component of the knowledge-based recommendation system. Although not essential for the functioning of the inference component, these

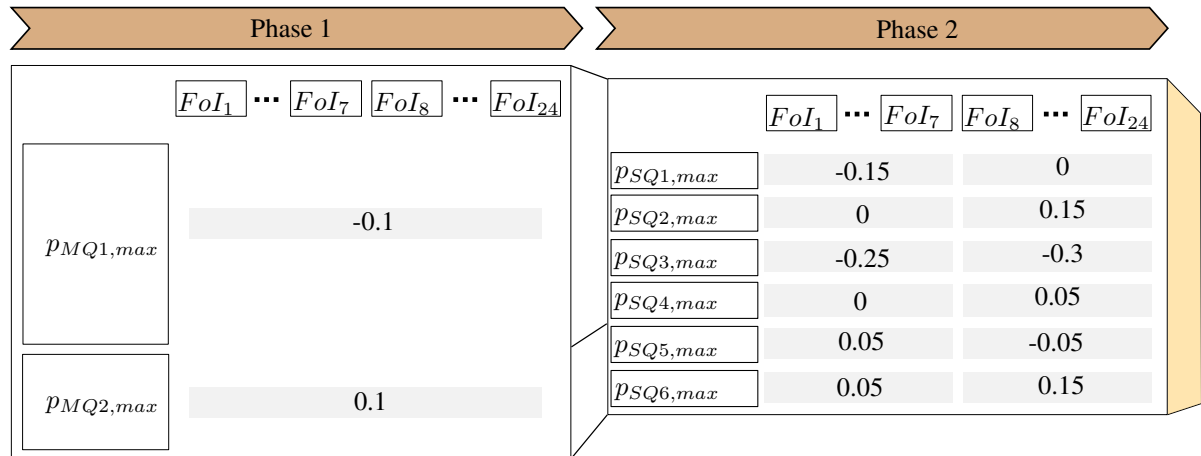


Figure 5.10: Summary of the identified Major Quality and Superior Quality aggregate values.

Qualities serve as an effective means of communicating the reasoning behind a recommendation to the user. By defining a Quality Profile for each GFPS, the user can comprehend a given recommendation by evaluating the addressed Qualities.

This results in a certain degree of design freedom for the Knowledge Engineer for defining the addressed Qualities. Since the main goal is user communication, both the specific terminology and the number of addressed Qualities are of secondary importance. The only requirements are: (1) the total influence on the Qualities must respect the predefined Superior Quality aggregate values, (2) the naming conventions for Qualities must be followed, and (3) redundancy should be avoided. With regard to redundancy, two perspectives apply: addressing more Qualities per PS can enhance user understanding, while excessive overlap between Qualities may hinder the user's ability to clearly distinguish the influence of different PSs. It is therefore acknowledged that the definition of Qualities is subjective to some extent.

Next, the Qualities are defined. For clarity, complete lists of previously defined Major Qualities and Superior Qualities are given in Tables E.5 and E.6. For the Qualities, defined in the following, it is referred to E.7 in the Appendix. The Qualities are derived based on the respective positive or negative influence of the PSs in a robot hand design and are defined during the collection of the PSs. For example, a great benefit of an underactuated finger design is the automatic passive compliance of the finger to any object geometry. The grasp benefits from that through improved contact conditions by increasing the contact surface between finger and object. This is thus defined that as a Quality (see q_{35} in Table E.7). As a second example, the Quality q_{41} "Keeping number of DOF" is introduced to distinguish the beneficial effect of joint elimination and underactuation: both reduces the DOA, but only the latter does so by keeping the number of DOF. It thus requires two Qualities. The list of input-independent Qualities

comprises eight elements ⁴. The complete list comprises 41 Qualities.

Once the Qualities have been identified, it can be continued with Phase 3. In this phase, the influence values of the best-performing PS for each FoI are determined. This process is largely intuitive, as not all 41 existing Qualities are relevant. For example, considering a FoI from the first FoI category: First, for each DOF eliminated by the PS, only one Quality from Block I (see Figure 5.7) is relevant. As a result, 11 influence values can be immediately set to zero. Further, the relevant Quality can be directly identified from the PS' name. Second, Block II is not addressed by FoIs in the first FoI category, resulting in 21 additional parameters set to zero. Third, the addressed Qualities in Block III logically follow from the corresponding PS and, thus, do not require elaborate identification either. Besides the addressed Qualities, the assigned values are directly derived from the aggregate values of the associated Superior Quality.

For clarity, the influence values for the PSs of all FoIs are given in Appendix L. There, a table is provided for each FoI. If multiple PSs exist for a given FoI, all are listed in the respective table. As described above, the influence values are identified for the best-performing PS. Additional relevant information regarding the selection of addressed Qualities and the resulting influence values is also included where appropriate. Furthermore, Phase 5 is also documented within these tables. The influence values of the remaining PSs within each FoI are derived through a pairwise comparison approach. This process ensures that the best-performing PS consistently retains the highest influence values across all relevant Qualities.

As the final step, the identified influence values of the PSs are propagated to the corresponding GFPSs. As outlined at the beginning of this section, this is achieved by defining appropriate loop variables that establish the group affiliation of each influence value. The corresponding implementation is detailed in the tables provided in Appendix L, where the loop variables used in the algorithm are highlighted for clarity.

Interested readers are referred to Appendix H.2 for a detailed explanation of how the generation of recommendation through the inference component is implemented from a programming perspective.

5.3 Interfaces

This section addresses the development of the interfaces for the knowledge-based system. It comprises two user interfaces and one interface for the Knowledge Engineer. The user interfaces involve the Dialog and the Explanation Component. The interface for the Knowledge Engineer represents the Knowledge Acquisition Component.

⁴The list of input-dependent Qualities has been derived in Chapter 4 for the Superior Qualities Anthropomorphic Movements and Movement Independence

The Dialog Component represents the interface through which the user communicates and provides the required input. The required input is defined in the preceding section. First, the user's preference between Motion Ability and Simplicity is required, as derived in Section 5.2.1. Second, the performance requirements need to be specified by the user. As derived before, the required performance is measured in the Motion Ability and shall be specified by the grasping tasks that need to be performed. Therefore, the user may choose required grasps from the taxonomy by Feix (2011).

According to the needs, an architecture of the Dialog Component is proposed in Figure 5.11. The Dialog Component is implemented as a GUI. The input interface of the GUI is composed of two major elements. On the left, the user specifies the performance requirements. The previously presented reduced Feix Taxonomy is given. Thereby, each grasp is implemented as a push button. This enables the user to specify the performance requirements with low level of required expertise, by choosing among the grasps. On the right side, the user specifies its performance quality preference. The relative relevance of the MQs can be defined by moving the order of the Qualities. Last, a push button allows the generation of recommendation, once the user has specified performance and preference.

The push button *Generate Recommendation* initializes the Inference Component. According to the procedure described in Section 5.2, for every identified Hand Concept (see Section 3.4), the computed constant Quality Profile is modified using the preference weight and relevance weight to determine the score x^{HC_i} and choose the Hand Concept with the highest one. The

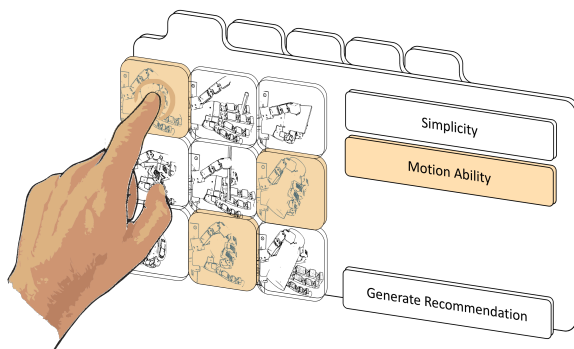


Figure 5.11: Design of the guidance's Dialog Component.

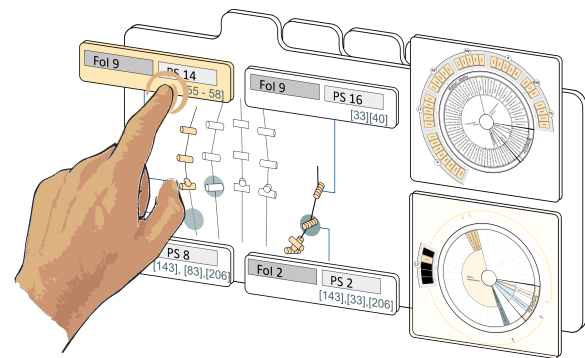


Figure 5.12: Design of the guidance's Explanation Component.

Explanation Component represents the interface through which the user receives the guidance's output. The designated output is a recommendation of a Hand Concept, according to the specified needs. This recommendation is the identified GFPS-combination. Further, As an important function, the output shall allow the user to comprehend the result.

To explain the output, a distinction is made between two aspects: explanation of the result and

explanation of the reasoning. The corresponding design is presented in Figure 5.12. For the explanation of the results, the selected GFPS-combination is visualized as a kinematic structure (left block). The notation used for joint coordination follows the convention introduced in Section 3.3. This allows for a clear identification of structural changes in comparison to the IMDC by assigning the corresponding GFPSs. For the explanation of the reasoning, two complementary approaches are applied. First, for each GFPS, references to relevant literature are provided. This enables interested readers to consult the associated publications and thereby understand the basis for the recommendation. Second, a visualization method developed in this dissertation is presented to illustrate the results of the utility analysis. The illustration is presented in more detail in Figures 5.14 and 5.15.

The Quality Criteria illustration provides the user with both an overview of the considered requirement criteria and an assessment of the qualitative influence of the selected GFPSs on these criteria. In Figure 5.14, all Quality Criteria are shown in the pie chart in gray. Along the outer circumference, the MQs are positioned. Adjacent to them are the Superior Quality, and further toward the center, the corresponding Qualities are assigned to each Superior Quality. Additionally, all FoIs are displayed along the outer edge of the diagram, grouped according to their respective Groups. Figure 5.15 presents an example visualization of the influences. For a given GFoI and GFPS that are applied to the Hand Concept, arrows indicate the affected Qualities. The arrow color reflects whether the influence is positive (brown) or negative (blue), while the color intensity of the addressed Qualities provides a qualitative indication of the influence strength.

The presented Explanation Component is generated for each of the three recommendations. Providing more than one recommendation serves multiple purposes. First, it allows the user to qualitatively compare the pie charts shown for each recommendation. Second, it addresses the challenge that, within a sorted set of preselected Hand Concepts, very similar Hand Concepts often appear close to each other, differing only in a few GFPSs. The multiple recommendations are represented as three tabs, as shown in Figure 5.12.

The Knowledge Acquisition Component allows the Knowledge Engineer to manually expand or modify the knowledge base. In particular for the identified FoIs and PSs, the knowledge can not be considered final. It must be taken into account that, on the one hand, completeness cannot be guaranteed in the course of the literature review, and on the other hand, knowledge is constantly evolving. Therefore, providing a means to expand the embedded knowledge is important, considering the objectives of this dissertation. The implemented Component provides two functionalities: screening the LoA and modifying it.

The architecture of the interface is given in Figure 5.13. As presented, drop down fields are provided to filter the content regarding FoIs, Groups, PSs, references, authors or robot hand names. As for the modification, push buttons are provided for every entity (e.g. PS). Once

chosen, a new window opens, asking for the required information to add or modify an entity. Information that are required depend on the entity and can be seen in the Entity-Relation model B.2. Similarly, push buttons are provided to add or modify relations between entities.

The interested reader is referred to the appendix for further information related to the programming implementation of the interfaces. The implementation of the interfaces was based on the methodology derived in the previous sections. An illustration of the implemented Dialog and Explanation Component is given in Figures I.1 and I.3, respectively. An illustration of the Knowledge Acquisition Component is given in Figure I.2.

Lastly, information on joint allocation are provided. As discussed in Section 2.5, no unique recommendation for task-dependent joint allocation can be given. Instead, a single set of working dimensional parameters is derived and provided for reference. Therefore, no extra tab is designated in the guidance's GUI. The reader is referred to Appendix A instead. The derivation is briefly given in the following. A detailed discussion can be found in the thesis by Polzin (2024), which was conducted under the author's supervision.

The established set of working dimensional parameters is mostly based on the information identified in the literature. For the joint configuration, the structure of the IMDC is applied. This intends to provide poses of all common joints, where individual joints can be easily removed if needed. For the joint ROM values, results from different studies (see summary in Section A) are combined to account for individual inconsistencies. The ROM values for the fingers are taken from the work of Cobos et al. (2008), the ROM values for HMC joints from the work of El-Shennawy et al. (2001) and the ROM values for the thumb from the work of Peña-Pitarch et al. (2014). For the lengths of the phalanges, the anthropomorphic relations discussed in Section 2.3.1 are used. A hand length of 195 mm was used, which corresponds to the average hand size of an adult male (Vergara et al. 2018). For the inclination and twist angles, values within the proposed ranges by Grebenstein (2016) are applied. For the remaining dimensions, such as the poses of the base joints (MCP, HMC, TMC) and the angles between the fingers, an X-ray image of the human hand from the National Library of Medicine (2024) was used.

All dimensions above discusses are then fine-tuned, according to the procedures described in Section 2.3.1. The cardboard model method by Grebenstein (2016) is implemented to identify optimal dimensions before prototyping. With the cardboard model, the Kapandji Opposition test and grasps from Feix' taxonomy are performed to optimize inclination and twist angles as well as base joint poses. The resulting finger dimensions are given in Table A.2. Overall hand dimensions are illustrated in Figure A.1.

Finally, a prototype is developed. The final robot hand design is depicted in Figure A.2. The successfully performed Kapandji Test and Feix taxonomy are presented in Figures A.3 and 2.6,

respectively. The exploded views in Figures A.4 and A.5, as well as the depiction of the MCP joint in Figure A.6, highlight the complexity and elaboration of the design. However, for the sake of conciseness, no detailed design information are provided, but reference is made to the thesis by Polzin (2024). Further, the complete CAD model is made available to the interested reader as an open-source resource.⁵

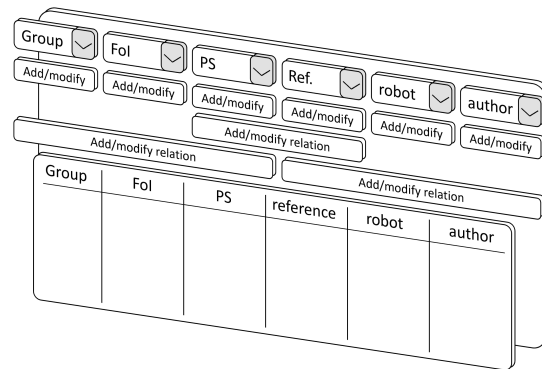


Figure 5.13: Design of the guidance's Knowledge Acquisition Component.

5.4 Conclusion

In this chapter, objective (O3) was addressed and, thus, the guidance's Control System was developed. The Control System is composed of four components. The Inference Component processes the information from the embedded knowledge base. The Dialog and Explanation Component are user interfaces for receiving input and presenting output, respectively. The Knowledge Acquisition Component allows the Knowledge Engineer to modify the embedded knowledge base derived in Chapter 3.

For the Inference Component, a method for identifying the most suitable Hand Concept based on a utility analysis was developed. Evaluation criteria were identified and collectively introduced as *Quality Criteria*. In total, 41 Qualities were proposed. These Qualities are divided into two Major Qualities *Motion Ability* and *Simplicity*. Within these, the Qualities are further grouped into six Superior Qualities. Furthermore, two necessary relevance and preference weights were introduced. A utility analysis was conducted for the GFPSs, with the individual evaluations defined as influences. Finally, a metric was derived that aggregates the overall utility values of each GFPS applied to an Hand Concept into a total utility value for the Hand Concept. The guidance selects the Hand Concept with the highest utility value.

For the development of the metric, three challenges were identified. The first challenge (Q7)

⁵<https://git-ce.rwth-aachen.de/robotic-hands/towards-quantitative-dof-relevance-identification>

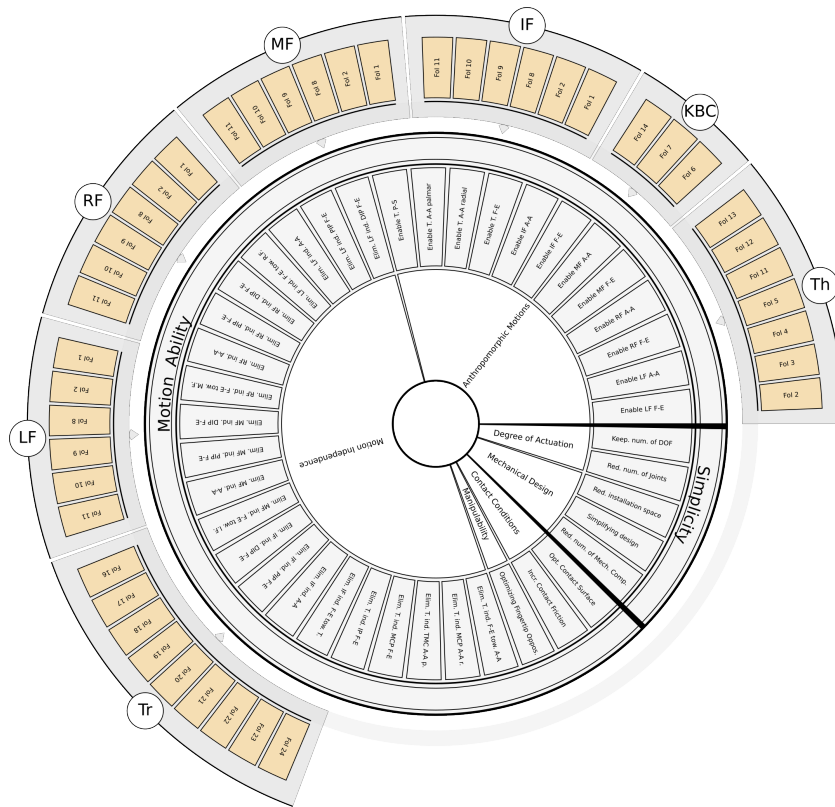


Figure 5.14: Illustration of the Quality Criteria (enlarged version in Figure K.1).

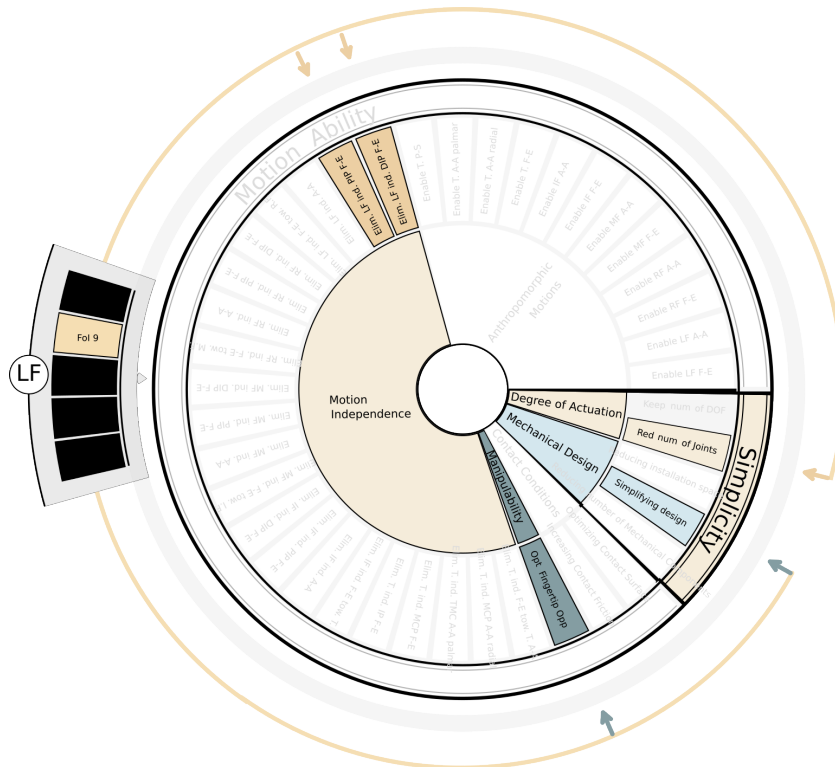


Figure 5.15: Example visualization of the Quality Profile for the PS p_{16} (enlarged version in Figure K.2).

concerns ease of implementation and scalability. The challenge consists in the manageability for the Knowledge Engineer to create a utility analysis across 41 Qualities for each of the 86 GFPSs. The second challenge (Q5) lies in the choice of influences and weights so that, depending on the user input, the system automatically evaluates unsuitable GFPSs negatively. The third challenge (Q6) lies in the choice of influences and weights to account for the trade-off of the decision.

The challenge (Q7) could be successfully addressed by (1) aggregating the Qualities and GFPSs, and (2) standardizing the influence values. The derived metric for calculating an Hand Concept's overall utility score showed that only the sum of influence values at the Superior Quality and Major Quality levels is relevant for the functioning of the guidance. The metric also indicated that a quantitative distinction between GFPS scores from different FoIs is not necessary. Only the binary distinction to identify the (un)suitability for the given user input is relevant. It was therefore decided that challenges (Q5) and (Q6) can be solved entirely via the weights, but without these, the Hand Concepts would exhibit identical overall utility scores. For this reason, the meaningful classification of Qualities into Superior Qualities and Major Qualities, and GFPSs into FoIs and these into FoI categories, was used. This classification suggests that all GFPSs of an FoI category address the same Superior Qualities of a Major Quality. Instead of considering 86 individual GFPSs, only 3 FoI categories need to be considered. For each FoI category, only 6 Superior Qualities instead of 41 Qualities must be considered. The influence values of the Superior Qualities are aggregate values of the influences of the associated Qualities and apply equally to all GFPSs of the respective FoI category. A single aggregate value is derived for the Major Qualities once, valid for every GFPS, which is applied negatively for the Motion Ability score and positively for the Simplicity score. Finally, an initial overall utility score assigned to an Hand Concept does not change in total through applied GFPSs (see Figure 5.3), but it does change in the distribution between Motion Ability and Simplicity (see Figure 5.4).

The challenge (Q5) could successfully be addressed by introducing a relevance weight. For four out of the six Superior Qualities, the associated Qualities are always considered relevant, regardless of the user input. For the remaining two Superior Qualities, the relevance of the associated Qualities depends on the user input. For each grasp specified by the user as a performance requirement, the relevance of these Qualities is defined. In the derived metric, the influences on Qualities that are not relevant for the given grasps are inverted. Considering the proposed standardization of aggregated Superior Quality values for GFPSs of a given FoI category, the aggregate values for the two input-dependent Superior Qualities are mathematically derived. If such a value is inverted (i.e., the addressed Qualities are not relevant), the aggregate value on the Major Quality decreases in such a way that any Hand Concept applying this GFPS will not be selected by the guidance (see Figure 5.5).

The challenge (Q6) could successfully be addressed by introducing a preference weight. According to the proposed standardization of influence values, the overall utility scores of all Hand Concepts are equal in total, but differ in their score components for the Motion Ability and Simplicity, depending on the number of reduced DoA (which is proportional to the number of applied GFPSs). To account for user preferences between Motion Ability and Simplicity, a weight is introduced that amplifies one of these two score components based on the input provided. As a result, Hand Concepts that align with the user's preference receive significantly higher scores and are thus selected by the guidance.

For the Dialog, Explanation, and Knowledge Acquisition Components, the required interfaces are developed. The design of the Dialog Component is presented in Figure 5.11. The interface allows the user to specify performance requirements by selecting required grasps and to express quality preferences by choosing between Motion Ability and Simplicity. The design of the Explanation Component is presented in Figure 5.12. The interface presents the recommended Hand Concept to the user and explains the recommendation by visualizing the GFPS combination as a kinematic structure and by providing reasoning through literature references and a novel illustration of the underlying utility analysis for the recommended GFPSs. The design of the Knowledge Acquisition Component is given in Figure 5.13. The interface leverages the modularity of the embedded knowledge: Each entity can be easily modified or extended without affecting any of the implemented methods.

With the completion of this chapter, all objectives of this dissertation have been addressed. The next chapter evaluates the developed guidance.

6 Application and Evaluation

This chapter addresses the evaluation of the developed guidance and comprises three parts. First, the developed method is manually applied to different requirements for validation purposes. Second, the outcome of the implemented guidance is investigated for chosen cases for verification purposes. Last, an example application of the guidance is presented.

6.1 Methodology Validation

In this section, the developed guidance is validated by examining whether the methodology was correctly derived. To this end, two example GFPSs, $gfps_8$ and $gfps_{78}$, are considered. The first describes the elimination of little finger MCP A-A DOF, while the second describes its coupling to the A-A of the ring finger and index finger. Both GFPSs are associated with FoIs that are in OR relation to one another, meaning that a given Hand Concept can apply only one of them. Furthermore, the three input scenarios introduced in Section 4.3.2 are considered. For an input corresponding to Scenario 1, an Hand Concept applying $gfps_8$ should be preferred over one applying $gfps_{78}$. For Scenario 3, the opposite is expected. Therefore, the input-independent Quality Profiles of both GFPSs are first defined. Based on the two scenarios, the relevance-weighted Quality Profiles are then defined and the results are evaluated for correctness.

The Quality Profiles are visualized in Figures 6.1 and 6.2. A full vector representation according to Equation 5.11 is omitted. However, the respective influence values can be found in Tables L.2 and L.20. A summary of the Major Quality and Superior Quality aggregate values is given in Figure 6.3. It can be seen that the sums for $gfps_{78}$ are higher, as two DoAs are eliminated. The change of aggregate values after application of relevance-weight is summarized for both scenarios in Figure 6.4. For scenario 1, the respective Qualities of both p_{SQ_1} and p_{SQ_2} are not defined as relevant (see Table 4.4). Therefore, the influence values are inverted. For scenario 3, the respective Qualities are considered relevant in both p_{SQ_1} and p_{SQ_2} . The influence values, thus, are not inverted.

The developed metric is validated to yield the expected recommendations by calculation of the overall score x , following Equation 5.19. For calculation, an example user preference towards Simplicity and the start vector $\mathbf{p}_S = (2, 0)$ is used. For scenario 1, the Hand Concept applying the $gfps_8$ features a higher score and is thus recommended. For scenario 3, the Hand Concept applying the $gfps_{78}$ features the higher score and is recommended.

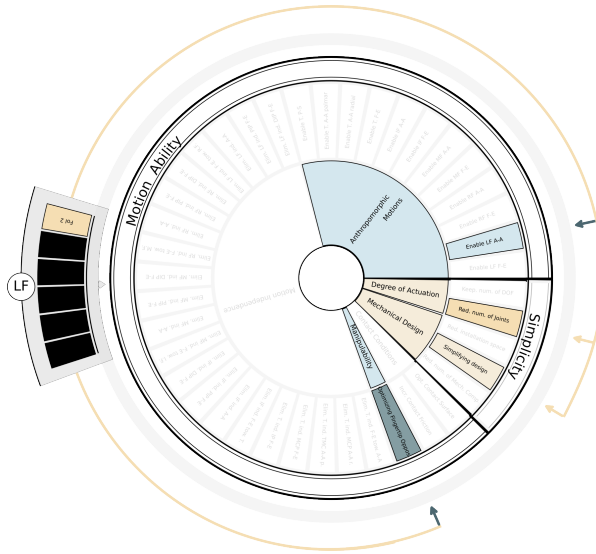


Figure 6.1: Quality Profile illustration of $gfps_8$ (enlarged version in Figure K.3).

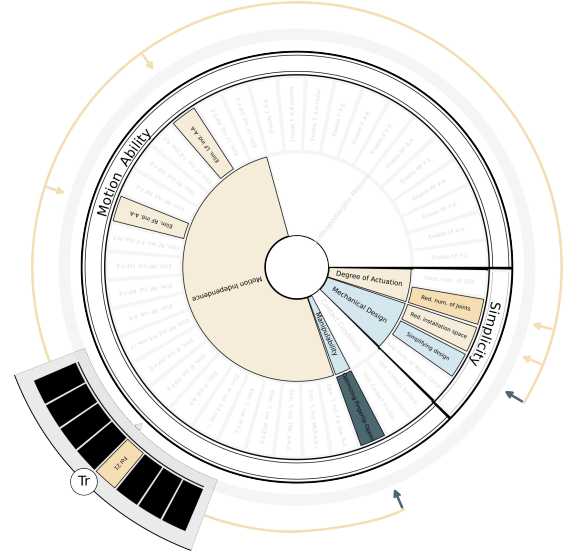


Figure 6.2: Quality Profile illustration of $gfps_{78}$ (enlarged version in Figure K.4).

| | $gfps_8$ | $gfps_{78}$ |
|---------|----------|-------------|
| PMQ_1 | -0.4 | -0.2 |
| PMQ_2 | 0.1 | 0.2 |

| | $gfps_8$ | $gfps_{78}$ |
|---------|----------|-------------|
| PSQ_1 | -0.15 | 0 |
| PSQ_2 | 0 | 0.3 |
| PSQ_3 | -0.25 | -0.5 |
| PSQ_4 | 0 | 0 |
| PSQ_5 | 0.04 | 0 |
| PSQ_6 | 0.06 | 0.2 |

Figure 6.3: Aggregate Quality Profile values for $gfps_8$ and $gfps_{78}$.

| | Scenario 1 | | Scenario 3 | |
|---------|------------|-------------|------------|-------------|
| | $gfps_8$ | $gfps_{78}$ | $gfps_8$ | $gfps_{78}$ |
| PMQ_1 | -0.1 | -0.8 | -0.4 | -0.2 |
| PMQ_2 | 0.1 | 0.2 | 0.1 | 0.2 |
| x | 2.2 | 1.8 | 1.9 | 2.4 |

| | Scenario 1 | | Scenario 3 | |
|---------|------------|-------------|------------|-------------|
| | $gfps_8$ | $gfps_{78}$ | $gfps_8$ | $gfps_{78}$ |
| PSQ_1 | 0.15 | 0 | -0.15 | 0 |
| PSQ_2 | 0 | -0.3 | 0 | 0.3 |
| PSQ_3 | -0.25 | -0.5 | -0.25 | -0.5 |
| PSQ_4 | 0 | 0 | 0 | 0 |
| PSQ_5 | 0.04 | 0 | 0.04 | 0 |
| PSQ_6 | 0.06 | 0.2 | 0.06 | 0.2 |

Figure 6.4: Relevance-weighted aggregate Quality Profile values for $gfps_8$ and $gfps_{78}$ in two scenarios.

6.2 Guidance Verification

In this section, the developed guidance is verified by examining whether the derived methodology has been correctly implemented. To this end, recommendations for selected inputs with known expected outcomes are evaluated. Therefore, the trade-off in the FoI category Joint Configuration is analyzed, to assess whether the guidance reproduces the expected results (see Figure 5.9). If successfully evaluated, the evaluation confirms the correct implementation of the metric, including the requirements (grasp-quality relation), the influences of GFPSs on Qualities, and the correct application of the relevance weight and preference weight.

The resulting recommendations are illustrated in Figure 6.5. On the left hand side, six recommendations for user preference towards Motion Ability are given. All six recommended Hand Concepts feature an overall score of $x^{HC} = 5.8$ and feature a single applied GFPS that eliminate a single DOF, respectively. On the right hand side, two recommendations for user preference towards Simplicity are given. Both feature an overall score of $x^{HC} = 3.4$ and have a total of seven eliminated DOFs. Further recommendations yield solutions with lower scores. For the left side, for example, these recommendations involve Hand Concepts with a single GFPS that eliminates two DOF, and Hand Concepts of different combination of the given GFPSs. For the sake of illustration, they are not given here.

Initially, three unexpected observations are identified in the recommendations with a preference for Motion Ability. First, the guidance recommends multiple Hand Concepts with identical scores, resulting in six equivalent solutions. This contradicts the expectation of a recommendation with decreasing scores - i.e., a clear primary recommendation followed by alternatives with comparatively lower significance. Second, finger structures appear in the recommendations that can not be found in the SRHs. For instance, a Hand Concept with an eliminated little finger A-A DOF is not present in the SRHs. Third, the IMDC, is not among the recommended options but was expected to be recommended with the highest score of six¹.

These observations can be explained after a detailed analysis. Regarding the first, the presence of multiple Hand Concepts with identical scores reflects the findings in Chapter 4: no quantitative measures currently exist to justify the superiority of any of the six recommendations. Consequently, the guidance yields a set of equivalent recommendations. This limitation was addressed in a study by the author (Gossen et al. 2025a), which proposed a method to quantify differences between Hand Concepts. A comprehensive identification of such values remains future work. Once available, the developed guidance allows their integration via the relevance weight. Currently, the relevance weight is limited to values of -1 or 1 . If a DOF is identified to be more important, its relevance weight can be scaled accordingly, resulting in a greater score reduction when eliminated. Regarding the second, the solutions that do not originate

¹Without applied GFPSs, the score is simply the preference weight multiplied with the start value

from the SRHs are the result of combining various sources from the literature in Chapter 4. As such, they represent new approaches towards minimal Hand Concepts derived as part of this dissertation. Regarding the third point, the IMDC is not listed because the recommendation is based on the list of GFPS combinations resulting from the exploration, which does not include the IMDC, as no GFPS is applied.

Subsequently, the recommendations with a preference for Simplicity are analyzed. The number of recommendations is relatively small, which was expected. For preference towards Simplicity, each applied GFPS from a suitable FoI contributes to a higher score. The resulting recommendation is therefore simply a collection of all GFPSs from suitable FoIs. The presence of two equivalent solutions, again, results from an OR configuration, for which no clear preference between the alternatives has yet been established. Furthermore, the recommended GFPSs do not contradict expectations either. Both the GFPSs from the SRHs and the newly derived GFPSs are considered. Notably, by incorporating the newly derived GFPSs, one Hand Concept emerges that is more minimal than the previously known SRHs and can be considered a new solution derived as part of this dissertation. It should be emphasized, however, that an (experimental) evaluation of these solutions is still pending, as previously discussed in Chapter 4.

In summary, the guidance accurately reflects the expected results. The scores correspond to

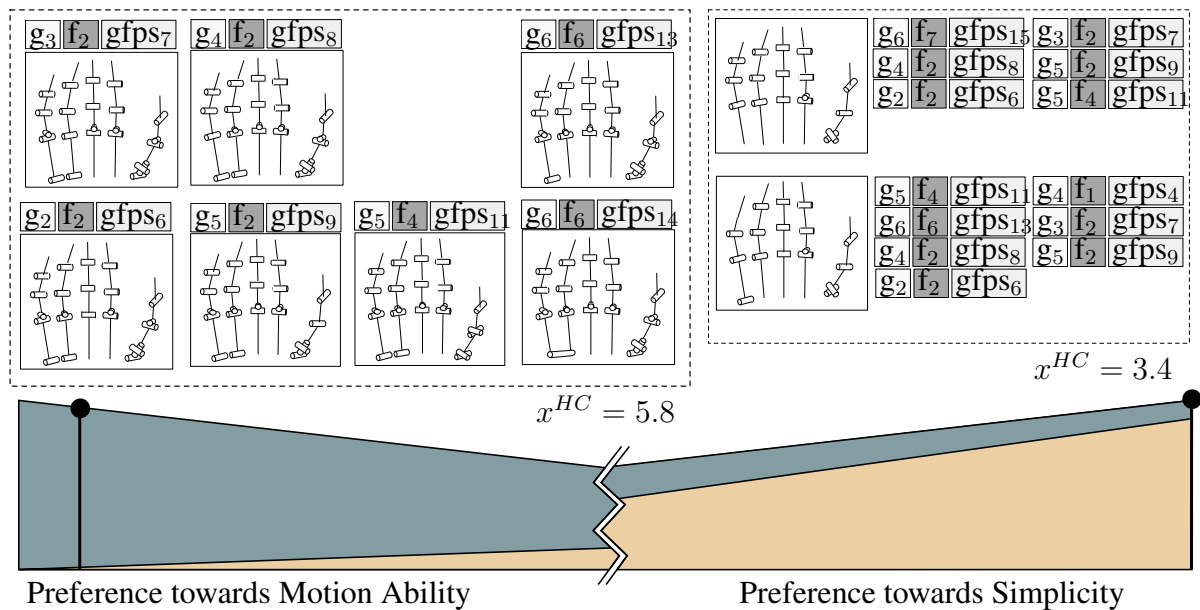


Figure 6.5: Guidance's recommendations for FoI-C Joint Configuration considering different user preferences.

those expected based on the number of applied GFPSs (indicating correct implementation of the metric, preference weight, and influences). GFPSs from unsuitable FoIs are not recommended

(indicating correct relevance weight application), and all expected GFPSs are included as intended (indicating correct application of the requirements and their combination). Further, contrary to initial expectations, the recommendations are not unique. However, this is due to the current state of the art (DOF relevance in anthropomorphic robot hands) rather than a shortcoming of the developed methodology or its implementation. Lastly, the recommended solutions appear, to the best of the author's knowledge, to be novel and not yet documented in the literature. Their experimental evaluation is therefore suggested as future work.

6.3 Example Application

This section presents an example application of the developed guidance. As outlined in Chapter 1, robotic hands offer a promising approach to meet the demand for versatile grippers when addressing the skilled labor shortage caused by demographic change through robotic assistance. An application of the developed guidance targets the high costs and mechanical complexity of current commercial robot hands. The guidance proposes a design of a versatile gripper that includes only the functionality necessary for the specific task.

The guidance thus supports the top-down design approach known from bionics. In bionics, the goal is to find a natural counterpart to a given technical problem and adapt the solution found in nature. In this case, the versatile human hand serves as the biological model that evolved to cope with different grasping tasks. For the technical adaptation, the guidance proposes to reduce its complexity according to user requirements, instead of aiming perfect replication.

Particularly relevant applications for this approach involve situations where objects must be grasped that are currently handled by humans - or even explicitly designed to be manipulated by the human hand. One especially relevant use case is the shortage of skilled workers in the care sector, as already mentioned in Chapter 1 in the context of humanoid applications. Robotic assistance is challenging in this field because the tasks involved require complex handling actions, each demanding a customized gripper. For humans, these tasks pose no difficulty, especially since the objects were often designed with the human hand in mind.

A collection of potentially required grasp types is shown in Figure 6.6. The first row illustrates grasps relevant to interactions in the patient's immediate environment, such as pushing a wheelchair, positioning an intravenous stand, grasping a bedsheet, and handling a bedpan. The second row shows grasps related to interaction with the surrounding space, such as operating a sliding door, interacting with a door leaf, a door knob, and a door handle.

The user input resulting from the performance requirements is shown in Figure 6.7. Grip number 1, "Large Cylinder", was selected for the wheelchair and the sliding door; grip number 13, "Adducted Thumb", for the intravenous stand and the door handle; grip number 8, "Tip Pinch", for the bedsheet; grip number 15, "Lateral", for the bedpan; and grip number 17,

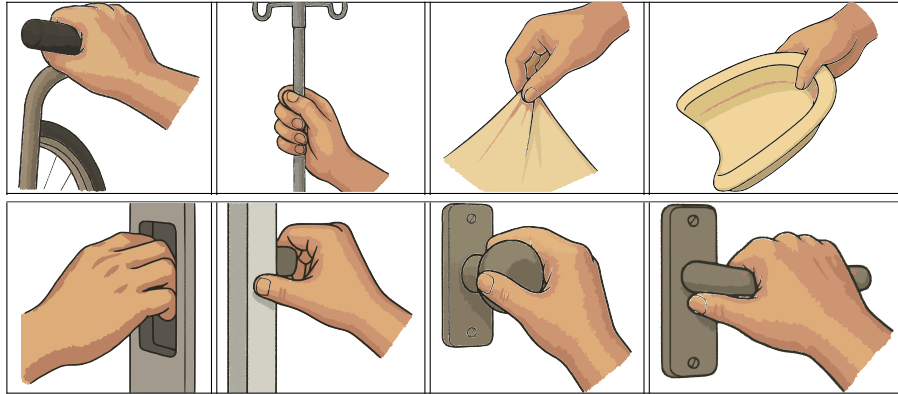


Figure 6.6: Consistent alignment of gripper images using fixed height and vertical centering.

"Parallel Extension", for the door leaf (compare Feix et al. 2015).

The guidance's recommendation for the example application "Care" is shown in Figure 6.8.

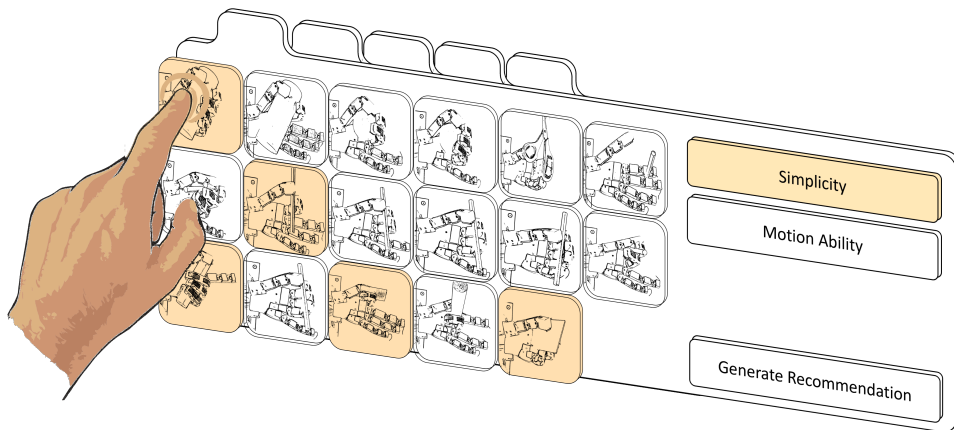


Figure 6.7: Required guidance input for the example application 'Care'.

Two guidance recommendations are illustrated as examples. They are examples, as all tendon UAs of the fingers are equally recommended as linkage UAs, resulting in many combinations. The recommendations have a core score of $x^{HC} = 5.8$ and 13 to 15 applied GFPSs.

A comparison with current commercial robot hands highlights the significance of a task-based design. The Shadow Hand, which was mentioned for the first time in the initial motivation of this dissertation, is used as a suitable example. Its conceptual design along with the GFPSs can be found in Figure 6.8 (H. Wang et al. 2017b; Shadow Robot Company 2025). While the Shadow Dexterous Hand has 20 DOF and an equal number of DOA, the guidance's recommendation has five DOA and 16 DOF. This demonstrates a reduction of six joints and 15 actuators. A qualitative comparison of the Quality Profiles is further used to assess the applied func-

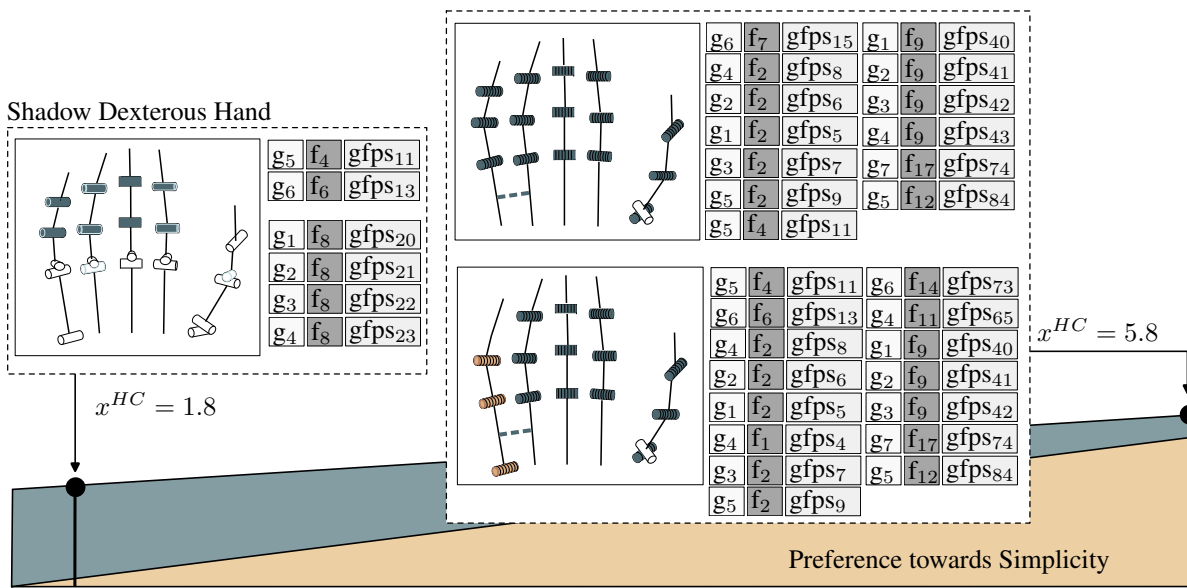


Figure 6.8: Guidance's recommendation for the example application 'Care' with example positioning of the commercially available Shadow Dexterous Hand.

tionalties. In Figure 6.9 and 6.10, the Quality Profile illustration for the recommended Hand Concept (see Figure 6.8, right) and the Shadow Dexterous Hand are shown, respectively. The Quality Profile illustrations of individual GFPSs considered so far are now linked to the Quality Profile of the IMDC (see Figure K.5), which features all Quality Criteria of the Superior Quality Anthropomorphic Movements due to its joint configuration. A quality marked in white in the given Quality Profiles is therefore one that is negatively addressed by an applied GFPS. A direct comparison of the two Quality Profiles in Figures 6.9 and 6.10 first reveals that the Shadow Hand still exhibits almost all Qualities of the Superior Quality Anthropomorphic Movements, whereas these are reduced by half in the recommendation. In addition, it is noticeable that the Shadow Hand coordinates only four anthropomorphic movements (chosen Qualities in the Superior Quality Movement Independence), whereas the recommended Hand Concept coordinates eleven. Both aspects are reflected in the Superior Quality Degree Of Actuation, which is strongly positively influenced for the recommended Hand Concept, as joints are simultaneously eliminated (q_{40} Reducing number of Joints/Motors) and coordinated (q_{41} Keeping number of DOF). Due to the coordination, the Superior Quality Contact Conditions is also positively influenced, qualitatively capturing the finger's passive compliance to objects. Finally, the Superior Quality Manipulability is much more negatively influenced in comparison to the Shadow Hand. This demonstrates that the manipulability of the Shadow Hand is better, and thus it is significantly more dexterous. However, it has been shown that this level of dexterity is not required for the defined tasks.

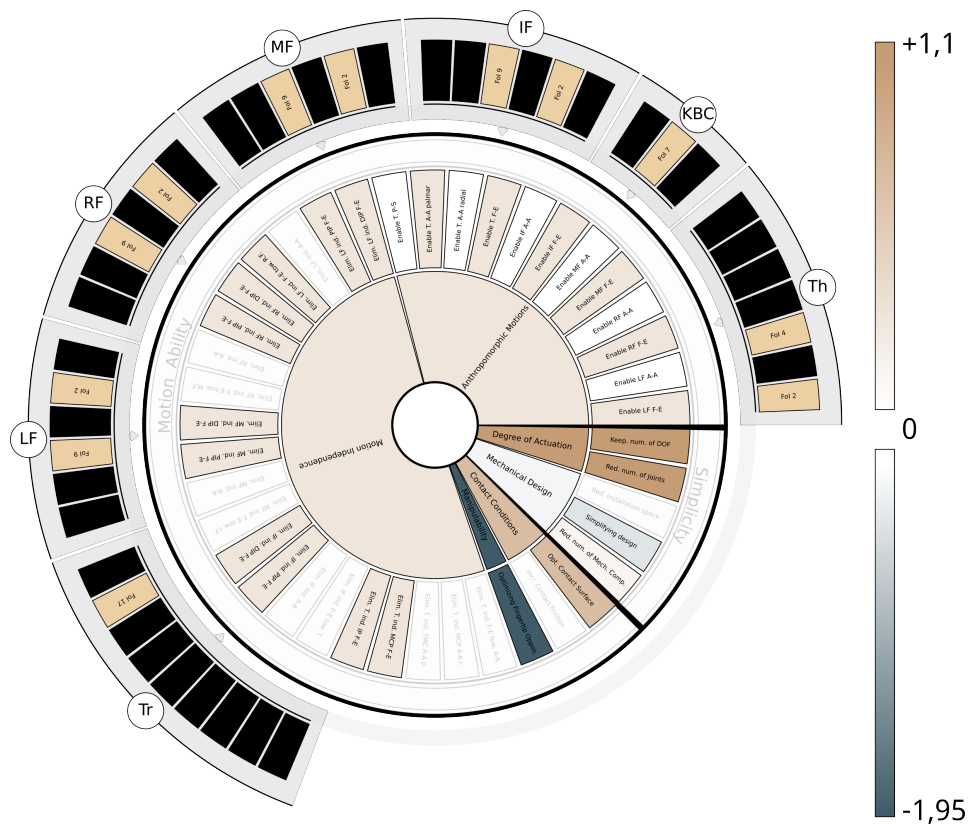


Figure 6.9: QP-illustration of the example recommendation (enlarged version in Figure K.6).

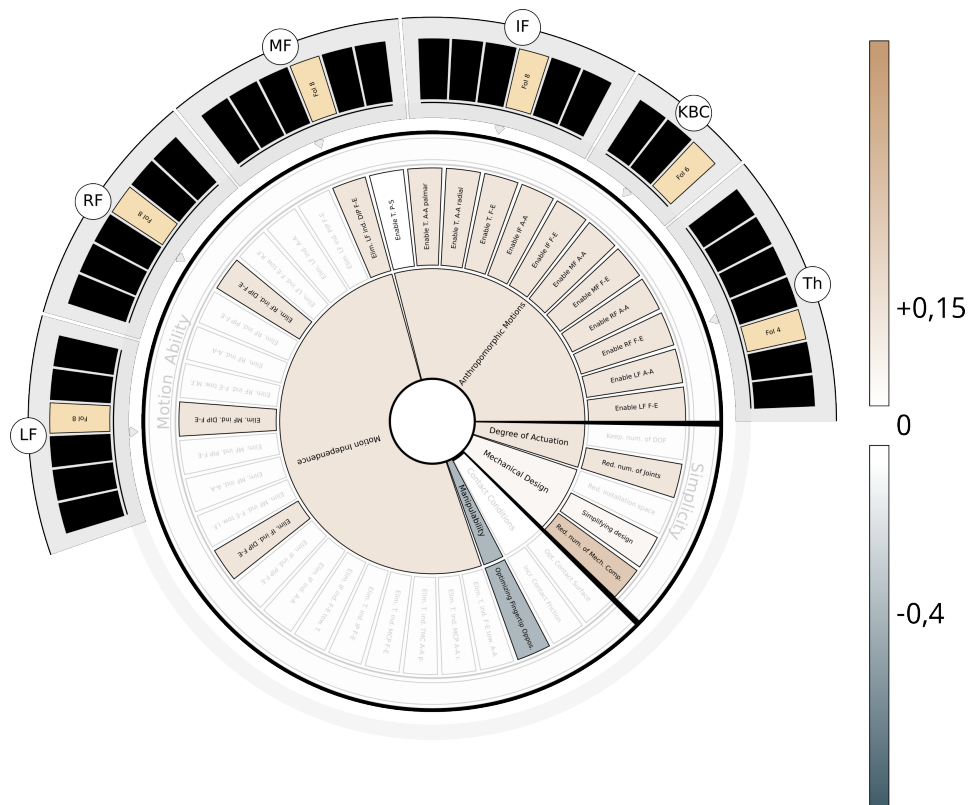


Figure 6.10: Quality Profile illustration of the Shadow Dexterous Robot Hand (enlarged version in Figure K.7).

7 Discussion

In this dissertation, the research question was defined as to how guidance can be developed for the conceptual design, whereby concrete functionalities were specified. A hypothesis was formulated that postulates the possible realization of such guidance in the form of a knowledge-based system. Three objectives were defined for the concretely specified functionalities of the guidance in order to develop these functionalities within the scope of this dissertation and test the hypothesis. Each of the objectives was addressed in separate Chapters 3, 4 and 5.

The results of this dissertation are discussed below. First, the research hypothesis is evaluated. To this end, the results of the individual objectives are discussed successively. They are briefly summarized, interpreted in the light of the hypothesis, discussed with regard to their implications, i.e. the impact and significance, and discussed with regard to their limitations. A detailed summary of the results is not provided, respectively. Instead, reference is made to the conclusions 3.5, 4.4 and 5.4, in which the respective summaries can be found. Finally, the research question of this dissertation will be discussed for the overall guidance developed. The chapter ends with a discussion of the limitations.

First Objective

The first objective (O1) requires the development of a database for design knowledge on joint configuration and joint coordination. On the one hand, the respective knowledge should reference relevant literature, on the other hand, it should be structured in such a way that it can be used for the systematic generation of conceptual design solutions.

The required database was developed in chapter 3 of this dissertation. A methodology was developed to collect literature-based knowledge on joint configuration and coordination and to structure it in the form of FoIs and PSs within morphological boxes, whereby the PSs are linked to the original references. Further, a methodology was developed to define the technically relevant DOF of the human hand. This was presented as the IMDC. Using both, it is proposed to define any robot hand conceptual design through the combination of the IMDC and corresponding PSs. Using a compatibility matrix, 8.5 billion possible robot hand conceptual designs could be determined.

The significance of the results can be discussed with regard to the research hypothesis. In summary, it can be said that the first objective was successfully fulfilled with the development

of the LoA, the IMDC and the Hand Concepts. As the first objective is derived directly from the hypothesis, it can therefore be said that this part of the hypothesis was successfully confirmed. Furthermore, the significance of the results can be discussed with regard to the state of the art. In the course of processing the first objective, five contributions to the state of the art could be realized. They are described below.

As a first contribution, the set of SRHs is defined. Performance requirements are commonly specified in robot hand designs. While these requirements may vary, grasping is a frequently used benchmark. To the best of the author's knowledge, no collection of robot hands that have successfully passed common and established grasping tests exists in the literature. The defined set of SRHs may serve as a valuable resource for the further analysis of applied design strategies.

As a second contribution, the derived IMDC identifies technically relevant anthropomorphic joints. The applied search systematic applied in Section 3.2 demonstrated that although many studies analyze the human hand's kinematic structure, no clear conclusion has yet been derived regarding which joints are technically relevant. For the first time, a methodology is presented that compares these findings with the joints used in currently successful robot hands. The IMDC may serve as a useful reference for designers seeking anthropomorphic inspiration.

As a third contribution, a database on design knowledge has been developed for the first time. As outlined in Section 2.4.1, no such database could be identified in the literature. Existing databases, such as the one by Piazza et al. (2019), present useful information on robot hands regarding their form and features. However, no work has yet introduced a database that enables filtering by design approaches. The presented *Library of Approaches* further allows users to locate relevant literature of the design approaches, associated authors and robot hands in which these approaches have been applied. In addition to the results presented in this dissertation, the database is available online through an easy-to-use GUI. The LoA can be helpful for both novice and experienced designers in exploring conceptual design options and retrieve relevant literature.

As fourth contribution, the developed database enables, for the first time, the categorization of robot hands based on their mechanical design. As outlined in Section 2.2.3, robot hands have so far been categorized according to factors such as form, features performance or simplicity. A categorization based on mechanical design has not been possible due to the lack of an appropriate foundation. Previous works have only allowed for grouping approaches based on fixed criteria (e.g., equal number of DOF, identical thumb configuration, etc.). The proposed definition of a Hand Concept as the combination of the IMDC and GFPSs enables, for the first time, categorization according to the mechanical design. An example application is performed in Section 6.3 using the Shadow Robot Hand. The categorization facilitates comparisons between different robot hands. For instance, it becomes evident after categorization, that

the design approaches $gfps_{11}$ and $gfps_9$ are implemented in nearly all SRHs. The developed illustration of Quality Profile additionally allows for qualitative comparison across multiple categorizations.

As a fifth contribution, the number of identified Hand Concepts is highlighted. By using the derived PSs, all possible conceptual designs were systematically identified. For the first time, the frequently claimed complexity and comprehensive nature of robot hand design could be illustrated in a systematic manner. The identified number of approximately 8.5 billion conceptual designs systematically reveals the extent of variation in literature. Furthermore, it confirms the initially stated impracticality of directly classifying existing conceptual designs; The applied methodology enables the description of hand designs that were unknown at the time of the method's derivation. Finally, it defines a broad solution space that supports innovation during the design process.

After discussing the significance of the results, the limitations are discussed. These are divided into two areas. Firstly, the limitations of the above-mentioned contributions are discussed. Secondly, the limitations that were defined at the beginning of this dissertation are discussed. As a first limitation, the SRHs are defined solely based on success in grasping tasks. For their identification, robot hands that achieved successful results in the Kapandji Test, Feix Taxonomy and Cutkosky Taxonomy were considered. While this definition is necessary for the scope of this dissertation, it does not imply the ineffectiveness of other robot hands. Similar sets of robot hands can be defined based on other Qualities, using different evaluation procedures. This limitation equally applies to the defined IMDC: the definition of 'technically relevant joints' may differ if other performance criteria, such as manipulation, are considered.

With regard to the database, the limitation of the developed solution space is discussed. While it is stated that *all possible* conceptual designs are derived, this solution space must be examined from two perspectives. On the one hand, it is emphasized that the completeness only applies in relation to the derived PS. On the other hand, it is acknowledged that the large number of Hand Concepts includes many designs that are of limited practical relevance. Concerning the first point, although the derived FoIs and PSs allow to categorize robot hands that were unknown during the derivation of the method, no general completeness can be claimed due to literature bias: It is impossible to cover all existing publications. As a result, alternative design approaches may exist that lead to new PS and thus to additional conceptual designs. Regarding the second point, identifying all possible GFPS combinations may result to Hand Concepts that are counterintuitive. For example, some Hand Concepts apply tendon coordination to one finger and linkage coordination to others. However, designers would normally choose a consistent coordination method across all fingers.

With regard to the developed solution space, the required computation time is also discussed. Considering all possible combinations of GFPSs demands significant computational resources.

The algorithm was executed on a Lenovo ThinkPad X13 Yoga (Intel Core i7-1165G7, 4 cores, 8 threads, 16 GB RAM). Taking all three FoI-Cs into account, the generation of the approximately 8.5 billion solutions required six hours of computing time when utilizing all available CPU cores in parallel. Using a single CPU core, the computation time took approximately five days. However, it is emphasized that the solution space needs to be generated only once and can subsequently be used as embedded knowledge. The addition of further literature sources does not require regeneration of the solution space, as it is composed of GFPS combinations that reference the stored literature. A new computation is only necessary if changes are made to the GFPS definitions themselves.

In reference to the limitations defined at the beginning of this dissertation, the omission of joint allocation is discussed. As established in the introduction, no universally valid joint allocation exists. Task-specific designs require parameterized joint allocation alongside optimization of inclination and twist angles, which depends on the joint configuration. As such definition would argue a dedicated dissertation, it lies outside the scope of this dissertation. Nevertheless, for the sake of completeness, a functioning joint allocation was implemented following standard procedures. The corresponding joint poses, inclination, and twist angles are documented in Appendix A. The presented set of working dimensions can be understood as an additional contribution: While various works provide individual working dimensions, no complete dataset including HMC joints was identified in the literature. Furthermore, the complete CAD design is made available as open source ¹.

Furthermore, the research was limited to rigid-sequential and tendon-driven designs. This focus was made in order to limit the scope of this dissertation. On the one hand, this limitation should be emphasized, as flexible and pneumatically driven designs are becoming increasingly popular and the information collected in the database does not include any design solutions for these robot hands. On the other hand, however, it must be emphasized that many of the findings are transferable. For example, the findings regarding the grasp-specific finger coordination requirements are equally relevant for pneumatically driven robot hands as for rigid-sequential designs.

The work was also limited to anthropomorphic designs. No FoIs and PSs were collected that lead to conceptual designs that contradict the definition established in Chapter 2.2.1. For example, complete fingers were not eliminated. On the one hand, this focus was chosen to limit the scope of this dissertation and focus the contribution to the design of anthropomorphic robot hands. On the other hand, the deviation from this approach is interesting with regard to the possible reduction of mechanical complexity and thus costs.

¹<https://git-ce.rwth-aachen.de/robotic-hands/towards-quantitative-dof-relevance-identification>

Second Objective

The second objective (O1) requires the development of a method that allows the selection of optimal conceptual designs from the set of Hand Concepts. An optimum is characterized by its dependence to user requirements, requiring thus the definition of those.

A heuristic is developed that uses user requirements to identify a Pareto-optimal solution. The user requirements are defined to include a performance requirement in form of required grasp types, as well as a preference among robot hand qualities. As an example, this dissertation uses the robot hand qualities *Motion Ability* and *Simplicity*. For each grasp type, appropriate joint configurations and coordination strategies are identified based on recommendations found in the literature. Put together, they form suitable Hand Concepts for each grasp type. The resulting set of suitable Hand Concepts for each grasp type is then ranked according to the selected qualities. For a single grasp type, a recommendation is made based on the user's preference: the right-hand side of the ranked set is selected when *Simplicity* is preferred, and the left-hand side when *Motion Ability* is preferred. In case of multiple selected grasp types, the same procedure is applied to the intersection of all corresponding sets.

The significance of the results can be discussed with regard to the research hypothesis. In summary, it can be said that the second objective was successfully fulfilled. Possible user requirements are analyzed and appropriate Qualities for the goal of this dissertation are defined. Further, a heuristic is developed to choose among the derived Hand Concepts the optimal solutions based on the defined Qualities. As the second objective is derived directly from the hypothesis, it can therefore be said that this part of the hypothesis was successfully confirmed. Regarding the implications of these results, for the first time, an heuristic for a task-based design is defined. First, requirement criteria are introduced for the definition of a task. Second, the distinct studies on joint relevance and joint coordination strategies are combined by translating their results into required criteria.

Regarding the limitations, the underlying motivation for the introduced heuristic for identification of an literature-based pareto optimal is discussed. As an alternative, a quantitative metric could have been developed. For example, a metric could be established that quantifies an Hand Concept's *Motion Ability* through defined characteristics, such as the addressable workspace (ROM), quality of fingertip opposition (coordination of ROMs) and number of suitable grasping points on a considered geometry. However, the development of such a metric involves issues. First, although allowing to identify theoretically an optimum, the practical implications would need to be verified experimentally. With the derived number of Hand Concepts, such experimental verification is impractical, requiring the development of an elaborated simulation. Second, the quantification of the defined characteristics, such as the addressable workspace, requires a fine-tuned joint allocation which depends on the considered Hand Concept. A single

set of defined dimensional parameters can not be used, as the comparison of multiple Hand Concepts requires them to be in their optimal configuration, which in turn requires fine-tuned inclination angles, twist angles, and base joint poses. To the best of the author's knowledge, no method exists for automated optimization of a given joint allocation based on the considered joint configuration. Concluding, a quantitative metric requires an exhaustive method, for which either practical implications are unclear, or elaborated verification is required. As the latter justifies the scope of a separate thesis, a heuristic is applied in this dissertation instead. As the applied heuristic leverages the results found in literature and allows to refer to these studies, it complies with the goal of this dissertation for the development of a guidance.

The limitations of the applied heuristic are also discussed. The reviewed literature is not well-suited for the intended purpose, revealing a gap in current research on task-based designs. This gap is examined in the following.

The task-based joint coordination results from Tavakoli et al. (2015) are partly subjective and lack experimental validation. In their recommended actuation strategies, hand appearance plays a key role but is considered only subjective. As a result, the actuation strategies for each grasp are based on theoretical reasoning rather than empirical data. However, experimental validation is not included here, as it falls outside the scope of this dissertation. The main objective is to develop a knowledge-based design assistance that refers to results found in literature.

The task-based joint configuration results from Saliba et al. (2013) are difficult to interpret in the context of this dissertation. This is due to three main limitations. First, the study involves three tasks, but it does not account for object variety: the geometries used are very similar and can all be approximated by a small cylinder. Second, the underlying evaluation metric is designed more for assessing manipulation skills than grasping: the computed dexterity score is based on task completion time, with most of the activity involving manipulation rather than grasping. Third, some joints were not sufficiently examined, because certain joints were difficult to restrict during the experiment. Reconstructing the results using a technical replica instead of a human hand, the Feix taxonomy, and a metric that evaluated grasp success rather than execution time would likely provide more relevant insights.

Such an approach was presented by the author (Gossen et al. 2025a) in a publication that was developed as part of this dissertation. In that study, the IMDC was implemented as a prototype, and successively reduced joint configurations were created as separate prototypes and compared experimentally. The experimental investigation determines the maximum graspable weight. The approach thus enabled a quantitative assessment of how eliminating specific joints affects performance, based on a Feix grasp. As proof of concept, the study evaluated the relevance of HMC joints. A comprehensive study of this kind would require significant effort, justifying a dedicated dissertation on the topic.

Third Objective

The third objective (O3) requires the development of the guidance's control system. An Inference Component must be designed that evaluates all Hand Concepts (from (O1)) in accordance with the derived heuristic (from (O2)).

The required control system behavior is successfully developed. A utility analysis is conducted once across all GFPSs, assigning each Hand Concept a base score. This score is then modified using preference and relevance weights, ensuring that the most suitable Hand Concepts receive the highest scores, according to the derived heuristic. The method was successfully validated in Section 6.1: for two example GFPSs, Hand Concept scores are manually calculated and found to match the expected results. The method was further successfully verified in Section 6.2, where the corresponding input yielded a correct replication of the set of SRHs. For a detailed summary, the reader is referred to Section 5.4.

The significance of the results can be discussed with regard to the research hypothesis. In summary, it can be said that the third objective was successfully fulfilled. The control system assigns each Hand Concept a score, considering user performance requirements and user preference requirements, and thus reflects the trade-off of the design decision. As the third objective is derived directly from the hypothesis, it can therefore be said that this part of the hypothesis was successfully confirmed.

Regarding the implications of the results, the derived method for identification of influence values is emphasized. First, the method significantly reduces manual effort and improves thus ease of implementation. It allows to reduce the initially assumed effort of evaluating 86 GFPSs over 41 evaluation criteria (resulting in a total of 3,526 parameters) to separated phases of evaluating three FoI-Cs over six SQs (resulting in a total of only 18 parameters). Second, the method's transferability is emphasized. It is independent of the specific content of the GFPSs and provides a systematic approach to defining weights and evaluation values (influences) to achieve the desired system behavior. As a result, the method can be applied in the same way to other GFPS datasets.

Regarding the limitations of the results, the subjectivity of the defined evaluation criteria is acknowledged. The selected terminologies and number of criteria reflect the author's perspective and may differ if developed by someone else. However, the goal is not to present a unique quantifiable solution, but to offer a systematic recommendation. As in product development, evaluation criteria and individual assessments are inherently subjective to some degree and depend on the developer's judgment. Nevertheless, the proposed method was developed systematically and is both traceable and repeatable.

As a second limitation, the required computation time is also discussed. The method assigns each Hand Concept a score (constant and thus embedded knowledge), modifies it according

to user requirements, and chooses the Hand Concepts with highest score for recommendation. Therefore, the applied strategy corresponds to a Dijkstra search. On the one hand, this search strategy identifies the global optimum. On the other hand, the exhaustive search requires substantial computation time. Considering all FoI-Cs at once, the generation of a single recommendation takes approximately ten hours.

A third limitation concerns the number of solutions considered in a recommendation. During validation of the inference component, it was found that the system does not produce a unique recommendation but rather a set of equivalent alternatives. These alternatives are identical in the number of eliminated DOFs (joint configuration) and DOAs (joint coordination), but differ in their specific implementation. As previously noted, this issue can be addressed through relevance weighting. Currently, the system uses a binary relevance weight (1 or -1) to distinguish relevant from irrelevant Quality Criteria. With defined joint relevances for a given grasp (see Gossen et al. (2025a)), the values can be extended. In this sense, it can be understood as both a limitation of the state of the art and a contribution that joint relevance - once identified - can be considered in the proposed framework.

Guidance System

This section presents the results related to the overarching guidance system. While the outcomes of the individual objectives are discussed above, this section focuses on the results arising from their integration into the complete guidance framework. Firstly, the verification in Section 6.2 replicated successfully the SRHs, but also suggested minimal designs with less DOA than the SRHs as they do not appear in the state of the art. Secondly, to the best of the author's knowledge, the example implementation of the guidance in Section 6.3 is the first task-based design of anthropomorphic robot hands. The result is a minimal conceptual design tailored specifically to the given task.

The significance of the results can be discussed with regard to the research hypothesis. As discussed above, all three objectives of this dissertation have been addressed, and the corresponding parts of the hypothesis from which they were derived have been confirmed. The consolidation of the individual results into a knowledge-based guidance system has been successfully validated, verified, and implemented in an example. Since the research hypothesis is fully represented by these three objectives and the results have been successfully integrated, it can be concluded that the hypothesis has been confirmed in the course of this dissertation.

Subsequently, the findings allow conclusions to be drawn about the research question. The hypothesis was derived based on assumptions. These assumptions were confirmed through the development and fulfillment of the objectives. First, the use of the lowest common denominator in form of PSs for generating conceptual designs rather than direct classification, proved

effective. As shown in Chapter 3, directly classifying eight billion possible conceptual designs is impractical. Second, designing recommendations based on user input also proved effective. Chapter 4 demonstrated that conceptual designs are Pareto-optimal solutions subjective to the user. In conclusion, the research question has been answered within the scope of this dissertation.

Besides the research question, the implications of the results for the current state of the art are also discussed. First, the importance of tailored, task-based designs is demonstrated. Second, the modularity and general applicability of the guidance framework is emphasized.

Regarding the first point, the findings show that incorporating task-specific requirements is not only valid but also beneficial when designing anthropomorphic robot hands. For example, the task-based design recommended by the guidance for selected care-related tasks (see Section 6.3) achieves a reduction of 15 actuators compared to a commercially available solution.

Regarding the second point, each component of the guidance system is developed in a modular and generalized way, allowing it to be applied to other domains if the data is appropriately adjusted. The methodology can be adopted to any robotic system that

- requires qualitatively justified design recommendations with reference to original sources.
- allows the definition of FoIs and PSs.
- represents a Pareto-optimal system, for which a set of user requirements can be specified, including at minimum performance requirements and a preference-based trade-off.
- allows definition of evaluation criteria for assessing PSs.

The corresponding data structure for these inputs can be easily adapted. The influence of individual PSs on the evaluation criteria can be identified using the generally applicable methodology presented in Chapter 5. The guidance system's inference component then processes these inputs independently of the specific data used.

Furthermore, the implications of the results are discussed in relation to the underlying motivations and goals of this dissertation. The research question arose from specific motivations. As shown earlier, the research question has been answered. Remaining is to assess whether the original motivations have also been successfully addressed. This involves examining whether (1) the tool is suitable for novice designers and helps lower entry barriers, (2) a semi-automation of the design process has been achieved, and (3) the system is not viewed as a closed body of knowledge.

Regarding the first point, the guidance system is proposed as a semi-automation of the conceptual design process, where the decision making for the knowledge parts is automated and the implementation parts remain manual. The respective components of the conceptual design process are color-coded in Figure 1.1. In the course of this dissertation, it has been demonstrated that the method enables this form of semi-automation. In the example application, the system not only generates a conceptual design recommendation but also provides task- and

preference-specific information on joint configuration and coordination, along with corresponding references to the literature. At the same time, users can extract general information on joint allocation from this dissertation, such as phalanx relations. As intended, the final evaluation and optimization steps must be performed manually. This process was also illustrated through the prototype implementation described in Chapter A.

Secondly, it is discussed if the guidance is appropriate for novice designers to lower entry hurdles. On the one hand, the tool is specifically designed to be intuitive in application. Users simply specify the required grasps, which are provided in a low-threshold format as images. In addition, the tool applies several measures to make the results understandable. For example, to explain the recommendation, a dedicated illustration is established. The user can identify on first glance which joints are present and how they are coordinated, if at all. To explain the reasoning, interested users are provided with literature sources for robot hands that incorporate similar design elements. To explain a variety of recommendations, another dedicated illustration is established and presented as the *Quality Profiles*. For a given conceptual design, a circle diagram visualizes the applied PSs and highlights the addressed Qualities. This qualitative depiction allows users to compare different recommendations or evaluate a recommendation against existing robot hands (see Section 6.3). On the other hand, it is acknowledged that the tool can not be used entirely without prior knowledge, as a certain level of interpretation is involved. For example, users must be familiar with the content of this dissertation, considering key terminologies, such as Feix Taxonomy, Motion Ability, FoIs and GFPSs. Further, the tool is intended for technically inclined individuals, as the manual part of the design process requires hands-on engineering skills. In conclusion, the tool is designed to be operated by novice designers and successfully lowers entry hurdles. However, a certain minimum level of expertise is required, which involves familiarity with the core concepts presented in this dissertation.

Thirdly, it is discussed if the system is viewed as a closed body of knowledge. While this is not explicitly stated as a motivation in the introduction, the underlying goal is to develop a design assistance system that refers to the literature. This concept inherently assumes that the system should not represent a fixed body of knowledge, but rather acknowledge the field as continuously evolving. In this context, it is emphasized that, in the current implementation, the referenced literature only includes sources published up to 2023, as outlined in the review strategy in Section 3.3. However, a Knowledge Acquisition Component has been developed and presented in Section 5.3. This interface allows the Knowledge Engineer to easily add new entities (references, PS, etc.) and relations. Additional references can be included without requiring changes to the derived Hand Concepts.

8 Conclusion and Outlook

This dissertation set out to develop a guidance system in the form of a knowledge-based design assistant for the conceptual design of anthropomorphic robot hands. The system aims to semi-automate the design process by providing recommendation and literature references for the knowledge-driven aspects of the design workflow. To answer the research question, a hypothesis is proposed, suggesting the implementation to follow the architecture of knowledge-based systems, with specific demands on the two main components: the knowledge base embeds literature-linked design knowledge that allows to systematically generate conceptual designs and the control system processes user requirements for evaluation of the systematically generated conceptual designs. Based on the hypothesis, three main objectives were defined: (1) to develop the corresponding knowledge base, (2) to develop a method for identification of optimal conceptual designs based on user requirements, and (3) to develop a method for the automated evaluation.

The first objective was successfully fulfilled through the application of three interlinked methodologies. The first enabled the collection and structuring of design knowledge and their literature references into principal solutions (PSs) within morphological boxes. The second derived an initial joint configuration that captures the technically relevant DOFs of the human hand. The third methodology defined conceptual designs as combinations of the initial joint configuration with the derived PSs, enabling systematic generation. By applying a compatibility matrix, the system identified approximately 8.5 billion feasible conceptual designs for anthropomorphic robot hands.

The second objective was successfully fulfilled by deriving a heuristic that uses user requirements to identify Pareto-optimal solutions. These requirements include both a performance aspect and a preference among robot hand qualities. The first is specified by required grasps. For the second, the qualities *Motion Ability* and *Simplicity* are used as illustrative examples. For each grasp type, suitable joint configurations and coordination strategies are identified based on literature recommendations, resulting in a set of suitable options that is selected from, depending on the user's preference. In case of multiple selected grasp types, the intersection of all corresponding sets is considered.

The third objective was successfully fulfilled by applying a utility analysis on all derived PSs, thereby assigning a score to each hand concept. A methodology was developed that significantly reduces the manual effort required to evaluate all PSs from an initial total of 3,526 parameters to just 18. User-specific input is incorporated by defining a baseline hand concept score and

adjusting it through input-dependent relevance and preference weightings. The method was successfully validated through manual calculation and verified by the automated replication of a known set of conceptual designs.

All individual results are successfully integrated into the intended guidance system. Beyond replicating the known set of conceptual designs, the verification also suggested new minimal designs with less DOA, as they do not appear in the state of the art. Further, an example application is performed, presenting a task-based design for application in the care sector. To the best of the author's knowledge, this presents the first automated task-based design of anthropomorphic robot hands.

With the successful fulfillment of all objectives - each derived directly from the hypothesis - the research hypothesis can be considered confirmed. As a result, the proposed solution effectively answers the research question posed in this dissertation. The underlying assumptions on which the hypothesis was based were also validated during the course of addressing the individual objectives. Specifically, it was shown that systematic generation of conceptual designs is necessary, as direct classification proved to be impractical, and that user requirements must be incorporated to produce meaningful design recommendations.

The primary contribution of this dissertation is the development of a semi-automated process for the conceptual design of anthropomorphic robot hands. For the first time, task-based conceptual designs can be systematically generated, with direct reference to literature where the corresponding design approaches have been applied. The framework's integrated explanatory components make it suitable for novice designers. The framework has, thus, the potential to significantly lower entry hurdles to this field of study. Moreover, the knowledge-based framework is both extendable and modular, allowing it to be adapted for use in other domains beyond robot hand design.

Additional contributions emerged in the course of fulfilling the objectives of this dissertation. First, a set of robot hands that successfully performed common grasping tasks is identified and presented as *Successful Robot Hands* (SRHs), a benchmark reference for future designs. Second, a unique definition of the technically relevant DOF of the human hand is proposed, based on a comparison between biological studies and the joint configurations of SRHs. Third, a design knowledge database is developed, which enables both the identification of mechanical design approaches and the categorization of robot hands based on their mechanical design. Fourth, a large number of conceptual designs were systematically generated, demonstrating the often claimed complexity of robot hand design and the significant variation across existing literature. Finally, for identification of user-specific recommendation, a heuristic was developed that combines findings from the literature.

While the guidance was successfully validated, verified and applied, several limitations remain. First, the approach is restricted to rigid-sequential, tendon-driven, and anthropomorphic designs.

Although much of the results and implications are transferable, the current database lacks reference for alternative actuation types such as pneumatic systems. Second, joint allocation is only partly addressed. A single example is derived, but a fully parameterized allocation method is beyond the scope of this dissertation. Third, due to limited data in the literature on joint relevance, the developed heuristic can not always produce a unique recommendation. Instead, it generates several (allegedly) equivalent alternatives with identical number of reduced DOF or DOA. Finally, the current implementation has high computational demands, with recommendations taking up to several hours. For demonstration purposes, the set of conceptual designs was reduced, resulting in significantly faster runtimes.

Based on the identified limitations, future work can be grouped into three main directions: (1) modifying, (2) transferring, and (3) extending the presented guidance system. Regarding the first, the framework can be optimized to reduce computation times. Besides general programming techniques for handling large datasets, the results of this dissertation could serve as training data for machine learning models, potentially enabling faster design recommendations. Second, the framework could be adapted for alternative robotic architectures, such as pneumatically driven robot hands, or transferred entirely to other domains. Third, the current heuristic could be expanded or replaced to enhance the precision of design recommendations. One promising option is to identify joint relevance values, enabling the framework to distinguish between conceptual designs not only by the number of eliminated joints, but also by their type. Alternatively, the heuristic could be replaced with a quantitative metric. In this approach, each conceptual design would need be optimized using a parameterized joint allocation strategy their Motion Ability be quantified based on defined characteristics.

Building on the extension strategies discussed above, relaxing the anthropomorphic constraints offers an intriguing opportunity to apply the presented guidance system in a top-down design approach for variable grippers. By allowing the elimination of entire finger, it would be possible to develop a library of minimal configurations for each grasp type, which may no longer be anthropomorphic. Selecting multiple grasps would lead to the combination of the corresponding minimal configurations into a gripper design capable of handling the different selected grasp types. Further assuming grasp types to be object agnostic, the gripper can handle different objects associated to the considered grasp types. The resulting variable gripper is then developed in a top-down approach, inspired by the human hand.

By lowering entry barriers in early stage design of anthropomorphic robot hands, this research lays a foundation to acceleration for both mechanical and control design and provides thus potential to meet the increasing demand of robot hands and to face currently high costs. At the same time, it offers for the first time a framework for task-based robot hand design with meaningful results, even though gaps in the state of the art do not justify an analysis of the entirety of these results.

Supervised Student Theses

This chapter provides information on student theses supervised and closely guided by the author. Table 8.1 lists theses that contributed to this dissertation, to ensure transparency regarding the scientific contributions. Table 8.2 lists theses that did not contribute directly to this dissertation. These are included to demonstrate the author's supervision experience, to document the author's academic duty in training and mentoring students, and to illustrate that the author's research activities extended beyond the scope of this dissertation. The author thanks the students for their work and their contribution.

| Name | Year | Type | Title |
|---|------|-----------------|---|
| Sebastian Polzin | 2022 | Bachelor Thesis | Analyse und Gegenüberstellung von (seilgetriebenen) Roboterhänden |
| Tianyi Jin | 2023 | Bachelor Thesis | Definition und Evaluation einer Taxonomie für die "Geschicklichkeit"(Dexterity) einer Roboter Hand im Rahmen der Qualitätskriterien |
| Ruiqi Zhang, Andrei Resceanu, Taiyang Tian, Tobias Mechsner | 2023 | Project Thesis | Design und Evaluierung eines Baukastensystems für die mechanische Konstruktion von anthropomorphen Roboterfingern |
| Eugen Schustermann | 2023 | Master Thesis | Identifikation und Analyse von Design Kriterien für die parametrische Entwicklung anthropomorpher Roboterdaumen |
| Ana Laura Urzua Quiroz | 2023 | Bachelor Thesis | Construction and Evaluation of Underactuated Mechanisms for Wire-driven Anthropomorphic Robot Hands and Analysis of their Modular Design |
| Mark Witte | 2023 | Master Thesis | Design und Evaluierung der Greifperformance einer auf Kontinuumsrobotik basierenden, seilgetriebenen Roboterhand unter Anwendung von Tendon-Routing |
| Sebastian Polzin | 2024 | Master Thesis | Einfluss der Gelenkkonfiguration auf die Greifperformance einer anthropomorphen Roboterhand |
| Andrei Resceanu | 2024 | Bachelor Thesis | Analyse der minimalen Anforderungen an den Aktuierungsgrad anthropomorpher Roboterhände |

Table 8.1: Student theses supervised in the doctoral period that contribute to this dissertation.

| Name | Year | Type | Title |
|--------------------|------|-----------------|--|
| Dhruva Singh Sewar | 2022 | Master Thesis | Konzeption und Konstruktion einer neuartigen Antriebseinheit für eine seilgetriebene Kontinuumsrobotik-Hand |
| David Bosen | 2022 | Bachelor Thesis | Underactuation in Robotic Hands: Design Adaption and Evaluation of a New Actuation Concept for Wire-driven Robotic Hands and Analysis of the General Context |
| Jungmin Lim | 2023 | Master Thesis | Design of Compliant Robot Leg using Variable Stiffness Mechanism |
| Disen Wang | 2023 | Master Thesis | Modeling and Control of Robotic Catheters |
| David Meyersieck | 2023 | Master Thesis | Untersuchung der Kriterien für das mechanische Design einer Roboterhand für einen definierten Anwendungsfall |
| Zhaohang Qiu | 2023 | Bachelor Thesis | Modellierung einer auf seilgetriebener Kontinuumsrobotik basierenden Roboterhand |
| Jonas Getmann | 2024 | Bachelor Thesis | Entwicklung und Evaluierung eines elastischen Gehäuses für die "CRoB Hand" |
| Tianyi Jin | 2025 | Master Thesis | Design Optimization of the RH5 Humanoid Robot For Reinforcement Learning-Driven Pull-Up Performance |
| Lennox Mart | 2025 | Master Thesis | Entwicklung eines Roboterendeffektors für das Lösen von Schrauben bei der Demontage von EV-Batteriesystemen |
| Jens Geuking | 2025 | Bachelor Thesis | Entwicklung eines Roboter-Endeffektors zur automatisierten Demontage von Steckerverbindern auf Leiterplatten |
| Rick Egetemaier | 2025 | Master Thesis | Learning from Demonstration — Identification and parameterization of disassembly operations from human observation |
| Omar Farooq | 2025 | Master Thesis | A Quantitative Evaluation of Thumb Degrees of Freedom Relevance in Anthropomorphic Robot Hands |
| Artem Ekimov | 2025 | Master Thesis | Finding Minimal Robotic Hand Configurations per Feix Taxonomy - A Top-Down Quality-Diversity Study |
| Lucas Maute | 2025 | Master Thesis | Development of a robotic end-effector for the automated disassembly of cables |

Table 8.2: Student theses supervised in the doctoral period that have not contributed to this dissertation.

Bibliography

- Altenkrüger, D. and W. Büttner (2013). *Wissensbasierte Systeme: Architektur, Entwicklung, Echtzeitanwendungen-Eine praxisgerechte Einführung*. ISBN: 978-3-528-05244-7.
- Ambrose, R. et al. (2000). “Robonaut: NASA’s space humanoid”. In: *IEEE Intelligent Systems and Their Applications* 15.4, pp. 57–63. DOI: 10.1109/5254.867913.
- Bain, G. et al. (2015). “The functional range of motion of the finger joints”. In: *The Journal of hand surgery, European volume* 40.4, pp. 406–411. DOI: 10.1177/1753193414533754.
- Barakat, M., J. Field, and J. Taylor (2013). “The range of movement of the thumb”. In: *Hand (New York, N.Y.)* 8.2, pp. 179–182. DOI: 10.1007/s11552-013-9492-y.
- Baril, M. et al. (2010). “Static Analysis of Single-Input/Multiple-Output Tendon-Driven Underactuated Mechanisms for Robotic Hands”. In: *ASME 2010 International Design Engineering Technical Conferences and Computers and Information in Engineering Conference*, pp. 155–164. DOI: 10.1115/DETC2010-28933.
- Baril, M. et al. (2013). “On the Design of a Mechanically Programmable Underactuated Anthropomorphic Prosthetic Gripper”. In: *Journal of Mechanical Design* 135.12. DOI: 10.1115/1.4025493.
- Becker, J. and N. Thakor (1988). “A study of the range of motion of human fingers with application to anthropomorphic designs”. In: *IEEE transactions on bio-medical engineering* 35.2, pp. 110–117. DOI: 10.1109/10.1348.
- Bekey George A and Tomovic, R. and I. Zeljkovic (1990). “Control Architecture for the Belgrade/USC Hand”. In: *Dextrous Robot Hands*. Ed. by T. Venkataraman Subramanian T. and Iberall. New York, NY: Springer New York, pp. 136–149. ISBN: 978-1-4613-8974-3. DOI: 10.1007/978-1-4613-8974-3_7. URL: https://doi.org/10.1007/978-1-4613-8974-3_7.
- Belter, J. and A. Dollar (2013). “Novel differential mechanism enabling two DOF from a single actuator: application to a prosthetic hand”. In: *IEEE International Conference on Rehabilitation Robotics*, p. 6650441. DOI: 10.1109/ICORR.2013.6650441.
- Belter, J., J. Segil, and A. Dollar (2013). “Mechanical design and performance specifications of anthropomorphic prosthetic hands: a review”. In: *Journal of rehabilitation research and development* 50.5, p. 599. DOI: 10.1682/JRRD.2011.10.0188.
- Berselli, G. et al. (2009). “Integrated Mechatronic Design for a New Generation of Robotic Hands”. In: *IFAC Proceedings Volumes* 42.16, pp. 8–13. ISSN: 14746670. DOI: 10.3182/20090909-4-JP-2010.00004.

- Biagiotti, L. et al. (2004). “How far is the human hand”. In: *A review on anthropomorphic robotic end-effectors*, p. 21. URL: <http://www.swisswuff.ch/files/biagiotti2002howfaristhehumanhand.pdf>.
- Bicchi, A. (2000). “Hands for dexterous manipulation and robust grasping: A difficult road toward simplicity”. In: *IEEE Transactions on robotics and automation* 16.6, pp. 652–662. DOI: 10.1109/70.897777.
- Biesecker, L. et al. (2009). “Elements of morphology: standard terminology for the hands and feet”. In: *American Journal of Medical Genetics Part A* 149A.1, pp. 93–127. DOI: 10.1002/ajmg.a.32596.
- Birglen, L. and C. Gosselin (Oct. 2006). “Force Analysis of Connected Differential Mechanisms: Application to Grasping”. In: *The International Journal of Robotics Research* 25.10, pp. 1033–1046. ISSN: 1741-3176. DOI: 10.1177/0278364906068942. URL: <http://dx.doi.org/10.1177/0278364906068942>.
- Birglen, L., T. Laliberté, and C. Gosselin (2008). *Underactuated Robotic Hands*. Springer Berlin Heidelberg. ISBN: 9783540774594. DOI: 10.1007/978-3-540-77459-4. URL: <http://dx.doi.org/10.1007/978-3-540-77459-4>.
- BMBF (2023). *Aktionsplan Robotikforschung - Innovationspotenziale der KI-basierten Robotik erschließen*. Zugriff am 26. Mai 2025. URL: https://www.bmbf.de/SharedDocs/Publikationen/DE/5/846858%5C_Aktionsplan%5C_Robotikforschung.pdf (visited on 05/26/2025).
- (2024). *Bekanntmachung der Richtlinie zur Förderung von Projekten zum Thema "Natürlichsprachliche Integration von Robotik in Gesundheitseinrichtungen"*. Accessed 2025-06-25. URL: <https://www.bmbf.de/SharedDocs/Bekanntmachungen/DE/2024/08/2024-08-16-Bekanntmachung-Robotik-Gesundheit.html> (visited on 05/26/2025).
- BMWK (2020). *Fachkräftesicherung: Strategien für den demografischen Wandel*. Accessed 2025-05-26. URL: <https://www.bmwk.de/Redaktion/DE/Dossier/fachkraeftesicherung.html> (visited on 05/26/2025).
- Bock, O. (2012). *Michelangelo operation manual*. Duderstadt, Germany.
- Bologni, L., S. Caselli, and C. Melchiorri (1988). *Design Issues for the UB Robotic hand*. Univ., School of Engineering.
- Bridgwater, L. et al. (2012). “The robonaut 2 hand-designed to do work with tools”. In: IEEE, pp. 3425–3430. DOI: 10.1109/ICRA.2012.6224772.
- Butterfass, J. et al. (2001). “DLR-Hand II: next generation of a dextrous robot hand”. In: *Proceedings of the 2001 IEEE International Conference on Robotics and Automation* 1, pp. 109–114. DOI: 10.1109/ROBOT.2001.932538.

- Butterfass, J. et al. (n.d.). “DLR’s multisensory articulated hand. I. Hard- and software architecture”. In: *Proceedings. 1998 IEEE International Conference on Robotics and Automation (Cat. No.98CH36146)*. Vol. 3. ROBOT-98. IEEE, pp. 2081–2086. DOI: 10.1109/robot.1998.680625. URL: <http://dx.doi.org/10.1109/ROBOT.1998.680625>.
- Calli, B. et al. (2015). “Benchmarking in manipulation research: The ycb object and model set and benchmarking protocols”. In: *arXiv preprint arXiv:1502.03143*. DOI: 10.48550/arXiv.1502.03143.
- Carrozza, M. et al. (2003). “Experimental analysis of an innovative prosthetic hand with proprioceptive sensors”. In: *2003 IEEE International Conference on Robotics and Automation (Cat. No.03CH37422)* (Taipei, Taiwan, Sept. 14–19, 2003), pp. 2230–2235. ISBN: 0-7803-7736-2. DOI: 10.1109/ROBOT.2003.1241925.
- Carrozza, M. et al. (2004). “The SPRING Hand: Development of a Self-Adaptive Prosthesis for Restoring Natural Grasping”. In: *Autonomous Robots* 16.2, pp. 125–141. DOI: 10.1023/B:AURO.0000016863.48502.98.
- Carrozza, M. et al. (2006). “Design of a cybernetic hand for perception and action”. In: *Biological cybernetics* 95, pp. 629–644. DOI: 10.1007/s00422-006-0124-2.
- Catalano, M. et al. (2014). “Adaptive synergies for the design and control of the Pisa/IIT SoftHand”. In: *The International Journal of Robotics Research* 33.5, pp. 768–782. DOI: 10.1177/0278364913518998.
- Catalano, M. et al. (2016). “From Soft to Adaptive Synergies: The Pisa/IIT SoftHand”. In: *Human and Robot Hands*. Ed. by M. Bianchi and A. Moscatelli. Springer Series on Touch and Haptic Systems. Cham: Springer International Publishing, pp. 101–125. ISBN: 978-3-319-26705-0. DOI: 10.1007/978-3-319-26706-7{_}8.
- Cerulo, I. et al. (2017). “Teleoperation of the SCHUNK S5FH under-actuated anthropomorphic hand using human hand motion tracking”. In: *Robotics and Autonomous Systems* 89, pp. 75–84. DOI: 10.1016/j.robot.2016.12.004.
- Chalon, M. et al. (2010). “The thumb: Guidelines for a robotic design”. In: *2010 IEEE/RSJ International Conference on Intelligent Robots and Systems*. IEEE, pp. 5886–5893. ISBN: 978-1-4244-6674-0. DOI: 10.1109/IROS.2010.5650454.
- Chalon, M. et al. (May 2011). “Dexhand: A Space qualified multi-fingered robotic hand”. In: *2011 IEEE International Conference on Robotics and Automation*. IEEE, pp. 2204–2210. DOI: 10.1109/icra.2011.5979923. URL: <http://dx.doi.org/10.1109/ICRA.2011.5979923>.
- Chang, L. and Y. Matsuoka (2006). “A kinematic thumb model for the ACT hand”. In: *Proceedings 2006 IEEE International Conference on Robotics and Automation, 2006. ICRA 2006*. IEEE, pp. 1000–1005. ISBN: 0-7803-9505-0. DOI: 10.1109/ROBOT.2006.1641840.

- Chew, M., G. Issa, and S. Shen (1991). “Expert System for Robot Hand Design Using Graph Representation”. In: *CAD/CAM Robotics and Factories of the Future '90*. Springer Berlin Heidelberg, pp. 466–471. ISBN: 9783642582141. DOI: 10.1007/978-3-642-58214-1_72. URL: http://dx.doi.org/10.1007/978-3-642-58214-1_72.
- Chu, D. et al. (2024). “Human Palm Performance Evaluation and the Palm Design of Humanoid Robotic Hands”. In: *IEEE Robotics and Automation Letters* 9, pp. 2463–2470. DOI: 10.1109/LRA.2024.3354619.
- Ciocarlie, M. and P. Allen (May 2010). “Data-driven optimization for underactuated robotic hands”. In: *2010 IEEE International Conference on Robotics and Automation*. IEEE, pp. 1292–1299. DOI: 10.1109/robot.2010.5509793. URL: <http://dx.doi.org/10.1109/ROBOT.2010.5509793>.
- Cipriani, C., M. Controzzi, and M. Carrozza (2010). “Objectives, criteria and methods for the design of the SmartHand transradial prosthesis”. In: *Robotica* 28.6, pp. 919–927. DOI: 10.1017/S0263574709990750.
- Cobos, S. et al. (2008). “Efficient human hand kinematics for manipulation tasks”. In: *IEEE. 2008 IEEE/RSJ International Conference on Intelligent Robots and Systems (Nice)*, pp. 2246–2251. ISBN: 978-1-4244-2057-5. DOI: 10.1109/IROS.2008.4651053.
- Connolly, C. (2008). “Prosthetic hands from touch bionics”. In: *Industrial Robot: An International Journal* 35.4, pp. 290–293. DOI: 10.1108/01439910810876364.
- Controzzi, M. et al. (2010). “Bio-inspired mechanical design of a tendon-driven dexterous prosthetic hand”. In: *2010 Annual International Conference of the IEEE Engineering in Medicine and Biology*. IEEE, pp. 499–502. DOI: 10.1109/IEMBS.2010.5627148.
- Cutkosky, M. (1989). “On grasp choice, grasp models, and the design of hands for manufacturing tasks”. In: *IEEE Transactions on Robotics and Automation* 5.3, pp. 269–279. DOI: 10.1109/70.34763.
- Dalley, S. et al. (2009). “Design of a Multifunctional Anthropomorphic Prosthetic Hand With Extrinsic Actuation”. In: *IEEE/ASME Transactions on Mechatronics* 14.6, pp. 699–706. DOI: 10.1109/TMECH.2009.2033113.
- Dalli, D. and M. Saliba (2016). “The University of Malta minimal anthropomorphic robot (UM-MAR) hand II”. In: *2016 IEEE International Conference on Advanced Intelligent Mechatronics (AIM)*. IEEE, pp. 371–376. DOI: 10.1109/AIM.2016.7576795.
- Davis, S., N. Tsagarakis, and D. Caldwell (2008). “The Initial Design and Manufacturing Process of a Low Cost Hand for the Robot iCub”. In: *IEEE-RAS International Conference on Humanoid Robots* 8, pp. 40–45. DOI: 10.1109/ICHR.2008.4755929.
- de Visser, H. and J. Herder (2000). “Force-directed design of a voluntary closing hand prosthesis”. In: *Journal of Rehabilitation Research and Development* 37, pp. 261–271. DOI: 10.1115/DETC2000/MECH-14149.

- Della Santina, C. et al. (2018). “Toward dexterous manipulation with augmented adaptive synergies: The pisa/iit soft hand 2”. In: *IEEE Transactions on Robotics* 34.5, pp. 1141–1156. DOI: 10.1109/TRO.2018.2830407.
- Deshpande, A. et al. (2013). “Mechanisms of the Anatomically Correct Testbed Hand”. In: *IEEE/ASME Transactions on Mechatronics* 18.1, pp. 238–250. ISSN: 1083-4435. DOI: 10.1109/TMECH.2011.2166801.
- Deutsches Institut für Normung e.V. (2020). *DIN 33402-2*. Norm. Beuth Verlag GmbH.
- Difonzo, E. et al. (2020). “Advances in finger and partial hand prosthetic mechanisms”. In: *Robotics* 9.4, p. 80. DOI: 10.3390/robotics9040080.
- Dollar, A. and R. Howe (2007). “The SDM Hand as a Prosthetic Terminal Device: A Feasibility Study”. In: *2007 IEEE 10th International Conference on Rehabilitation Robotics* (Noordwijk, Netherlands, June 13–15, 2007), pp. 978–983. ISBN: 978-1-4244-1319-5. DOI: 10.1109/ICORR.2007.4428542.
- Duruoz, M. (2014). *Hand Function: A Practical Guide to Assessment*. Springer New York. ISBN: 9781461494492. DOI: 10.1007/978-1-4614-9449-2. URL: <http://dx.doi.org/10.1007/978-1-4614-9449-2>.
- Eusebi, A. et al. (1994). “The UB Hand II control system: design features and experimental results”. In: vol. 2. IEEE, pp. 782–787. DOI: 10.1109/IECON.1994.397885.
- Farinha, A. and P. Lima (2016). “A novel underactuated hand suitable for human-oriented domestic environments”. In: *2016 International Conference on Autonomous Robot Systems and Competitions (ICARSC)*. IEEE, pp. 106–111. DOI: 10.1109/ICARSC.2016.21.
- Feix, T. (2011). “Anthropomorphic Hand Optimization based on a Latent Space Analysis”. PhD thesis. Wien: TU Wien.
- Feix, T. et al. (2015). “The grasp taxonomy of human grasp types”. In: *IEEE Transactions on Human-Machine Systems* 46.1, pp. 66–77. DOI: 10.1109/THMS.2015.2470657.
- Fortune Editors (2025). *Elon Musk reveals massive plans for Tesla Optimus, self-driving cars, and humanoid robots*. Accessed on 26 May 2025. URL: <https://fortune.com/2025/01/30/elon-musk-reveals-massive-plans-tesla-optimus-self-driving-cars-humanoid-robots/> (visited on 05/26/2025).
- Frommelt, P. and H. Lösslein (2011). *NeuroRehabilitation: Ein praxisbuch für interdisziplinäre teams*. ISBN: 978-3-662-66956-3.
- Fukaya, N. et al. (2000). “Design of the TUAT/Karlsruhe humanoid hand”. In: *IEEE/RSJ International Conference on Intelligent Robots and Systems (IROS)*, pp. 1754–1759. DOI: 10.1109/IROS.2000.895225.
- Gaiser, I. et al. (2009). “The FLUIDHAND III: A multifunctional prosthetic hand”. In: *JPO: Journal of Prosthetics and Orthotics* 21.2, pp. 91–96. DOI: 10.1097/JPO.0b013e3181a1ca54.

- Gama Melo, E., O. Aviles Sanchez, and D. Amaya Hurtado (June 2014). “Anthropomorphic robotic hands: a review”. In: *ingeniería y desarrollo* 32.2, pp. 279–313. ISSN: 2145-9371. DOI: 10.14482/inde.32.2.4715.
- Gao, G., A. Dwivedi, and M. Liarokapis (2023). “The New Dexterity Adaptive Humanlike Robot Hand: Employing a Reconfigurable Palm for Robust Grasping and Dexterous Manipulation”. In: *2023 IEEE International Conference on Robotics and Automation (ICRA)*. IEEE, pp. 10310–10316. ISBN: 979-8-3503-2365-8. DOI: 10.1109/ICRA48891.2023.10161369.
- Gazeau, J.-P. et al. (1996). “A Polyarticulated mechanical hand with 16 degrees of freedom—Synthesis in the different sides of experimental site”. In:
- Gazeau, J.-P. et al. (2001). “The LMS hand: force and position controls in the aim of the fine manipulation of objects”. In: vol. 3, 2642–2648 vol.3. DOI: 10.1109/ROBOT.2001.933021.
- Gosselin, C. (2006). “Adaptive Robotic Mechanical Systems: A Design Paradigm”. In: *Journal of Mechanical Design* 128.1, pp. 192–198. DOI: 10.1115/1.2120781.
- Gosselin, C., F. Pelletier, and T. Laliberté (2008). “An anthropomorphic underactuated robotic hand with 15 dofs and a single actuator”. In: pp. 749–754. DOI: 10.1109/ROBOT.2008.4543295.
- Gossen, D. et al. (Aug. 2025a). “Quantitative Evaluation of Joint Relevance in Anthropomorphic Robot Hands”. In: *2025 International Conference on Advanced Robotics and Mechatronics (ICARM)*. IEEE, pp. 1–7. DOI: 10.1109/icarm65671.2025.11293489.
- Gossen, D. et al. (Dec. 2025b). “The Library of Approaches: A systematic mapping of approaches for the mechanical design of tendon-driven, rigid-sequential anthropomorphic robot hands”. In: *Mechanism and Machine Theory* 218, p. 106257. ISSN: 0094-114X. DOI: 10.1016/j.mechmachtheory.2025.106257.
- Grebenstein, M. (2016). *Approaching Human Performance: The Functionality-Driven AWIWI Robot Hand*. ISBN: 978-3-319-03593-2.
- Grebenstein, M. et al. (2010). *A Method for Hand Kinematics Designers: 7 Billion Perfect Hands*. 1st International Conference on Applied Bionics and Biomechanics ICABB-2010.
- Güçlü, H. and A. Cora (2023). “A survey on wearable hand robotics design for assistive, rehabilitative, and haptic applications”. In: *International Journal of Intelligent Robotics and Applications* 7.2, pp. 227–252. DOI: 10.1007/s41315-023-00282-2.
- Hassanzadeh, N., X. He, and A. Perez-Gracia (2016). “A Design Implementation Process for Robotic Hand Synthesis”. In: The American Society of Mechanical Engineers. ISBN: 978-0-7918-5714-4. DOI: 10.1115/detc2015-46098.

- Hazard, C., N. Pollard, and S. Coros (2020). “Automated Design of Robotic Hands for In-Hand Manipulation Tasks”. In: *International Journal of Humanoid Robotics* 17.1, p. 1950029. DOI: 10.1142/S0219843619500294.
- Hirt, B. et al. (2015). *Anatomie und biomechanik der hand*. Vol. 160. 1, p. 23. DOI: 10.1055/a-1708-5828.
- Hume, M. et al. (1990). “Functional range of motion of the joints of the hand”. In: *The Journal of Hand Surgery* 15.2, pp. 240–243. DOI: 10.1016/0363-5023(90)90102-W.
- Inc, T. B. (2013). *Touch Bionics website*. <http://www.touchbionics.com/>. [Internet]. Mansfield, MA. URL: <http://www.touchbionics.com/>.
- Ingram, J. et al. (2008). “The statistics of natural hand movements”. In: *Experimental brain research* 188.2, pp. 223–236. DOI: 10.1007/s00221-008-1355-3.
- Interact Analysis (2024). *Humanoid Robots: Large Opportunity but Limited Uptake in the Short to Mid-Term*. Accessed on 26 May 2025. URL: <https://interactanalysis.com/insight/humanoid-robots-large-opportunity-but-limited-uptake-in-the-short-to-mid-term/> (visited on 05/26/2025).
- International, 3. (2024). *3d Model Human Hand Bones*. URL: <https://www.turbosquid.com/3d-models/human-hand-bones-1023475> (visited on 06/12/2024).
- Iwata, H. and S. Sugano (2009). “Design of anthropomorphic dexterous hand with passive joints and sensitive soft skins”. In: *Proceedings of the 2009 IEEE/SICE International Symposium on System Integration*, pp. 129–134. DOI: 10.1109/SI.2009.5384542.
- Jacobsen, S. et al. (1986). “Design of the Utah/M.I.T. Dextrous Hand”. In: vol. 3, pp. 1520–1532. DOI: 10.1109/ROBOT.1986.1087395.
- Jee, S.-C. et al. (2016). “Anthropometric classification of human hand shapes in Korean population”. In: *Proceedings of the Human Factors and Ergonomics Society Annual Meeting*. Vol. 60. 1. SAGE Publications Sage CA: Los Angeles, CA, pp. 1200–1204. DOI: 10.1177/1541931213601281.
- Kamikawa, Y. and T. Maeno (2008). “Underactuated five-finger prosthetic hand inspired by grasping force distribution of humans”. In: *2008 IEEE/RSJ International Conference on Intelligent Robots and Systems* (Nice, Sept. 22–26, 2008), pp. 717–722. ISBN: 978-1-4244-2057-5. DOI: 10.1109/IROS.2008.4650628.
- Kapandji, I. (1986). “Clinical test of apposition and counter-apposition of the thumb”. In: *Annales de chirurgie de la main: organe officiel des sociétés de chirurgie de la main* 5.1, pp. 67–73. DOI: 10.1016/s0753-9053(86)80053-9.
- (Jan. 1987). “Biomécanique du carpe et du poignet”. In: *Annales de Chirurgie de la Main* 6.2, pp. 147–169. ISSN: 0753-9053. DOI: 10.1016/s0753-9053(87)80031-5. URL: [http://dx.doi.org/10.1016/S0753-9053\(87\)80031-5](http://dx.doi.org/10.1016/S0753-9053(87)80031-5).
- (2007). *The physiology of the joints: volume one the upper limb*.

- Kawasaki, H. and T. Komatsu (Aug. 1999). “Mechanism Design of Anthropomorphic Robot Hand: Gifu Hand I”. In: *Journal of Robotics and Mechatronics* 11.4, pp. 269–273. ISSN: 0915-3942. DOI: 10.20965/jrm.1999.p0269. URL: <http://dx.doi.org/10.20965/jrm.1999.p0269>.
- Kawasaki, H., T. Komatsu, and K. Uchiyama (2002a). “Dexterous Anthropomorphic Robot Hand With Distributed Tactile Sensor: Gifu Hand II”. In: *IEEE/ASME Transactions on Mechatronics* 7.3, pp. 296–303. ISSN: 1083-4435. DOI: 10.1109/TMECH.2002.802720.
- Kawasaki, H., T. Mouri, and T. Endo (2011). “Review of Gifu Hand and Its Application”. In: *Mechanics Based Design of Structures and Machines* 39.2, pp. 210–228. ISSN: 1539-7734. DOI: 10.1080/15397734.2011.550857.
- Kawasaki, H., T. Mouri, and S. Ito (2004). “Toward Next Stage of Kinetic Humanoid Hand”. In: *Proceedings World Automation Congress, 2004*. Pp. 129–134. ISBN: 1-889335-21-5.
- Kawasaki, H. et al. (2002b). “Anthropomorphic Robot Hand: Gifu Hand III”. In: *International Conference on Control, Automation and Systems (ICCAS)*, pp. 1288–1293. URL: https://mindtrans.narod.ru/pdfs/Gifu%5C_Hand%5C_III.pdf.
- Konda, R. et al. (2022). “Anthropomorphic twisted string-actuated soft robotic gripper with tendon-based stiffening”. In: *IEEE Transactions on Robotics* 39.2, pp. 1178–1195. DOI: 10.1109/TRO.2022.3224774.
- Konnaris, C. et al. (2016). “EthoHand: A dexterous robotic hand with ball-joint thumb enables complex in-hand object manipulation”. In: *2016 6th IEEE International Conference on Biomedical Robotics and Biomechatronics (BioRob)*. IEEE, pp. 1154–1159. ISBN: 978-1-5090-3287-7. DOI: 10.1109/BIOROB.2016.7523787.
- Kontoudis, G., M. Liarokapis, and K. Vamvoudakis (2019). “A Compliant, Underactuated Finger for Anthropomorphic Hands”. In: *IEEE International Conference on Rehabilitation Robotics*, pp. 682–688. DOI: 10.1109/ICORR.2019.8779435.
- Kontoudis, G. et al. (2015). “Open-source, anthropomorphic, underactuated robot hands with a selectively lockable differential mechanism: Towards affordable prostheses”. In: *IEEE/RSJ International Conference on Intelligent Robots and Systems (IROS)*, pp. 5857–5862. DOI: 10.1109/IROS.2015.7354209.
- Kurita, Y. et al. (2009). “NAIST hand 2: Human-sized anthropomorphic robot hand with detachable mechanism at the wrist”. In: *2009 IEEE/RSJ International Conference on Intelligent Robots and Systems*. IEEE, pp. 2271–2276. DOI: 10.1109/IROS.2009.5354439.
- Kyberd, P. and P. Chappell (1994). “The Southampton Hand: an intelligent myoelectric prosthesis”. In: *Journal of Rehabilitation Research & Development* 31.4.
- Kyberd, P. et al. (2001). “The design of anthropomorphic prosthetic hands: A study of the Southampton Hand”. In: *Robotica* 19.6, pp. 593–600. DOI: 10.1017/S0263574701003538.
- Laliberté, T. and C. Gosselin (2001). “Underactuation in space robotic hands”. In:

- Laliberté, T. et al. (2010). “Towards the design of a prosthetic underactuated hand”. In: *Mechanical Sciences* 1.1, pp. 19–26. DOI: 10.5194/ms-1-19-2010.
- Le, T.-H.-L. et al. (2016). “Skinning a Robot: Design Methodologies for Large-Scale Robot Skin”. In: *IEEE Robotics & Automation Magazine* 23.4, pp. 150–159. DOI: 10.1109/MRA.2016.2548800.
- Lee, K.-S. and M.-C. Jung (2015). “Ergonomic evaluation of biomechanical hand function”. In: *Safety and health at work* 6.1, pp. 9–17. DOI: 10.1016/j.shaw.2014.09.002.
- Lee, P. et al. (2023). “Naturally Compliant Dexterous Anthropomorphic Hand via Novel Modular Soft-Rigid Hybrid Robotics Approach: Design Rationale, Assembly Methods, and Evaluation”. In: *2023 32nd IEEE International Conference on Robot and Human Interactive Communication (RO-MAN)*. IEEE, pp. 2281–2287. DOI: 10.1109/RO-MAN57019.2023.10309552.
- Leonardis, D. and A. Frisoli (2020). “CORA hand: a 3D printed robotic hand designed for robustness and compliance”. In: *Meccanica* 55.8, pp. 1623–1638. DOI: 10.1007/s11012-020-01188-0.
- Light, C. and P. Chappell (2000). “Development of a lightweight and adaptable multiple-axis hand prosthesis”. In: *Medical engineering & physics* 22.10, pp. 679–684. DOI: 10.1016/S1350-4533(01)00017-0.
- Liu, H. et al. (2008). “Multisensory five-finger dexterous hand: The DLR/HIT Hand II”. In: IEEE, pp. 3692–3697. ISBN: 978-1-4244-2057-5. DOI: 10.1109/IROS.2008.4650624.
- Liu, H. et al. (2020). “Design of a Lightweight Single-Actuator Multi-Grasp Prosthetic Hand With Force Magnification”. In: *Journal of Mechanisms and Robotics* 12.5. DOI: 10.1115/1.4047438.
- Lotti, F. et al. (2004). “UBH 3: an anthropomorphic hand with simplified endo-skeletal structure and soft continuous fingerpads”. In: *IEEE International Conference on Robotics and Automation, 2004. Proceedings. ICRA '04. 2004*. IEEE, 4736–4741 Vol.5. ISBN: 0-7803-8232-3. DOI: 10.1109/ROBOT.2004.1302466.
- Lotti, F. et al. (2005a). “Development of UB Hand 3: Early Results”. In: *Proceedings of the 2005 IEEE International Conference on Robotics and Automation*. IEEE, pp. 4488–4493. ISBN: 0-7803-8914-X. DOI: 10.1109/ROBOT.2005.1570811.
- Lotti, F. et al. (2005b). “Development of UB Hand 3: Early Results”. In: *Proceedings of the 2005 IEEE International Conference on Robotics and Automation*, pp. 4488–4493. DOI: 10.1109/ROBOT.2005.1570811.
- Ma, R., L. Odhner, and A. Dollar (2013). “A modular, open-source 3D printed underactuated hand”. In: *2013 IEEE International Conference on Robotics and Automation (Karlsruhe,*

- Germany, May 6–10, 2013), pp. 2737–2743. ISBN: 978-1-4673-5643-5. DOI: 10.1109/ICRA.2013.6630954.
- Mansoor, M., P. Prajapati, and M. Suhaib (2023). “Some Study on Multifinger Robotic Gripper”. In: IEEE, pp. 460–465. DOI: 10.1109/REEDCON57544.2023.10150807.
- Marieb, E. and K. Hoehn (2007). *Human anatomy & physiology*. ISBN: 978-0-321-37294-9.
- Martell, J. and G. Gini (2007). “Robotic hands: design review and proposal of new design process”. In: *World Academy of Science, Engineering and Technology* 26.5, pp. 85–90. DOI: 10.5281/zenodo.1071071.
- Martell, J. and G. Giuseppina (2007). *Robotic hands: design review and proposal of new design process*.
- Martin, J. and M. Grossard (2014). “Design of a fully modular and backdrivable dexterous hand”. In: *The International Journal of Robotics Research* 33.5, pp. 783–798. ISSN: 0278-3649. DOI: 10.1177/0278364913511677.
- Mason, M. (2018). “Toward Robotic Manipulation”. In: *Annual Review of Control, Robotics, and Autonomous Systems* 1.1, pp. 1–28. DOI: 10.1146/annurev-control-060117-104848.
- Massa, B. et al. (2002). “Design and development of an underactuated prosthetic hand”. In: IEEE, pp. 3374–3379. ISBN: 0-7803-7272-7. DOI: 10.1109/ROBOT.2002.1014232.
- Medynski, C. and B. Rattray (2011). “Bebionic prosthetic design”. In: Myoelectric Symposium.
- Melchiorri, C. and M. Kaneko (2016). “Robot hands”. In: *Springer Handbook of Robotics*, pp. 463–480. DOI: 10.1007/978-3-319-32552-1_19.
- Melchiorri, C. et al. (2013). “Development of the UB Hand IV: Overview of Design Solutions and Enabling Technologies”. In: *IEEE Robotics & Automation Magazine* 20.3, pp. 72–81. ISSN: 1070-9932. DOI: 10.1109/MRA.2012.2225471.
- Mendez, V. et al. (2021). “Current solutions and future trends for robotic prosthetic hands”. In: *Annual Review of Control, Robotics, and Autonomous Systems* 4.1, pp. 595–627. DOI: 10.1146/annurev-control-071020-104336.
- Mitchell, M. and R. Weir (2008). “Development of a clinically viable multifunctional hand prosthesis”. In: Myoelectric Symposium.
- Mizushima, K. et al. (2018). “Multi-fingered robotic hand based on hybrid mechanism of tendon-driven and jamming transition”. In: (Livorno, Apr. 24–28, 2018), pp. 376–381. ISBN: 978-1-5386-4516-1. DOI: 10.1109/ROBOSOFT.2018.8404948.
- Mottard, A., T. Laliberté, and C. Gosselin (2017). “Underactuated tendon-driven robotic/prosthetic hands: Design issues.” In: (Boston, USA, July 12–16, 2017). Vol. 7, pp. 1–9. DOI: 10.15607/rss.2017.xiii.019.

- Nanayakkara, V. et al. (2017). “The Role of Morphology of the Thumb in Anthropomorphic Grasping: A Review”. In: *Frontiers in Mechanical Engineering* 3. DOI: 10.3389/fmech.2017.00005.
- National Library of Medicine (2024). *X-ray image of the human hand*. Accessed: 2024-05-02. URL: <https://medpix.nlm.nih.gov/search?allen=true%5C&allt=true%5C&alli=true%5C&query=hand>.
- Nazma, E. and S. Mohd (2012). “Tendon driven robotic hands: A review”. In: *Int. J. Mech. Eng. Robot. Res* 1.3, pp. 350–357.
- Ngeo, J., T. Tamei, and T. Shibata (2014). “Continuous and simultaneous estimation of finger kinematics using inputs from an EMG-to-muscle activation model”. In: *Journal of neuroengineering and rehabilitation* 11, p. 122. DOI: 10.1186/1743-0003-11-122.
- Nikafrooz, N. and A. Leonessa (2021). “A Single-Actuated, Cable-Driven, and Self-Contained Robotic Hand Designed for Adaptive Grasps”. In: *Robotics* 10.4, p. 109. DOI: 10.3390/robotics10040109.
- Niola, V. et al. (2014). “An underactuated mechanical hand: A first prototype”. In: (Smolenice, Slovakia, Sept. 3–5, 2014), pp. 1–6. ISBN: 978-1-4799-6798-8. DOI: 10.1109/RAAD.2014.7002225.
- Okada, T. (1982). “Computer Control of Multijointed Finger System for Precise Object-Handling”. In: *IEEE Transactions on Systems, Man, and Cybernetics* 12.3, pp. 289–299. DOI: 10.1109/TSMC.1982.4308818.
- Page, M. et al. (2021). “The PRISMA 2020 statement: An updated guideline for reporting systematic reviews”. In: *BMJ* 372, n71. DOI: 10.1136/bmj.n71.
- Palli, G. and S. Pirozzi (May 2013). “An optical joint position sensor for anthropomorphic robot hands”. In: *2013 IEEE International Conference on Robotics and Automation*. IEEE, pp. 2765–2770. DOI: 10.1109/icra.2013.6630958. URL: <http://dx.doi.org/10.1109/ICRA.2013.6630958>.
- Palli, G. et al. (2014). “The DEXMART hand: Mechatronic design and experimental evaluation of synergy-based control for human-like grasping”. In: *The International Journal of Robotics Research* 33.5, pp. 799–824. ISSN: 0278-3649. DOI: 10.1177/0278364913519897.
- Parveen, S., M. Suhaib, and M. Majid (2023). “Multifinger Robotic Gripper: A Review”. In: *IEEE*, pp. 466–470. DOI: 10.1109/REEDCON57544.2023.10150673.
- Peerdeman, B. et al. (2014). “UT hand I: A lock-based underactuated hand prosthesis”. In: *Mechanism and Machine Theory* 78, pp. 307–323. ISSN: 0094114X. DOI: 10.1016/j.mechmachtheory.2014.03.018.
- Peña-Pitarch, E., N. Falguera, and J. Yang (2014). “Virtual human hand: model and kinematics”. In: *Computer methods in biomechanics and biomedical engineering* 17.5, pp. 568–579. DOI: 10.1080/10255842.2012.702864.

- Peña-Pitarch, E., N. Falguera Ticó, and J. Yang (2012). “Virtual human hand: model and kinematics”. In: *Computer methods in biomechanics and biomedical engineering* 17.5, pp. 568–579. DOI: 10.1080/10255842.2012.702864.
- Piazza, C. et al. (2019). “A century of robotic hands”. In: *Annual Review of Control, Robotics, and Autonomous Systems* 2.1, pp. 1–32. DOI: 10.1146/annurev-control-060117-105003.
- Polzin, S. (2024). “Einfluss der Gelenkkonfiguration auf die Greifperformance einer anthropomorphen Roboterhand”. Supervised by the author of this thesis. Master’s Thesis. RWTH Aachen University, Institute of Mechanism Theory, Machine Dynamics and Robotics.
- Pons, J. et al. (2004). “The MANUS-HAND dextrous robotics upper limb prosthesis: mechanical and manipulation aspects”. In: *Autonomous Robots* 16, pp. 143–163. DOI: 10.1023/B:AURO.0000016862.38337.f1.
- Prensilia (2024). *MIA Hand*. Accessed: 2024-11-22. URL: <https://www.prensilia.com/mia-hand/>.
- Puig, J., N. Rodriguez, and M. Ceccarelli (2008a). “A Methodology for the Design of Robotic Hands with Multiple Fingers”. In: *International Journal of Advanced Robotic Systems* 5.2, p. 22. DOI: 10.5772/5600.
- (2008b). “A methodology for the design of robotic hands with multiple fingers”. In: *International Journal of Advanced Robotic Systems* 5.2, p. 22. DOI: 10.5772/5600.
- Pulleyking, S., D. Das, and J. Schultz (2016). “Simplified robotic thumb inspired by surgical intervention”. In: *2016 6th IEEE International Conference on Biomedical Robotics and Biomechatronics (BioRob)*. IEEE, pp. 1200–1206. ISBN: 978-1-5090-3287-7. DOI: 10.1109/BIOROB.2016.7523794.
- Pulleyking, S. and J. Schultz (2020). “Flexure Hinge-based Biomimetic Thumb with a Rolling-Surface Metacarpal Joint”. In: *2020 IEEE International Conference on Robotics and Automation (ICRA)*, pp. 2960–2966. DOI: 10.1109/ICRA40945.2020.
- (2023). *A Compliant Rolling Ellipsoidal Thumb Joint for the TU Hand*. DOI: 10.36227/techrxiv.22199395.v1.
- Roa, M. and R. Suárez (2015). “Grasp quality measures: review and performance”. In: *Autonomous robots* 38, pp. 65–88. DOI: 10.1007/s10514-014-9402-3.
- Roccella, S. et al. (2004). “Design, fabrication and preliminary results of a novel anthropomorphic hand for humanoid robotics: RCH-1”. In: vol. 1. IEEE, pp. 266–271. DOI: 10.1109/IROS.2004.1389363.
- Rodriguez, N., G. Carbone, and M. Ceccarelli (2006). “Optimal design of driving mechanism in a 1-DOF anthropomorphic finger”. In: *Mechanism and machine theory* 41.8, pp. 897–911. DOI: 10.1016/j.mechmachtheory.2006.03.016.

- Ruehl, S. et al. (2014). “Experimental evaluation of the schunk 5-finger gripping hand for grasping tasks”. In: IEEE, pp. 2465–2470. DOI: 10.1109/ROBIO.2014.7090710.
- Saliba, M., A. Chetcuti, and M. Farrugia (2013). “Towards the rationalization of anthropomorphic robot hand design: Extracting knowledge from constrained human manual dexterity testing”. In: *World Scientific* 10.02, p. 1350001. DOI: 10.1142/S0219843613500011.
- Saliba, M., M. Cutajar, and G. Pascalidis (2022). “Prototype development of a prosthetic derivative of the minimal anthropomorphic artificial hand”. In: *2022 31st IEEE International Conference on Robot and Human Interactive Communication (RO-MAN)*. IEEE, pp. 14–21. DOI: 10.1109/RO-MAN53752.2022.9900648.
- Salisbury, J. and J. Craig (1982). “Articulated Hands: Force Control and Kinematic Issues”. In: *The International Journal of Robotics Research* 1.1, pp. 4–17. DOI: 10.1177/027836498200100102.
- Sardo, A., P. Tiezzi, and G. Vassura (Dec. 2006). “A Methodological Approach to Design of Soft Fingertips for Humanoid Robot Hands”. In: *2006 6th IEEE-RAS International Conference on Humanoid Robots*. IEEE, pp. 370–375. DOI: 10.1109/ichr.2006.321299. URL: <http://dx.doi.org/10.1109/ICHR.2006.321299>.
- Savić, S. et al. (2016). “Design of an Underactuated Adaptive Robotic Hand with Force Sensing”. In: *International Conference on Electrical, Electronic and Computing Engineering IcETRAN*.
- Schmitz, A. et al. (2010). “Design, realization and sensorization of the dexterous iCub hand”. In: *2010 10th IEEE-RAS International Conference on Humanoid Robots*. IEEE, pp. 186–191. ISBN: 978-1-4244-8688-5. DOI: 10.1109/ICHR.2010.5686825.
- Schulz, S., C. Pylatiuk, and G. Bretthauer (2001). “A new ultralight anthropomorphic hand”. In: vol. 3, 2437–2441 vol.3. DOI: 10.1109/ROBOT.2001.932988.
- Shadow Robot Company (2020). *Internal price list for robotic systems*. Unpublished company document, received via email.
- (2025). *Shadow Dexterous Hand - Technical Specification*. <https://www.shadowrobot.com/products/dexterous-hand/>. Accessed: 2025-07-13. URL: <https://www.shadowrobot.com/products/dexterous-hand/>.
- Sharma, D. et al. (2014). “Shadow Hand”. In: *Journal of Advance Research in Applied Science (ISSN: 2208-2352)* 1.1, pp. 04–07. DOI: 10.53555/nnas.v1i1.692.
- El-Shennawy, M. et al. (2001). “Three-dimensional kinematic analysis of the second through fifth carpometacarpal joints”. In: *The Journal of Hand Surgery* 26.6, pp. 1030–1035. DOI: 10.1053/jhsu.2001.28761.
- Shorthose, O. et al. (2022). “Design of a 3D-printed soft robotic hand with integrated distributed tactile sensing”. In: *IEEE Robotics and Automation Letters* 7.2, pp. 3945–3952. DOI: 10.1109/LRA.2022.3149037.

- Stillfried, G. and P. van der Smagt (2010). *Movement model of a human hand based on magnetic resonance imaging (MRI)*. URL: <https://archive.air.in.tum.de/Main/Publications/StiSma2010.pdf>.
- Stillfried, G. et al. (2009). “Human hand kinematics based on MRI imaging”. In: *Understanding the Human Hand for Advancing Robotic Manipulation Workshop at Robotics: Science and Systems 2009*. URL: https://www.researchgate.net/profile/Patrick-Van-Der-Smagt/publication/259896284%5C_Human%5C_hand%5C_kinematics%5C_based%5C_on%5C_MRI%5C_imaging/links/0c960530648cb14eb7000000/Human-hand-kinematics-based-on-MRI-imaging.pdf.
- Stillfried, G. et al. (2014). “MRI-Based Skeletal Hand Movement Model”. In: *The Human Hand as an Inspiration for Robot Hand Development*, pp. 49–75. DOI: 10.1007/978-3-319-03017-3_3.
- Sun, B.-Y. et al. (2022). “Design Principle of a Dual-Actuated Robotic Hand With Anthropomorphic Self-Adaptive Grasping and Dexterous Manipulation Abilities”. In: *IEEE Transactions on Robotics* 38.4, pp. 2322–2340. DOI: 10.1109/TRO.2021.3132532.
- Sureshbabu, A., G. Metta, and A. Parmiggiani (2015). “A new cost effective robot hand for the iCub humanoid”. In: *2015 IEEE-RAS 15th International Conference on Humanoid Robots (Humanoids)*. IEEE, pp. 750–757. ISBN: 978-1-4799-6885-5. DOI: 10.1109/HUMANOIDS.2015.7363454.
- (2019). “A systematic approach to evaluating and benchmarking robotic hands—the FFP index”. In: *Robotics* 8.1, p. 7. DOI: 10.3390/robotics8010007.
- Systems, V. (2013). *VINCENT hand*. <http://handprothese.de/vincent-hand/>. [Internet]. Weingarten, Germany. URL: <http://handprothese.de/vincent-hand/>.
- Tae-uk, K. and O. Yonghwan (2014). “Design of spatial adaptive fingered gripper using spherical five-bar mechanism”. In: *Proceedings of the 2014 International Conference on Advanced Mechatronic Systems*, pp. 145–150. DOI: 10.1109/icamechs.2014.6911640.
- Tasi, B., M. Koller, and G. Cserey (2019). “Design of the Anatomically Correct, Biomechatronic Hand”. In: *arXiv preprint arXiv:1909.07966*. DOI: 10.48550/arXiv.1909.07966.
- Tavakoli, M. et al. (2015). “Underactuated anthropomorphic hands: Actuation strategies for a better functionality”. In: *Robotics and Autonomous Systems* 74, pp. 267–282. DOI: 10.1016/j.robot.2015.08.011.
- Ten Kate, J., G. Smit, and P. Breedveld (2017). “3D-printed upper limb prostheses: a review”. In: *Disability and Rehabilitation: Assistive Technology* 12.3, pp. 300–314. DOI: 10.1080/17483107.2016.1253117.

- The Robot Report (2025). *Despite the Hype, Interact Analysis Expects Humanoid Adoption to Remain Slow*. Accessed: 2025-05-15. URL: <https://www.therobotreport.com/despite-the-hype-interact-analysis-expects-humanoid-adoption-to-remain-slow/>.
- Tian, L. et al. (2020). *Fast 3D Modeling of Anthropomorphic Robotic Hands Based on A Multi-layer Deformable Design*.
- Tian, L. et al. (2021). “Towards complex and continuous manipulation: a gesture based anthropomorphic robotic hand design”. In: *IEEE Robotics and Automation Letters* 6.3, pp. 5461–5468. DOI: 10.1109/LRA.2021.3076960.
- Tomovic, R. and G. Boni (1962). “An adaptive artificial hand”. In: *IRE Transactions on Automatic Control* 7.3, pp. 3–10. DOI: 10.1109/TAC.1962.1105456.
- Townsend, W. (2000). “The BarrettHand grasper—programmably flexible part handling and assembly”. In: *Industrial Robot: an international journal* 27.3, pp. 181–188. DOI: 10.1108/01439910010371597.
- Ueda, J., M. Kondo, and T. Ogasawara (2010). “The multifingered NAIST hand system for robot in-hand manipulation”. In: *Mechanism and Machine Theory* 45.2, pp. 224–238. DOI: 10.1016/j.mechmachtheory.2009.08.007.
- Van Der Hulst, F. et al. (2012). “A functional anatomy based kinematic human hand model with simple size adaptation”. In: IEEE, pp. 5123–5129. DOI: 10.1109/ICRA.2012.6225350.
- van der Hulst, F. et al. (2012). “A functional anatomy based kinematic human hand model with simple size adaptation”. In: *ICRA 2012. 2012 IEEE International Conference on Robotics and Automation (ICRA)* (St Paul, MN, USA), pp. 5123–5129. ISBN: 978-1-4673-1405-3. DOI: 10.1109/ICRA.2012.6225350.
- van der Smagt, P. and G. Stillfried (2007). “Using MRT data to compute a hand kinematic model”. In: *Proceedings of MOVIC 2008* 35, pp. 1989–2002. DOI: 10.1007/s10439-007-9364-0.
- Vanderzanden, J., B. Adams, and J. Guan (2014). “MCP arthrodesis using an intramedullary interlocking device”. In: *Hand* 9.2, pp. 209–213. DOI: 10.1007/s11552-013-9579-5.
- Vergara, M., M. Agost, and V. Gracia-Ibáñez (2018). “Dorsal and palmar aspect dimensions of hand anthropometry for designing hand tools and protections”. In: *Human Factors and Ergonomics in Manufacturing & Service Industries* 28.1, pp. 17–28. DOI: 10.1002/hfm.20714.
- Vertongen, J. et al. (2020). “Mechanical aspects of robot hands, active hand orthoses, and prostheses: A comparative review”. In: *IEEE/ASME Transactions on Mechatronics* 26.2, pp. 955–965. DOI: 10.1109/TMECH.2020.3014182.

- Wang, H., S. Fan, and H. Liu (2012). “An anthropomorphic design guideline for the thumb of the dexterous hand”. In: *2012 IEEE International Conference on Mechatronics and Automation*, pp. 777–782. DOI: 10.1109/ICMA.2012.6283241.
- (2017a). “Thumb Configuration and Performance Evaluation for Dexterous Robotic Hand Design”. In: *Journal of Mechanical Design* 139.1. ISSN: 1050-0472. DOI: 10.1115/1.4034837.
- (2017b). “Thumb configuration and performance evaluation for dexterous robotic hand design”. In: *American Society of Mechanical Engineers* 139.1, p. 012304. DOI: 10.1115/1.4034837.
- Wang, L. et al. (2011). “A highly-underactuated robotic hand with force and joint angle sensors”. In: (San Francisco, CA, Sept. 25–30, 2011), pp. 1380–1385. ISBN: 978-1-61284-456-5. DOI: 10.1109/IROS.2011.6095147.
- Weiner, P. et al. (2018). *The KIT Prosthetic Hand: Design and Control*. DOI: 10.1109/IROS.2018.8593851. URL: <https://h2t.anthropomatik.kit.edu/pdf/Weiner2018a.pdf> (visited on 05/14/2023).
- Weir, R. et al. (2008). “The intrinsic hand—a 22 degree-of-freedom artificial hand-wrist replacement”. In: *Proc Myoelectric Controls/Powered Prosthetics Symposium*. Duke University Durham, NC, pp. 233–237. DOI: 10.1016/j.triboint.2009.02.005.
- Wiste, T. and M. Goldfarb (2017). “Design of a simplified compliant anthropomorphic robot hand”. In: *2017 IEEE International Conference on Robotics and Automation (ICRA)* (Singapore, Singapore, May 29–June 3, 2017), pp. 3433–3438. ISBN: 978-1-5090-4633-1. DOI: 10.1109/ICRA.2017.7989391.
- Woo, S. (2019). *The Thumb: A Guide to Surgical Management*. Springer Singapore. ISBN: 9789811044007. DOI: 10.1007/978-981-10-4400-7. URL: <http://dx.doi.org/10.1007/978-981-10-4400-7>.
- Xinhua (2025). “China to promote use of humanoid robots for elderly care”. In: *english.www.gov.cn*. Zugriff am 4. Februar 2025. URL: https://english.www.gov.cn/policies/latestreleases/202501/07/content%5C_WS677d340ac6d0868f4e8ee95d.html.
- Xiong, C.-H. et al. (2016). “Design and implementation of an anthropomorphic hand for replicating human grasping functions”. In: *IEEE Transactions on Robotics* 32.3, pp. 652–671. DOI: 10.1109/TRO.2016.2558193.
- Xu, Z. and E. Todorov (2016). “Design of a highly biomimetic anthropomorphic robotic hand towards artificial limb regeneration”. In: *2016 IEEE International Conference on Robotics and Automation (ICRA)*. IEEE, pp. 3485–3492. ISBN: 978-1-4673-8026-3. DOI: 10.1109/ICRA.2016.7487528.

- Yang, H., G. Wei, and L. Ren (2019). “Design and Development of a Linkage-Tendon Hybrid Driven Anthropomorphic Robotic Hand”. In: *Intelligent Robotics and Applications*. Ed. by H. Yu et al. Vol. 11740. Lecture Notes in Computer Science. Cham: Springer International Publishing, pp. 117–128. ISBN: 978-3-030-27525-9. DOI: 10.1007/978-3-030-27526-6{\textunderscore}11.
- Yang, H. et al. (2021a). “An Affordable Linkage-and-Tendon Hybrid-Driven Anthropomorphic Robotic Hand—MCR-Hand II”. In: *Journal of Mechanisms and Robotics* 13.2. ISSN: 1942-4302. DOI: 10.1115/1.4049744.
- (2021b). “An affordable linkage-and-tendon hybrid-driven anthropomorphic robotic hand—MCR-Hand II”. In: *Journal of Mechanisms and Robotics* 13.2. DOI: 10.1115/1.4049744.
- Yang, J. et al. (2004). “A multi-fingered hand prosthesis”. In: *Mechanism and Machine Theory* 39.6, pp. 555–581. ISSN: 0094-114X. DOI: 10.1016/j.mechmachtheory.2004.01.002. URL: <https://www.sciencedirect.com/science/article/pii/S0094114X04000229>.
- Yang, D.-p. et al. (2009). “An anthropomorphic robot hand developed based on underactuated mechanism and controlled by EMG signals”. In: *Journal of Bionic Engineering* 6.3, pp. 255–263. DOI: 10.1016/S1672-6529(08)60119-5.
- You, W., Y. Lee, et al. (2019). “Kinematic design optimization for anthropomorphic robot hand using Interactivity of Fingers (IF)”. In: *Springer International Journal of Mechatronics and International Systems (S M J)* 12.2, pp. 197–208. DOI: 10.1007/s11370-019-00274-x.
- Zhang, C. et al. (2023). “An anthropomorphic robotic hand with a soft-rigid hybrid structure and positive-negative pneumatic actuation”. In: *IEEE Robotics and Automation Letters* 8.7, pp. 4346–4353. DOI: 10.1109/LRA.2023.3280829.
- Zhang, Z. et al. (2018). “CATCH-919 Hand: Design of a 9-actuator 19-DOF Anthropomorphic Robotic Hand”. In: *arXiv:1809.04290 [cs.RO]*. DOI: 10.48550/arXiv.1809.04290.
- Zhou, H. et al. (2019). “A Novel Monolithic Soft Robotic Thumb for an Anthropomorphic Prosthetic Hand”. In: *IEEE Robotics and Automation Letters* 4.2, pp. 602–609. DOI: 10.1109/LRA.2019.2892203.
- Zhou, J. et al. (2019). “A soft-robotic approach to anthropomorphic robotic hand dexterity”. In: *IEEE Access* 7, pp. 101483–101495. DOI: 10.1109/ACCESS.2019.2929690.
- Zilles, K. and B. Tillmann (2010). *Anatomie*. Springer Berlin Heidelberg. ISBN: 9783540694830. DOI: 10.1007/978-3-540-69483-0. URL: <http://dx.doi.org/10.1007/978-3-540-69483-0>.

- Zimmer, P. and H.-J. Appell (2021a). “Funktionelle Anatomie des Bewegungsapparates”. In: *Funktionelle Anatomie: Grundlagen sportlicher Leistung und Bewegung*, pp. 27–104. DOI: 10.1007/978-3-662-61482-2.
- (2021b). *Funktionelle Anatomie: Grundlagen sportlicher Leistung und Bewegung*. Springer Berlin Heidelberg. ISBN: 9783662614822. DOI: 10.1007/978-3-662-61482-2. URL: <http://dx.doi.org/10.1007/978-3-662-61482-2>.

Appendix

A Joint Allocation Information

In this chapter, the interested reader is provided with information on the dimensional parameter. The chapter begins with summaries of the data identified in the literature. Subsequently, an overview of the dimensions of the robotic hand developed and successfully evaluated in this dissertation is given. The presented dimensions can be adapted for custom prototype development and iteratively optimized according to the procedure introduced in Section 2.3.1. The information presented is taken from the thesis by Polzin (2024), which was conducted under the author's supervision.

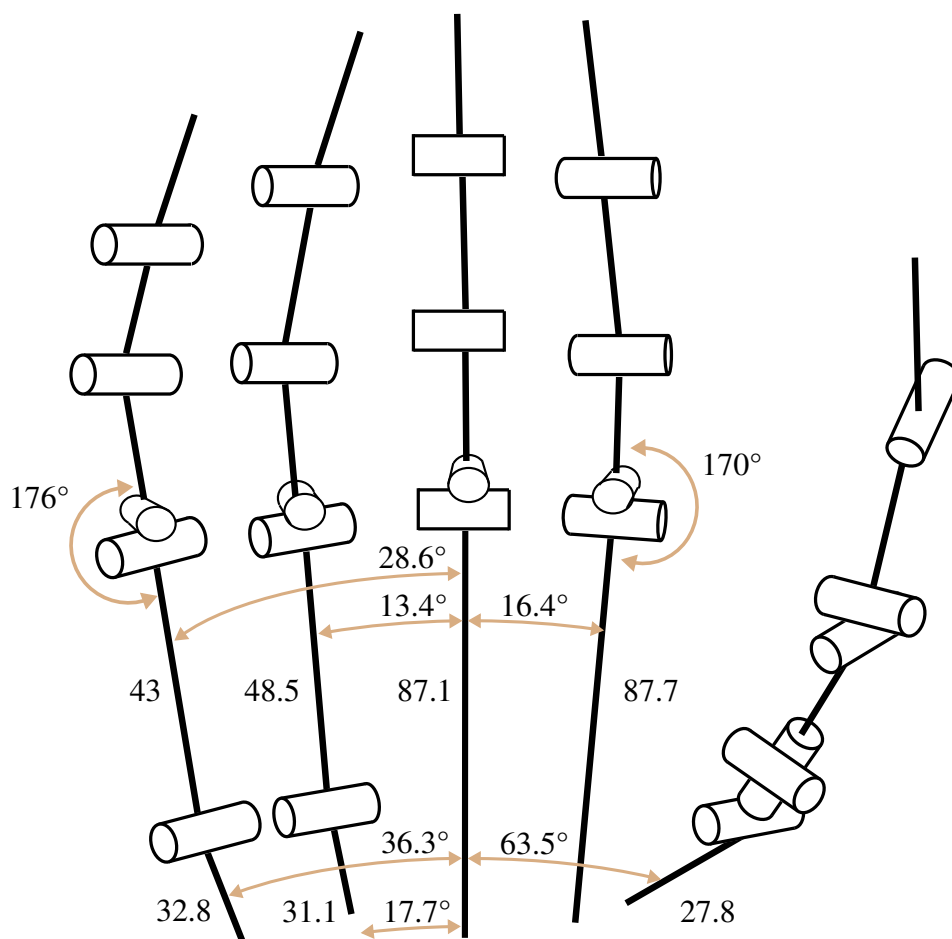


Figure A.1: Developed robot hand dimensions. Measures without unit are given in mm.

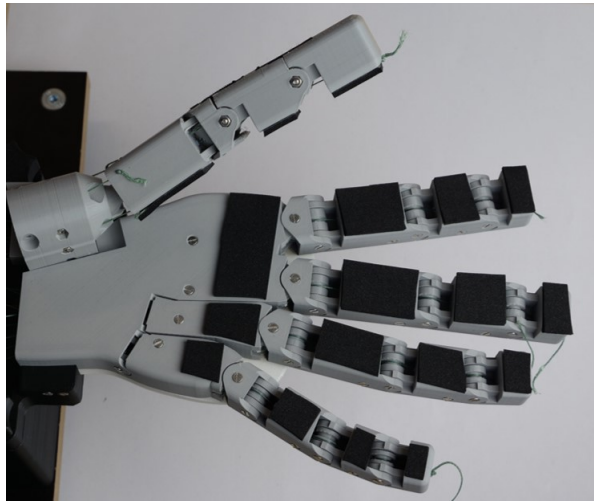


Figure A.2: Developed robot hand prototype according to the IMDC joint structure.

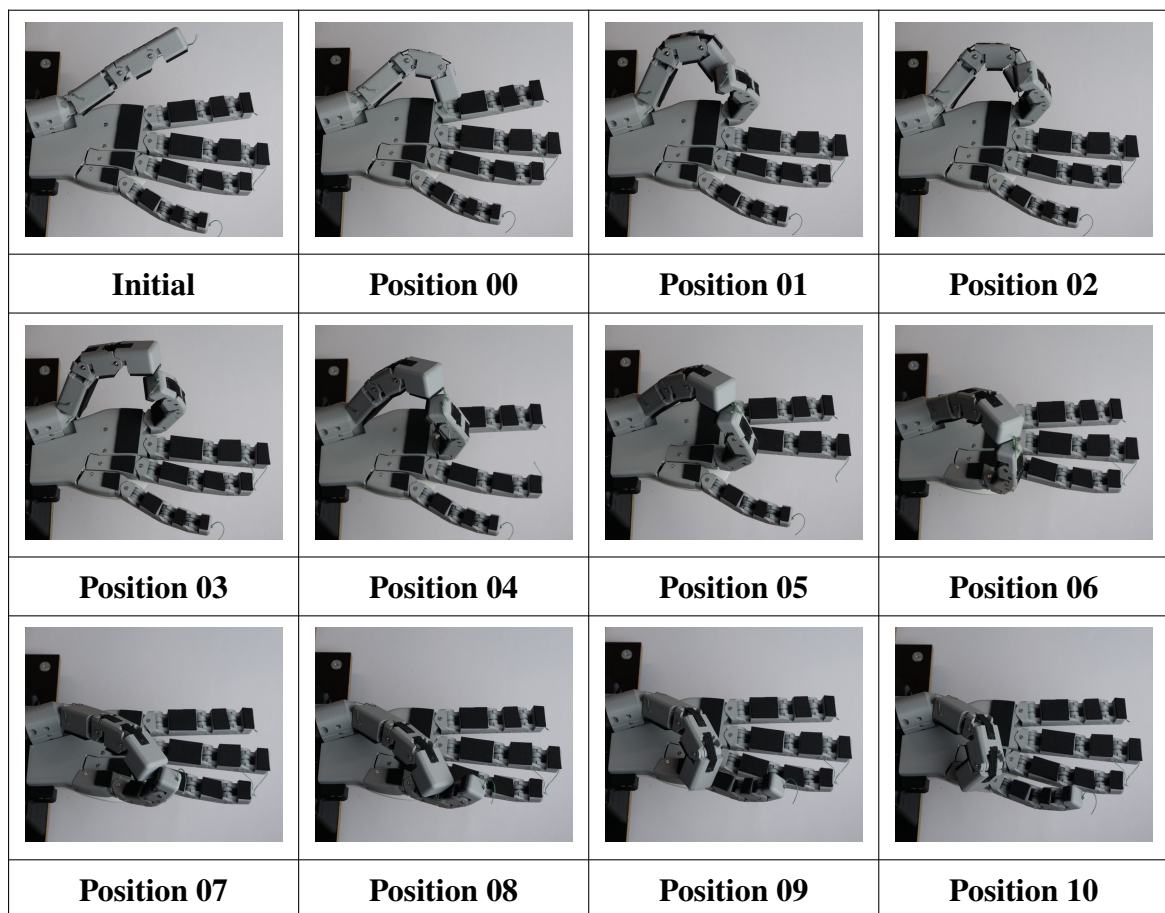


Figure A.3: Developed robot hand Kapandji Test results.

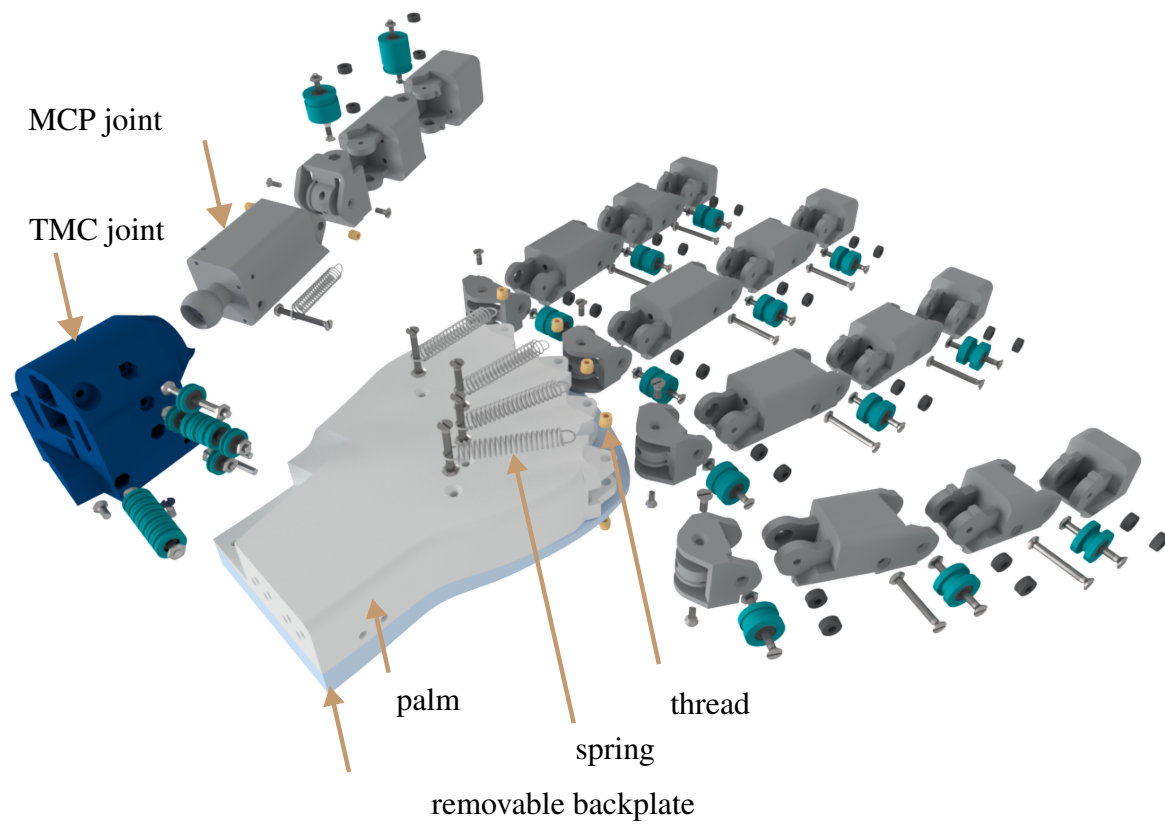


Figure A.4: Exploded view of the developed robot hand prototype.

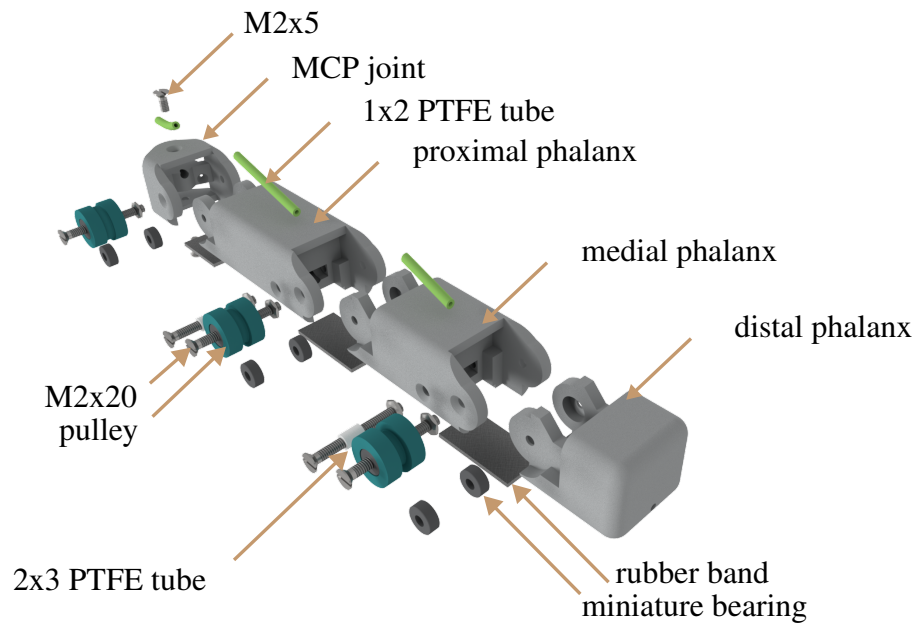


Figure A.5: Exploded view of the developed robot hand's middle finger.

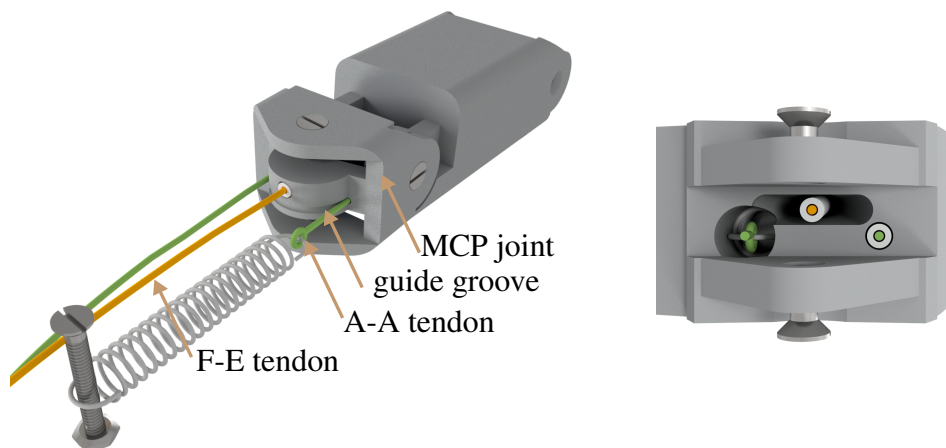


Figure A.6: Illustration of MCP joint design.

| Digit | Joint | Movement | ROM values [°] | | | | | | | | | | | | | | |
|---------------|-------|----------|----------------|------|------|------|------|------|------|------|------|------|------|----|-----|----|----|
| | | | 1988 | 1990 | 2001 | 2008 | 2013 | 2014 | 2015 | 2015 | 2015 | 2014 | 2014 | | | | |
| Thumb | TMC | Pa. A-A | - | - | - | 90 | 15 | 61.2 | 31 | amb. | - | - | 60 | 0 | | | |
| | MCP | Ra. A-A | - | - | - | 60 | | 62.9 | 10.2 | | - | - | 25 | 35 | | | |
| | | A-A | - | - | - | - | | - | - | - | - | - | 60 | 0 | | | |
| IP | F-E | - | 0 | 56 | - | 0 | 80 | 8.1 | 60 | 10 | 55 | 0 | 61 | 10 | 55 | | |
| | F-E | - | -5 | 73 | - | 10 | 80 | 12 | 90 | 15 | 80 | 0 | 81 | 15 | 80 | | |
| Index finger | HMC | F-E | - | - | - | 3 | 0 | 5 | - | - | - | - | - | - | - | | |
| | MCP | A-A | - | - | - | 60 | | - | - | - | - | - | 13 | 42 | | | |
| | | F-E | - | 0 | 100 | - | 40 | 90 | - | - | 45 | 90 | 19 | 90 | 0 | 80 | |
| PIP | F-E | - | 0 | 105 | - | 0 | 110 | - | - | 0 | 100 | 7 | 101 | 0 | 100 | | |
| | DIP | F-E | - | 0 | 85 | - | 5 | 90 | - | 0 | 80 | 6 | 84 | 0 | 80 | 10 | 90 |
| Middle finger | HMC | F-E | - | - | - | 3 | 0 | 5 | - | - | - | - | - | - | - | | |
| | MCP | A-A | - | - | - | 60 | | - | - | - | - | - | 8 | 35 | | | |
| | | F-E | - | 0 | 100 | - | 40 | 90 | - | - | 45 | 90 | 19 | 90 | 0 | 80 | |
| PIP | F-E | - | 0 | 105 | - | 0 | 110 | - | - | 0 | 100 | 7 | 101 | 0 | 100 | | |
| | DIP | F-E | - | 0 | 85 | - | 5 | 90 | - | 0 | 80 | 6 | 84 | 0 | 80 | 10 | 90 |
| Ring finger | HMC | F-E | - | - | - | 15 | 0 | 10 | - | - | - | - | - | - | - | | |
| | MCP | A-A | - | - | - | 45 | | - | - | - | - | - | 14 | 20 | | | |
| | | F-E | - | 0 | 100 | - | 40 | 90 | - | - | 45 | 90 | 19 | 90 | 0 | 80 | |
| PIP | F-E | - | 0 | 105 | - | 0 | 120 | - | - | 0 | 100 | 7 | 101 | 0 | 100 | | |
| | DIP | F-E | - | 0 | 85 | - | 5 | 90 | - | 0 | 80 | 6 | 84 | 0 | 80 | 20 | 90 |
| Little finger | HMC | F-E | - | - | - | 30 | 0 | 15 | - | - | - | - | - | - | - | | |
| | MCP | A-A | - | - | - | 50 | | - | - | - | - | - | 19 | 33 | | | |
| | | F-E | - | 0 | 100 | - | 40 | 90 | - | - | 45 | 90 | 19 | 90 | 0 | 80 | |
| PIP | F-E | - | 0 | 105 | - | 0 | 135 | - | - | 0 | 100 | 7 | 101 | 0 | 100 | | |
| DIP | F-E | - | 0 | 85 | - | 5 | 90 | - | - | 0 | 80 | 6 | 84 | 0 | 80 | 30 | 90 |

Becker and Thakor (1988), Hume et al. (1990), El-Shennawy et al. (2001), Cobos et al. (2008), Barakat et al. (2013), Ngeo et al. (2014)

Pa.: palmar, Ra.: radial, amb.: ambiguous

Bain et al. (2015), K.-S. Lee and Jung (2015), Peña-Pitarch et al. (2014)

Table A.1: ROM value from literature for different finger

| Finger | Phalanx Length Proximal; Medial; Distal | Width | Thickness |
|---------------|--|--------------|------------------|
| Index Finger | 47.775; 27.885; 18.915 | 20.5 | 16 |
| Middle Finger | 51.87; 33.15; 21.06 | 19 | 16 |
| Ring Finger | 47.58; 32.175; 20.865 | 18 | 16 |
| Little Finger | 39.78; 22.815; 18.135 | 16 | 16 |

Table A.2: Robot hand finger phalanx dimensions in mm for a hand length of 195 mm.

B Entity-Relation Models

In this chapter, Entity-Relation Models established in this dissertation are given. They are presented in the Appendix to improve readability of the main body and presented here for the sake of completeness.

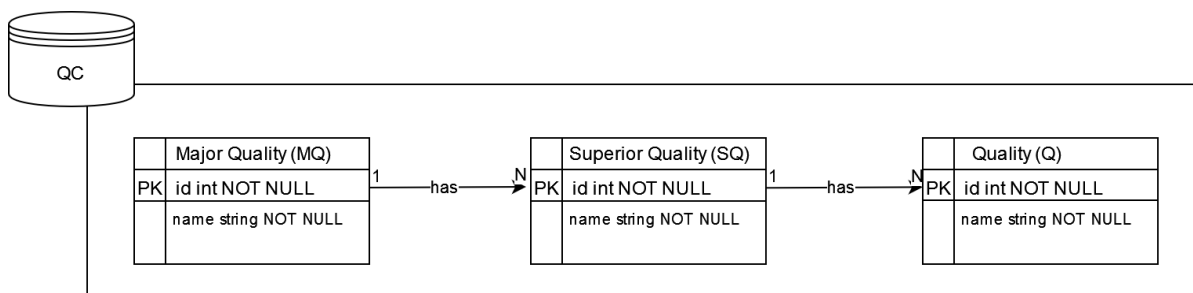


Figure B.1: Entity-Relation model of the Quality Criteria data structure.

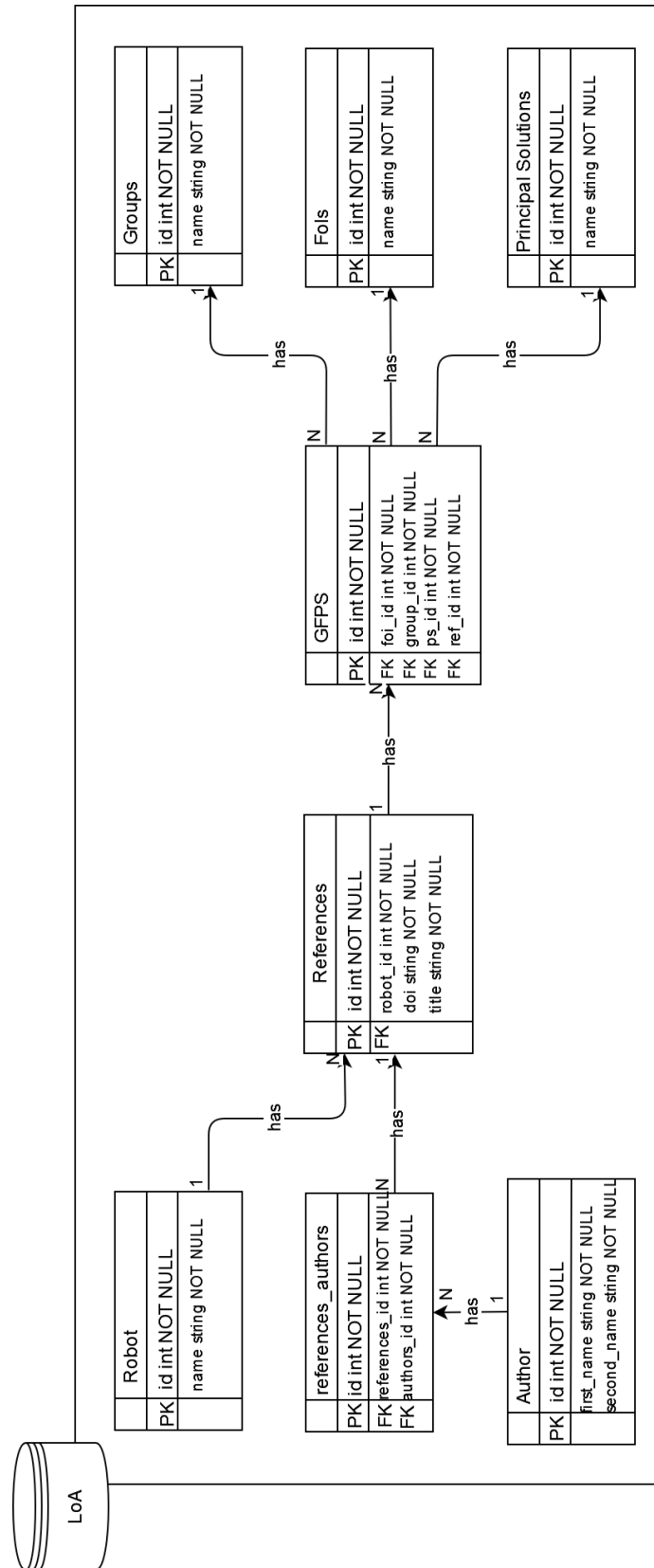


Figure B.2: Entity-Relation Model of the LoA data structure.

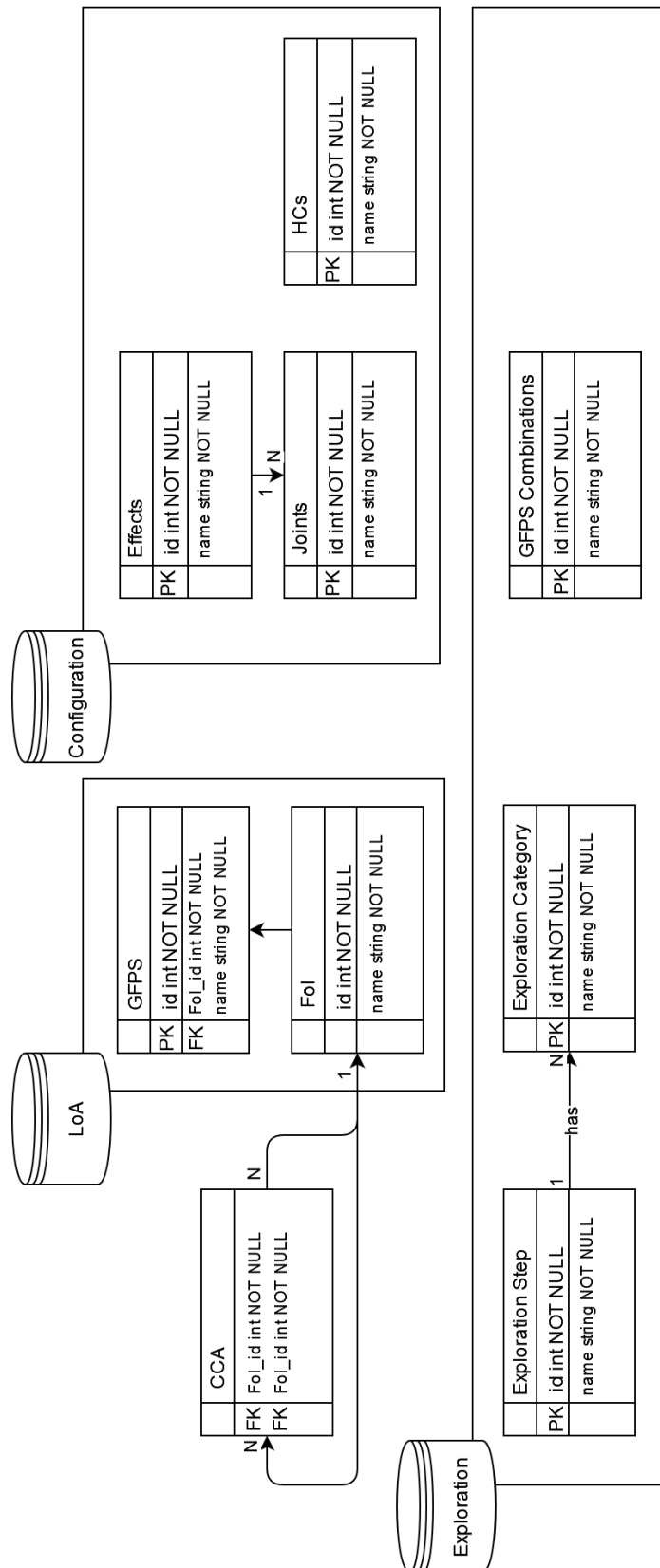


Figure B.3: Entity-Relation Model of three data bases: LoA, Configuration, and Exploration.

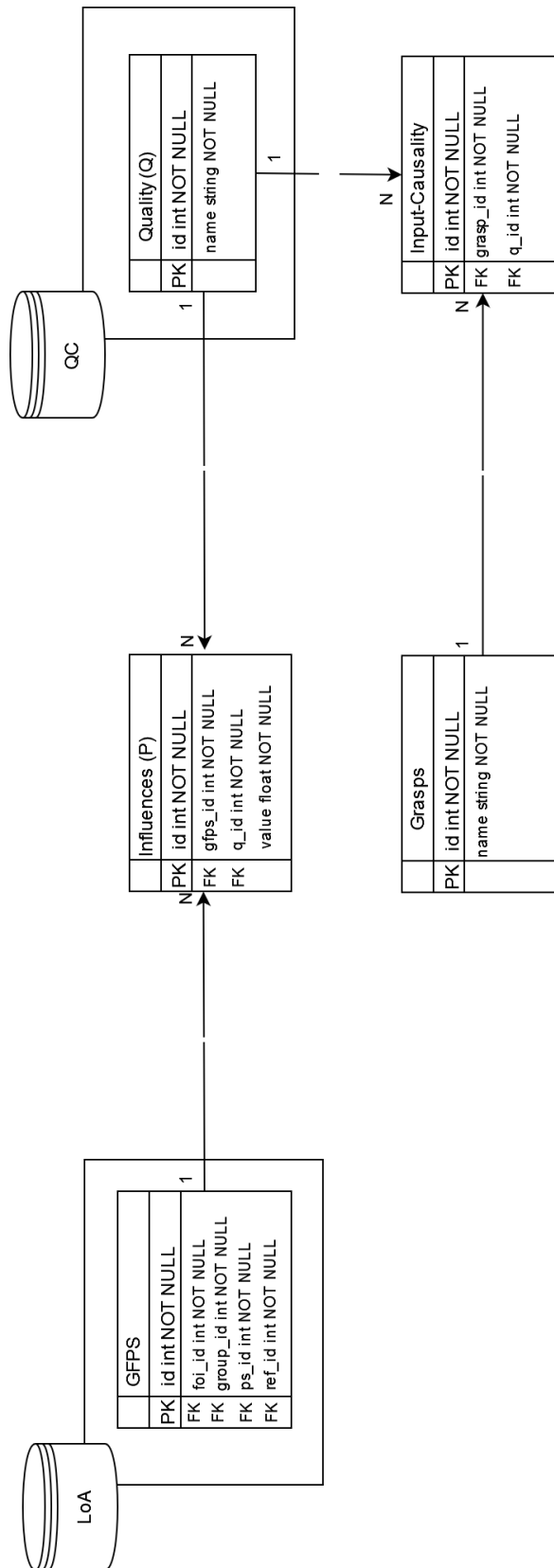


Figure B.4: Entity-Relationship model for the relationship between the data files Qualities, GFPS, and Grasps.

C Collected Robot Hands

In this chapter, the robot hands collected in this dissertation are given for different purposes are given on a timeline, respectively. They are presented in the Appendix to improve readability of the main body and presented here for the sake of completeness.

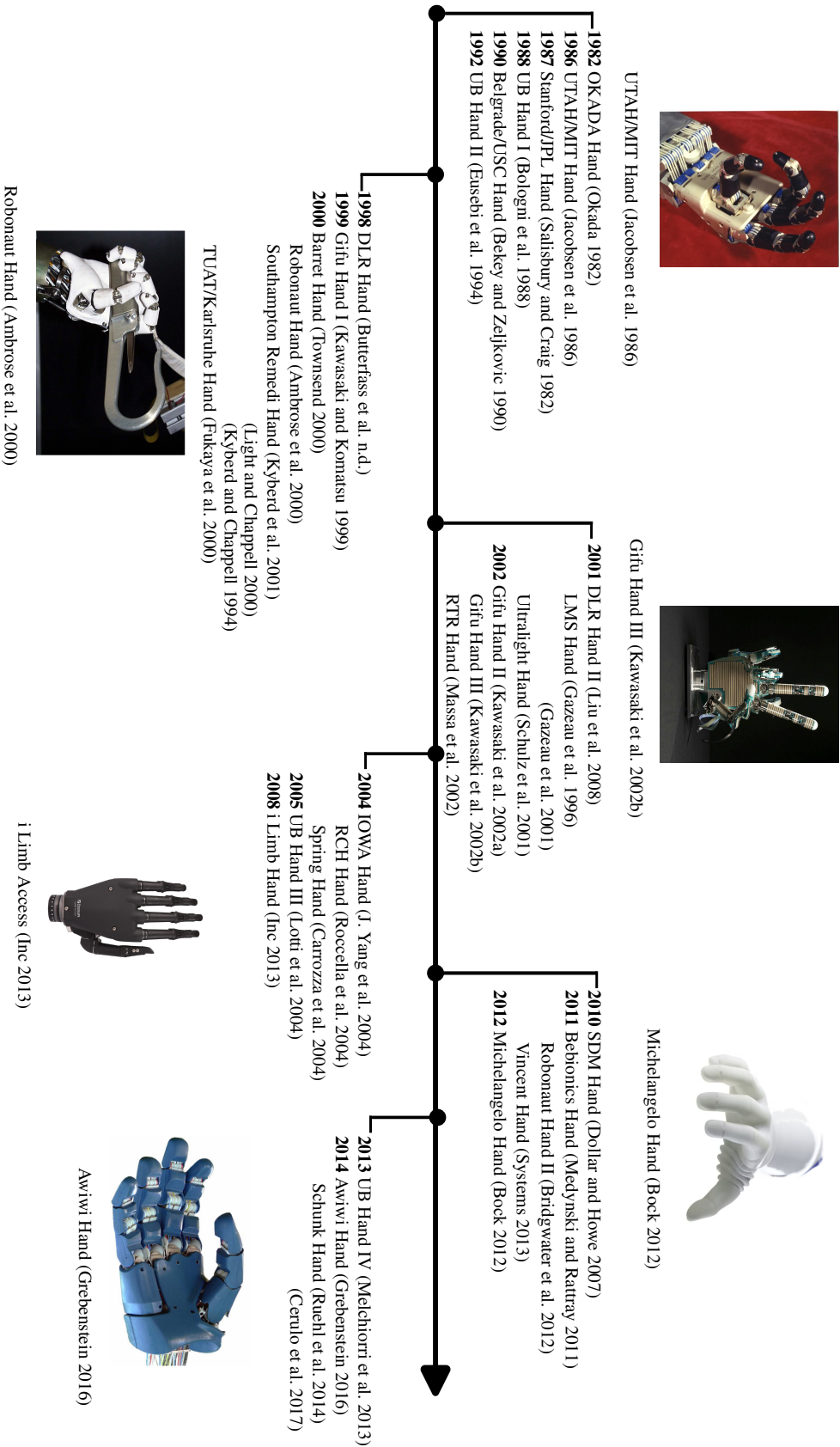


Figure C.1: Time line of the collected Significant Robot Hands †.

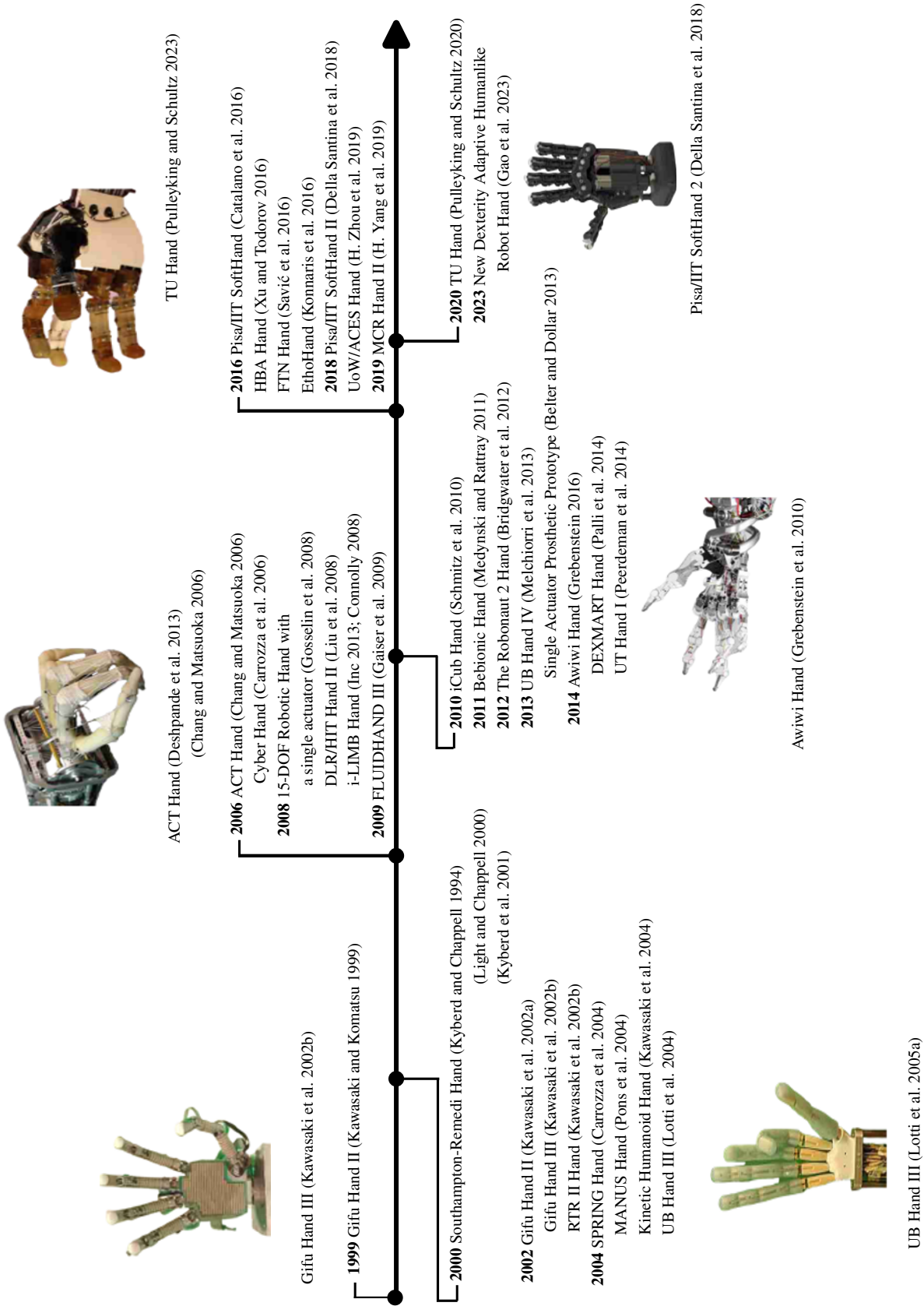


Figure C.2: Time line of the collected robot hands analyzed for thumb contributions †.

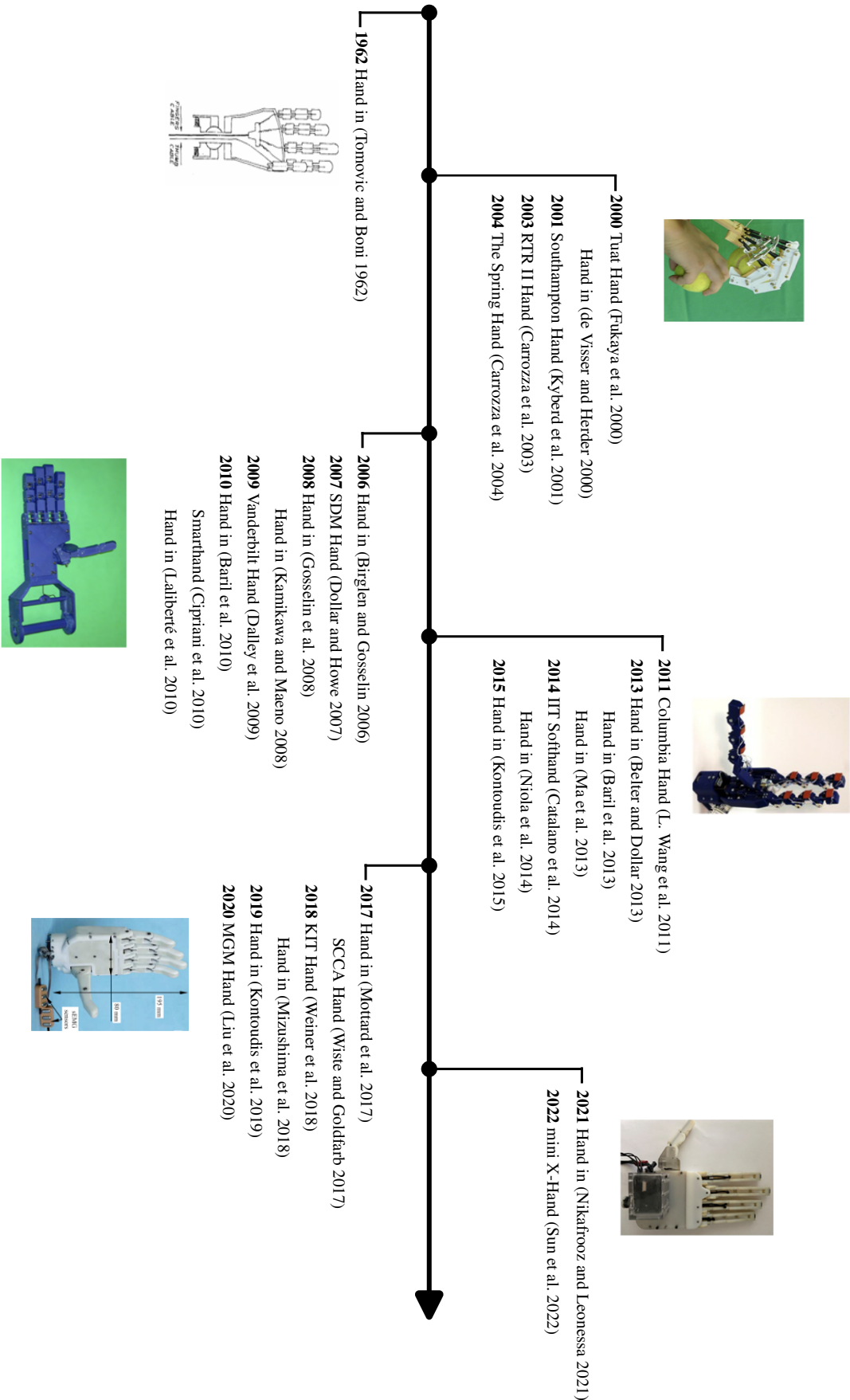


Figure C.3: Time line of the collected robot hands analyzed for interfinger underactuation contributions †.

D Library of Approaches Examples

In this chapter, examples for given Principal Solutions of specific FoIs are presented. They serve as additional information for the interested reader. The LoA examples are reproduced from the author's prior publication (Gossen et al. 2025b).

| Elim. 1 TMC Joint DOF | Elim. TMC P-S DOF |
|--|-------------------|
| 2-2-1 configuration (3.9 (a)) | |
| <p>The 2-2-1 (3.9 (a)) configuration type has been proposed and discussed in detail in the work by H. Wang et al. (2017a). For further information, readers are referred to the work by Wang et al. The 2-2-1 configuration is defined by simplifications of the TMC joint and closely resembles the human thumb in terms of DOF, although it is more challenging to implement. As a result, this configuration is comparably uncommon to find. (H. Wang et al. 2017a)</p> | |
| <p>Shadow Hand (Sharma et al. 2014), CEA Dexterous Hand (Martin and Grossard 2014), UB Hand 3 (Lotti et al. 2005b)</p> | |

Table D.1: LoA examples: Thumb - elim. 1 TMC P-S DOF

| Elim. 2 DOA TMC-MCP-IP Joints | Tendon UA of three joints |
|---|---------------------------|
| <p>In the FTN hand (Savić et al. 2016), the F-E degrees of freedom of all three joints (IP, MCP and CMC) are connected together by a tendon. This allows for the utilisation of underactuation, whereby the F-E movement of the entire thumb is achieved with a single actuator. The combination of tendon drive and torsion springs in the pin joints results in an underactuated movement of the thumb joints. This allows the phalanges of the thumb to adapt passively to the shape of the object to be gripped. Should the first phalanx of the thumb encounter an obstacle during flexion, the second and third phalanges will continue to flex until either the obstacle or their mechanical limits are reached. (Savić et al. 2016)</p> | |
| <hr/> <p>FTN hand (Savić et al. 2016)</p> | |

Table D.2: LoA examples: Thumb - Elim. 2 DOA - tendon underactuation

| Elim. 1 MCP Joint DOF | Elim. MCP A-A DOF |
|---|-------------------|
| <p>3-1-1 configuration (3.9 (c))</p> | |
| <p>The 3-1-1 (3.9 (c)) configuration type has been proposed and discussed in detail in the work by H. Wang et al. (2017a). For further information, readers are referred to the work by Wang et al. The TMC joint's critical role in enabling the thumb's axial rotation is incorporated in this design to specifically support pronation. This design allows all pronation-related mechanisms in the IP and MCP joints to be disregarded, effectively giving the TMC joint three DOFs. According to Wang et al., no robotic hand with this configuration had been developed, due to the challenges of realizing a compact structure that maintains functional appearance and size. However, in the course of this dissertation, the Ethohand Konnaris et al. (2016) was identified, being published after the study by Wang et al. was conducted. The Ethohand incorporates a three DOF ball joint for the TMC joint. Notably, however, efforts in this dissertation to replicate the Ethohand's ball joint design failed, as the third DOF is highly restricted by the tendon routing. This highlights the design challenges.</p> | |
| <hr/> <p>Ethohand (Konnaris et al. 2016)</p> | |

Table D.3: LoA examples: Thumb - elim. 1 MCP A-A DOF

| | |
|--|-------------------|
| Elim. 1 TMC Joint DOF | Elim. TMC P-S DOF |
| Elim. 1 MCP Joint DOF | Elim. MCP A-A DOF |
| 2-1-1 configuration (3.9 (c)) | |
| <p>The 2-1-1 (3.9 (b)) configuration type has been proposed and discussed in detail in the work by H. Wang et al. (2017a). For further information, readers are referred to the work by Wang et al. The 2-1-1 configuration is characterized by simplifications in both the MCP and TMC joints, combining the approaches of the 3-1-1 and 2-2-1 configurations. This configuration offers a lower number of DOF, simplifying both structure and control. Consequently, the majority of thumb configurations in advanced robotic hands utilize this configuration type. A total of 20 robot hands that apply the 2-1-1 configuration have been identified in the literature. (H. Wang et al. 2017a)</p> | |
| <p>DLR Hand Serie (Butterfass et al. n.d.)(Butterfass et al. 2001)(Liu et al. 2008), DexHand (Chalon et al. 2011), UTAH/MIT Hand (Jacobsen et al. 1986), Gifu Hand Serie (Kawasaki et al. 2002a)(Kawasaki et al. 2002b), NAIST Hand Serie (Ueda et al. 2010)(Kurita et al. 2009), TUAT/Karlsruhe Hand (Fukaya et al. 2000), TWENDY-ONE Hand (Iwata and Sugano 2009), Awiwi Hand (Grebenstein 2016), iCub Hand (Schmitz et al. 2010), DARPA Intrinsic Hand (Weir et al. 2008), DEXMART Hand (Palli et al. 2014), UBH-IV Hand (Palli and Pirozzi 2013), Robonaut 2 Hand (Bridgwater et al. 2012), DARPA Extrinsic Hand (Mitchell and Weir 2008), ARTS Hand (Controzzi et al. 2010)</p> | |

Table D.4: LoA examples: Thumb - elim. 1 TMC P-S and 1 MCP A-A DOF

| | |
|---|-------------------|
| Elim. 1 TMC Joint DOF | Elim. TMC P-S DOF |
| Elim. 2 MCP Joint DOF | Elim. MCP joint |
| 2-0-1 configuration (3.9 (d)) | |
| <p>The 2-0-1 (3.9 (d)) configuration type is inspired by the surgical procedure known as MCP joint arthrodesis. Arthrodesis is typically recommended for patients with severe arthritis, instability, or deformity of the MCP joint, conditions commonly associated with rheumatoid arthritis. Due to the limited angular movement of the MCP joint in routine activities and grasps, surgeons have found that stiffening the MCP joint can effectively reduce pain while preserving functional grasping ability. (Vanderzanden et al. 2014) Technically implemented in a robot hand, this specific configuration has only been observed in the TU hand (Pulleyking et al. 2016), (Pulleyking and Schultz 2020). In this configuration, the MCP joint’s DOF is reduced from two to zero, fully immobilizing it at 10 degrees of flexion and 15 degrees of abduction (Pulleyking et al. 2016), (Pulleyking and Schultz 2020). Analysis of this design shows approximately a 50 percent reduction in the thumb’s workspace volume compared to an unstiffened thumb, with the restricted movement primarily affecting positions that bring the thumb close to the palm — a movement that is considered infrequent in daily tasks according to the authors (Pulleyking et al. 2016). Additionally, the reduction in joint count compared to conventional robotic thumbs notably decreases both cost and structural complexity, as highlighted by the authors Pulleyking et al. (2016), Pulleyking and Schultz (2020).</p> | |
| TU hand (Pulleyking et al. 2016), (Pulleyking and Schultz 2020) | |

Table D.5: LoA examples: Thumb - elim. 1 TMC P-S and 2 MCP DOF

| | |
|--|------------------------|
| Elim. 2 TMC Joint DOF | Elim. TMC F-E, P-S DOF |
| Elim. 1 MCP Joint DOF | Elim. MCP A-A DOF |
| 1-1-1 configuration (3.9 (c)) | |
| <p>The 1-1-1 (3.9 (e)) configuration type comprises three DOF. It could only be found in the following two robot hands: The UT Hand I (Peerdeman et al. 2014) and the RTR II Hand (Massa et al. 2002). In both hands, the thumb is oriented at a specific angle relative to the palm and the other fingers. The A-A movement for the opposition of the thumb is achieved through a TMC joint with a single DOF. The F-E movement of the thumb is achieved through the MCP and IP joints.</p> | |
| UT Hand I (Peerdeman et al. 2014), RTR II Hand (Massa et al. 2002) | |

Table D.6: LoA examples: Thumb - elim. TMC P-S and F-E and MCP A-A DOF

| Elim. 1 DOA MCP-PIP Joints | Tendon coupling of two joints |
|---|-------------------------------|
| <p>In the DLR/HIT Hand II (Liu et al. 2008), the thumb exhibits three DOF. The final two joints are mechanically coupled to one another. The coupling mechanism in the MCP and IP joints of the thumb is achieved through the use of a steel wire with a tensioning mechanism. The utilisation of the steel wire ensures the transmission of force in the thumb is both flexible and secure. The coupling mechanism precludes the possibility of controlling the movements of the proximal and distal phalanges individually. The transmission ratio between them is precisely 1:1 throughout the entire range of motion (Liu et al. 2008).</p> | |
| <p>DLR/HIT Hand II (Liu et al. 2008)</p> | |
| <p>Berselli et al. (2009) coupled the MCP and the IP joint with one of the drive tendons. This coupling restricts the movements of the two joints in analogy to the human hand. This tendon is not connected to an actuator, but is attached to different phalanges at both ends.</p> | |
| <p>No robot hand name</p> | |
| <p>The rotation of the IP joint of the thumb of UT Hand I (Peerdeman et al. 2014) is also flexibly coupled to the rotation of the MCP joint via a tendon coupling. The apparatus comprises a connection of two crossed nylon ropes, guided around two pulleys. The crossed cables enable bidirectional coupling of the angle of the distal phalanx. The transmission ratio is defined by the radius ratio and is set to 2:1 by Peerdeman et al. (2014). The advantage of this configuration is that the compliance of the tendon coupling also contributes to a more flexible grip. (Peerdeman et al. 2014)</p> | |
| <p>UT Hand I (Peerdeman et al. 2014)</p> | |

Table D.7: LoA examples: Elim. 1 DOA - Tendon Coupling

| Elim. 1 DOA MCP-PIP Joints | Linkage coupling of two joints |
|--|--------------------------------|
| <p>In the MCR Hand II (H. Yang et al. 2019), (H. Yang et al. 2021a), the movement of the IP joint is coupled with that of the MCP joint via a four bar linkage. This implies that the angle of the IP joint is a passive degree of freedom, undergoing alteration in accordance with the angle of the MCP joint. Both the IP and MCP joints are driven by a single servomotor. The angular ratio between the MCP and IP joints of the thumb is approximately 1.41. (H. Yang et al. 2019), (H. Yang et al. 2021a)</p> | |
| <p>MCR Hand II (H. Yang et al. 2019), (H. Yang et al. 2021a)</p> | |

Table D.8: LoA examples: Thumb: Elim. 1 DOA - Linkage Coupling

E Lists of Entities and Instances

In this chapter, the lists of entities and their instances established in this dissertation are given. The entities correspond to the graphically given entities in the Entity-Relation models in Chapter B. While all established entities and instances are given in the main body at the appropriate locations, this chapter serves as a summarizing source, where each entity and instance can be located with their unique identifier. The lists are presented in the Appendix to improve readability of the main body.

| Group | Name |
|---------|----------------------|
| Group 1 | Index Finger |
| Group 2 | Middle Finger |
| Group 3 | Ring Finger |
| Group 4 | Little Finger |
| Group 5 | Thumb |
| Group 6 | Kinematic-Base-Chain |
| Group 7 | Transmission |

Table E.1: List of instances of the entity "Group" (see Entity-Relation model in Figure B.2).

| FoI | Name |
|--------|--------------------------------------|
| FoI 01 | Eliminating 1 IP Joint DOF |
| FoI 02 | Eliminating 1 MCP Joint DOF |
| FoI 03 | Eliminating 2 MCP Joint DOF |
| FoI 04 | Eliminating 1 TMC Joint DOF |
| FoI 05 | Eliminating 2 TMC Joint DOF |
| FoI 06 | Eliminating 1 HMC Joint DOF |
| FoI 07 | Eliminating 2 HMC Joint DOF |
| FoI 08 | Eliminating 1 DOA DIP-PIP Joints |
| FoI 09 | Eliminating 2 DOA MCP-DIP-PIP Joints |
| FoI 10 | Eliminating 3 DOA MCP-DIP-PIP Joints |
| FoI 11 | Eliminating 1 DOA MCP-PIP Joints |
| FoI 12 | Eliminating 2 DOA TMC-MCP-IP Joints |
| FoI 13 | Eliminating 3 DOA TMC-MCP-IP Joints |
| FoI 14 | Eliminating 1 DOA HMC Joint |
| FoI 15 | Eliminating 2 DOA HMC Joint |
| FoI 17 | Eliminating 1 DOA F-E LF-RF |
| FoI 18 | Eliminating 1 DOA F-E MF-IF |
| FoI 19 | Eliminating 2 DOA F-E RF-MF-IF |
| FoI 20 | Eliminating 2 DOA F-E MF-IF-Tb |
| FoI 21 | Eliminating 2 DOA A-A LF-RF-IF |
| FoI 22 | Eliminating 3 DOA F-E LF-RF-MF-IF |
| FoI 23 | Eliminating 4 DOA F-E LF-RF-MF-IF-Tb |

Table E.2: List of instances of the entity "FoI" (see Entity-Relation model in Figure B.2).

| Principal Solution | Name |
|-----------------------|--|
| Principal Solution 1 | Eliminating DIP Joint |
| Principal Solution 2 | Eliminating MCP A-A DOF |
| Principal Solution 3 | Eliminating MCP Joint |
| Principal Solution 4 | Eliminating TMC P-S DOF |
| Principal Solution 5 | Eliminating TMC A-A and P-S DOF |
| Principal Solution 6 | Eliminating HMC Ring Finger |
| Principal Solution 7 | Implementing joined HMC for Little and Ring Finger |
| Principal Solution 8 | Eliminating HMC Little and Ring finger |
| Principal Solution 9 | Coupling (linkage) two joints |
| Principal Solution 10 | Coupling (tendon) two joints |
| Principal Solution 11 | Underactuating (linkage) two joints |
| Principal Solution 12 | Underactuating (tendon) two joints |
| Principal Solution 13 | Coupling (linkage) three joints |
| Principal Solution 14 | Coupling (tendon) three joints |
| Principal Solution 15 | Underactuating (linkage) three joints |
| Principal Solution 16 | Underactuating (tendon) three joints |
| Principal Solution 17 | Coupling (linkage) HMC-MCP Joints |
| Principal Solution 18 | Coupling (linkage) Grebenstein |
| Principal Solution 19 | Underactuating (linkage) HMC-MCP Joints |
| Principal Solution 20 | Underactuating (tendon) HMC-MCP Joints |
| Principal Solution 21 | Underact./Coupl. (tendon) F-E LF-RF |
| Principal Solution 22 | Underact./Coupl. (tendon) F-E MF-IF |
| Principal Solution 23 | Underact./Coupl. (tendon) F-E RF-MF-IF |
| Principal Solution 24 | Underact./Coupl. (tendon) F-E MF-IF-Tb |
| Principal Solution 25 | Underact./Coupl. (tendon) A-A LF-RF-IF |
| Principal Solution 26 | Underact./Coupl. (tendon) F-E LF-RF-MF-IF |
| Principal Solution 27 | Underact./Coupl. (tendon) F-E LF-RF-MF-IF-Tb |
| Principal Solution 28 | Underact./Coupl. (tendon) A-A LF-RF-MF-IF-Tb |
| Principal Solution 29 | Underact./Coupl. (linkage) F-E LF-RF |
| Principal Solution 30 | Underact./Coupl. (linkage) F-E MF-IF |

Table E.3: List of instances of the entity "Principal Solutions" (see Entity-Relation model in Figure B.2).

| GFPS | Name | PS | FoI | Group |
|---------|---|-----------------------|-------|---------|
| GFPS 1 | IF: Elim. DIP Joint | Principal Solution 1 | FoI 1 | Group 1 |
| GFPS 2 | MF: Elim. DIP Joint | Principal Solution 1 | FoI 1 | Group 2 |
| GFPS 3 | RF: Elim. DIP Joint | Principal Solution 1 | FoI 1 | Group 3 |
| GFPS 4 | LF: Elim. DIP Joint | Principal Solution 1 | FoI 1 | Group 4 |
| GFPS 5 | IF: Elim. MCP A-A DOF | Principal Solution 2 | FoI 2 | Group 1 |
| GFPS 6 | MF: Elim. MCP A-A DOF | Principal Solution 2 | FoI 2 | Group 2 |
| GFPS 7 | RF: Elim. MCP A-A DOF | Principal Solution 2 | FoI 2 | Group 3 |
| GFPS 8 | LF: Elim. MCP A-A DOF | Principal Solution 2 | FoI 2 | Group 4 |
| GFPS 9 | Th: Elim. MCP A-A DOF | Principal Solution 2 | FoI 2 | Group 5 |
| GFPS 10 | Th: Elim. MCP Joint | Principal Solution 3 | FoI 3 | Group 5 |
| GFPS 11 | Th: Elim. TMC P-S DOF | Principal Solution 4 | FoI 4 | Group 5 |
| GFPS 12 | Th: Elim. TMC A-A and P-S DOF | Principal Solution 5 | FoI 5 | Group 5 |
| GFPS 13 | KBC: Elim. HMC Ring Finger | Principal Solution 6 | FoI 6 | Group 6 |
| GFPS 14 | KBC: Implement. joined HMC LF RF | Principal Solution 7 | FoI 6 | Group 6 |
| GFPS 15 | KBC: Elim. HMC Little and Ring finger | Principal Solution 8 | FoI 7 | Group 6 |
| GFPS 16 | IF: Coupling (linkage) two joints | Principal Solution 9 | FoI 8 | Group 1 |
| GFPS 17 | MF: Coupling (linkage) two joints | Principal Solution 9 | FoI 8 | Group 2 |
| GFPS 18 | RF: Coupling (linkage) two joints | Principal Solution 9 | FoI 8 | Group 3 |
| GFPS 19 | LF: Coupling (linkage) two joints | Principal Solution 9 | FoI 8 | Group 4 |
| GFPS 20 | IF: Coupling (tendon) two joints | Principal Solution 10 | FoI 8 | Group 1 |
| GFPS 21 | MF: Coupling (tendon) two joints | Principal Solution 10 | FoI 8 | Group 2 |
| GFPS 22 | RF: Coupling (tendon) two joints | Principal Solution 10 | FoI 8 | Group 3 |
| GFPS 23 | LF: Coupling (tendon) two joints | Principal Solution 10 | FoI 8 | Group 4 |
| GFPS 24 | IF: Underactuating (linkage) two joints | Principal Solution 11 | FoI 8 | Group 1 |
| GFPS 25 | MF: Underactuating (linkage) two joints | Principal Solution 11 | FoI 8 | Group 2 |
| GFPS 26 | RF: Underactuating (linkage) two joints | Principal Solution 11 | FoI 8 | Group 3 |
| GFPS 27 | LF: Underactuating (linkage) two joints | Principal Solution 11 | FoI 8 | Group 4 |
| GFPS 28 | IF: Coupling (linkage) three joints | Principal Solution 13 | FoI 9 | Group 1 |
| GFPS 29 | MF: Coupling (linkage) three joints | Principal Solution 13 | FoI 9 | Group 2 |
| GFPS 30 | RF: Coupling (linkage) three joints | Principal Solution 13 | FoI 9 | Group 3 |
| GFPS 31 | LF: Coupling (linkage) three joints | Principal Solution 13 | FoI 9 | Group 4 |
| GFPS 32 | IF: Coupling (tendon) three joints | Principal Solution 14 | FoI 9 | Group 1 |
| GFPS 33 | MF: Coupling (tendon) three joints | Principal Solution 14 | FoI 9 | Group 2 |
| GFPS 34 | RF: Coupling (tendon) three joints | Principal Solution 14 | FoI 9 | Group 3 |

(continued on next page)

| | | | | |
|---------|---|-----------------------|--------|---------|
| GFPS 35 | LF: Coupling (tendon) three joints | Principal Solution 14 | FoI 9 | Group 4 |
| GFPS 36 | IF: Underactuating (linkage) three joints | Principal Solution 15 | FoI 9 | Group 1 |
| GFPS 37 | MF: Underactuating (linkage) three joints | Principal Solution 15 | FoI 9 | Group 2 |
| GFPS 38 | RF: Underactuating (linkage) three joints | Principal Solution 15 | FoI 9 | Group 3 |
| GFPS 39 | LF: Underactuating (linkage) three joints | Principal Solution 15 | FoI 9 | Group 4 |
| GFPS 40 | IF: Underactuating (tendon) three joints | Principal Solution 16 | FoI 9 | Group 1 |
| GFPS 41 | MF: Underactuating (tendon) three joints | Principal Solution 16 | FoI 9 | Group 2 |
| GFPS 42 | RF: Underactuating (tendon) three joints | Principal Solution 16 | FoI 9 | Group 3 |
| GFPS 43 | LF: Underactuating (tendon) three joints | Principal Solution 16 | FoI 9 | Group 4 |
| GFPS 44 | IF: Underactuating (linkage) three joints | Principal Solution 15 | FoI 10 | Group 1 |
| GFPS 45 | MF: Underactuating (linkage) three joints | Principal Solution 15 | FoI 10 | Group 2 |
| GFPS 46 | RF: Underactuating (linkage) three joints | Principal Solution 15 | FoI 10 | Group 3 |
| GFPS 47 | LF: Underactuating (linkage) three joints | Principal Solution 15 | FoI 10 | Group 4 |
| GFPS 48 | IF: Underactuating (tendon) three joints | Principal Solution 16 | FoI 10 | Group 1 |
| GFPS 49 | MF: Underactuating (tendon) three joints | Principal Solution 16 | FoI 10 | Group 2 |
| GFPS 50 | RF: Underactuating (tendon) three joints | Principal Solution 16 | FoI 10 | Group 3 |
| GFPS 51 | LF: Underactuating (tendon) three joints | Principal Solution 16 | FoI 10 | Group 4 |
| GFPS 52 | IF: Coupling (linkage) two joints | Principal Solution 9 | FoI 11 | Group 1 |
| GFPS 53 | MF: Coupling (linkage) two joints | Principal Solution 9 | FoI 11 | Group 2 |
| GFPS 54 | RF: Coupling (linkage) two joints | Principal Solution 9 | FoI 11 | Group 3 |
| GFPS 55 | LF: Coupling (linkage) two joints | Principal Solution 9 | FoI 11 | Group 4 |
| GFPS 56 | Th: Coupling (linkage) two joints | Principal Solution 9 | FoI 11 | Group 5 |
| GFPS 57 | IF: Coupling (tendon) two joints | Principal Solution 10 | FoI 11 | Group 1 |
| GFPS 58 | MF: Coupling (tendon) two joints | Principal Solution 10 | FoI 11 | Group 2 |
| GFPS 59 | RF: Coupling (tendon) two joints | Principal Solution 10 | FoI 11 | Group 3 |
| GFPS 60 | LF: Coupling (tendon) two joints | Principal Solution 10 | FoI 11 | Group 4 |
| GFPS 61 | Th: Coupling (tendon) two joints | Principal Solution 10 | FoI 11 | Group 5 |
| GFPS 62 | IF: Underactuating (linkage) two joints | Principal Solution 11 | FoI 11 | Group 1 |
| GFPS 63 | MF: Underactuating (linkage) two joints | Principal Solution 11 | FoI 11 | Group 2 |
| GFPS 64 | RF: Underactuating (linkage) two joints | Principal Solution 11 | FoI 11 | Group 3 |
| GFPS 65 | LF: Underactuating (linkage) two joints | Principal Solution 11 | FoI 11 | Group 4 |
| GFPS 66 | Th: Underactuating (linkage) two joints | Principal Solution 11 | FoI 11 | Group 5 |
| GFPS 67 | Th: Coupling (linkage) three joints | Principal Solution 13 | FoI 12 | Group 5 |
| GFPS 68 | Th: Coupling (tendon) three joints | Principal Solution 14 | FoI 12 | Group 5 |

(continued on next page)

| | | | | |
|---------|--|-----------------------|--------|---------|
| GFPS 69 | Th: Underactuating (linkage) three joints | Principal Solution 15 | FoI 12 | Group 5 |
| GFPS 70 | Th: Underactuating (linkage) three joints | Principal Solution 15 | FoI 13 | Group 5 |
| GFPS 71 | KBC: Coupling (linkage) HMC-MCP Joints | Principal Solution 17 | FoI 14 | Group 6 |
| GFPS 72 | KBC: Coupling (linkage) Grebenstein | Principal Solution 18 | FoI 14 | Group 6 |
| GFPS 73 | KBC: Underact. (linkage) HMC-MCP Joints | Principal Solution 19 | FoI 14 | Group 6 |
| GFPS 74 | Tr: Underact./Coupl. (tendon) F-E LR-RF | Principal Solution 21 | FoI 17 | Group 7 |
| GFPS 75 | Tr: Underact./Coupl. (tendon) F-E MF-IF | Principal Solution 22 | FoI 18 | Group 7 |
| GFPS 76 | Tr: Underact./Coupl. (tendon) F-E RF-MF-IF | Principal Solution 23 | FoI 19 | Group 7 |
| GFPS 77 | Tr: Underact./Coupl. (tendon) F-E MF-IF-Tb | Principal Solution 24 | FoI 20 | Group 7 |
| GFPS 78 | Tr: Underact./Coupl. (tendon) A-A LF-RF-IF | Principal Solution 25 | FoI 21 | Group 7 |
| GFPS 79 | Tr: Underact./Coupl. (tendon) F-E LF-RF-MF-IF | Principal Solution 26 | FoI 22 | Group 7 |
| GFPS 80 | Tr: Underact./Coupl. (tendon) F-E LF-RF-MF-IF-Tb | Principal Solution 27 | FoI 23 | Group 7 |
| GFPS 81 | Tr: Underact./Coupl. (tendon) A-A LF-RF-MF-IF-Tb | Principal Solution 28 | FoI 24 | Group 7 |
| GFPS 82 | Tr: Underact./Coupl. (linkage) F-E LF-RF | Principal Solution 29 | FoI 17 | Group 7 |
| GFPS 83 | Tr: Underact./Coupl. (linkage) F-E MF-IF | Principal Solution 30 | FoI 18 | Group 7 |
| GFPS 84 | Th: Underactuating (tendon) three joints | Principal Solution 16 | FoI 12 | Group 5 |
| GFPS 85 | LF: Underactuating (tendon) two joints | Principal Solution 12 | FoI 11 | Group 4 |
| GFPS 86 | KBC: Underact. (tendon) HMC-MCP Joints | Principal Solution 20 | FoI 14 | Group 6 |

Table E.4: List of instances of the entity "GFPS" (see Entity-Relation model in Figure B.2).

| Major Quality | Name |
|---------------|-----------------------|
| MQ 1 | Motion Ability (M.A.) |
| MQ 2 | Simplicity |

Table E.5: List of instances of the entity "Major Quality" (see Entity-Relation model in Figure B.1).

| Superior Quality | Name |
|------------------|----------------------------------|
| SQ 1 | Anthropomorphic Movements (A.M.) |
| SQ 2 | Movement Independence (M.I.) |
| SQ 3 | Manipulability (M.) |
| SQ 4 | Contact Conditions (C.C.) |
| SQ 5 | Mechanical Design (M.D.) |
| SQ 6 | Degree of Actuation (D.o.A.) |

Table E.6: List of instances of the entity "Superior Quality" (see Figure B.1).

| Quality | Name |
|---------|-----------------------------|
| Q1 | Enable LF F-E |
| Q2 | Enable LF A-A |
| Q3 | Enable RF F-E |
| Q4 | Enable RF A-A |
| Q5 | Enable MF F-E |
| Q6 | Enable MF A-A |
| Q7 | Enable IF F-E |
| Q8 | Enable IF A-A |
| Q9 | Enable T. F-E |
| Q10 | Enable T. A-A radial |
| Q11 | Enable T. A-A palmar |
| Q12 | Enable T. P-S |
| Q13 | Elim. LF ind. DIP F-E |
| Q14 | Elim. LF ind. PIP F-E |
| Q15 | Elim. LF ind. A-A |
| Q16 | Elim. LF ind. F-E tow. R.F. |
| Q17 | Elim. RF ind. DIP F-E |
| Q18 | Elim. RF ind. PIP F-E |
| Q19 | Elim. RF ind. A-A |
| Q20 | Elim. RF ind. F-E tow. M.F. |

(continued on next page)

| Quality | Name |
|---------|--|
| Q21 | Elim. MF ind. DIP F-E |
| Q22 | Elim. MF ind. PIP F-E |
| Q23 | Elim. MF ind. A-A |
| Q24 | Elim. MF ind. F-E tow. I.F. |
| Q25 | Elim. IF ind. DIP F-E |
| Q26 | Elim. IF ind. PIP F-E |
| Q27 | Elim. IF ind. A-A |
| Q28 | Elim. IF ind. F-E tow. T. |
| Q29 | Elim. T. ind. IP F-E |
| Q30 | Elim. T. ind. MCP F-E |
| Q31 | Elim. T. ind. TMC A-A palmar |
| Q32 | Elim. T. ind. MCP A-A radial |
| Q33 | Elim. T. ind. F-E tow. T. A-A |
| Q34 | Increasing Contact Friction |
| Q35 | Optimizing Contact Surface |
| Q36 | Optimizing Fingertip Opposition |
| Q37 | Reducing number of Mechanical Components |
| Q38 | Simplifying design |
| Q39 | Reducing installation space |
| Q40 | Reducing number of Joints/Motors |
| Q41 | Keeping number of DOF |

Table E.7: List of instances of the entity "Quality" (see Entity-Relation model in Figure B.1).

F Fields of Interest Compatibility Matrix

In this chapter, the compatibility matrix of the FoIs established in this dissertation is given. The compatibility matrix is derived by assessing whether two FoIs can be applied at the same time. The table is presented in the Appendix to improve readability of the main body.

| | FoI 1 | FoI 2 | FoI 3 | FoI 4 | FoI 5 | FoI 6 | FoI 7 | FoI 8 | FoI 9 | FoI 10 | FoI 11 | FoI 12 | FoI 13 | FoI 14 | FoI 15 | FoI 16 | FoI 17 | FoI 18 | FoI 19 | FoI 20 | FoI 21 | FoI 22 | FoI 23 | |
|--------|-------|-------|-------|-------|-------|-------|-------|-------|-------|--------|--------|--------|--------|--------|--------|--------|--------|--------|--------|--------|--------|--------|--------|---|
| FoI 1 | | ■ | ■ | ■ | ■ | ■ | ■ | | | | ■ | | ■ | ■ | ■ | ■ | ■ | ■ | ■ | ■ | ■ | ■ | ■ | ■ |
| FoI 2 | | | | ■ | ■ | ■ | ■ | ■ | ■ | | ■ | ■ | ■ | ■ | ■ | ■ | ■ | ■ | ■ | ■ | ■ | ■ | ■ | ■ |
| FoI 3 | | | | | ■ | ■ | ■ | ■ | | | | | ■ | ■ | ■ | ■ | ■ | ■ | ■ | ■ | ■ | ■ | ■ | ■ |
| FoI 4 | | | | | | ■ | ■ | ■ | ■ | ■ | ■ | ■ | ■ | ■ | ■ | ■ | ■ | ■ | ■ | ■ | ■ | ■ | ■ | ■ |
| FoI 5 | | | | | | | ■ | ■ | ■ | ■ | ■ | ■ | ■ | ■ | ■ | ■ | ■ | ■ | ■ | ■ | ■ | ■ | ■ | ■ |
| FoI 6 | | | | | | | | ■ | ■ | ■ | ■ | ■ | ■ | ■ | | ■ | ■ | ■ | ■ | ■ | ■ | ■ | ■ | ■ |
| FoI 7 | | | | | | | | | ■ | ■ | ■ | ■ | ■ | ■ | | ■ | ■ | ■ | ■ | ■ | ■ | ■ | ■ | ■ |
| FoI 8 | | | | | | | | | | | | ■ | ■ | ■ | ■ | ■ | ■ | ■ | ■ | ■ | ■ | ■ | ■ | ■ |
| FoI 9 | | | | | | | | | | | | ■ | ■ | ■ | ■ | ■ | ■ | ■ | ■ | ■ | ■ | ■ | ■ | ■ |
| FoI 10 | | | | | | | | | | | | ■ | ■ | ■ | ■ | ■ | ■ | ■ | ■ | ■ | ■ | ■ | ■ | ■ |
| FoI 11 | | | | | | | | | | | | | ■ | ■ | ■ | ■ | ■ | ■ | ■ | ■ | ■ | ■ | ■ | ■ |
| FoI 12 | | | | | | | | | | | | | | ■ | ■ | ■ | ■ | ■ | ■ | ■ | ■ | ■ | ■ | ■ |
| FoI 13 | | | | | | | | | | | | | | | ■ | ■ | ■ | ■ | ■ | ■ | ■ | ■ | ■ | ■ |
| FoI 14 | | | | | | | | | | | | | | | | ■ | ■ | ■ | ■ | ■ | ■ | ■ | ■ | ■ |
| FoI 15 | | | | | | | | | | | | | | | | | ■ | ■ | ■ | ■ | ■ | ■ | ■ | ■ |
| FoI 16 | | | | | | | | | | | | | | | | | | ■ | ■ | ■ | ■ | ■ | ■ | ■ |
| FoI 17 | | | | | | | | | | | | | | | | | | | ■ | ■ | ■ | ■ | ■ | ■ |
| FoI 18 | | | | | | | | | | | | | | | | | | | | ■ | ■ | ■ | ■ | ■ |
| FoI 19 | | | | | | | | | | | | | | | | | | | | | ■ | ■ | ■ | ■ |
| FoI 20 | | | | | | | | | | | | | | | | | | | | | | ■ | ■ | ■ |
| FoI 21 | | | | | | | | | | | | | | | | | | | | | | | ■ | ■ |
| FoI 22 | | | | | | | | | | | | | | | | | | | | | | | | ■ |
| FoI 23 | | | | | | | | | | | | | | | | | | | | | | | | |
| FoI 24 | | | | | | | | | | | | | | | | | | | | | | | | |

Table F.1: Compatibility Matrix for FoIs with beige illustrating compatibility.

G Illustration of Derivation of Hand Concepts

In this chapter, it is shown, how the high number of HCs result from the comparably low number of defined FoIs. Therefore, first, it is demonstrated that the identification of FoI combinations alone lead to a large number of resulting HCs. Second, it is demonstrated how the application of the expansion rules finally lead to the high number of HCs.

In a first step, thus, possible FoI combinations are derived from the compatibility matrix. For example, using the FoI-C₁, a total of only seven FoIs ($f_1 - f_7$) are relevant. However, considering the compatibility matrix, given in Table F.1, 53 possible combinations of FoIs can be identified for FoIs in FoI-C₁. The identified FoI-combinations are summarized in Table G.1. The illustration of FoI combinations in Figure G.1 visualizes how the combinations are

| 1 FoI | 2 FoIs | 3 FoIs | 4 FoIs |
|-------|--------------|---------------------|----------------------------|
| FoI 2 | FoI 2, FoI 5 | FoI 2, FoI 5, FoI 6 | FoI 2, FoI 5, FoI 6, FoI 1 |
| FoI 5 | FoI 2, FoI 4 | FoI 2, FoI 5, FoI 7 | FoI 2, FoI 5, FoI 7, FoI 1 |
| FoI 4 | FoI 2, FoI 6 | FoI 2, FoI 5, FoI 1 | FoI 2, FoI 4, FoI 6, FoI 1 |
| FoI 3 | FoI 2, FoI 7 | FoI 2, FoI 4, FoI 6 | FoI 2, FoI 4, FoI 7, FoI 1 |
| FoI 6 | FoI 2, FoI 1 | FoI 2, FoI 4, FoI 7 | FoI 5, FoI 3, FoI 6, FoI 1 |
| FoI 7 | FoI 5, FoI 3 | FoI 2, FoI 4, FoI 1 | FoI 5, FoI 3, FoI 7, FoI 1 |
| FoI 1 | FoI 5, FoI 6 | FoI 2, FoI 6, FoI 1 | FoI 4, FoI 3, FoI 6, FoI 1 |
| | FoI 5, FoI 7 | FoI 2, FoI 7, FoI 1 | FoI 4, FoI 3, FoI 7, FoI 1 |
| | FoI 5, FoI 1 | FoI 5, FoI 3, FoI 6 | |
| | FoI 4, FoI 3 | FoI 5, FoI 3, FoI 7 | |
| | FoI 4, FoI 6 | FoI 5, FoI 3, FoI 1 | |
| | FoI 4, FoI 7 | FoI 5, FoI 6, FoI 1 | |
| | FoI 4, FoI 1 | FoI 5, FoI 7, FoI 1 | |
| | FoI 3, FoI 6 | FoI 4, FoI 3, FoI 6 | |
| | FoI 3, FoI 7 | FoI 4, FoI 3, FoI 7 | |
| | FoI 3, FoI 1 | FoI 4, FoI 3, FoI 1 | |
| | FoI 6, FoI 1 | FoI 4, FoI 6, FoI 1 | |
| | FoI 7, FoI 1 | FoI 4, FoI 7, FoI 1 | |
| | | FoI 3, FoI 6, FoI 1 | |
| | | FoI 3, FoI 7, FoI 1 | |

Table G.1: 53 valid FoI combinations for FoI-C₁ grouped by size (1-4 FoIs)

derived. Illustrated is the IMDC on the lower bottom, combined with five FoIs on the layer

above. Assuming all of these five FoIs are compatible with one another, combinations of the IMDC with two FoIs are identified on the second layer from the bottom. Within the illustration, only combinations of up to two FoIs are given. A single example for combinations of three FoIs is given, to depict the increasingly confusing illustration. In a second step, the identified

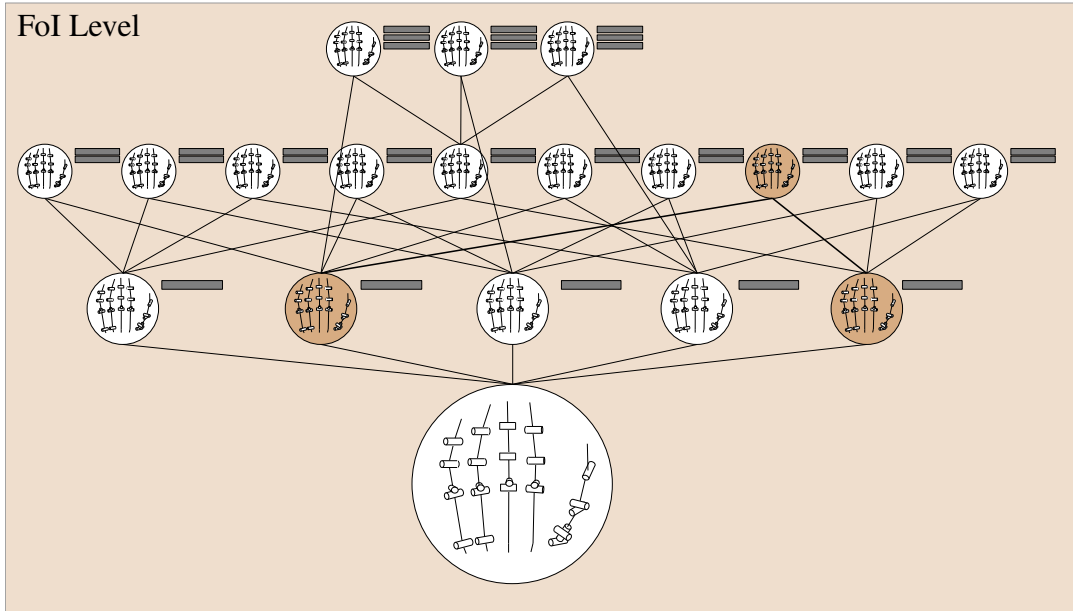


Figure G.1: Illustration of FoI combinations for five FoIs with up to two combined FoIs.

set of possible FoI combinations can be expanded according to the rules. For better explanation, the process of expansion is illustrated and implemented on two example FoIs f_2 and f_8 from across FoI-Cs. The FoI combinations using these two FoIs is illustrated in Figure G.2.

For each FoI combination, a PS-expansion can be applied. The PS-expansion is illustrated in

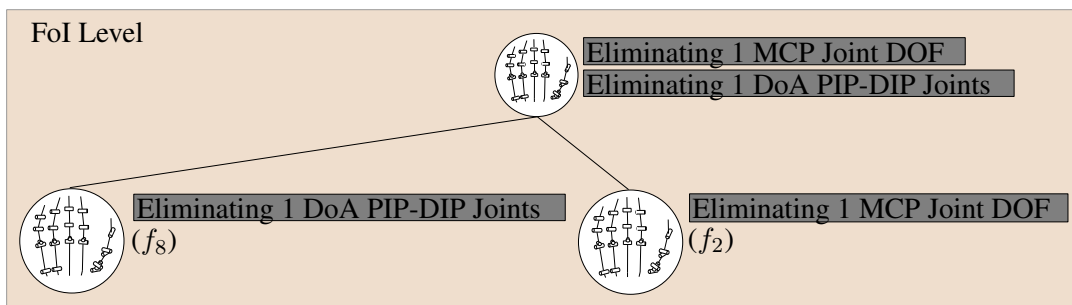


Figure G.2: Illustration of IMDC combination with FoI₂ and FoI₈.

Figure G.3. For the given FoIs, one and three PSs are available, respectively. Thus, the three initially defined FoI combinations lead to seven PS combinations with the IMDC. At this point, no HCs are defined, as no GFPSs are considered yet: it is not clear to what group the PSs are applied.

Therefore, a G-expansion is applied to the FoI combinations, as illustrated in Figure G.4. In the

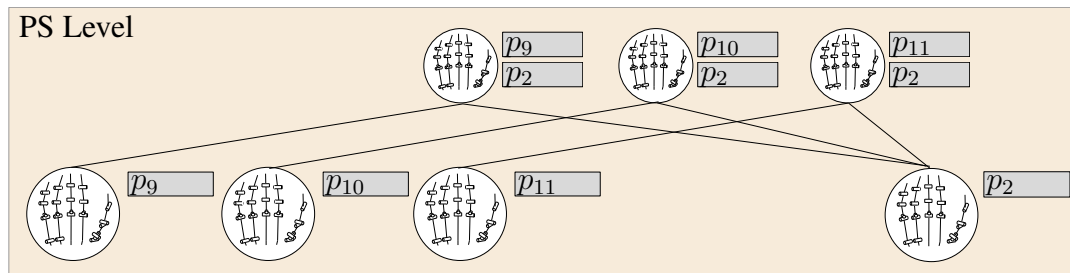
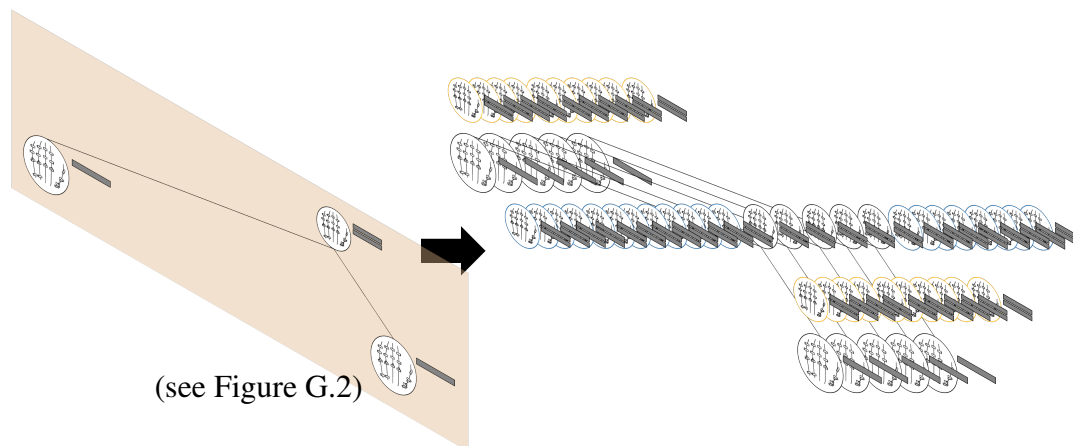


Figure G.3: Illustration of IMDC combination with PSs from FoI₂ and FoI₈.

given example, FoIs f_2 and f_8 can both be applied to the groups Index Finger, Middle Finger, Ring Finger, Little Finger, and Thumb. As a result, the single FoI layer results in five layers with the corresponding GFoIs (black circles on the right side in Figure G.4). Furthermore, where IMDCs are represented with two applied FoIs, more options arise: Firstly, GFoI combinations with the two FoIs applied to different groups arise (blue circles on the right side in Figure G.4), resulting in 15 further options. Secondly, GFoI combinations with one of the two FoI applied multiple times with association to different groups arise (yellow circles on the right side in Figure G.4). This results in an additional five-over-two (= 10) options on each side. As a result, starting from initial three defined FoI combinations, a total of $15 + 15 + 20 = 50$ GFoI combinations can be identified.

Finally, applying both the G-expansion and the PS-expansion to the FoI combinations, the



(see Figure G.2)

Figure G.4: Illustration of G-expansion from a given FoI combinations to a GFoI combination with FoI₂ and FoI₆.

resulting HCs can be defined. The previously introduced PS-expansion can equally be applied to a GFoI. The concatenated expansion is illustrated in Figure G.5. For the given example, through the concatenation, the initially defined three FoI combinations lead to a total of 195 HCs, illustrated on the right hand side of the figure.

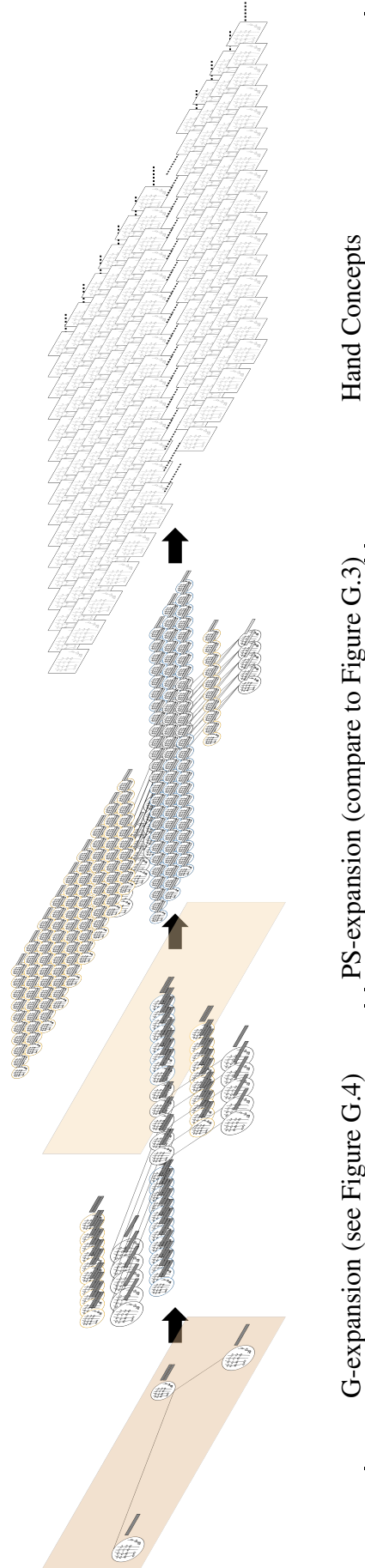


Figure G.5: Illustration of concatenated expansion from a given FoI combinations to a GFPS combination with FoI_2 and FoI_6 .

H Programming Implementation Details

In this chapter, the interested reader is provided with additional information on the implementation from a programming perspective. The programming of the user interfaces was carried out in collaboration with Tianyi Jin, who worked at the IGMR as a research assistant at the time. The programming of the publicly launched graphical user interface for the LoA was carried out in collaboration with Axel Sommer, who worked at the IGMR in the IT department.

H.1 Hand Concept Creation

In this chapter, the implementation of the Hand Concept creation from a programming perspective is explained. The overall process is given in the flowchart in Figure H.2. All algorithms are written in Python.

In a first step, the scope of the designated exploration is read in. It is distinguished between the *Exploration Step* and the *Exploration Categories*. Both data files are given in the ER model in Figure B.3 as part of the data base *Exploration*. In the current implementation, only a single Exploration Step is implemented, namely the conceptual design. However, the algorithm is equipped to perform an exploration with FoIs and PSs of other design phases, such as the detailed design, provided the FoIs and PSs are elaborated. The exploration categories are the FoI-Cs. Depending on the user's intention, Hand Concepts can be generated that consider only selected categories. The user may specify its intention about the scope in a tab of the guidance' GUI. This tab is illustrated in Figure I.4. The algorithm starts then with a loop (yellow), iterating through each FoI-C.

In a second step, the FoI-combinations are derived. Therefore, the established compatibility matrix (CCA) in Table F.1 is read in. Using the CCA, all possible FoI combinations are derived. The corresponding flowchart for the responsible function is given in Figure H.3.

In a third step, the G-expansion is performed. For each FoI combination, all possible GFoI combinations are created, leveraging the two previously introduced expansion rules. The corresponding flowchart for the responsible function is given in Figure H.4.

In a fourth step, the PS-expansion is performed. For each GFoI combination, all possible GFPS combinations are created, leveraging the two previously introduced rules. The corresponding flowchart for the responsible function is given in Figure H.5. The algorithm continues in a loop,

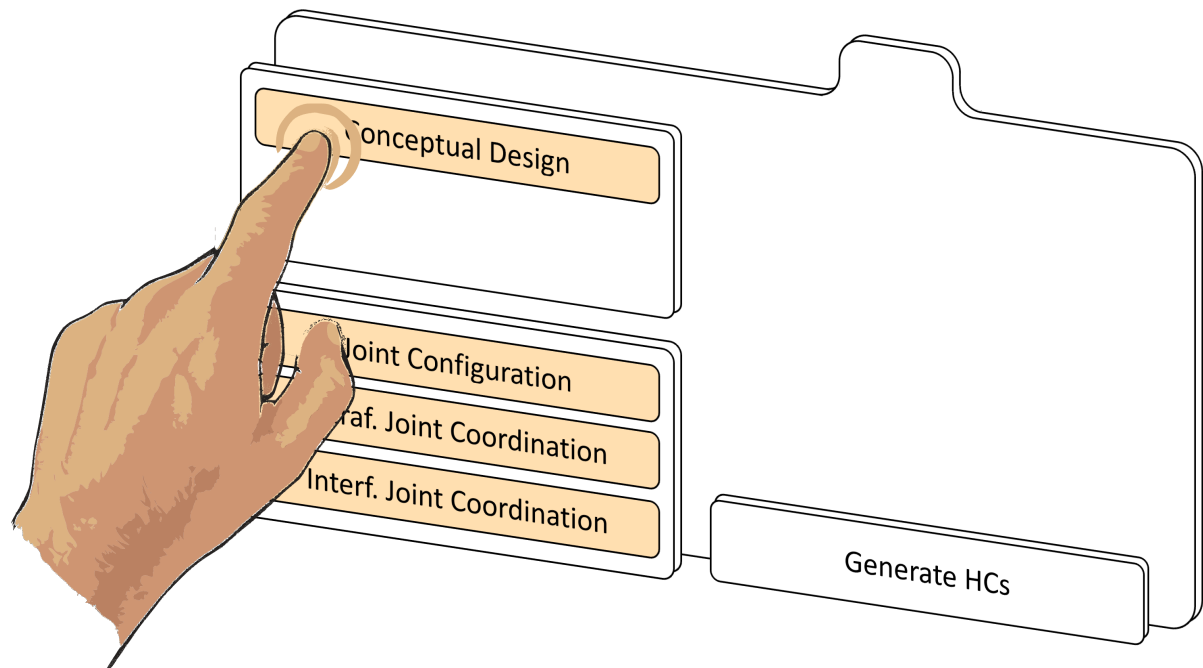


Figure H.1: Design of the guidance' tab for advanced settings.

covering iteratively every identified GFPS combination.

The GFPS combinations represent the established Hand Concepts. For the guidance' Explanation Component, described in Section 5.3, the Hand Concepts are visualized by combining the identified GFPSs with the IMDC.

H.2 Recommendation Generation

In this chapter, the identification of Hand Concept recommendations from a programming perspective is explained. The overall process is given in the flowchart in Figure H.7. Embedded functions are also presented in alone-standing flowcharts. In all flowcharts, individual steps are briefly given as steps. All algorithms are written in Python.

The algorithm starts with an initialization of the GUI to receive user input. The given input can only be processed, if the exploration (see Chapter 3 and Section H.1) is performed.

In a second step, the input is processed, as depicted in flowchart H.8. The set of grasps, identified by the user as performance requirements, and the preference towards either Motion Ability or Simplicity is captured.

In a third step, the recommendation is generated, as depicted in flowchart H.9. The Hand Concept score x is calculated for every GFPS-combination identified in the Exploration, as described in Section 5.2.4. Thereby, the value is sequentially identified for every GFPS-combination.

A vector m of three elements capture (and update) the three highest scores with reference to the responsible GFPS-combination. Finally, the three Hand Concepts to be recommended are captured, by referencing to the score x and the responsible GFPS-combination.

All associated data files are given in the ER model in Figure B.4. The specified personal keys (PK) and foreign keys (FK) shall allow the interested reader to understand how these data files are implemented from a programming perspective.

H.3 Hand Concept Illustration

In this chapter, the illustration of the Hand Concept recommendations is explained from a programming perspective. The explanation is divided into two parts, as the depiction is partly embedded in the previously described Exploration (see H.1) and the main program (see H.2).

First, the last step of the Exploration needs to be explained. In the explanation of the Exploration in Section H.1, the creation of GFPS-combinations is explained. It was left out that the GFPS-combinations are further used to create updated configuration files, as it is created for the IMDC (see Listing H.1).

For the generation of exploration related configuration files, the loop in flowchart H.2 is considered. Three data files must be explained in advance in order to understand the process. First, an excerpt from the implementation of the identified IMDC from Section 3.2 is given in Listing H.1. In that data file, each joint is defined by an ID (e.g. "J011"), name, and a number of parameters. The first parameters are solely for illustration reasons: a distinct algorithm uses the the dimensions and pose of the cylinder to plot the given configuration. The parameter "generate-cylinder" defines the existence of the particular joint. The remaining six variables define its coordination to the neighboring joint. Second, an excerpt from the effect data file is given in Listing H.2. In that data file, so called effects are defined, where each effect refers to certain joints with (updated) parameters. Third and last, an excerpt from the effect-GFPS data file is given in Listing H.3. In that data file, effects are assigned to GFPSs.

Then, for each GFPS-combination, a combination of effects is defined. The corresponding flowchart for the responsible function is given in Figure H.6. The algorithm outputs in "Exploration Result" the identified GFPS-combinations, updated by the effect-combinations, referring to the respective joints.

Second, the last step of the main program can be explained, using the configuration files. The last two steps of the main algorithm, presented in flowchart H.7, are considered.

The creation of recommended configuration files is depicted in flowchart H.10. In this algorithm,

depictions for the three identified recommendations are generated. For the three identified recommendations, the associated GFPS-combinations have been identified (see H.2). They are used to locate the associated effect-combination from the exploration result. In combination to the IMDC data file, updated configuration files are generated. In a last step, the updated recommendation configuration files are depicted by visualizing the specified joints with their given poses and dimensions. The illustration is presented to the user in respective pages in the GUI.

H.4 Data Files Programming Excerpts

Listing H.1: IMDC data file excerpt

```
1  {
2    "J011": {
3      "name": "little_finger_HMC_joint",
4      "height": 3,
5      "radius": 0.5,
6      "color": "blue",
7      "x": -12,
8      "y": 4,
9      "z": 29.39,
10     "alpha": 90.0,
11     "beta": 0.0,
12     "gamma": 0.0,
13     "generate_cylinder": true,
14     "tendon_coupling": false,
15     "linkage_coupling": false,
16     "linkage_underactuation": false,
17     "joint_elimination": false,
18     "inter_coupling": false,
19     "inter_underactuation": false
20   },
21   ...
22 }
```

Listing H.2: Extract from the Effect data file

```
1  {
2    "Effect001": {
3      "joint": {
```

```
4     "J021": {
5         "generate_cylinder": true} } },
6     ...
7 }
```

Listing H.3: Extract from the Effect-GFPS data file

```
1 {
2     "Effect001" : "GFPS032",
3     "Effect002" : "GFPS012",
4     ...
5 }
```

H.5 Flow Charts

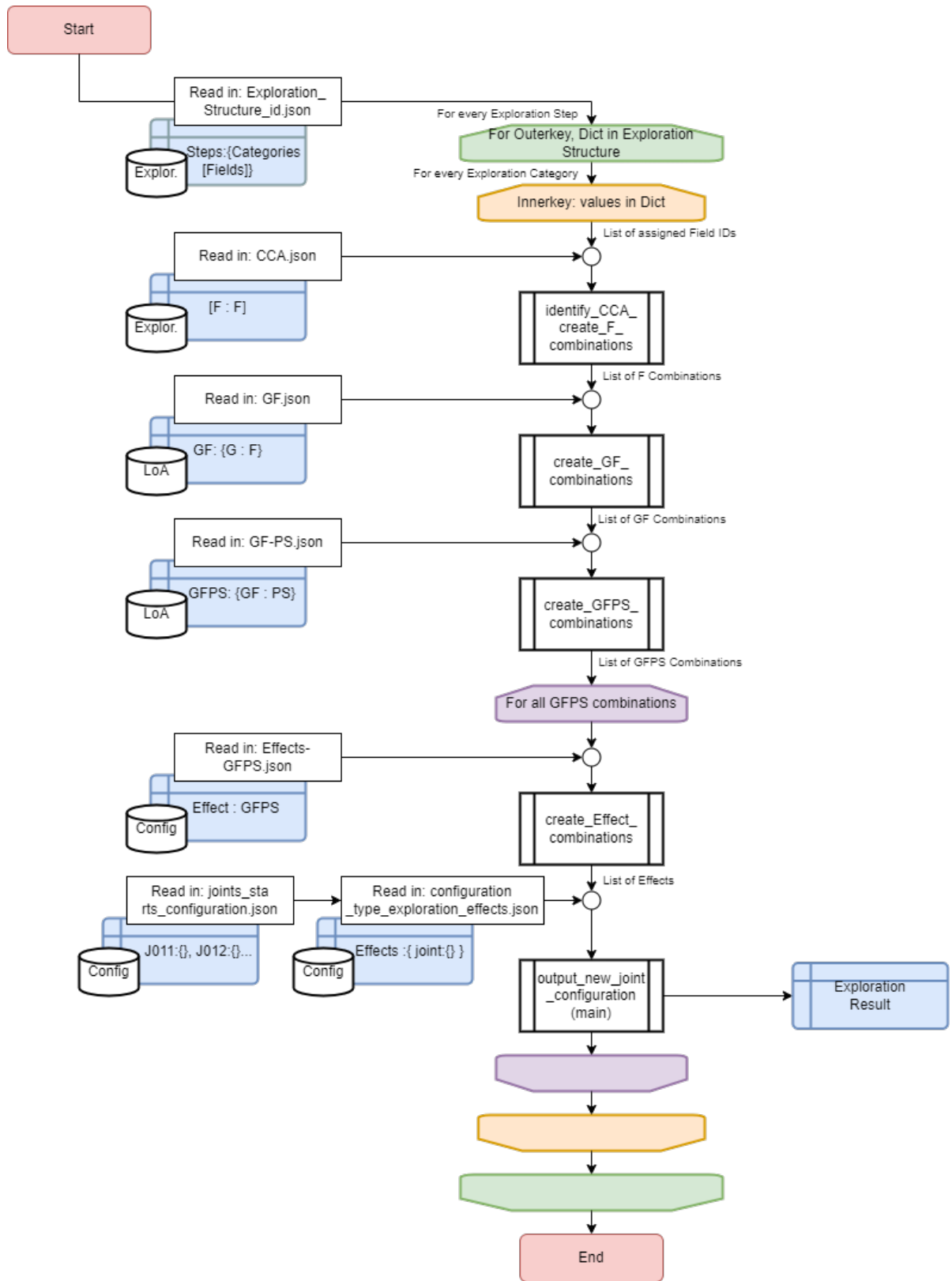


Figure H.2: Flowchart for Hand Concept creation.

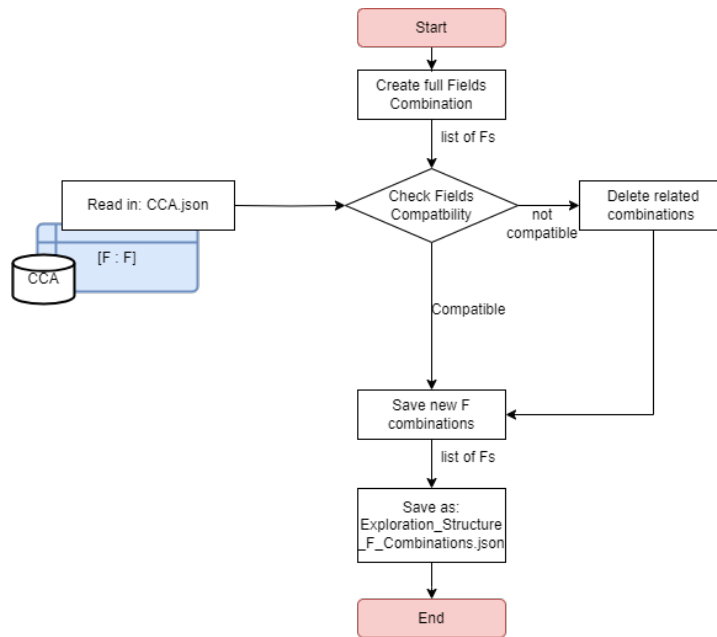


Figure H.3: Flowchart for FoI combinations creation.

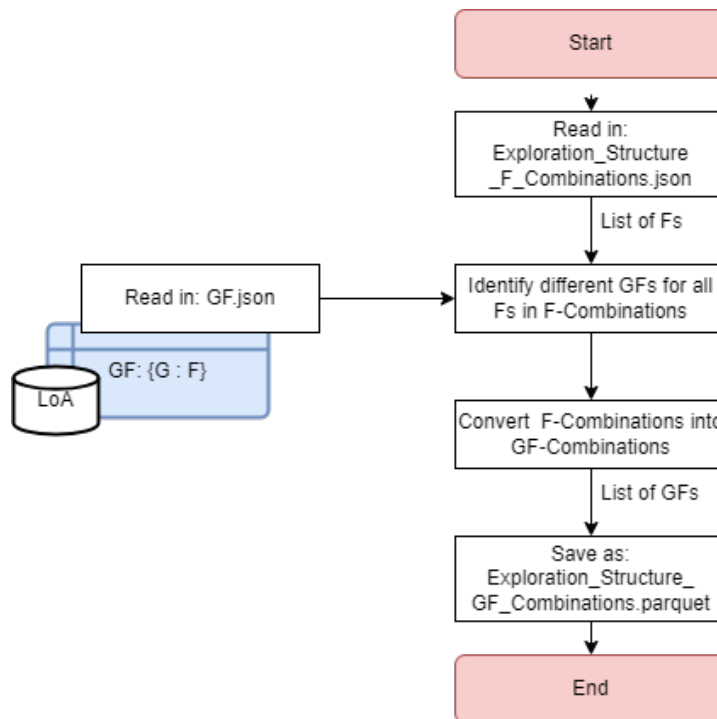


Figure H.4: Flowchart for GFoI combinations creation.

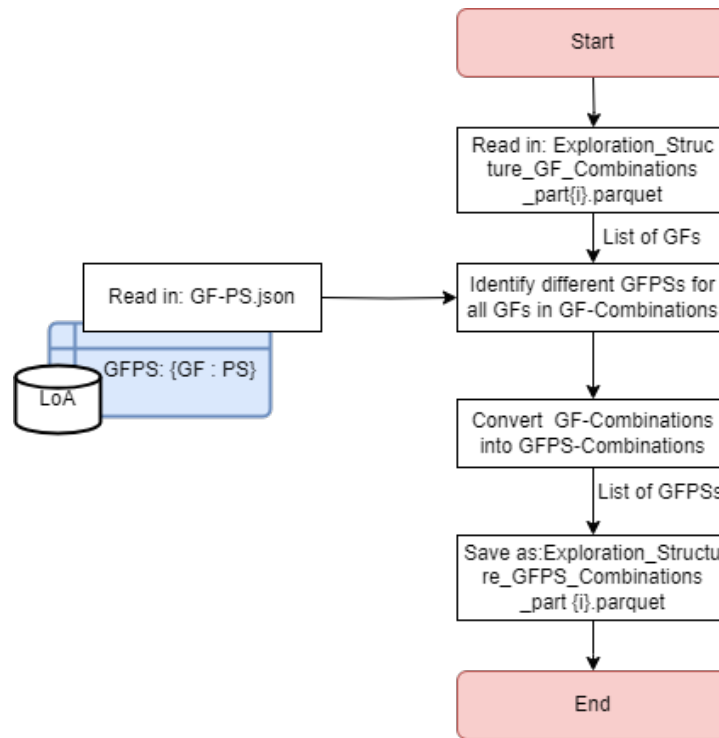


Figure H.5: Flowchart for GFPS combinations creation.

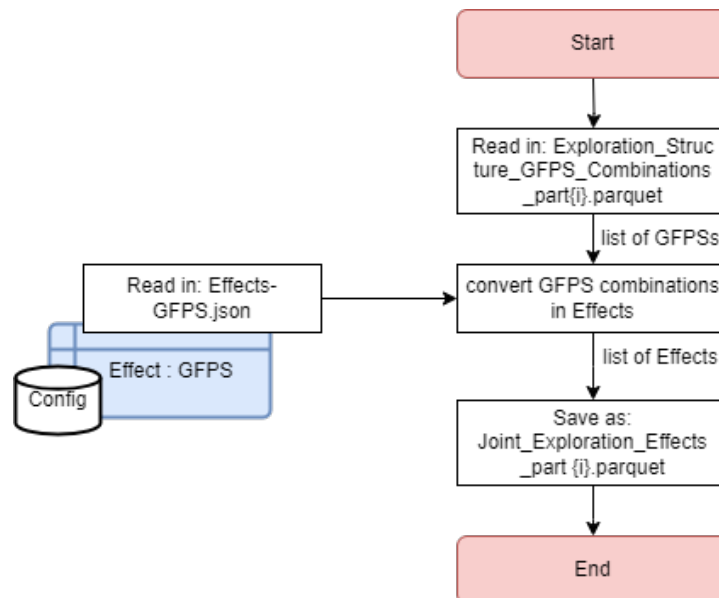


Figure H.6: Flowchart for Effect combinations creation.

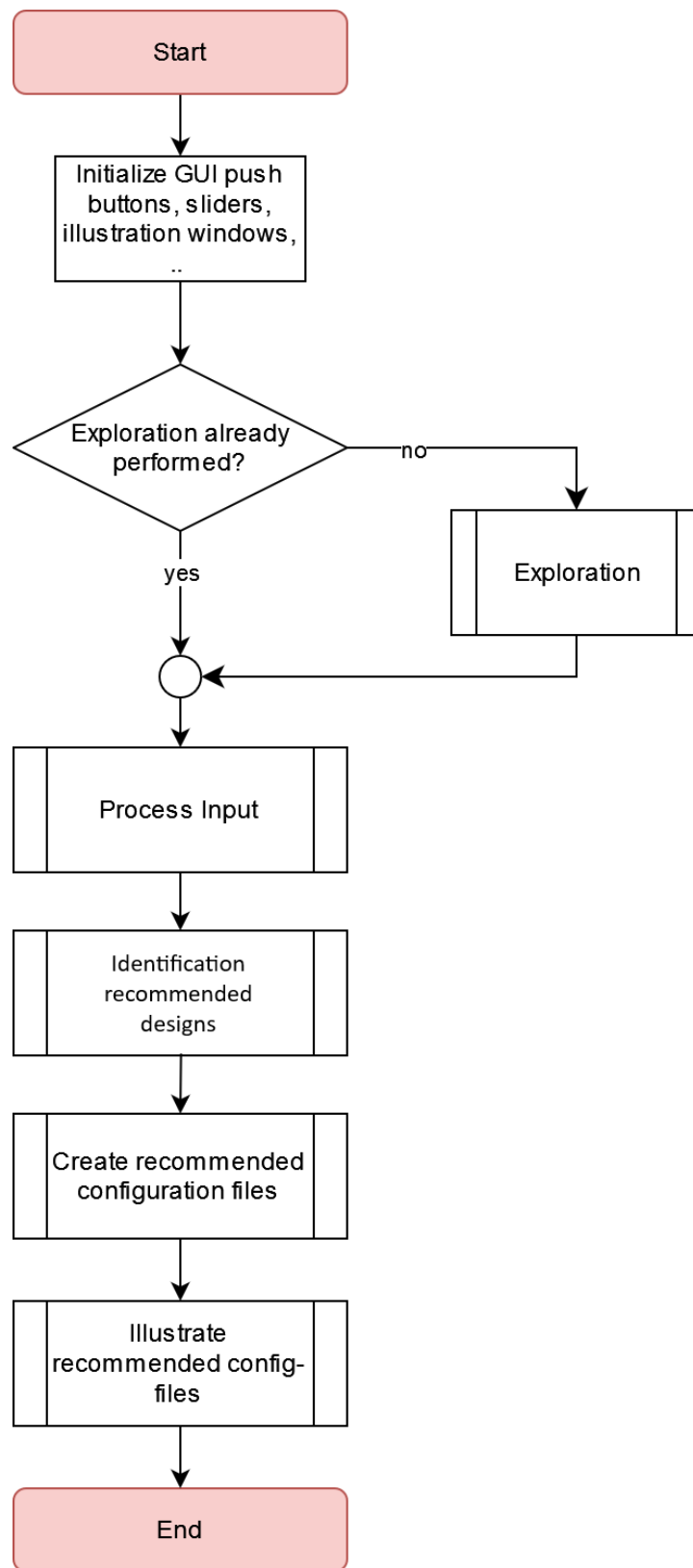


Figure H.7: Flowchart for main process.

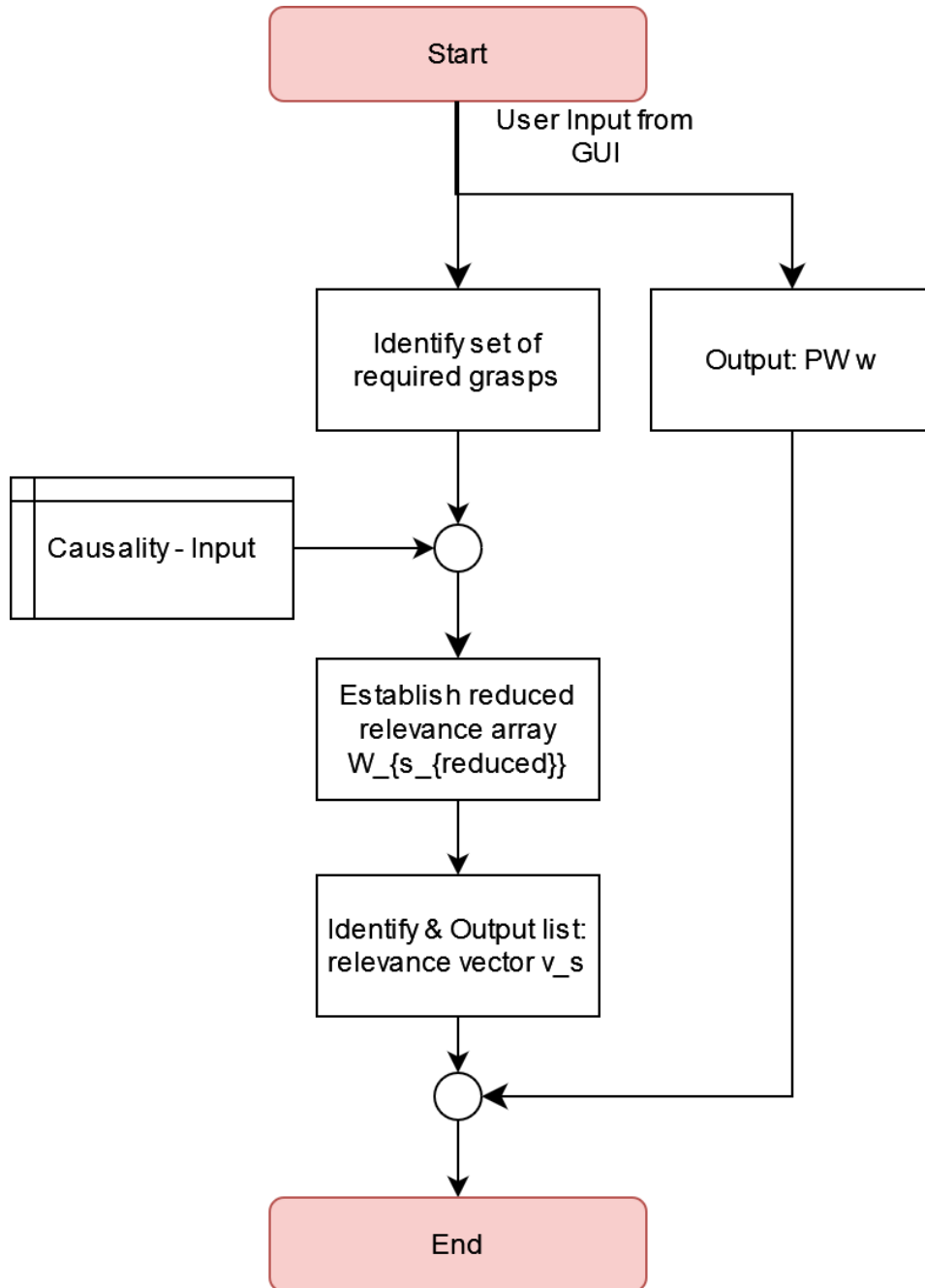


Figure H.8: Flowchart for input processing.

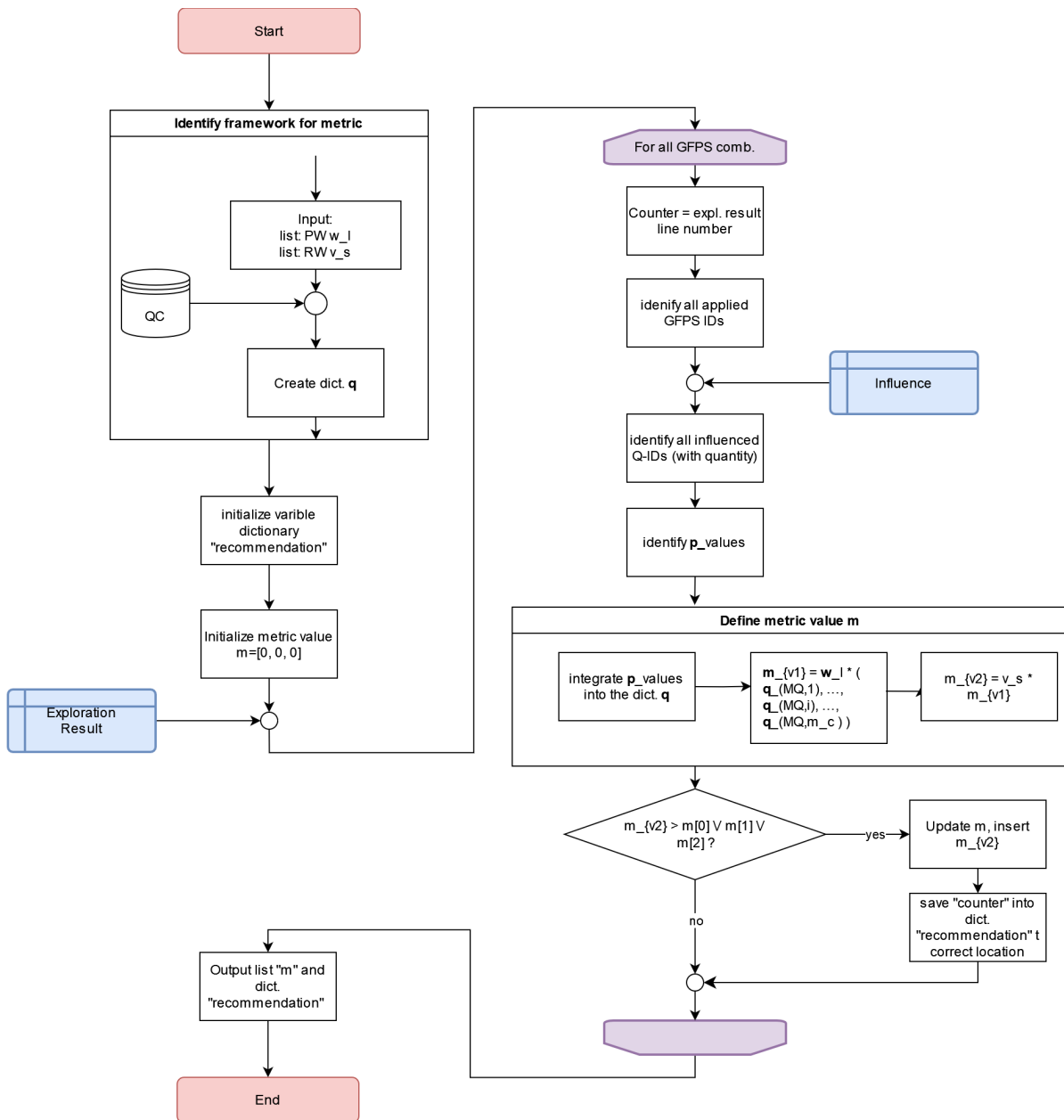


Figure H.9: Flowchart for identification of recommended Hand Concepts.

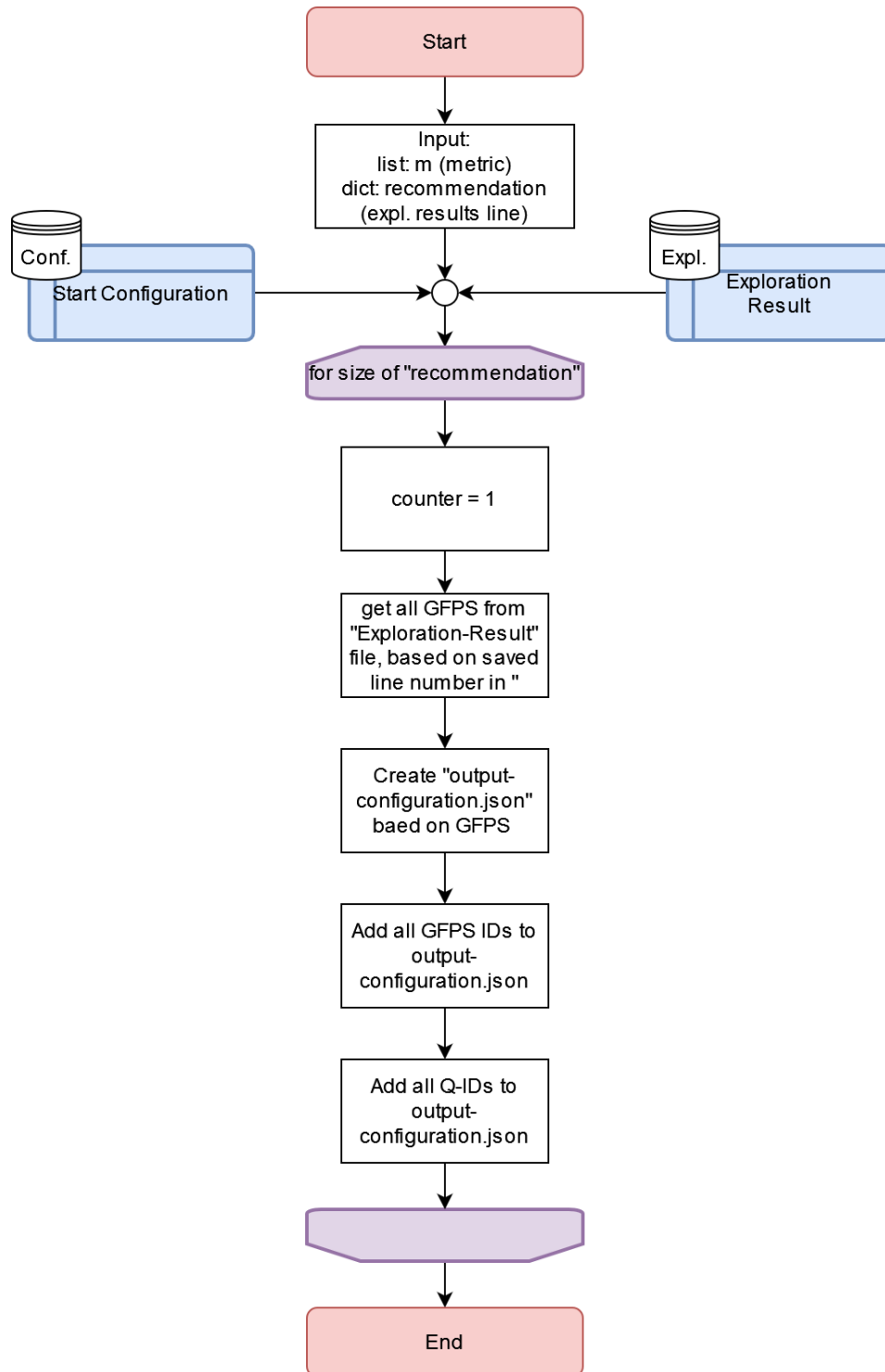


Figure H.10: Flowchart for creation of recommendation.

I Guidance GUI Design Illustrations

In this chapter, the interested reader is provided with screenshots of the actual interfaces of the graphical user interface for the guidance, developed in this dissertation.

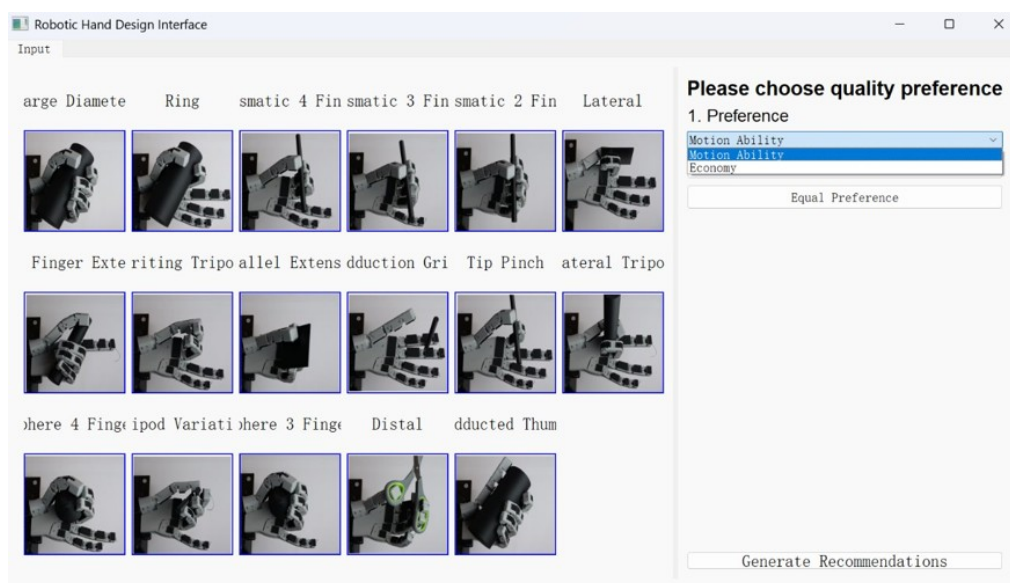


Figure I.1: Implementation of the guidance’s Dialog Component.

The screenshot shows a 'Library of Approaches DB Editor' window. At the top, there are search filters for Field, Group, Principle Solution, Reference, Author, and Robot Hand. Below the filters are buttons for 'Add field', 'Add group', 'Add P/S', 'Add reference', 'Add author', and 'Add robot'. The main area is a table with the following columns: ID, Field, Group, Principle Solution, Reference, Comment, Robot, and Author(s). The table contains 48 rows of data, including entries like '4) Pshiere Design', '1) Finger Structure', '2) Phalnx Length', etc.

| ID | Field | Group | Principle Solution | Reference | Comment | Robot | Author(s) |
|----|---|-----------------|--|--|---|----------------------|-----------------------|
| 0 | 4) Pshiere Design | 1) Finger_Index | 150) Eoskeleton | 5) https://doi.org/10.1109/BIOCIB.2016.7927387 | Hollow Cylinder | 5) Etho Hand | 5) Konami, C. |
| 1 | 1) Finger Structure | 1) Finger_Index | 1) rigid-sequential | 3) https://doi.org/10.1109/ICORR.2019.09113 | | 3) Robust Hand | 3) Lovish, C.V. |
| 2 | 1) Finger Structure | 1) Finger_Index | 1) rigid-sequential | 4) https://doi.org/10.1007/978-3-319-03993-2 | | 4) Awika Hand | 4) Grebenster, M. |
| 3 | 1) Finger Structure | 1) Finger_Index | 1) rigid-sequential | 5) https://doi.org/10.1109/BIOCIB.2016.7927387 | | 5) Etho Hand | 5) Konami, C. |
| 4 | 1) Finger Structure | 1) Finger_Index | 2) flexible | 40) https://doi.org/10.1109/ICORR.2007.4423542 | | 34) SCMA Hand | 43) Duller, Aaron M. |
| 5 | 1) Finger Structure | 1) Finger_Index | 2) flexible | 48) https://doi.org/10.1109/MRA.2012.225471 | | 38) UB Hand IV | 47) Melchior, Claudio |
| 6 | 1) Finger Structure | 1) Finger_Index | 2) flexible | 49) https://doi.org/10.1109/IECON.1994.397385 | | 39) UB Hand I | 48) Eweli, A. |
| 7 | 2) Phalnx Length | 1) Finger_Index | 142) Anisopomorphc | 4) https://doi.org/10.1007/978-3-319-03993-2 | between 5.77 and 10.37 of pully diameter | 4) Awika Hand | 4) Grebenster, M. |
| 8 | 3) Finger Size | 1) Finger_Index | 143) Anisopomorphc | 4) https://doi.org/10.1007/978-3-319-03993-2 | within 25th and 75th percentile of human size | 4) Awika Hand | 4) Grebenster, M. |
| 9 | 3) Finger Size | 1) Finger_Index | 143) Anisopomorphc | 5) https://doi.org/10.1109/BIOCIB.2016.7927387 | average dimension of a male person | 5) Etho Hand | 5) Konami, C. |
| 12 | 6) Flexing | 1) Finger_Index | 1) torsional spring | 6) https://doi.org/10.1109/MCH.2011.5906025 | used for extending MCP and IP joints | 6) Cub Hand | 6) Schmitz, A. |
| 13 | 7) IP Joint Structural Design (1 DOF) | 1) Finger_Index | 84) 1 axis | 4) https://doi.org/10.1007/978-3-319-03993-2 | | 4) Awika Hand | 4) Grebenster, M. |
| 14 | 7) IP Joint Structural Design (1 DOF) | 1) Finger_Index | 84) 1 axis | 7) https://doi.org/10.1109/TRO.2018.2830407 | | 7) P54/IT SoftHand 2 | 7) Sentina, C. |
| 15 | 7) IP Joint Structural Design (1 DOF) | 1) Finger_Index | 84) 1 axis | 8) https://doi.org/10.1109/MCH.2011.2168001 | | 8) ACT Hand | 8) Delpandre, A. D. |
| 16 | 8) DP Mechanical Joint Design | 1) Finger_Index | 164) Passive Hyperextension | 9) https://arxiv.org/pdf/1805.04290 | Sliding Chute | 9) Catch-919 Hand | 9) Zhang, Z. |
| 17 | 8) Passive Joint Extension | 1) Finger_Index | 13) Interchangeable Spring System | 7) https://doi.org/10.1109/TRO.2018.2830407 | Reduction of Joint Impedance | 7) P54/IT SoftHand 2 | 7) Sentina, C. |
| 18 | 10) MCP Joint Structural Design (1 DOF) | 1) Finger_Index | 84) 1 axis | 9) https://arxiv.org/pdf/1805.04290 | pruned linkage | 9) Catch-919 Hand | 9) Zhang, Z. |
| 19 | 10) MCP Joint Structural Design (1 DOF) | 1) Finger_Index | 84) 1 axis | 44) https://doi.org/10.1109/ICORR.2007.4423542 | | 34) SCMA Hand | 43) Duller, Aaron M. |
| 21 | 12) MCP Joint Structural Design (2 DOF) | 1) Finger_Index | 19) 2 axis orthogonal and non-intersecting - Adducto | 4) https://doi.org/10.1007/978-3-319-03993-2 | | 4) Awika Hand | 4) Grebenster, M. |
| 22 | 12) MCP Joint Structural Design (2 DOF) | 1) Finger_Index | 20) 2 axis orthogonal and non-intersecting - Abduction-Add | 2) https://doi.org/10.1109/MCH.2011.5906025 | | 2) Etho Hand | 2) Estefania, J. |
| 46 | 12) MCP Joint Structural Design (2 DOF) | 1) Finger_Index | 21) 2 axis not orthogonal and non-intersecting - Adduct | 8) https://doi.org/10.1109/TMCH.2011.2168001 | | 8) ACT Hand | 8) Delpandre, A. D. |
| 47 | 13) Bimimicng 1-Dof PIP-DIP Joints | 1) Finger_Index | 22) linkage coupling of two joints | 1) https://arxiv.org/pdf/1805.04290 | 4-bar linkage | 1) Gifu Hand II | 1) Mizui, T. |
| 48 | 13) Bimimicng 1-Dof PIP-DIP Joints | 1) Finger_Index | 22) linkage coupling of two joints | 13) https://doi.org/10.1109/ICRA.2012.622772 | 4-bar linkage | 13) Robust Hand 2 | 13) Birkawater, I. B. |

Figure I.2: Implementation of the guidance’s Knowledge Acquisition Component.

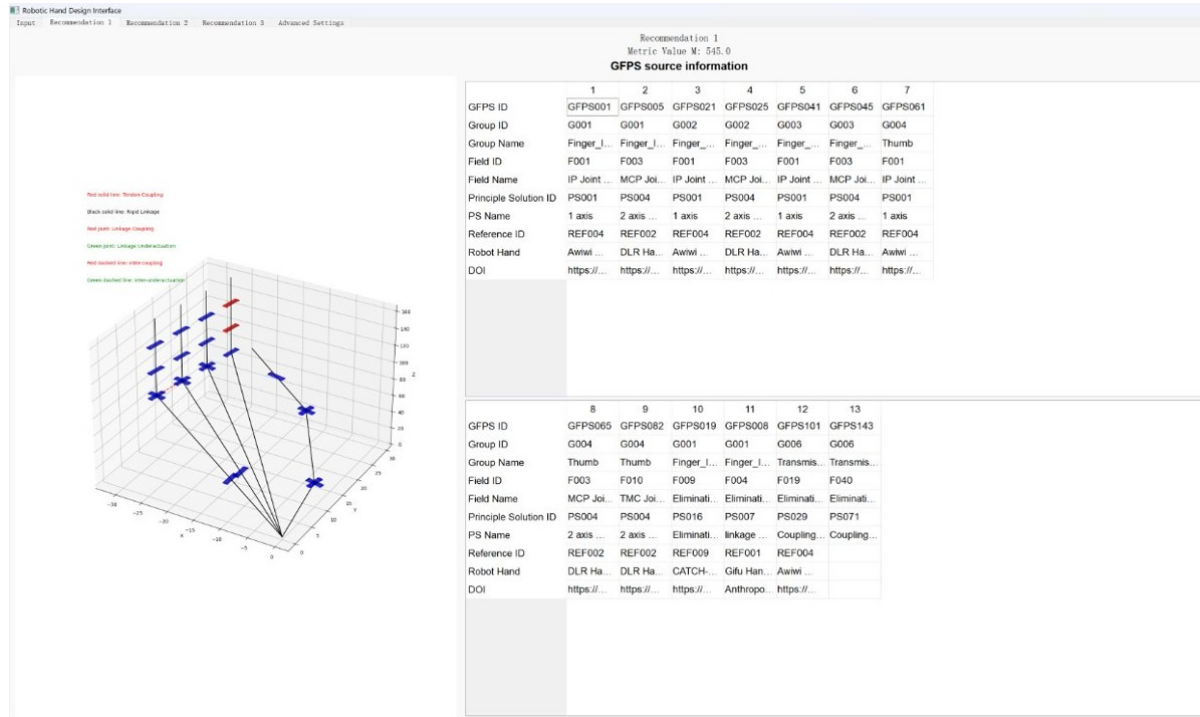


Figure I.3: Implementation of the guidance's Explanation Component.

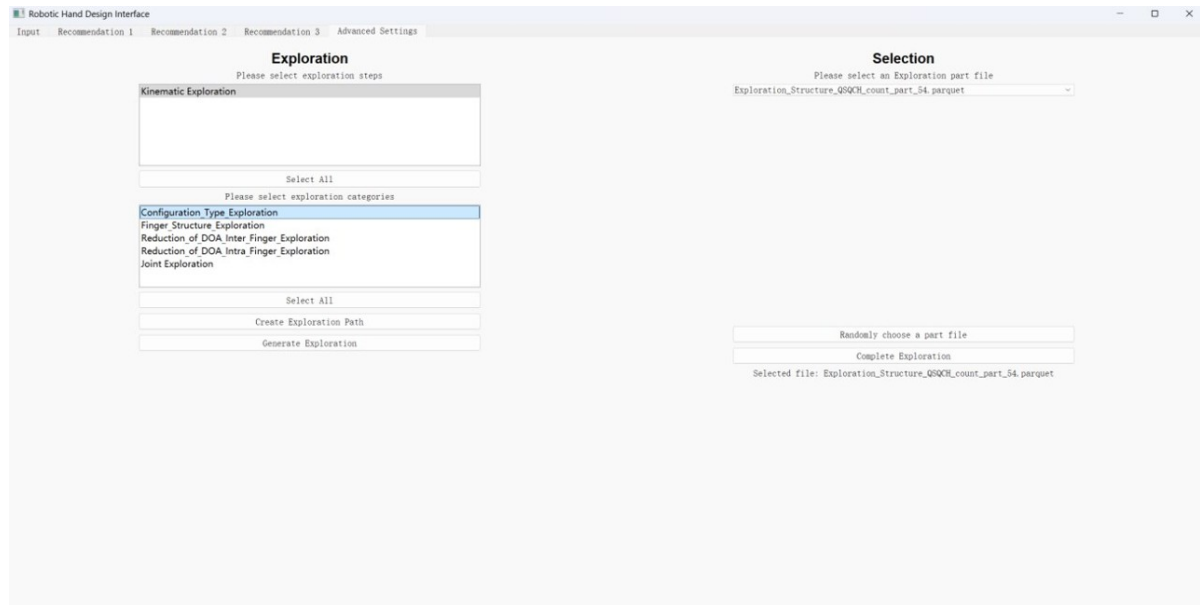


Figure I.4: Implementation of the guidance's advanced settings tab.

J Influence Value Derivation

This chapter demonstrates the derivation of the Major Quality and Superior Quality aggregate values for the FoI-C₂. This derivation was repeated after derivation for the FoI-C₁ to demonstrate the general applicability of the approach. It is shown that, first, the method can be applied in the same way to other FoI categories, and second, that selections within different FoI categories do not interfere with one another.

Major Quality Aggregate Values

Figure J.1 shows the corresponding discretization for the FoI category Intrafinger Joint Coordination. The same procedure is applied with the applied variables adjusted to the FoI-C₂ (e.g., $p_{MQ}^{FoI-C_2}$). However, the starting value for the Major Quality Motion Ability is now, in general, a value that results from a previous selection made in another FoI category for the Hand Concept under consideration ($p_{S_1} - bp_{MQ}^{FoI-C_1}$). Analogous to (5.21) and (5.22), setting up the relationship for the suitable FoIs on the left side yields the following inequality for the weighting on the Motion Ability side:

$$\begin{aligned}
 3 \cdot (p_{S_1} - bp_{MQ}^{FoI-C_1}) + 1 \cdot bp_{MQ}^{FoI-C_1} &> 3 \cdot ((p_{S_1} - bp_{MQ}^{FoI-C_1}) - cp_{MQ}^{FoI-C_2}) + 1 \cdot (bp_{MQ}^{FoI-C_1} + cp_{MQ}^{FoI-C_2}) \\
 3p_{S_1} - 2bp_{MQ}^{FoI-C_1} &> 3p_{S_1} - 2bp_{MQ}^{FoI-C_1} - 2cp_{MQ}^{FoI-C_2} \\
 0 &> -2cp_{MQ}^{FoI-C_2}
 \end{aligned} \tag{J.1}$$

and the inequality for the weighting on the Simplicity side:

$$\begin{aligned}
 3 \cdot (bp_{MQ}^{FoI-C_1} + cp_{MQ}^{FoI-C_2}) + 1 \cdot ((p_{S_1} - bp_{MQ}^{FoI-C_1}) - cp_{MQ}^{FoI-C_2}) &> 3 \cdot bp_{MQ}^{FoI-C_1} + (p_{S_1} - bp_{MQ}^{FoI-C_1}) \\
 3bp_{MQ}^{FoI-C_1} + 3cp_{MQ}^{FoI-C_2} + p_{S_1} - bp_{MQ}^{FoI-C_1} - cp_{MQ}^{FoI-C_2} &> 2bp_{MQ}^{FoI-C_1} + p_{S_1} \\
 2bp_{MQ}^{FoI-C_1} + 2cp_{MQ}^{FoI-C_2} + p_{S_1} &> 2bp_{MQ}^{FoI-C_1} + p_{S_1} \\
 2cp_{MQ}^{FoI-C_2} &> 0
 \end{aligned} \tag{J.2}$$

The variable $c \in \mathbb{Z}$, $c > 0$ represents an arbitrary number of suitable FoIs. The inequalities show that the previously chosen joint configuration (i.e., the initial value appearing here) has no influence and cancels out. To satisfy the conditions, it is sufficient that $p_{MQ}^{FoI-C_2} > 0$ holds

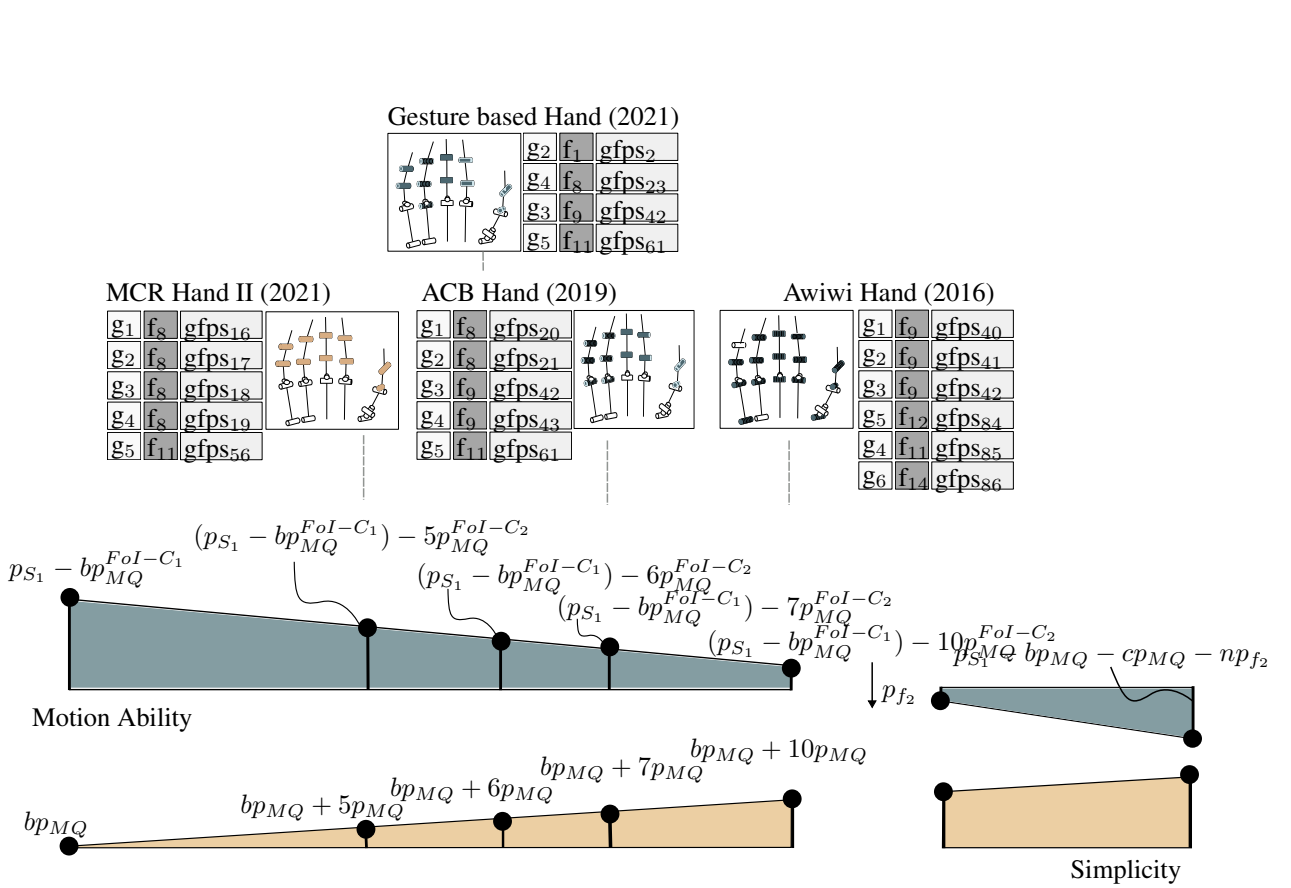


Figure J.1: Discretized Trade-Off Illustration of Hand Concepts (FoI-C Intrafinger Joint Coordination)

for any value of c .

The derivation of the required amount p_{f_2} by which $p_{MQ}^{FoI-C_2}$ is reduced after inversion through the Relevance Weight in case of an unsuitable FoI leads to the same conditions as in the previous approach. Again, hypothetical Hand Concepts are defined. For a Hand Concept with c suitable FoIs, the Motion Ability score component is $(p_{S_1} - bp_{MQ}^{FoI-C_1}) - cp_{MQ}^{FoI-C_2}$ and the Simplicity score component is $bp_{MQ}^{FoI-C_1} + cp_{MQ}^{FoI-C_2}$. For a Hand Concept with n unsuitable FoIs in addition to the c suitable ones, the Motion Ability score component becomes $p_{S_1} - bp_{MQ}^{FoI-C_1} - cp_{MQ}^{FoI-C_2} - np_{f_2}$ and the Simplicity score component is $bp_{MQ}^{FoI-C_1} + (c + n)p_{MQ}^{FoI-C_2}$.

To ensure that the system always selects the concept containing only suitable FoIs, the following condition must hold:

$$\begin{aligned}
 & 3 \cdot (bp_{MQ}^{FoI-C_1} + cp_{MQ}^{FoI-C_2}) + 1 \cdot (p_{S_1} - bp_{MQ}^{FoI-C_1} - cp_{MQ}^{FoI-C_2}) \\
 & > 3 \cdot (bp_{MQ}^{FoI-C_1} + cp_{MQ}^{FoI-C_2} + np_{MQ}^{FoI-C_2}) \\
 & \quad + 1 \cdot (p_{S_1} - bp_{MQ}^{FoI-C_1} - cp_{MQ}^{FoI-C_2} - np_{f_2}) \\
 \Rightarrow & \quad p_{f_2} > 3p_{MQ}^{FoI-C_2} \tag{J.3}
 \end{aligned}$$

Once again, it becomes evident that the number of suitable FoIs c and the number of unsuitable FoIs n are irrelevant.

Superior Quality Aggregate Values

According to the derivation in Section 5.2.2.2, the Superior Qualities Movement Independence, Manipulability, and Contact Conditions are addressed. Among these, Movement Independence is the input-dependent Superior Quality, and the influence on Contact Conditions is positive. Mathematically, this leads to the definition of two equations that capture the respective conditions:

$$p_{M.I.} - p_M + p_{C.C.} = -p_{MQ} \tag{J.4}$$

$$(-1) \cdot p_{M.I.} - p_M + p_{C.C.} = -4p_{MQ} \tag{J.5}$$

Rearranging Equation (J.5) yields:

$$p_M = 4p_{MQ} + p_{C.C.} - p_{M.I.} \tag{J.6}$$

Substituting this into Equation (J.4) gives:

$$\begin{aligned}
 p_{M.I.} - (4p_{MQ} + p_{C.C.} - p_{M.I.}) + p_{C.C.} &= -p_{MQ} \\
 \dots \\
 p_{M.I.} &= \frac{3}{2}p_{MQ}
 \end{aligned} \tag{J.7}$$

which defines the required aggregate value of the M.I.

Substituting this into Equation (J.4) yields:

$$\begin{aligned}
 \frac{3}{2}p_{MQ} - p_{M.} + p_{C.C.} &= -p_{MQ} \\
 -p_{M.} + p_{C.C.} &= -\frac{5}{2}p_{MQ}
 \end{aligned} \tag{J.8}$$

which establishes a relationship between the influences on Qualities in the Superior Qualities M. and Contact Conditions

There are, therefore, infinitely many possible values for the influence upper bounds on Contact Conditions and M. However, this range of values can be exploited in terms of qualitative interpretation. For example, $p_{C.C.}$ should be positive, as the influence of underactuation on the contact conditions is considered beneficial. Consequently, $p_{M.} > 2.5p_{MQ}$ must hold, and this value is rounded up to the next integer. This yields the following values for the Superior Quality aggregate values:

$$p_{M.} = 3p_{MQ} \quad p_{C.C.} = 0.5p_{MQ}. \tag{J.9}$$

K Quality Criteria and Quality Profile Illustrations

In this chapter, illustrations from the main body are presented in full size. Some illustration of Quality Criteria and Quality Profiles are given in the main body in small for depiction of the addressed qualities and "first glance" comparisons between different Quality Profiles. These illustrations are given bigger here for the sake of readability.

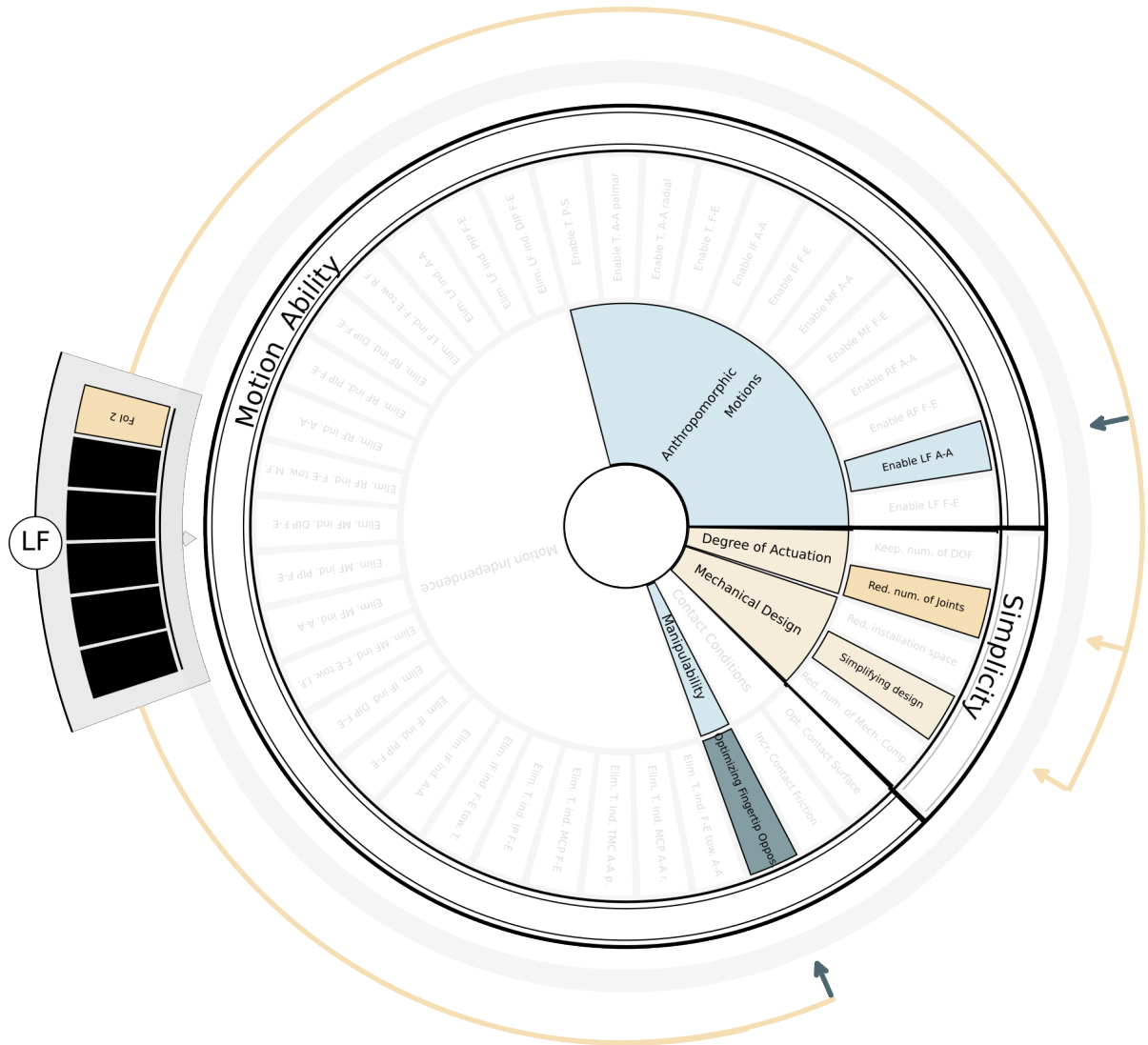


Figure K.3: Quality Profile illustration of gfp_{s8} (enlarged version of Figure 6.1).

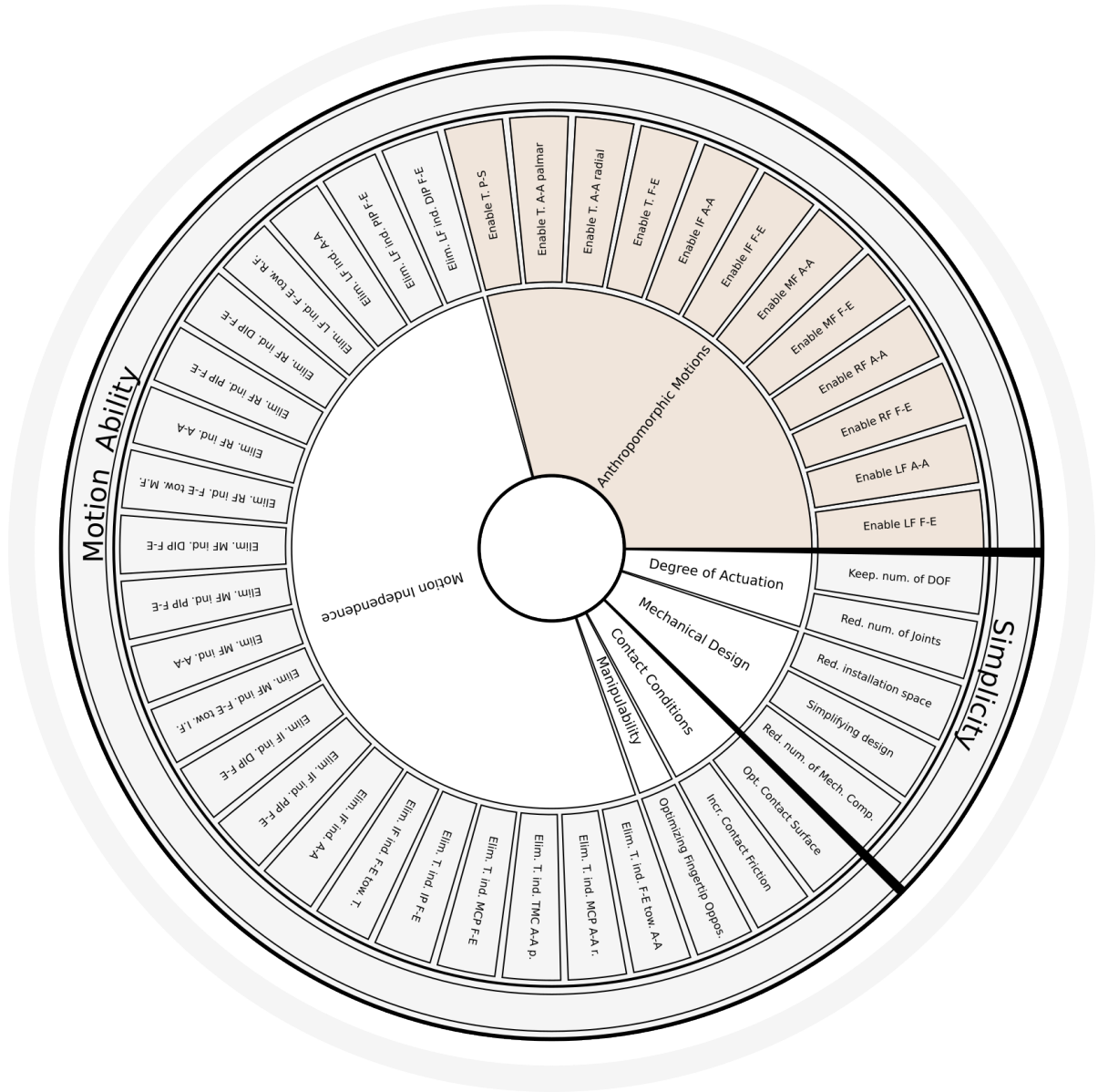


Figure K.5: Quality Profile illustration of the IMDC.

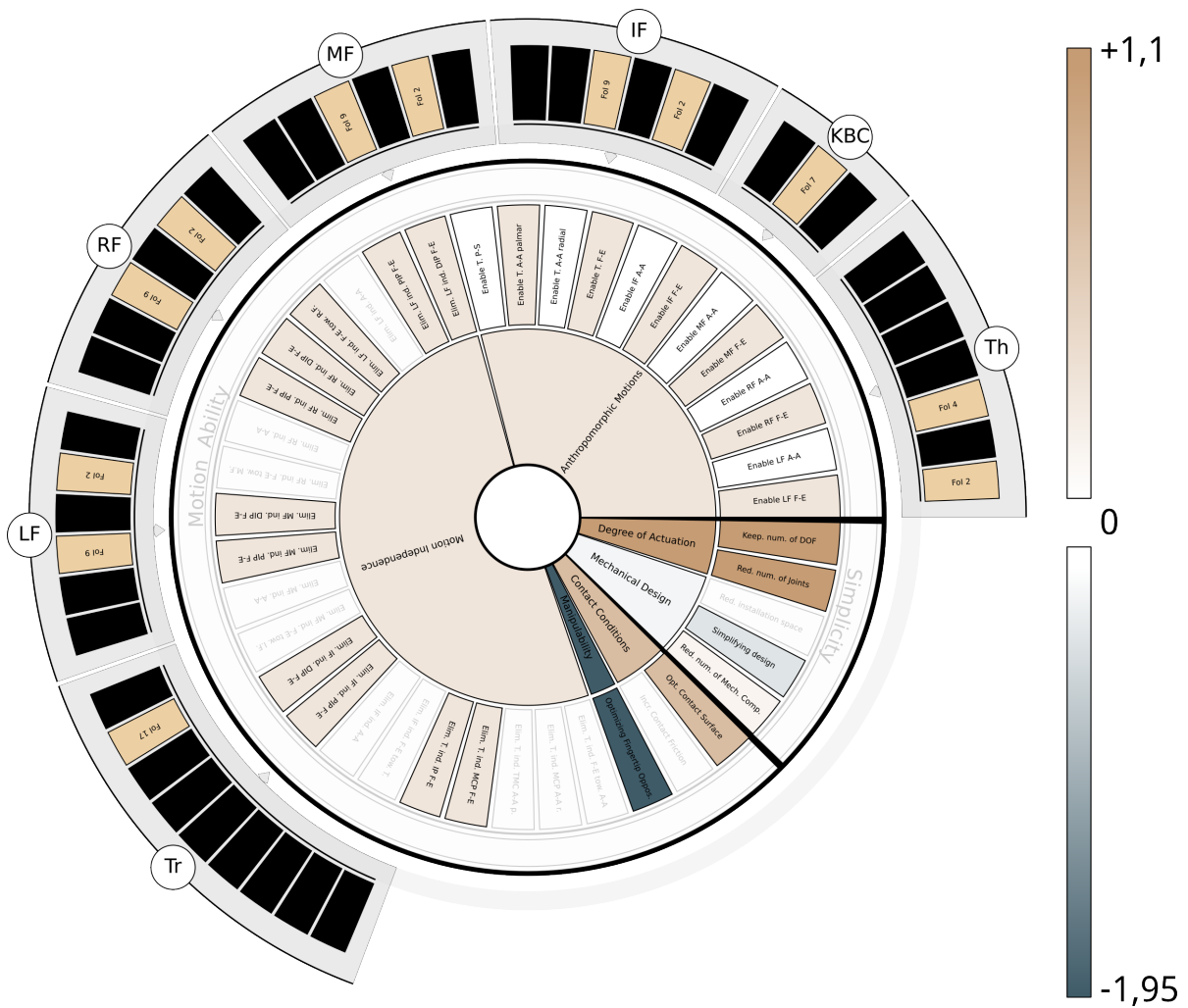


Figure K.6: Quality Profile illustration of the example recommendation (enlarged version of Figure 6.9).

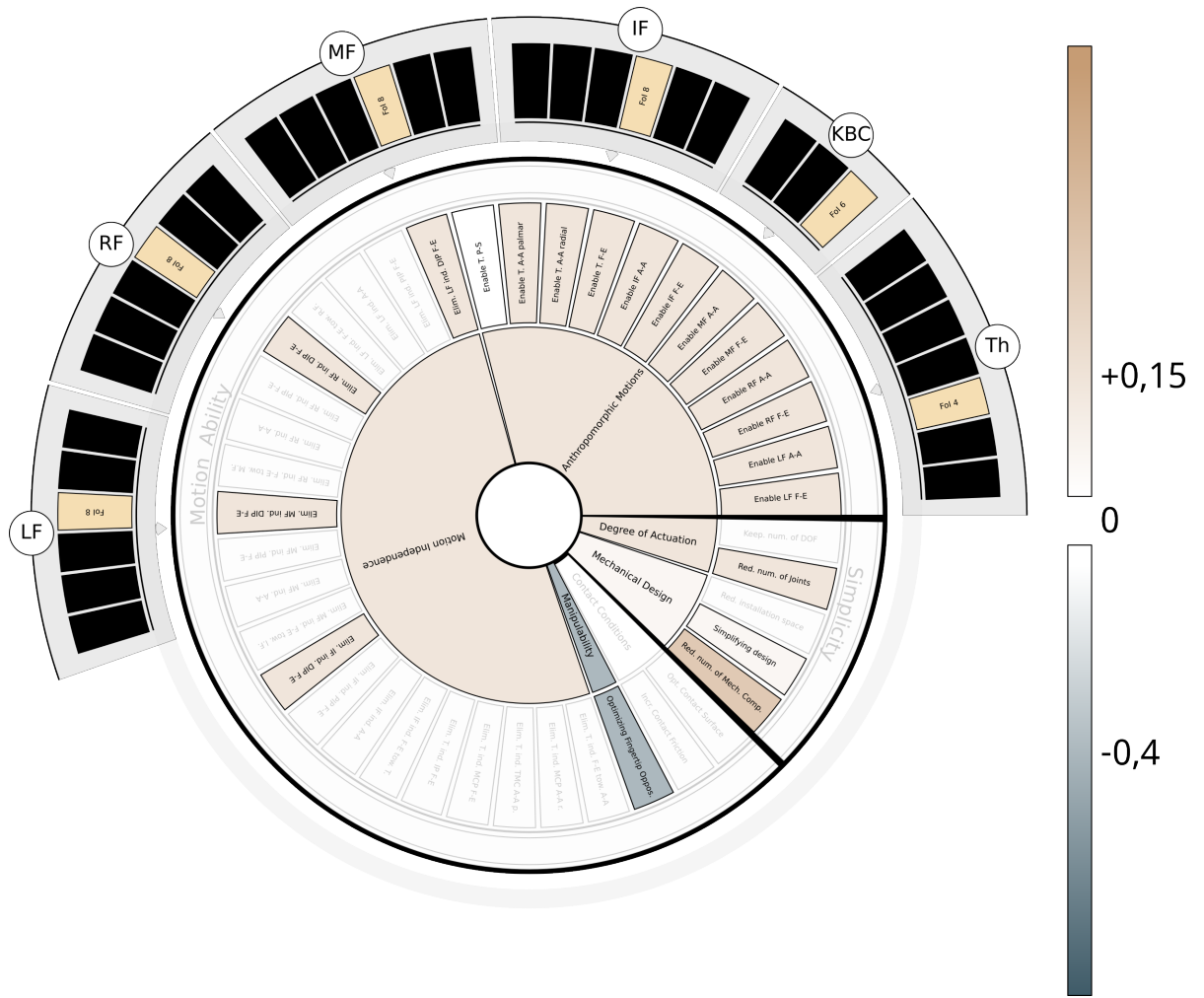


Figure K.7: Quality Profile illustration of the Shadow Dexterous Robot Hand (enlarged version of Figure 6.10).

L Influence Values

In this chapter, the influence value identifications for each FoI are presented. For chosen FoIs, further information and remarks are given that assist an interested reader in understanding the mechanics of chosen the addressed qualities and influence values they are addressed with.

The procedure for the FoI *Eliminating 1 TMC Joint DOF* in table L.1 presents the simplest standard procedure. For each influenced Superior Quality, a single Quality is addressed. The Quality of the input-dependent Superior Quality is uniquely associated to the PS. As only a single Quality per Superior Quality is addressed, the influence values correspond to the identified influence limits of the respective Superior Qualities. Further, no multiple expansion into the GFPS layer takes place, as the presented FoI and FPS directly corresponds to a single G-FoI and GFPS for the Thumb Group.

The procedure for the FoI *Eliminating 1 MCP Joint DOF* in table L.2 is identical. However,

| Eliminating 1 TMC Joint DOF | | | |
|-----------------------------|---------------------------|----------------------------------|---------------------|
| MQ | SQ | Q | Elim. TMC Pro./Sup. |
| Motion Ability | Manipulability | Optimizing Fingertip opposition | -0.25 |
| Motion Ability | Anthropomorphic Movements | Enable Th P-S | -0.15 |
| Simplicity | Mechanical Design | Simplifying design | +0.06 |
| Simplicity | DOA | Reducing number of Joints/Motors | +0.04 |

Table L.1: Influence values for FoI: Eliminating 1 TMC Joint DOF

it is subject to multiple expansion. The FPS can be assigned to five different groups, ranging from LF to Thumb. For the expansion into a group (in the GFPS level), only the addressed input-dependent Quality is altered. More specifically, only the assignment of the A-A DOF to a finger changes, which is thus marked with an "X". Therefore, the presented table can be transferred to any of the five groups, modifying the "X" to the respective group name¹. Another

¹For the Thumb Group, an exception is applied and the Quality *Enable T. A-A radial* is addressed

interesting difference to the FoI *Eliminating 1 MCP Joint DOF* are the different influence values of the Major Quality Simplicity. As derived, the individual influences on Qualities of that Major Quality are irrelevant as long as the sum corresponds to the identified influence limit. They are thus used as a mean of communication to the user. In this case, the elimination of the third DOF of the TMC joint is considered as a significant simplification of the mechanical design and thus correspondingly marked in the influences.

The FoI *Eliminating 1 IP Joint DOF* is a good example in which the influence value is

| Eliminating 1 MCP Joint DOF | | | |
|-----------------------------|--------------------|---------------------|-------------------------|
| MQ | SQ | Q | Eliminating MCP A-A DOF |
| Motion Ability | Anthrop. Movements | Enable X A-A | -0.15 |
| Motion Ability | Manipulability | Opt. Fingertip Opp. | -0.25 |
| Simplicity | Mechanical Design | Simplifying Design | 0.04 |
| Simplicity | D.o.A. | Red. num. of Joints | 0.06 |

Table L.2: Influence values for FoI *Eliminating 1 MCP Joint DOF*.

dependent on other GFPS. Generally speaking, it can occur that certain design options affect one another. In this FoI, it is demonstrated how that can be taken into account. In the given table, it is shown that the elimination of the DIP joint affects the respective finger F-E. If that F-E is given through the user input as required, the influence value is taken as it is depicted, the overall sum of the influence on the Major Quality Motion Ability is -0.4 , and the GFPS is considered undesired. Considering the defined user requirements per grasp, this will always be the case. However, a SRH has demonstrated that the LF DIP joint can be eliminated if a LF HMC joint is present. Thus, elimination of LF DIP Joint should be eligible in case the LF HMC is present. As a result, the influence value is not a single integer, but a conditional statement, as given in Table L.4, where GFPS₉₆ is referring to the PS *Eliminating HMC LF and RF*. The procedure for the FoI *Eliminating 2 TMC Joint DOF* is a good example of an FPS with a step size greater than 1. As shown, the same addressed qualities and influence values are simply doubled, since the influence limits are defined per step size.

The procedure for the FoI *Eliminating 1 HMC Joint DOF* is a good example in which no input-dependent qualities are addressed. In Figure 5.7, the number of addressed qualities in Block I and Block II is given as at most equal to the respective step size k . This formulation was chosen because eliminating a DOF does not necessarily impact any anthropomorphic movements. This is the case for the elimination of the HMC joint, as research has shown that its removal does not impair grasping performance.

| Eliminating 1 IP Joint DFF | | | |
|----------------------------|---------------------------|----------------------------------|-----------------|
| MQ | SQ | Q | Elim. DIP Joint |
| Motion Ability | Manipulability | Optimizing Fingertip opposition | -0.25 |
| Motion Ability | Anthropomorphic Movements | Enable X F-E | -0.15 |
| Simplicity | Mechanical Design | Reducing num. of Mech. Comp. | +0.04 |
| Simplicity | DOA | Reducing number of Joints/Motors | +0.06 |

Table L.3: Influence values for FoI *Eliminating 1 IP Joint DOF*.

| LF - Eliminating 1 IP Joint DOF | | | |
|---------------------------------|---------------------------|----------------------------------|---------------------------|
| MQ | SQ | Q | Elim. LF DIP Joint |
| Motion Ability | Manipulability | Optimizing Fingertip opposition | -0.25 if GFPS96 else -0.1 |
| Motion Ability | Anthropomorphic Movements | Enable X F-E | -0.15 if GFPS96 else 0 |
| Simplicity | Mechanical Design | Reducing num. of Mech. Comp. | +0.04 |
| Simplicity | DOA | Reducing number of Joints/Motors | +0.06 |

Table L.4: Influence values for G-FoI *LF-Eliminating 1 IP Joint DOF*.

The procedure for the FoI *Eliminating 1 DOA HMC Joint* is a good example in which multiple FPS are present. As derived, for the purpose of backward engineering, the strongest FPS is assigned the full influence limits. This ensures that it is treated as the most desirable option among the FPSs associated with the given FoI. The remaining FPSs are assigned lower influence values, with the specific reductions serving explanatory purposes only. In this example, a pairwise comparison between underactuation (UA) and coupling is illustrated. For instance, unlike UA, coupling neither preserves the number of degrees of freedom nor improves the contact conditions—accordingly, the associated qualities are reduced.

| Eliminating 2 TMC Joint DOF | | | |
|-----------------------------|---------------------------|----------------------------------|---------------------|
| MQ | SQ | Q | Elim. TMC A-A & P-S |
| Motion Ability | Manipulability | Optimizing Fingertip opposition | -0.25 |
| Motion Ability | Manipulability | Optimizing Fingertip opposition | -0.25 |
| Motion Ability | Anthropomorphic Movements | Enable Th P-S | -0.15 |
| Motion Ability | Anthropomorphic Movements | Enable Th A-A palmar | -0.15 |
| Simplicity | Mechanical Design | Simplifying design | +0.10 |
| Simplicity | DOA | Reducing number of Joints/Motors | +0.10 |

Table L.5: Influence values for FoI *Eliminating 2 TMC Joint DOF*

| Eliminating 2 MCP Joint DOF | | | |
|-----------------------------|---------------------------|----------------------------------|-----------------|
| MQ | SQ | Q | Elim. MCP Joint |
| Motion Ability | Manipulability | Optimizing Fingertip opposition | -0.25 |
| Motion Ability | Manipulability | Optimizing Fingertip opposition | -0.25 |
| Motion Ability | Anthropomorphic Movements | Enable Th A-A radial | -0.15 |
| Motion Ability | Anthropomorphic Movements | Enable Th F-E | -0.15 |
| Simplicity | Mechanical Design | Reducing num. of Mech. Comp. | +0.10 |
| Simplicity | DOA | Reducing number of Joints/Motors | +0.10 |

Table L.6: Influence values for FoI *Eliminating 2 MCP Joint DOF*

| Eliminating 1 HMC Joint DoF | | | | | |
|-----------------------------|--------------------|----------------------------------|--------------------|------------|----------------|
| MQ | SQ | Q | Impl. HMC L.F+R.F. | joined for | Elim. HMC R.F. |
| Motion Ability | Manipulability | Optimizing Fingertip opposition | -0.1 | | -0.1 |
| Motion Ability | Anthropomorphic M. | Enable L.F. F-E | 0 | | 0 |
| Motion Ability | Anthropomorphic M. | Enable R.F. F-E | 0 | | 0 |
| Simplicity | Mechanical Design | Reducing num of Mech. Comp. | +0.04 | | +0.04 |
| Simplicity | DOA | Reducing number of Joints/Motors | +0.06 | | +0.06 |

Table L.7: Influence values for FoI *Eliminating 1 HMC Joint DOF*

| Eliminating 2 HMC Joint DOF | | | | |
|-----------------------------|---------------------------|----------------------------------|--|--|
| MQ | SQ | Q | | Eliminating HMC Little and Ring finger |
| Motion Ability | Manipulability | Optimizing Fingertip opposition | | -0.1 |
| Motion Ability | Manipulability | Optimizing Fingertip opposition | | -0.1 |
| Motion Ability | Anthropomorphic Movements | Enable L.F. F-E | | 0 |
| Motion Ability | Anthropomorphic Movements | Enable R.F. F-E | | 0 |
| Simplicity | Mechanical Design | Reducing num. of Mech. Comp. | | +0.1 |
| Simplicity | DOA | Reducing number of Joints/Motors | | +0.1 |

Table L.8: Influence values for FoI *Eliminating 2 HMC Joint DOF*

| Elim. 1 DOA HMC Joint | | | | | | |
|-----------------------|----------------------------|--|--|-----------------------------------|-----------------------------|----|
| MQ | SQ | Q | | Linkage coupling of two joints | Linkage UA of two joints | of |
| Motion Ability | Manipulability | Optimizing Fin- gertip opposition | | -0.3 | -0.3 | |
| Motion Ability | Contact Conditions | Optimizing Con- tact Surface | | 0 | +0.05 | |
| Motion Ability | Movement Inde- pendence | Elim. L.F. indi- vidual PIP F-E | | +0.15 | +0.15 | |
| Simplicity | Mechanical Design | Simplifying De- sign | | -0.08 | -0.08 | |
| Simplicity | Mechanical Design | Reducing mainte- nance | | +0.03 | +0.03 | |
| Simplicity | DOA | Reducing number of Joints/Motors | | +0.05 | +0.05 | |
| Simplicity | DOA | Keeping num. of DOF | | 0 | +0.1 | |

Table L.9: Influence values for FoI *Elim. 1 DOA HMC Joint*

| Elim. 1 DOA MCP-PIP Joints | | | | | | | |
|----------------------------|--|-----------------------|--------------|----------------------------------|-------------------------------|--------------------------------|--------------------------|
| MQ | | SQ | | Q | Tendon coupling of two joints | Linkage coupling of two joints | Linkage UA of two joints |
| Motion Ability | | Manipulability | | Optimizing Fingertip opposition | -0.3 | -0.3 | -0.3 |
| Motion Ability | | Contact Conditions | Conditions | Optimizing Contact Surface | 0 | 0 | +0.05 |
| Motion Ability | | Movement Independence | Independence | Elim. X individual PIP F-E | +0.15 | +0.15 | +0.15 |
| Simplicity | | Mechanical Design | Design | Simplifying Design | -0.05 | -0.08 | -0.08 |
| Simplicity | | Mechanical Design | Design | Reducing maintenance | 0 | +0.03 | +0.03 |
| Simplicity | | DOA | | Reducing number of Joints/Motors | +0.05 | +0.05 | +0.05 |
| Simplicity | | DOA | | Keeping num of DOF | 0 | 0 | +0.1 |

Table L.10: Influence values for FoI *Elim. 1 DOA MCP-PIP Joints*

| Elim. 2 DOA TMC-MCP-IP Joints | | | | | | | |
|-------------------------------|-----------------------|----------------------------------|---------------------------------|----------------------------------|----------------------------|--|--|
| MQ | SQ | Q | Tendon coupling of three joints | Linkage coupling of three joints | Linkage UA of three joints | | |
| Motion Ability | Manipulability | Optimizing Fingertip opposition | -0.6 | -0.6 | -0.6 | | |
| Motion Ability | Contact Conditions | Optimizing Contact Surface | 0 | 0 | +0.1 | | |
| Motion Ability | Movement Independence | Elim. T. individual IP F-E | +0.15 | +0.15 | +0.15 | | |
| Motion Ability | Movement Independence | Elim. T. individual MCP F-E | +0.15 | +0.15 | +0.15 | | |
| Simplicity | Mechanical Design | Simplifying Design | -0.1 | -0.16 | -0.16 | | |
| Simplicity | Mechanical Design | Reducing maintenance | 0 | +0.06 | +0.06 | | |
| Simplicity | DOA | Reducing number of Joints/Motors | +0.1 | +0.1 | +0.1 | | |
| Simplicity | DOA | Keeping num. of DOF | 0 | 0 | +0.2 | | |

Table L.11: Influence values for FoI *Elim. 2 DOA TMC-MCP-IP Joints*

| Elim. 3 DOA TMC-MCP-IP Joints | | | | |
|-------------------------------|-----------------------|--------|----------------------------------|----------------------------|
| MQ | SQ | | Q | Linkage UA of three joints |
| Motion Ability | Manipulability | | Optimizing Fingertip opposition | -0.9 |
| Motion Ability | Contact Conditions | | Optimizing Contact Surface | +0.15 |
| Motion Ability | Movement Independence | Indep- | Elim. T. individual IP F-E | +0.15 |
| Motion Ability | Movement Independence | Indep- | Elim. T. individual MCP F-E | +0.15 |
| Motion Ability | Movement Independence | Indep- | Elim. T. ind. F-E towards T. A-A | +0.15 |
| Simplicity | Mechanical Design | | Simplifying Design | -0.24 |
| Simplicity | Mechanical Design | | Reducing maintenance | +0.09 |
| Simplicity | DOA | | Reducing number of Joints/Motors | +0.15 |
| Simplicity | DOA | | Keeping num. of DOF | +0.3 |

Table L.12: Influence values for FoI *Elim. 3 DOA TMC-MCP-IP Joints*

| Elim. 1 DOA PIP-DIP Joints | | | | | | | |
|----------------------------|-----------------------|----------------------------------|-------------------------------|--------------------------------|--------------------------|----|--|
| MQ | SQ | Q | Tendon coupling of two joints | Linkage coupling of two joints | Linkage UA of two joints | UA | |
| Motion Ability | Manipulability | Optimizing Fingertip opposition | -0.3 | -0.3 | -0.3 | | |
| Motion Ability | Contact Conditions | Optimizing Contact Surface | 0 | 0 | +0.05 | | |
| Motion Ability | Movement Independence | Elim. X individual DIP F-E | +0.15 | +0.15 | +0.15 | | |
| Simplicity | Mechanical Design | Simplifying Design | -0.05 | -0.08 | -0.08 | | |
| Simplicity | Mechanical Design | Reducing maintenance | 0 | +0.03 | +0.03 | | |
| Simplicity | DOA | Reducing number of Joints/Motors | +0.05 | +0.05 | +0.05 | | |
| Simplicity | DOA | Keeping num. of DOF | 0 | 0 | +0.1 | | |

Table L.13: Influence values for FoI *Elim. 1 DOA PIP-DIP Joints*

| Elim. 2 DOA MCP-PIP-DIP Joints | | | | | | | |
|--------------------------------|-----------------------|-----------------------------------|---------------------------------|----------------------------------|----------------------------|---------------------------|--|
| MQ | SQ | Q | Tendon coupling of three joints | Linkage coupling of three joints | Linkage UA of three joints | Tendon UA of three joints | |
| Motion Ability | Manipulability | Optimizing Fingertip opposition | -0.6 | -0.6 | -0.6 | -0.6 | |
| Motion Ability | Contact Conditions | Optimizing Contact Surface | 0 | 0 | +0.1 | +0.1 | |
| Motion Ability | Movement Independence | Elim. X individual DIP F-E | +0.15 | +0.15 | +0.15 | +0.15 | |
| Motion Ability | Movement Independence | Elim. X individual PIP F-E | +0.15 | +0.15 | +0.15 | +0.15 | |
| Simplicity | Mechanical Design | Simplifying Design | -0.1 | -0.16 | -0.16 | -0.1 | |
| Simplicity | Mechanical Design | Reducing maintenance | 0 | +0.06 | 0.06 | 0 | |
| Simplicity | DOA | Reducing number of Joints/-Motors | +0.1 | +0.1 | +0.1 | +0.1 | |
| Simplicity | DOA | Keeping num of DOF | 0 | 0 | +0.2 | +0.2 | |

Table L.14: Influence values for FoI *Elim. 2 DOA MCP-PIP-DIP Joints*

| Elim. 3 DOA MCP-DIP-PIP Joints | | | | |
|--------------------------------|--------------------|-----------------|---|--------------------------|
| MQ | SQ | | Q | Linkage UA of two joints |
| Motion Ability | Manipulability | | Optimizing Fingertip opposition | -0.9 |
| Motion Ability | Contact Conditions | | Optimizing Contact Surface | +0.15 |
| Motion Ability | Movement | Indep- dence | Elim. X individual DIP F-E | +0.15 |
| Motion Ability | Movement | Indep- dence | Elim. X individual PIP F-E | +0.15 |
| Motion Ability | Movement | Indep- dence | Elim. X individual F- E towards A-A | +0.15 |
| Simplicity | Mechanical Design | | Simplifying Design | -0.24 |
| Simplicity | Mechanical Design | | Reducing mainte- nance | +0.09 |
| Simplicity | DOA | | Reducing number of Joints/Motors | +0.15 |
| Simplicity | DOA | | Keeping num. of DOF | +0.3 |

Table L.15: Influence values for FoI *Elim. 3 DOA MCP-DIP-PIP Joints*

| Eliminating 1 DOA F-E LF-RF | | | | |
|-----------------------------|--------------------|-----------------|---|--------------------------------------|
| MQ | SQ | | Q | Tendon Underactua- tion F-E LF-RF |
| Motion Ability | Manipulability | | Optimizing Fingertip opposition | -0.3 |
| Motion Ability | Contact Conditions | | Optimizing Contact Surface | +0.05 |
| Motion Ability | Movement | Indep- dence | Elim. L.F. individual F-E towards R.F. | +0.15 |
| Simplicity | Mechanical Design | | Simplifying Design | -0.05 |
| Simplicity | DOA | | Reducing number of Joints/Motors | +0.05 |
| Simplicity | DOA | | Keeping num. of DOF | +0.1 |

Table L.16: Influence values for FoI *Eliminating 1 DOA F-E LF-RF*

| Eliminating 1 DOA F-E MF-IF | | | | |
|-----------------------------|----------------------------|---|--------------------------------------|--|
| MQ | SQ | Q | Tendon Underactua- tion F-E MF-IF | |
| Motion Ability | Manipulability | Optimizing Fingertip opposition | -0.3 | |
| Motion Ability | Contact Conditions | Optimizing Contact Surface | +0.05 | |
| Motion Ability | Movement Indepen- dence | Elim. M.F. individual F-E towards I.F. | +0.15 | |
| Simplicity | Mechanical Design | Simplifying Design | -0.05 | |
| Simplicity | DOA | Reducing number of Joints/Motors | +0.05 | |
| Simplicity | DOA | Keeping num. of DOF | +0.1 | |

Table L.17: Influence values for FoI *Eliminating 1 DOA F-E MF-IF*

| Eliminating 2 DOA F-E RF-MF-IF | | | | |
|--------------------------------|----------------------------|---|---|--|
| MQ | SQ | Q | Tendon Underactua- tion F-E RF-MF-IF | |
| Motion Ability | Manipulability | Optimizing Fingertip opposition | -0.6 | |
| Motion Ability | Contact Conditions | Optimizing Contact Surface | +0.1 | |
| Motion Ability | Movement Indepen- dence | Elim. R.F. individual F-E towards M.F. | +0.15 | |
| Motion Ability | Movement Indepen- dence | Elim. M.F. individual F-E towards I.F. | +0.15 | |
| Simplicity | Mechanical Design | Simplifying Design | -0.1 | |
| Simplicity | DOA | Reducing number of Joints/Motors | +0.1 | |
| Simplicity | DOA | Keeping num. of DOF | +0.2 | |

Table L.18: Influence values for FoI *Eliminating 2 DOA F-E RF-MF-IF*

| Eliminating 2 DOA F-E LF-RF-MF | | | | |
|--------------------------------|-----------------------|--------|--|------------------------------------|
| MQ | SQ | | Q | Tendon Underactuation F-E LF-RF-MF |
| Motion Ability | Manipulability | | Optimizing Fingertip opposition | -0.6 |
| Motion Ability | Contact Conditions | | Optimizing Contact Surface | +0.1 |
| Motion Ability | Movement Independence | Indep- | Elim. L.F. individual F-E towards R.F. | +0.15 |
| Motion Ability | Movement Independence | Indep- | Elim. R.F. individual F-E towards M.F. | +0.15 |
| Simplicity | Mechanical Design | | Simplifying Design | -0.1 |
| Simplicity | DOA | | Reducing number of Joints/Motors | +0.1 |
| Simplicity | DOA | | Keeping num. of DOF | +0.2 |

Table L.19: Influence values for FoI *Eliminating 2 DOA F-E LF-RF-MF*

| Eliminating 2 DOA A-A LF-RF-IF | | | | |
|--------------------------------|-----------------------|--------|----------------------------------|------------------------------|
| MQ | SQ | | Q | Tendon Coupling A-A LF-RF-IF |
| Motion Ability | Manipulability | | Optimizing Fingertip opposition | -0.5 |
| Motion Ability | Contact Conditions | | Optimizing Contact Surface | 0 |
| Motion Ability | Movement Independence | Indep- | Elim. L.F. individual A-A | +0.15 |
| Motion Ability | Movement Independence | Indep- | Elim. R.F. individual A-A | +0.15 |
| Simplicity | Mechanical Design | | Simplifying Design | -0.1 |
| Simplicity | Mechanical Design | | Reducing installation space | +0.1 |
| Simplicity | DOA | | Reducing number of Joints/Motors | +0.2 |

Table L.20: Influence values for FoI *Eliminating 2 DOA A-A LF-RF-IF*

| Eliminating 3 DOA F-E LF-RF-MF-IF | | | | |
|-----------------------------------|--------------------|-------------------|---|--|
| MQ | SQ | | Q | Tendon Underactua- tion F-E LF-RF-MF- IF |
| Motion Ability | Manipulability | | Optimizing Fingertip opposition | -0.9 |
| Motion Ability | Contact Conditions | | Optimizing Contact Surface | +0.15 |
| Motion Ability | Movement | Indepen- dence | Elim. L.F. individual F-E towards R.F. | +0.15 |
| Motion Ability | Movement | Indepen- dence | Elim. R.F. individual F-E towards M.F. | +0.15 |
| Motion Ability | Movement | Indepen- dence | Elim. M.F. individual F-E towards I.F. | +0.15 |
| Simplicity | Mechanical Design | | Simplifying Design | -0.15 |
| Simplicity | DOA | | Reducing number of Joints/Motors | +0.15 |
| Simplicity | DOA | | Keeping num. of DOF | +0.3 |

Table L.21: Influence values for FoI *Eliminating 3 DOA F-E LF-RF-MF-IF*

| Eliminating 4 DOA F-E LF-RF-MF-IF-Tb | | | | |
|--------------------------------------|------------------------|-------------------|---|---|
| MQ | SQ | | Q | Tendon Underactua- tion F-E LF-RF-MF- IF-Tb |
| Motion Ability | Manipulability | | Optimizing Fingertip opposition | -1.2 |
| Motion Ability | Contact Conditions | | Optimizing Contact Surface | +0.2 |
| Motion Ability | Movement dependence | Indepen- dence | Elim. L.F. individual F-E towards R.F. | +0.15 |
| Motion Ability | Movement dependence | Indepen- dence | Elim. R.F. individual F-E towards M.F. | +0.15 |
| Motion Ability | Movement dependence | Indepen- dence | Elim. M.F. individual F-E towards I.F. | +0.15 |
| Motion Ability | Movement dependence | Indepen- dence | Elim. I.F. individual F-E towards T. | +0.15 |
| Simplicity | Mechanical Design | | Simplifying Design | -0.2 |
| Simplicity | DOA | | Reducing number of Joints/Motors | +0.2 |
| Simplicity | DOA | | Keeping num. of DOF | +0.4 |

Table L.22: Influence values for FoI *Eliminating 4 DOA F-E LF-RF-MF-IF-Tb*

| Eliminating 4 DOA A-A LF-RF-MF-IF-Tb | | | | |
|--------------------------------------|--------------------|-------------------|-------------------------------------|---|
| MQ | SQ | | Q | Tendon Underactua- tion A-A LF-RF-MF- IF-Tb |
| Motion Ability | Manipulability | | Optimizing Fingertip opposition | -1.2 |
| Motion Ability | Contact Conditions | | Optimizing Contact Surface | +0.2 |
| Motion Ability | Movement | Indepen- dence | Elim. L.F. individual A-A | +0.15 |
| Motion Ability | Movement | Indepen- dence | Elim. R.F. individual A-A | +0.15 |
| Motion Ability | Movement | Indepen- dence | Elim. M.F. individual A-A | +0.15 |
| Motion Ability | Movement | Indepen- dence | Elim. I.F. individual A-A | +0.15 |
| Simplicity | Mechanical Design | | Simplifying Design | -0.2 |
| Simplicity | DOA | | Reducing number of Joints/Motors | +0.2 |
| Simplicity | DOA | | Keeping num. of DOF | +0.4 |

Table L.23: Influence values for FoI *Eliminating 4 DOA A-A LF-RF-MF-IF-Tb*

With demographic change driving the demand for robotic assistance in complex grasping tasks, robot hands are emerging as a promising solution. However, the growing interest in anthropomorphic robot hands is difficult to address: The complex and multifaceted mechanical design creates high entry hurdles for new designers. This slows the growth in the number of experts and complicates finding relevant information, even for experienced designers. This is particularly evident in the conceptual design phase, when determining joint configuration, their coordination, and relative allocation. Guidance in the form of a knowledge-based design assistance system could address these problems by automating the decision-making parts of the design process, presenting solutions with reference to literature and offering recommendations for the conceptual design. This dissertation addresses the question of how such a guidance can be developed.

A hypothesis is formulated and three objectives are pursued to test it: (1) develop a literature-linked knowledge base on joint configuration and coordination of tendon-driven rigid-sequential anthropomorphic robot hands to systematically generate conceptual designs, (2) develop a method to identify optimal designs based on user requirements, and (3) develop an automated evaluation method to select the most suitable design from the generated options.

For the first objective, a knowledge base is developed, organizing relevant information into a non-redundant list of 23 fields of interest and 30 principal solutions, each linked to its original references. Arranged in morphological boxes, the knowledge base is applied to a methodically derived joint configuration of the human hand to generate approximately 8.5 billion conceptual designs. For the second, a heuristic is developed to identify Pareto-optimal designs based on desired grasp types (performance) and a choice between dexterity and design simplicity (preference). Suitable joint configurations and coordination strategies, drawn from literature, are ranked according to the user's preference. For the third, the developed control system evaluates designs using a utility analysis of the principal solutions, with scores adjusted by preference and relevance weights to align with the heuristic.

The resulting guidance is implemented as a graphical user interface and verified to replicate the intended recommendations. An example application of the guidance presents, to the best of the author's knowledge, the first task-based design of an anthropomorphic robot hand with references to original sources.

By lowering entry barriers in early-stage anthropomorphic robot hand design, this dissertation lays a foundation for accelerating mechanical and control development, with potential to meet growing demand and reduce costs. It also presents the first framework for task-based robot hand design with meaningful results, despite gaps in the state of the art limiting a full analysis.

